# Cervical Total Level Arthroplasty System With PEEK All-Polymer Articulations

by

Gordon Daniel George Langohr

A thesis
presented to the University of Waterloo
in fulfillment of the
thesis requirement for the degree of
Master of Applied Science
in
Mechanical Engineering

Waterloo, Ontario, Canada, 2010

I hereby declare that I am the sole author of this thesis. This is a true copy of the thesis, including any required final revisions, as accepted by my examiners.

I understand that my thesis may be made electronically available to the public.

# Abstract

Chronic back pain and related nerve damage is a significant contributor to the use of the healthcare system generating an estimated 13 million doctor and 50 million chiropractor visits annually in the United States and almost certainly proportional numbers in Canada. In particular, the prevalence of neck pain and associated nerve impingement has been reported to be within the range of 9% to 12% of the general population with the combined effects of neck and back pain accounting for up to 65% of cases of disability. Neck pain is specifically related to the cervical spine. This represents notable cost to society in terms of healthcare expenses plus lost work time and suffering for those afflicted.

The cervical spine must perform somewhat contradictory roles. It must provide adequate structural support for the head while allowing range of motion to complete everyday activities. Also, it must protect one of the most vital components of the central nervous system, the spinal cord and its related branching nerves. The motion and protection of the cervical spinal cord with its branching nerves depends a large extent on the condition of the joints. There are two types of joints: the intervertebral discs which are a flexible connection and the facets, which are articulating synovial joints. Both joints carry axial load and torque during rotational motion with the discs carrying most of the axial load and providing axial shock absorption. Both degenerate with age. A recent study of the lumbar spine suggests that disc degeneration usually occurs before facet joint degeneration. This sequence is likely to occur in the cervical spine as well and it has been estimated that up to 62% of neck pain cases arise from the facet joint degeneration.

Current surgical procedures to alleviate severe dysfunction and pain associated with disc degeneration include spinal arthrodesis (fusion) and disc arthroplasty (replacement with a joint). If severe dysfunction and pain are also associated with the facet joints, spinal fusion is the only option. Occasionally, when only the facet joints seem to be the cause of pain and there is little dysfunction (major nerve impingement), the small nerves to the facet joints can be killed. However, the continued structural collapse of the facet joints is likely to cause disc degeneration and thus eventually fusion may be required.

In spinal fusion the intervertebral disc is removed and, with the *in vivo* spacing preserved, the adjacent vertebrae are fused together with a combination of bone grafts and implants. Fusion prevents or severely limits the intervertebral motion, which causes abnormally high stress levels in adjacent discs.

In disc replacement, the damaged disc is removed and an articulating device is inserted in place of the disc and allows intervertebral motion that attempts to mimic the healthy spine. Disc arthroplasty is a significant improvement over spinal fusion, particularly in the cervical region, with regards to the reduction in adjacent level motion and stresses. However, the lack of rotational constraint causes increased facet contact pressure at both the surgical and adjacent levels especially in extension with axial rotation when the facets are the most heavily loaded.

Current FDA (U.S. Food and Drug Administration) approved devices for cervical disc arthroplasty are the Prestige® and Bryan® implants both from Medtronic Spinal & Biologics and the ProDisc™-C from Synthes Spine, Inc.. Metallic alloys provide the main structural components. These metallic alloys introduce medical imaging problems that would disappear if a polymer such as medical grade polyetheretherkeytone (PEEK) could

be substituted. There are also several facet arthroplasty devices that have been proposed and are under current investigation/promotion but they too include metallic alloys and none of them have been specifically designed to function in conjunction with cervical disc arthroplasty.

Thus, opportunities exist for improving disc arthroplasty and developing facet arthroplasty in the cervical spine. Efforts should be made, in disc arthroplasty, to reduce postoperative facet pressures. This could involve a disc implant design that better restores the load sharing between the disc and facet joints. Furthermore, there may be merit in an approach that integrates both geometry and structure to give a combined replacement of the disc and facets for a cervical total level arthroplasty system (CTLAS) solution for patients afflicted with both disc and facet degeneration. The only current treatment option in this case is fusion. Thus, there is a need for modular CTLAS implant system that has a disc implant specifically designed to preserve the facet joints and an implant or set of implants for facet arthroplasty that can act together with the disc implant in an integrated and co-operative manner. In some cases, there may be a need for one or two stand-alone facet joint implants.

The design of a modular cervical CTLAS implant system is proposed that would replace both the disc and the facet joints. PEEK (polyetheretherkeytone) was proposed as the main structural material to improve medical imaging and some thought was given to using shock absorbing materials to protect the branching nerves. An all-polymer PEEK articulation was specified that reproduced the natural helical axis of the cervical spine. The facet joints were to be replaced with an all-polymer PEEK surface replacement. The proposed CTLAS design was considered an important first step in realizing such a technological advance in clinical practice. The proposed design was incomplete because there were still fixation issues to consider along with optimization for manufacturing. Furthermore, pre-clinical investigations would be required and probably include animal testing of fixation methods involving PEEK surfaces plus extensive simulator testing to show acceptably low levels of both fatigue and wear.

In the present thesis, pre-clinical testing was initiated with pin-on-plate wear testing of PEEK-on-PEEK to explore the tribology of this rather uncommon contact configuration. This testing contributed to an existing body of knowledge on this material pairing that was obtained in previous pin-on-plate and simulator studies done at various research centres. The present study used a protocol of testing under an adverse loading regime to investigate the sensitivity of all-polymer PEEK articulations to previous wear damage and extreme conditions. A gravimetric wear assessment protocol was used that avoided vacuum drying. The lower wear of polyacrylonitrile carbon fibre reinforced (CFR) PEEK compared with unfilled PEEK, as found by many other studies, was confirmed. PEEK was shown to have remarkably low wear despite previous adverse load testing. CFR PEEK was found to have much lower and more predictable wear than the unfilled PEEK, under a variety of test conditions. The wear of unfilled PEEK pairs seemed to show sensitivity to lubricant protein concentration. The coefficient of friction in all testing was found to be quite high (up to 0.5) and this might have clinical implications. Finally, it was noted that the comparison of wear factors and wear amounts from the present study (and other previous studies at Waterloo by Austin et al) with those of the very similar study by Scholes and Unsworth (Durham University, UK) suggested that their laboratory model might be overstating the wear of all-polymer PEEK articulations for potential applications in orthopaedic tribology. Also, the present study suggested that PEEK-on-

PEEK articulations could carry loads for a certain number of cycles up to some threshold condition after which the surfaces could no longer resist the energy input without sustaining a severe and cascading damage. This situation may or may not occur in clinical application.

The CFR PEEK had a higher elastic modulus, smaller contact areas, higher contact stresses and lower wear than the unfilled PEEK. While this clearly made the CFR look better than the unfilled PEEK, the possibility of subsurface fatigue exposing carbon fibers to direct contact and wear remains a concern. If this concern is adequately addressed with further wear test data including simulator studies of the proposed design, then CFR is clearly better than unfilled PEEK for use in a spinal disc and facet arthroplasty device because its low wear under a variety of conditions.

# Acknowledgements

The author would like to thank his supervisor, Professor John B. Medley for providing guidance in research and a multitude of opportunities including attendance to several local and international conferences, observation of orthopaedic surgeries, as well as an overall introduction to the field of biomedical engineering. Professor Medley provided invaluable insight during the preparation of various publications including the present thesis, and was an excellent sounding board for discussion.

The author wishes to thank Medtronic Spine and Biologics (Memphis, TN) for supplying the specimens used in the present work and Invibio Ltd. (Thornton Cleveleys, LAN) for providing specimens and funding support. Also, scholarship support for the author was received from the Natural Science and Engineering Research Council (NSERC) of Canada and an Ontario Government Scholarship (OGS). Guidance was provided on the operation of the OrthoPOD™ with general training from Heather Austin and some specific technical support from Alan Walsh (AMTI, Watertown, MA). Also, Nupur Maheshwari gave valuable assistance in the some of the laboratory testing.

# Table of Contents

# List of Tables

# List of Figures

# List of Acronyms

| | |
|---|---|
| ALL | anterior longitudinal ligament |
| CFR | carbon fibre reinforced PEEK |
| CNF | carbon-nano fibre reinforced PEEK |
| CSM | cervical spinal myelopathy |
| CSR | cervical spinal radiculopathy |
| CTLAS | cervical total level arthroplasty system |
| FDA | food and drug administration |
| F-E | flexion-extension |
| IDE | investigational device exemption |
| ICR | instantaneous center of rotation |
| IVD | intervertebral disc |
| MRI | magnetic resonance imaging |
| NGF | nerve growth factor |
| OPT | PEEK OPTima |
| PAN | polyacrylonitrile |
| PBS | phosphate buffer solution |
| PCM | porous coated motion prosthesis |
| PE | polyethylene |
| PEK | polyetherkeytone |
| PEEK | polyetheretherkeytone |
| PG | proteoglycans |
| PLL | posterior longitudinal ligament |
| ROM | range of motion |
| TDA | total disc arthroplasty |
| TFAS | total facet arthroplasty system |
| TOPS | total posterior system (facet replacement) |
| UHMWPE | ultra-high-molecular-weight polyethylene |

# Nomenclature

| | |
|---|---|
| $A$ | area of wear scar on the pin tip |
| $\Delta m_W$ | real mass loss |
| $F$ | load (N) |
| $k$ | wear factor ($mm^3\ N^{-1}\ m^{-1}$) |
| $m$ | specimen mass at the beginning of wear testing (mg) |
| $Mc$ | millions of cycles |
| $\rho$ | density of PEEK material ($mg\ mm^{-3}$) |
| $V$ | volumetric wear ($mm^3$) |
| $x$ | sliding distance (m) |

# Chapter 1

# Introduction

The spine is an integral component of the human physiology as it provides structural support for the entire body by transmitting the gravitational and muscular loading from the extremities to the lower structures and ultimately the ground. The spine must be stiff enough to support the significant loading to which it is subjected but, at the same time, flexible enough to allow motion in many different directions. It must also protect the spinal cord which is responsible for the transmission of neural information that occurs between the body and brain.

The spine is subdivided into three main sections: the lumbar, thoracic and cervical regions (Figure 1-1). The spine is comprised of 24 independent vertebrae which are made of bone. These vertebrae support the applied axial loads, constrain the range of motion and protect the spinal cord which is located within its posterior elements. Compared with the lumbar spine, the vertebrae of the cervical spine are smaller in size and have a similar but distinctive geometry. In particular, they have a smaller axial thickness than those of the lumbar spine.

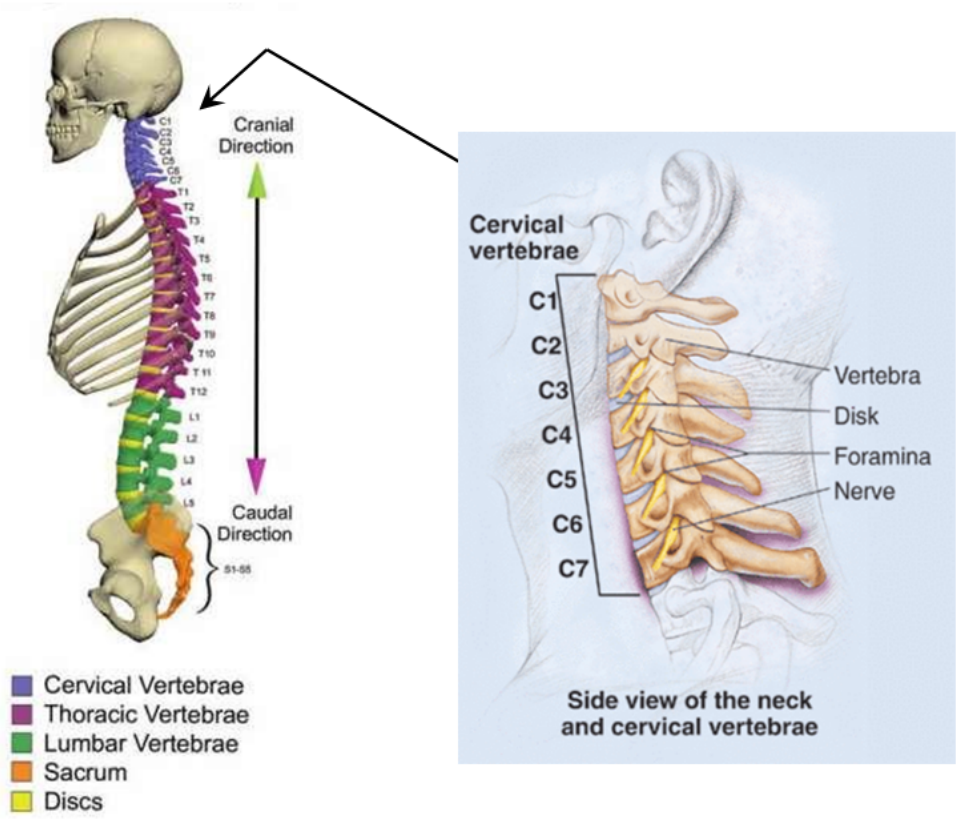


(Adapted from www.eorthopod.com and Kurtz & Edidin, 2006)

**Figure 1-1: Regions of the human spine with details for the cervical spine**

The vertebrae of the cervical spine are smaller in size and have a similar but distinctive geometry compared with the vertebrae of the lumbar spine. Also, the intervertebral discs are smaller and in particular have a smaller axial dimension (thickness) than those of the lumbar spine.

Adjacent vertebrae are separated by flexible joints known as intervertebral discs that consist of a liquid gel core contained within a fibrous multi-layered annular shell. The discs transmit axial load, shear load and torsion while providing enough compliance between the bony structures to allow flexion-extension, rotation and lateral motions of the spine. Besides these flexible intervertebral discs, there are also facet joints that share in the load transmission of the spine. The facet joints are classified as synovial joints and have conforming bony ends covered with articular cartilage that slides over each other in the presence of synovial fluid. In the cervical spine, the facet joints are oriented at an angle of about $45^{o}$ in the sagittal plane and thus carry a significant portion of the axial load particularly during extension (rearward motion) of the neck as well as torsion. During flexion-extension, rotation and lateral bending motions, both the discs and the facet joints transmit tensile forces through their fibrous outer shells. Also, the facet joint alignment depends to a large extent on the ability of the disc to maintain the correct vertical spacing between the vertebrae. Thus, both disc and facet joints are related in terms of loading, geometry and overall spinal kinematics.

Because the spine plays an important role in human locomotion and the distribution of motor and sensory information to and from the brain, spinal disorders are of particular interest from the point of view of both patients and healthcare providers. The results of spinal disorders most commonly include the presence of occasional back pain but may also incorporate significant dysfunction and disability due to persistent discomfort, numbness, loss of coordination and in severe cases some degree of paralysis.

The prevalence of chronic back pain is fairly common in the general population. Spivak and Bendo (2002) estimated that back pain generates a total of 13 million doctor visits and 50 million chiropractor visits each year in the United States (U.S.). The most common sources of pain generation are the lumbar region due to the high loads transmitted and the cervical region due to the large range of motion. Typically the thoracic spine is only problematic if it is the site of a localized injury. Chronic neck pain has been reported by Clark (2005) to range from 9% to 12% of the general population, with one third of all people surveyed having recalled at least one painful episode. The degeneration of both the disc and the facets play an integral role in the overall health of the spine. Fujiwara *et al* (1999) have shown both to be adversely affected by age with disc degeneration in the lumbar spine most commonly occurring before degeneration of the facets.

The typical progression of treatment for chronic and recurring back pain often starts with moderate physical therapy in the early stages. However, persistent pain and/or the prevalence of sensory complications (nerve impingement and/or numbness of extremities) are often indications that a surgical technique is required to mitigate the observed symptoms. The two most common surgical procedures utilized for discogenic pain (from the nerves embedded in the annular wall of the disc) are spinal fusion and spinal disc arthroplasty. Pain associated with the facet joints can sometimes be reduced and/or eliminated with the use of radiofrequency facet nerve ablation or eliminated in the spinal fusion procedure.

## 1.1 Spinal Fusion

Spinal fusion is an effective and common surgical procedure and is sometimes referred to as the 'gold standard' for the treatment of severe spinal disc degeneration. It is most often used in the lumbar spine for the treatment of low back pain related to degenerative disc disease but it is also widely used in the cervical spine for similar reasons. The procedure usually involves the removal of the intervertebral disc followed by the fusion of the adjacent vertebrae into a single unit. Fusion is accomplished by placing a bone graft, a fusion cage implant, or a combination of both in the intervertebral disc space to restore the original disc height. An anterior rigid plate or a set of posterior rods are also affixed to the vertebral body to provide temporary fixation immediately after the operation to prevent motion while the bone graft and/or fusion cage assimilates with the vertebral bone (Figure 1-2).

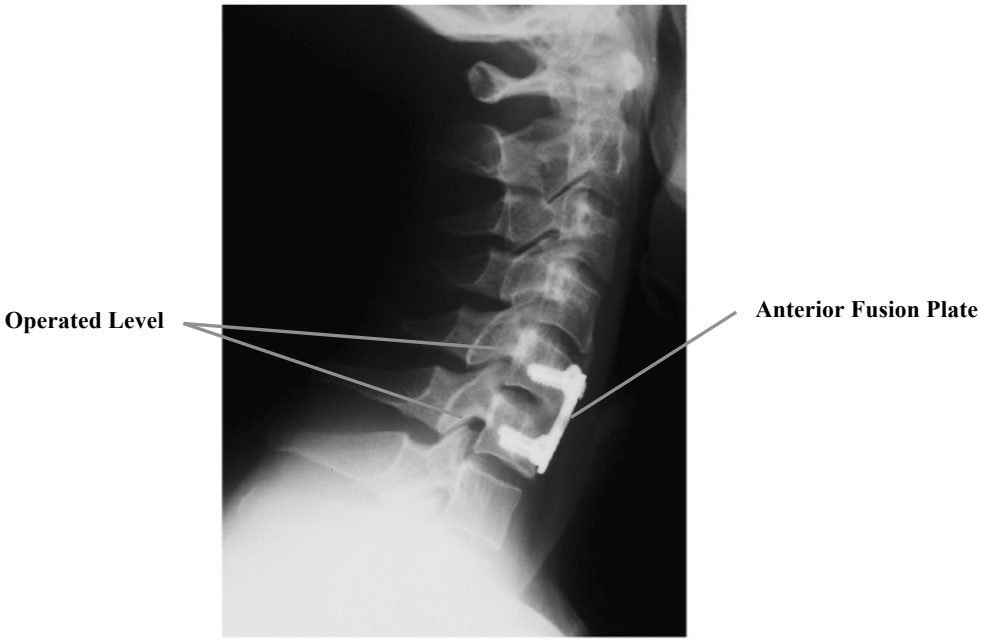


(Adapted from Kasimatis *et al*, 2009)

**Figure 1-2: Postoperative imaging following an anterior C5-C6 spinal fusion**

The fusion mitigates the resulting pain and/or nerve impingement by significantly reducing intervertebral motion. However, due to the loss of motion caused by the removal of the disc, the stress increases at the adjacent discs in order to provide the same overall range of motion in the spine; Matsumoto *et al* (2009) have found that this can lead to accelerated degeneration of adjacent spinal segments. Also, finite element studies of the lumbar spine after fusion show that at the adjacent levels there is increased intradiscal pressures, range of motion, annulus stress and facet joint pressures (Chen *et al*, 2009).

Although the use of anterior cervical fusion has been increasing at a significant rate in recent years and the procedure-related complication rates hover at relatively low values in the range of 3-5% (Marawar *i*, 2010), the risk of accelerated adjacent level degeneration post operatively may pose significant risks to the long-term application of this procedure.

## 1.2 Spinal Disc Arthroplasty

Spinal disc arthroplasty is a procedure which allows for the replacement of the natural disc with an articulating implant that attempts to re-establish the natural range of motion and kinematics of the spine (Figure 1-3).

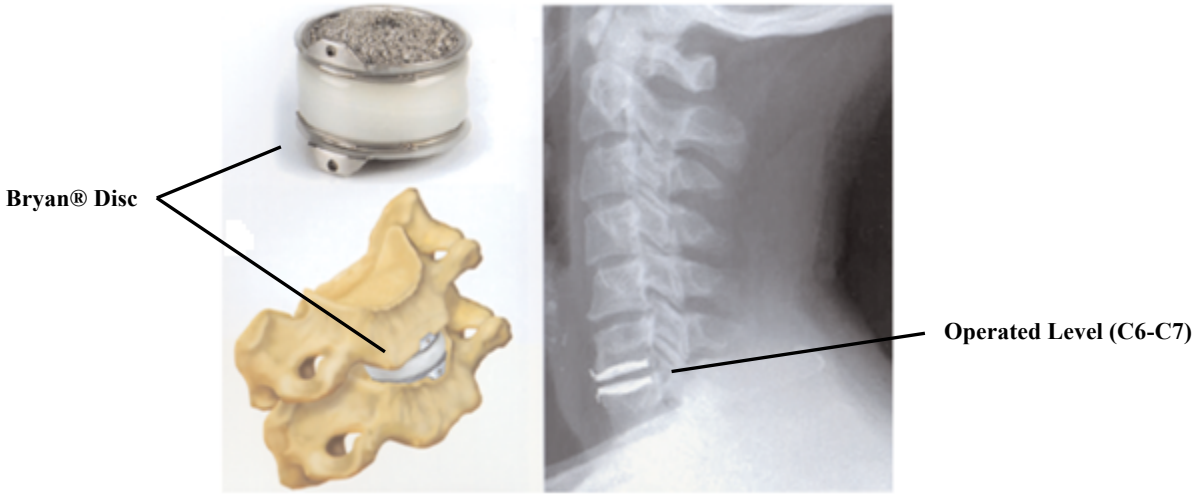


(Adapted from Le & Kim, 2004)

**Figure 1-3: The Bryan(R) Disc from Medtronic Spine & Biologics**

Spinal disc arthroplasty using commercially available devices is most mature in the lumbar region where initial designs were developed in the early 1970s which include the AcroFlex®, Charite® and Maverick® artificial discs. These lumbar disc replacements have evolved continually and use various metal-metal or metal-polymer material pairings. In the cervical region, artificial discs are reduced in size to accommodate the smaller cervical vertebrae. The cervical disc implants that are approved by the FDA (U.S. Food and Drug Administration) are the Prestige® and the Bryan®, both of which are from Medtronic Spine & Biologics (Memphis, TN), and the ProDisc™-C which is from Synthes Spine (West Chester, PA). The field of cervical disc arthroplasty is relatively young with all three of the above implants receiving FDA approval since 2007 (U.S. FDA, 2009).

Spinal disc arthroplasty alleviates pain and nerve impingement by removing damaged structures such as a herniated disc and also by restoring natural disc height. Some segmental motion is also retained with arthroplasty which is a major difference in comparison to fusion which eliminates virtually all intervertebral motion. Although cervical disc arthroplasty retains some motion at the operated level and produces close to natural intradiscal pressures at the adjacent segments (above and below the operated level), Chang *et al* (2007a) have found significant increases in the facet contact pressure at the operated level. This may lead to accelerated facet joint degeneration at the level of implantation. This could be a result of the implant causing a change in the natural centre of rotation of the vertebrae, requiring the facet joints to sustain higher loads as they constrain segmental motion. This constraint of motion must occur to protect the posteriorly located spinal cord and prevent hyperextension, shearing or impingement of the vital neurologic elements. Thus, degeneration of the facet joints after disc arthroplasty may result in spinal instability and thus the need for spinal fusion thereby eliminating the

motion retention of the original disc implant and potentially causing adjacent level degeneration. However, in the cervical spine, there is little clinical data regarding the long-term performance of disc arthroplasty because the first round of long term patient data is just now being collected.

## 1.3 Facet Joint Treatments

Occasionally, just the facet joints degeneration the cervical spine. While this can be treated by spinal fusion, less drastic treatments are often tried.

### 1.3.1 Facet Nerve Removal

If the cause of pain can be isolated to the facet joints and there is no immediate impingement on nerves to the arms and upper body, the small nerves to the facet joints can be ablated (or killed) to stop the pain. This procedure can be done in a minimally invasive manner using radiofrequency facet rhizotomy and can also be performed in the lumbar spine in a similar manner (Figure 1-4). Alternatively, endoscopic laser removal of the nerve branches can be done under direct vision. The intent of the procedure is to halt the transmission of pain sensory information along the nerve which innervates the damaged facet joint. Damage is accomplished by heating the local area or by severing the nerve using a laser.

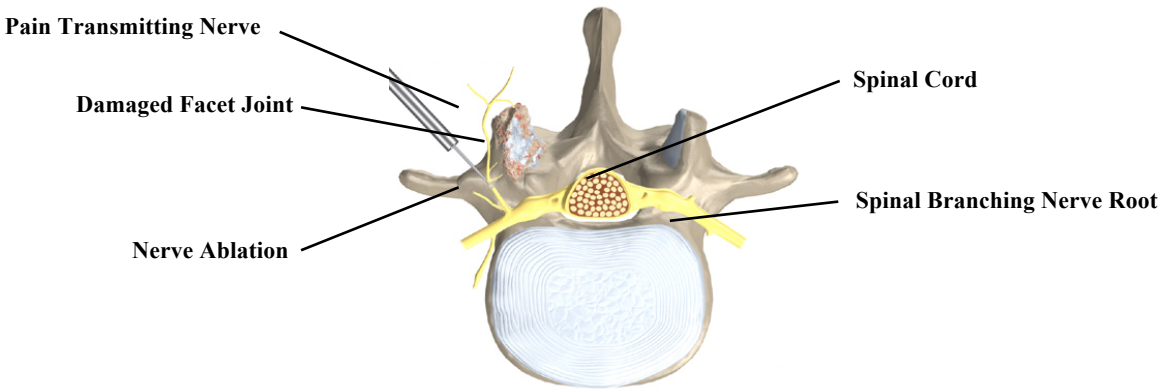


(Adapted from www.eorthopod.com)

**Figure 1-4: Lumbar facet rhizotomy**

The efficacy of this procedure has been disputed because it is unlikely to be a permanent solution with some studies reporting a mean effective length of 10.5 months but then some 85% of patients have successful subsequent treatments (Cohen, 2007; Ozgur, 2009). However, although the pain associated with the facet joints will be mitigated, the continued degeneration and structural collapse of the facet joints is likely to cause disc degeneration and thus eventually fusion may be required.

### 1.3.3 Facet Removal

If the facet degeneration includes arthritic bony ridging causing compression of the spinal cord and/or nerve roots then a facetectomy can be performed to decompress the associated neurological components. Dillon *et al* (1986) estimated that 51% of the adult population that will experience neck and arm pain due to cervical spondylosis at some point, and Scoville (1961) has observed that as this population ages, this pain is commonly accompanied by bony arthritic ridging.

In order to accomplish the decompression of the nerve root, the medial half to two-thirds of the facet is removed using a cutting burr under constant irrigation to prevent heat damage to the underlying structures (Figure 1-1). This medial section is removed because it includes the arthritic bony ridges.

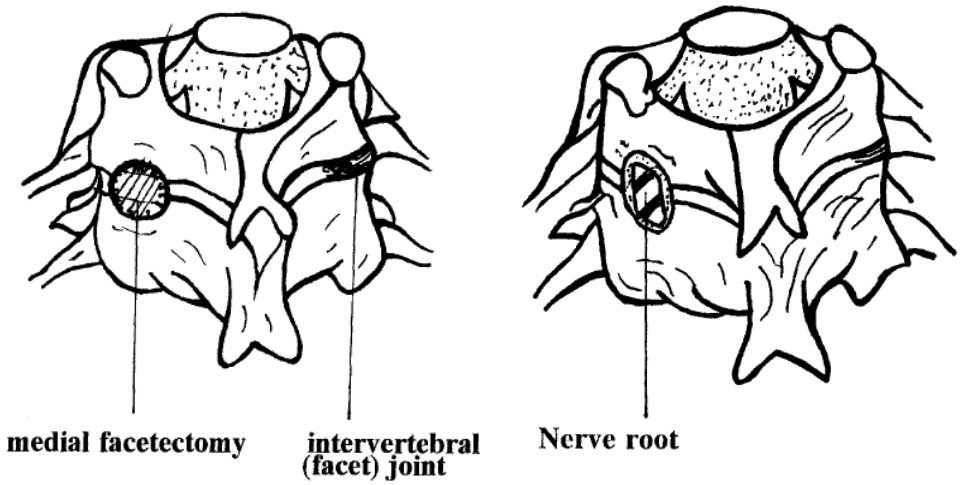


(Adapted from Tan, 1999)

**Figure 1-5: Location of keyhole medial facetectomy (left) to expose and decompress the nerve root (right)**

Tan (1999) reported that in a study of 71 facetectomy patients 76% of patients had a good outcome, 15.5% a moderate improvement and the remaining 8.4% showed a poor result. Raynor *et al* (1985) performed a study on the effects of facetectomy on spinal strength and stability and noted that removal of more than 50% of the facet would result in a significant increase in the chance of fracture of the bony support structures under normal physiological activities. Thus, although this procedure is relatively effective in the short term, the partial removal of the articulating surface of an already damaged facet joint may affect spinal stability in the more severe cases. Also, the reduced articulating area could also result in increase contact pressures and accelerated degeneration of the spinal disc possibly requiring future fusion.

## 1.4 Problem Specification

The use of fusion for facet degeneration can eventually lead to adjacent level degradation. Disc arthroplasty is typically not performed if the facets exhibit degeneration as the implanted prosthesis commonly causes increased contact forces in the facet joints. These increased forces can apparently be caused by both the

constraints and the lack of constraints of the typical ball-and-socket or ball-and-trough artificial disc design (Chen *et al*, 2009). The incidence of contraindication to total spinal arthroplasty due to facet joint degeneration has been reported by Wong *et al* (2007) to be 97% in the lumbar spine. Therefore, at the present time, a patient exhibiting both disc and facet degeneration is limited to the spinal fusion procedure and is typically not a candidate for any disc arthroplasty procedures. It is significant that patients presenting with severe facet degeneration are not considered for disc arthroplasty and are often treated with fusion (Chang *et al*, 2007a). Even if disc degeneration is accompanied by relatively mild facet degeneration, patients are often denied disc arthroplasty because the previously-mentioned increase in facet contact forces is believed to accelerate facet degeneration. Thus, facet joint degeneration limits the use of disc arthroplasty in the cervical spine.

To address the problems with facet degeneration in the lumbar spine, there are a small number of proposed designs for total facet joint replacement and some discussion of an integrated disc and facet joint replacement solution (Voronov *et al*, 2009). However peer-reviewed literature on this topic is limited. All of these designs are currently affixed on the posterior side of the vertebral body and replace the removed facet and pedicle structures and there has been little discussion of an integrated disc and facet joint replacement solution. Both Zigler (2005) and Kim et al (2006) state that in the lumbar spine there is a need to develop a set of implants to better treat patients exhibiting disc and/or facet degeneration. This need also exists for the cervical spine but there are distinct differences in the loading, motion and geometry of the cervical compared with the lumbar spine that must be addressed.

## 1.5 Objectives

Based on the current state of technologies used to accommodate spinal degneration, there currently exists the need to develop an implant or set of implants to better treat patients exhibiting spinal disc and/or facet joint degeneration in the lumbar spine as agreed by Zigler (2005). This need can also be extended to the cervical spine, an area of the spine where historically, spinal implant technology is adapted after proving efficacy in the lumbar spine. If the facet joints are in good shape but the disc is degenerated, a disc arthroplasty device designed to maintain the same share of the loading as the natural disc is needed and may discourage facet degeneration. The present work seeks to achieve all this with a set of implants that can be used in a modular fashion. While this need exists in both the lumbar and cervical spine, it is more acute in the cervical spine and the present work addresses only the cervical spine treatment. This will also expedite the application of this technology to the cervical spine rather than following the typical primary application to the lumbar spine followed by future adaptation to the cervical spine.

Three clinical situations are envisioned in which a cervical total level arthroplasty system (CTLAS) could be partially or fully applied. If the facet joints are healthy but the disc is degenerated, a disc arthroplasty device designed to maintain the same share of loading as the natural disc is needed that will discourage facet degeneration. If both disc and facet joints have degenerated, the fully integrated CTLAS is needed. If only the facet joints are degenerated, which occasionally occurs, just the facet replacement component is needed.

Such a CTLAS design will be far in advance of clinical practice and, as such, should only serve as a template for future development. Since long term new directions are being considered, a novel material selection can also be contemplated. Several fusion devices used in the cervical spine incorporate non-metallic materials including cages, plates and rods (Kurtz and Devine, 2007). However, all cervical disc arthroplasty devices approved by the American Food and Drug Administration (FDA) have some metallic components. These metals distort and mask medical imaging to some extent. This results in a reduction in the precision of post-operative monitoring which is important because of the proximity of the cervical disc to the spinal cord. Thus, there is some incentive to use a suitable non-metallic material in a CTLAS design.

It is the first objective of the present thesis to investigate the aforementioned design problem. Many aspects of the proposed CTLAS design merit research attention. These include fixation, fatigue, surgical procedures and instrumentation, manufacturing procedures and cost, component sterilization and tribology. Wear is a particularly important aspect of the tribology because wear particles can cause an adverse tissue reaction that results in a destruction (or lysis) of the bone supporting the implant (Amstutz *et al*, 1992; Harris, 1995). Furthermore, a novel and unconventional bearing has been suggested using non-metallic materials which, depending on the lubrication, can have high friction when they articulate, and consequently they can develop high surface temperatures and significant surface damage. So, many aspects of the tribology are likely to be important in the CTLAS design. Thus, the second objective of the present thesis is to investigate the tribology of the chosen pairing of non-metallic materials.

## 1.6 Thesis Organization

A literature review is presented in Chapters 2-5 that includes a description of the anatomy and physiology of the spine, the in-vivo motion and loading of the spine, degenerative disorders of the spinal structures and the medical treatment currently available for degeneration. The design process used to develop the CTLAS and the resulting proposed design is outlined in Chapter 6. The experimental procedures, methods, and results of the PEEK-on-PEEK pin-on-plate wear testing are presented in Chapter 7. Finally, Chapter 8 summarizes the key findings of the current study and proposes direction for future work.

# Chapter 2

# Anatomy and Physiology

In seeking to develop an implant or system of implants to replace one or more components of the spine, a detailed understanding of this complex structure of the human body is required. This includes the study of both anatomy; the shape and size of each component, as well as physiology; the purpose and use of each component. Several biological structures including the intervertebral disc, vertebrae, facet joints, as well as the attached ligaments and spinal musculature provide different degrees of mobility, motion constraints that when combined produce the unique motion and stiffness of the spine.

The standard human anatomical planes are used throughout the literature as seen in Figure 2-1. These descriptions represent theoretical planes that can be used to section the body at any point and include the coronal (or frontal) plane, the sagittal plane and the transverse plane.

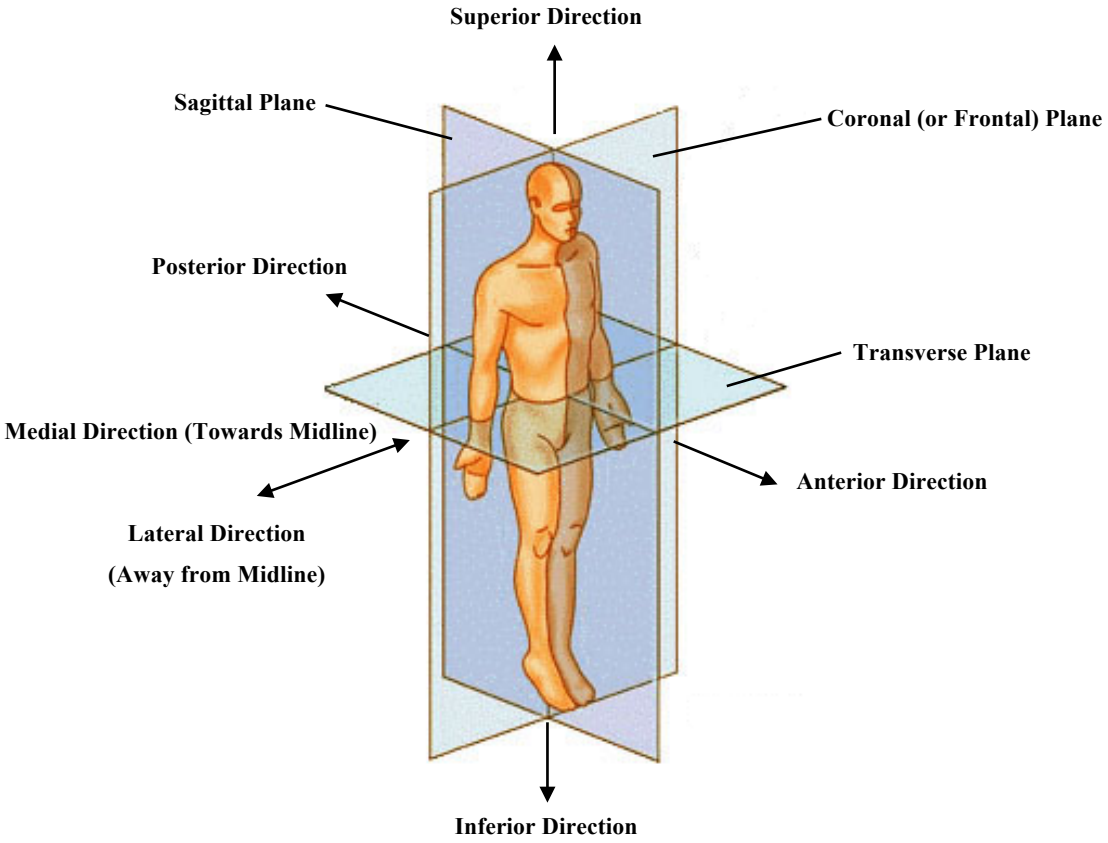


(Adapted from www.wikipedia.com)

**Figure 2-1: Standard Human Anatomical Plane and Direction Descriptors**

The standard anatomical directions include the superior direction which is upwards towards the top of the head, the inferior direction which is downwards away from the head, the anterior direction which is frontward facing, the posterior direction which is rearward facing, the lateral direction which lies along the coronal plane

and is away from the midline of the body and finally the medial direction which directs towards the midline of the body.

The motion of the spine is also classified using standard anatomical terms (Figure 2-2). These include extension which is rearward motion of the spine, front ward motion of the spine is classified as flexion, lateral bending is motion of the spine in the coronal plane, axial rotation is rotation about the intersection of the coronal and sagittal plane and finally traction is axial motion in the vertical direction.

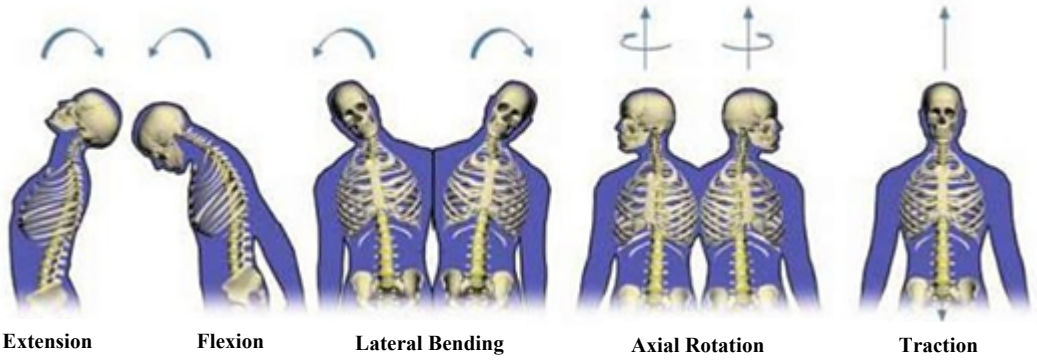


(Adapted from Kurtz and Edidin, 2006)

**Figure 2-2: Standard Spinal Motion Descriptors**

The motion that is provided by the spine *in vivo* is usually a combination of two or more of the above individual motions. In the cervical spine the lateral bending and axial rotation are inherently coupled due to the orientation of the posterior elements; therefore any lateral bending in the cervical spine is accompanied by axial rotation and vice versa.

## 2.1 Vertebrae of the Spine

The vertebral column (Figure 2-3) is a mobile structure that provides flexible columnar support for the upper human body that is comprised of a series of bones known as the vertebrae. The spine is subdivided into three main sections: moving in the inferior direction from the head there is the cervical spine, the thoracic spine and finally the lumbar spine. The sacral and coccygeal regions of the spine are located at the inferior end of the spinal column and consist of false (or fixed) vertebrae because during the transition to adulthood the sacrum and coccyx are formed via the fusion of nine lowest vertebral bodies. These regions therefore do not provided articulation in adulthood as the other three main regions of the spine.

There are a total of 33 vertebrae in the entire spinal column: there exist seven in the cervical region, twelve in the thoracic, five in the lumbar, as well as five in the sacral and four in the coccygeal (which constitute the 9 vertebrae which fuse in adulthood). The number of vertebrae in each region is sometimes increased or diminished in a particular region due to a deformation during development; however, the number of cervical vertebrae is very rarely modified. After the fusion of the lower 9 vertebrae to form the sacrum and coccyx, the total number of remaining articulating vertebrae is 24.

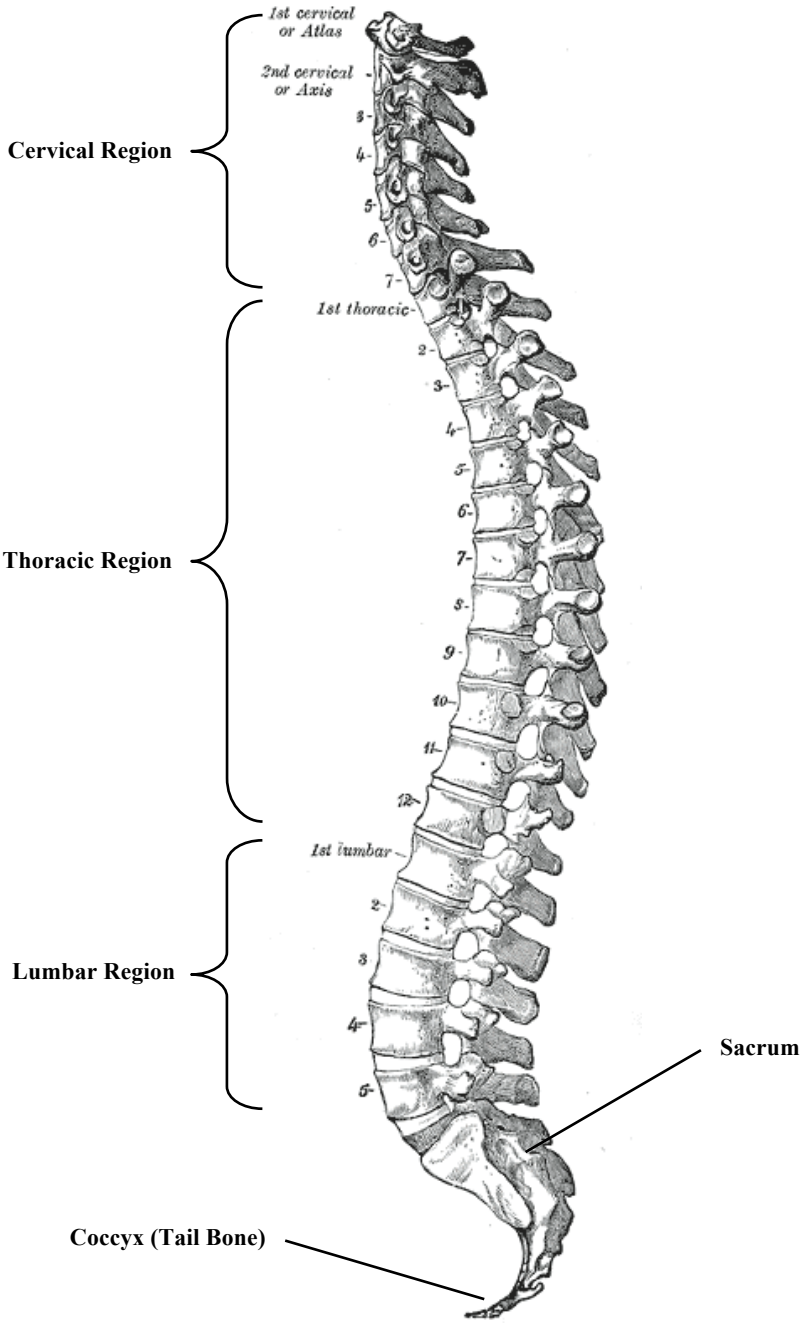


(Adapted from Gray, 1918)

**Figure 2-3: Lateral view of the vertebral column**

### 2.1.1 Anatomy of the Vertebrae

The typical vertebra consists of two main components; the anterior segment which includes the body, and the posterior segment which includes the vertebral arch (Figure 2-4). The vertebral arch encloses the vertebral

foramen and consists of a set of pedicles and laminae, and supports seven processes; four of which are articular (facet joints), two transverse and one spinous.

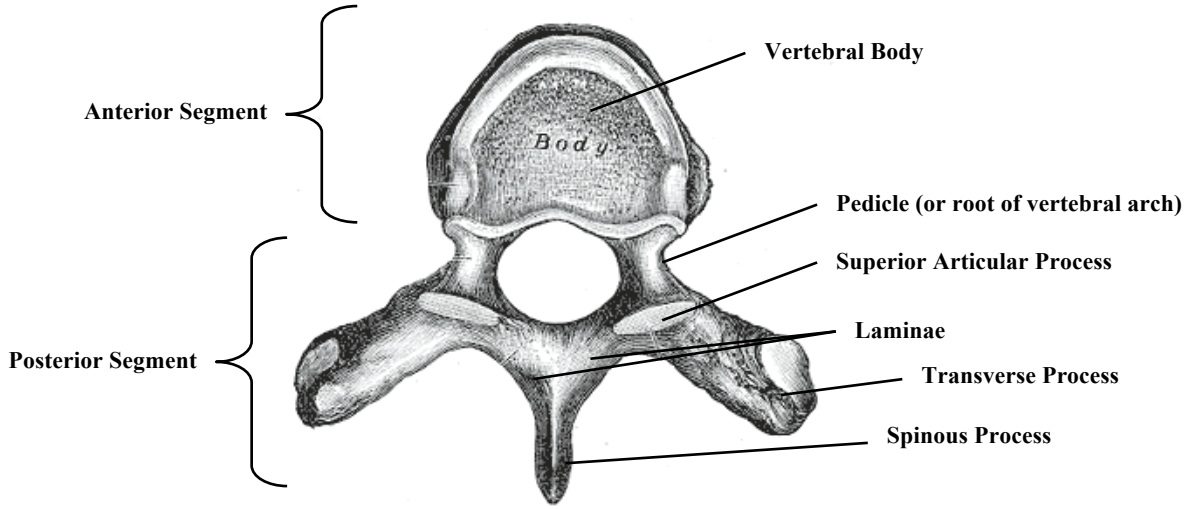


(Adapted from Gray, 1918)

**Figure 2-4: Typical vertebra as viewed from above**

The vertebral body is the main component and is elliptically cylindrical in shape. It is the point of attachment for the intervertebral fibrocartilages and each presents a rim around its circumference. The upper and lower surfaces are the mating surface to which the vertebral bodies interact with the intervertebral discs, the contact surfaces of which are flattened and rough. On the anterior aspect the body is convex from side to side and concave from the superior. The posterior aspect is flat from the superior and slightly concave from side to side. There are several apertures for the passage of nutrient vessels as well as for the exit of vertebral veins from the body of the vertebra.

The pedicles are directed in the posterior direction and provide the point of attachment of the posterior segment of the vertebra to the body. The point of connection is at the junction of the posterior and lateral superior surfaces of the vertebral body. The pedicles are visibly notched between the body and the laminae which form concavities termed the intervertebral foramina through which the spinal branching nerves pass. The laminae form the posterior boundary of the foramen and are the attachment point of the ligament flava. The spinous process projects in the posterior direction slightly downward and serves as the attachment point for several muscles and ligaments. The transverse processes are located on both sides of the vertebra at the point where the laminae meet the pedicle and are also the point of attachment for muscles and ligaments.

The articular processes consist of two superior and two inferior components which form the facet joints of the spinal segment. The orientations of the articular surfaces are different in each region of the spine and are coated with hyaline cartilage.

The osseous structure of the vertebra consists of a distribution of both cancellous and cortical bone as seen in Figure 2-5. The body is comprised mainly of cancellous tissue covered by a thin layer of cortical bone which is

perforated by a number of passageways to allow for the passage of vessels. The posterior part of the body is the point of convergence of the one or two large vein canals. The structure of the cancellous lamellae in the body is markedly vertical and perpendicular to the superior and inferior surface to accommodate the compressive loadings and pressure experienced on these locations. The vertebral arch and various processed share the same general composition however the thickness of the cortical bone covering the cancellous bone in these regions is thicker to accommodate the higher loadings and smaller cross sectional areas of these components.

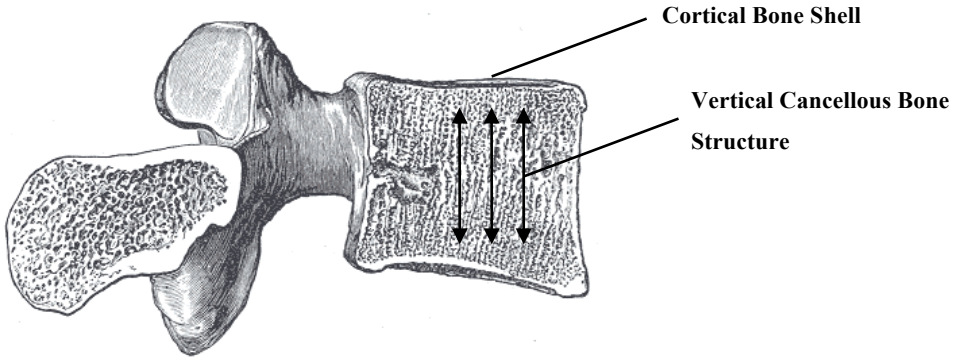


(Adapted from Gray, 1918)

**Figure 2-5: Sagittal vertebral section with view of osseous composition**

The large amount of cancellous tissue located between the two endplates of the vertebral body can be likened to the anatomy of other articulations in the human body where the presence of the sponge like bone is thought to provide some shock absorption under loading. In the case of the spine the disc accommodates much of the shock absorption; however it is clear that the vertebral body is also capable of this to some extent.

The cervical vertebrae are visibly the smallest of the articulating vertebrae and include the presence of an added passageway in each transverse process. The vertebrae of the cervical spine also observe the largest chance in geometry from the superior to the inferior level than either of the other two regions of the spine. For this reason the cervical spine is further subdivided into three regions known as the upper (C1-C2), the middle (C3-C5) and the lower (C6-T1) cervical spine (Figure 2-6).

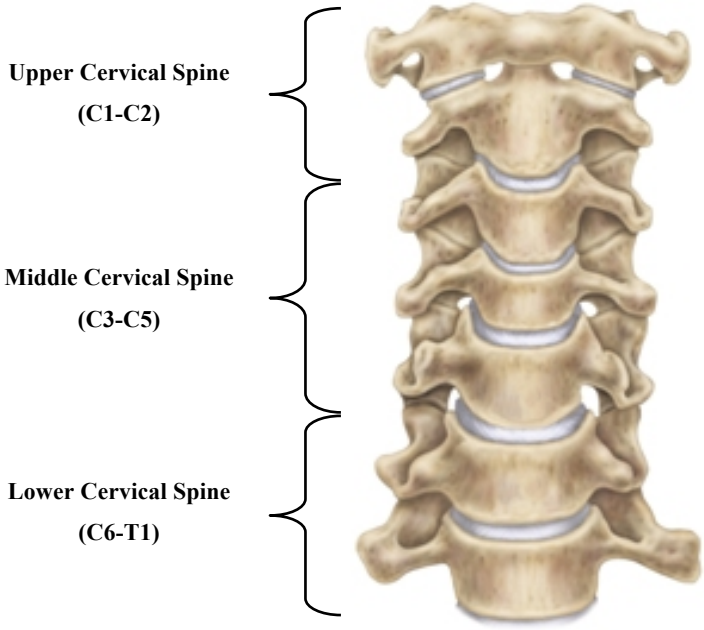


(Adapted from www.prestigedisc.com)

**Figure 2-6: Regions of the cervical spine**

The body of the vertebrae in the cervical spine (Figure 2-7 and Figure 2-8) is notably smaller and wider in the lateral direction than in the anterior-posterior direction. The superior endplate is concave transversely with projecting lips on either side which are known as the uncovertebral joints. The inferior surface is concave from before backward, convex from side to side and has laterally shallow concavities which receive the projecting uncovertebral joints of the adjacent inferior vertebral body.

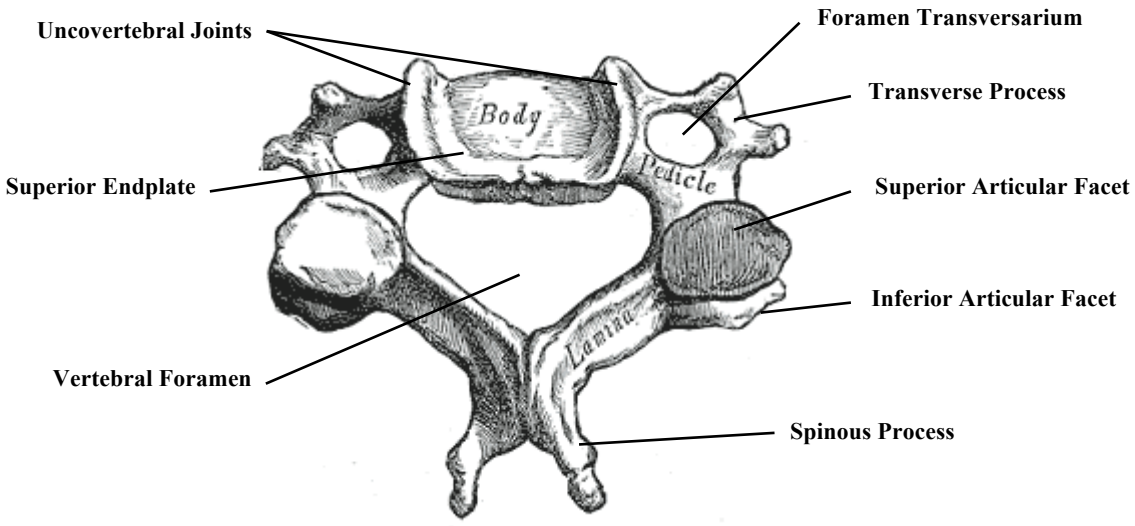


(Adapted from Gray, 1918)

**Figure 2-7: Superior view of typical cervical vertebra**

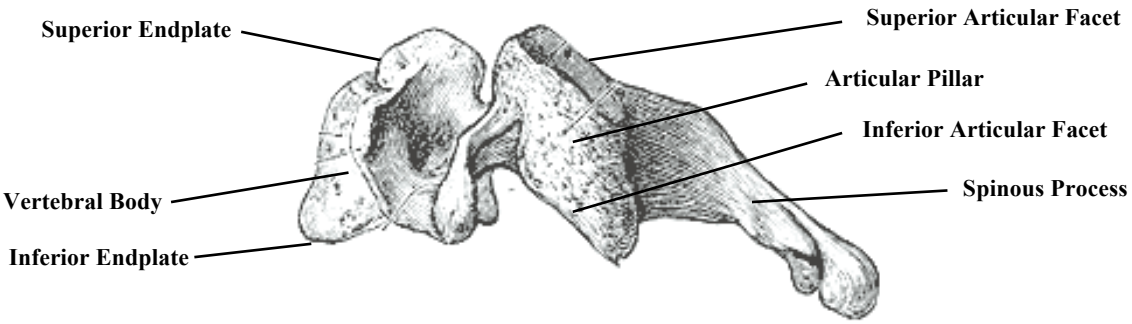


(Adapted from Gray, 1918)

**Figure 2-8: Side view of a typical cervical vertebra**

The pedicles are projected lateral and to the posterior and are attached to the vertebral body at the midpoint between the superior and inferior endplate surfaces such that both the inferior and superior pedicles form the vertebral notch through which the spinal branching nerves pass. A elliptical cylindrical articular pillar is formed between the superior and inferior articular facets which themselves are flat and oval in shape. The upper six vertebrae include the foramen Transversarium which gives passage to the vertebral artery, vein and a plexus of sympathetic nerves. The vertebral foramen formed by the laminae is large and triangular in shape.

The first cervical vertebra (Figure 2-9) has no distinct vertebral body and no spinous process and the vertebra itself is ring-like in form. The anterior arch forms about one fifth of the ring, the anterior surface of which is convex and on it is the anterior tubercle which acts as a muscle attachment point. The posterior arch forms about two fifths of the ring and presents the posterior tubercle which is another muscle attachment point.

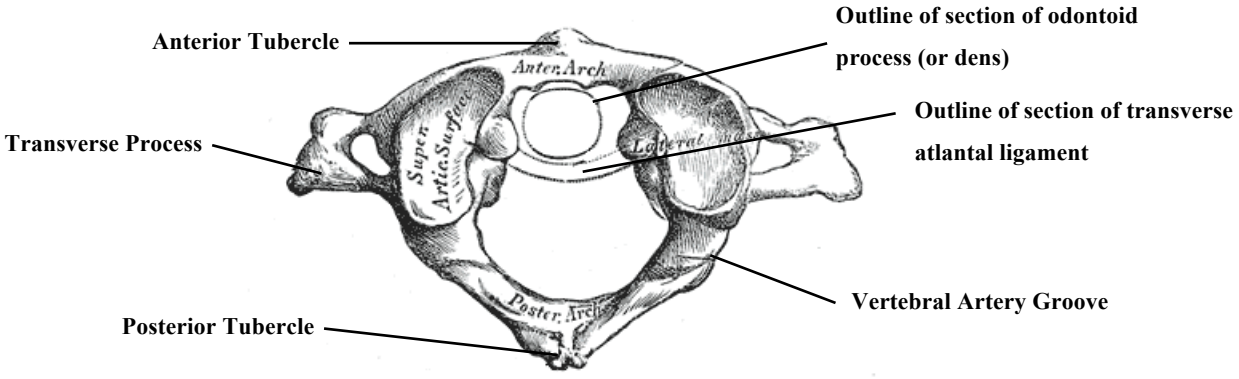


(Adapted from Gray, 1918)

**Figure 2-9: First cervical vertebra (atlas)**

The superior articular facets are large, oval in shape, condylar concave structures that form a cup for the corresponding condyle of the occipital bone. They are notably adapted to the nodding motion of the head. The inferior articular facets are flattened but slightly convex and circular in form and articulate with the axis to permit

rotation of the head. Just below the medial division of each superior facet is a small tubercle to allow for ligament attachment. The transverse processes act as the attachment point for several muscles that assist in rotation of the head.

The second cervical vertebra is termed the axis and forms the pivot upon which the first vertebra rotates about. The dens process protrudes perpendicularly from the upper surface of the body and interacts with the atlas. The vertebral foramen is markedly smaller on the axis than the atlas, which accommodates the fact that the atlas pivots about the axis and thus the spinal cord requires more motion in the superior component.

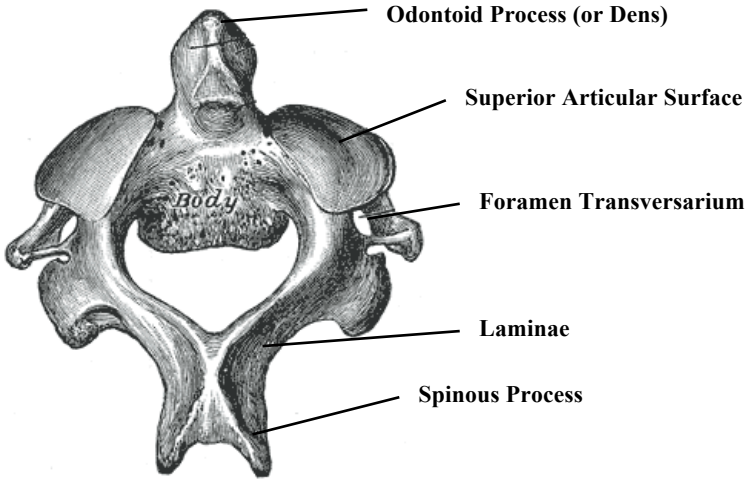


(Adapted from Gray, 1918)

**Figure 2-10: Second cervical vertebra (axis)**

The seventh cervical vertebra (Figure 2-11) of the lower cervical spine exhibit significant differences from the upper cervical spine including the presence of a large posterior spinous process (or vertebra prominens) which is nearly horizontal. At the end of the process is a tubercle to which the ligamentum nuchae is attached. Sometimes the vertebral vein passes through both foramen transversarium but in their absences (which commonly occurs) both the artery and vein pass in front of the transverse process.

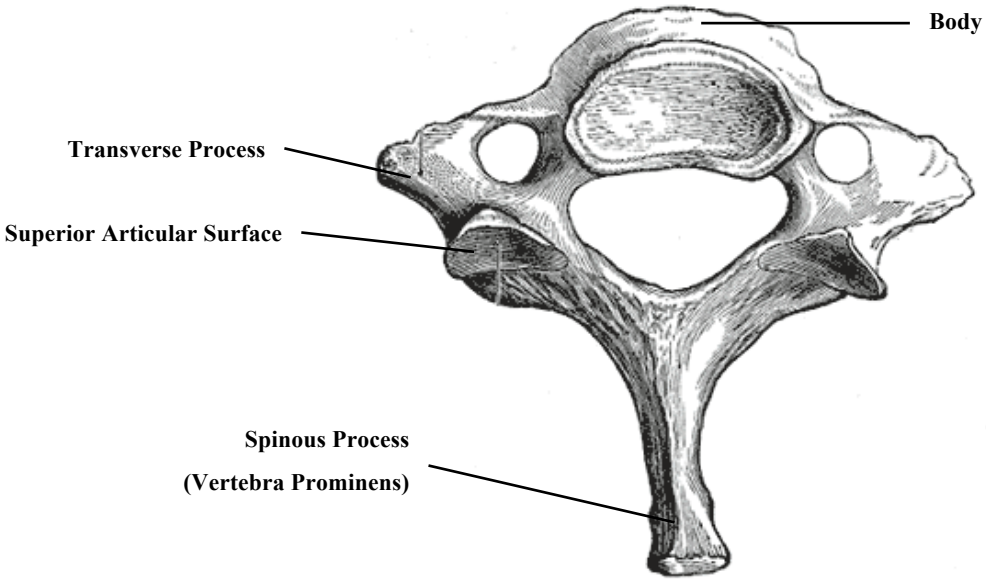


(Adapted from Gray, 1918)

**Figure 2-11: Seventh cervical vertebra**

The thoracic vertebrae (Figure 2-12) are larger than those in the cervical region and continually increase in size moving in the inferior direction. There are also facets on the sides of the vertebral bodies for articulation with the heads of the ribs in addition to the facets on the transverse processes.

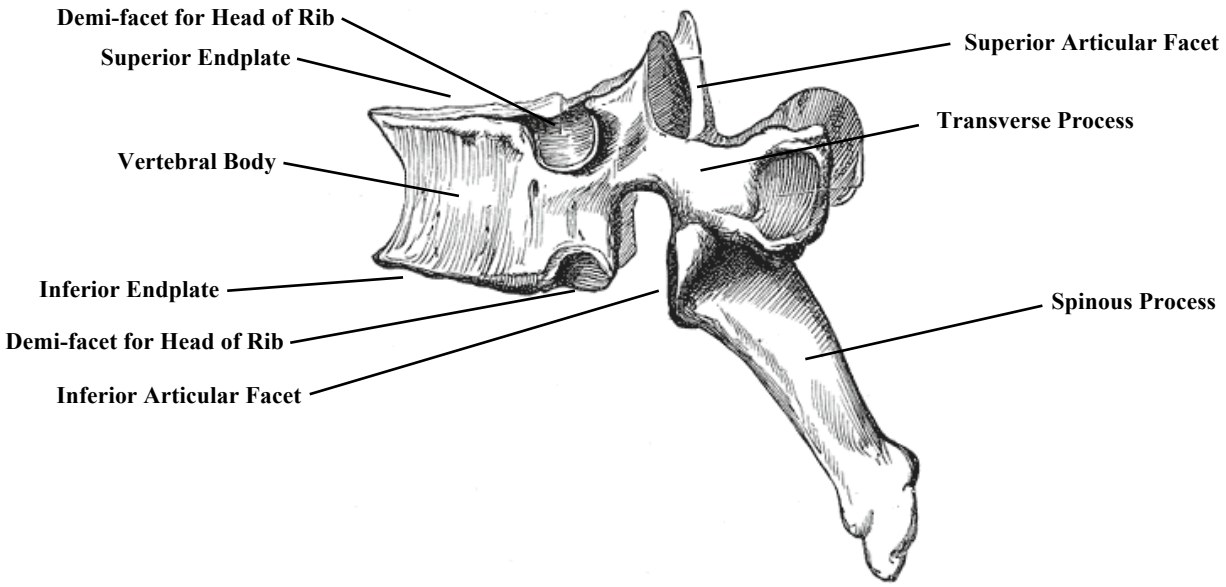


(Adapted from Gray, 1918)

**Figure 2-12: Side view of a typical thoracic vertebra**

The vertebral bodies in the thoracic region of the spine are heart-shaped and blend the transition in shape from the slender ovular cervical vertebrae to the more circular shape found in the lumbar spine. The endplates are

convex from side to side in front and deeply concave behind and slightly constricted laterally and in front. Two cartilaginous facets are present above and below the root of the pedicle on each side to form oval surfaces that articulate with the heads of ribs. The pedicles exhibit vertebral notches that are larger than any others in the spine and are bridged by overlapping laminae. The vertebral foramen is small and circular in shape which is a result of the lower range of motion provided by this region of the spine and therefore less of a need for spinal cord mobility within the vertebral bodies. The transverse process is oriented to the posterior and points significantly in the inferior direction at the end of which a ligament attachment point. The articular facets are flat and oriented posteriorly with a slight lateral and superior orientation. The presence of demi-facets typically ceases at the ninth or tenth thoracic vertebra.

The lumbar vertebrae (Figure 2-13, Figure 2-14) are the largest components of the articulating spinal column and do not include a foramen in the transverse process or the presence of rib articulating facets. The vertebral bodies are larger in the lateral direction than in the anterior-posterior direction and the endplates are slightly concave above and below with deep constriction in front and at the sides. The posterior of the body is concave. The pedicles protrude in the posterior direction from the superior part of the body. The vertebral foramen is again triangular in shape and is larger than that found in the thoracic spine but smaller than in the cervical region.

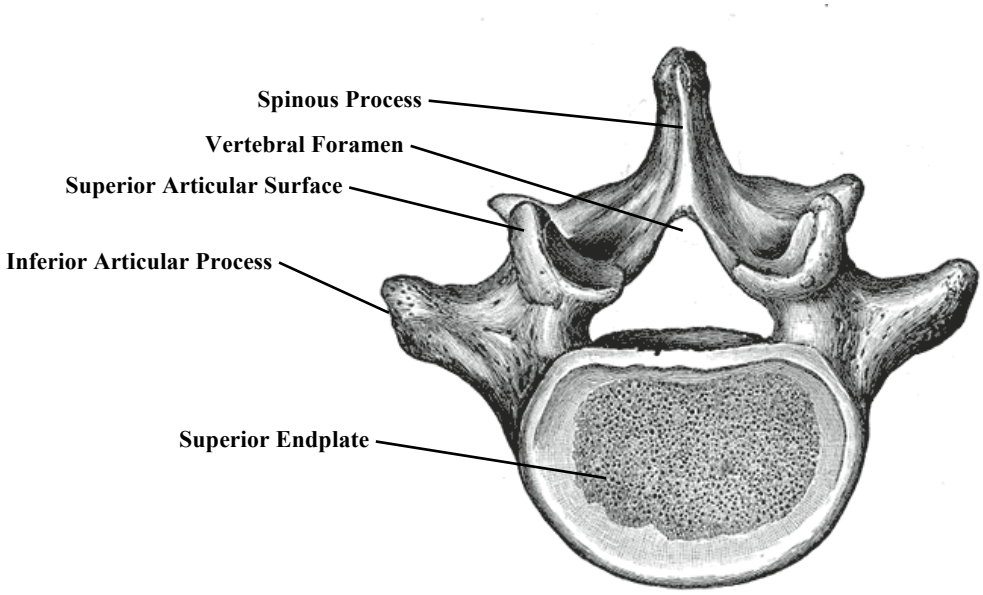


(Adapted from Gray, 1918)

**Figure 2-13: Fifth lumbar vertebra viewed from above**

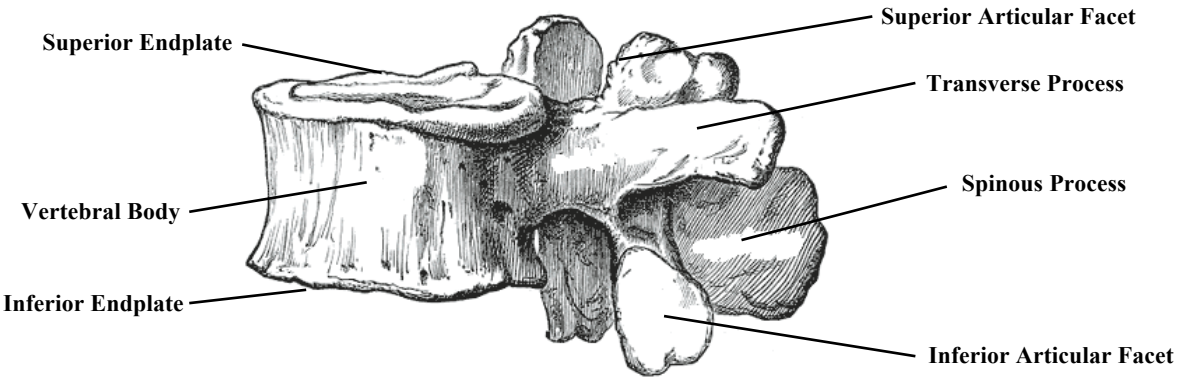


(Adapted from Gray, 1918)

**Figure 2-14: Side view of a typical lumbar vertebra**

Both the superior and inferior articular processes are well defined, projecting upward and downward from the junctions of the pedicles and the laminae. The superior facets are concave and are oriented to the posterior laterally. The inferior articular facets are convex and are oriented laterally to the anterior of the vertebral body. The superior facets are wider than the inferior surfaces.

The sacral and coccygeal vertebrae are comprised of nine individual vertebral segments until they are united in the adult to form two bones; five forms the sacrum and four forms the coccyx (Figure 2-15).

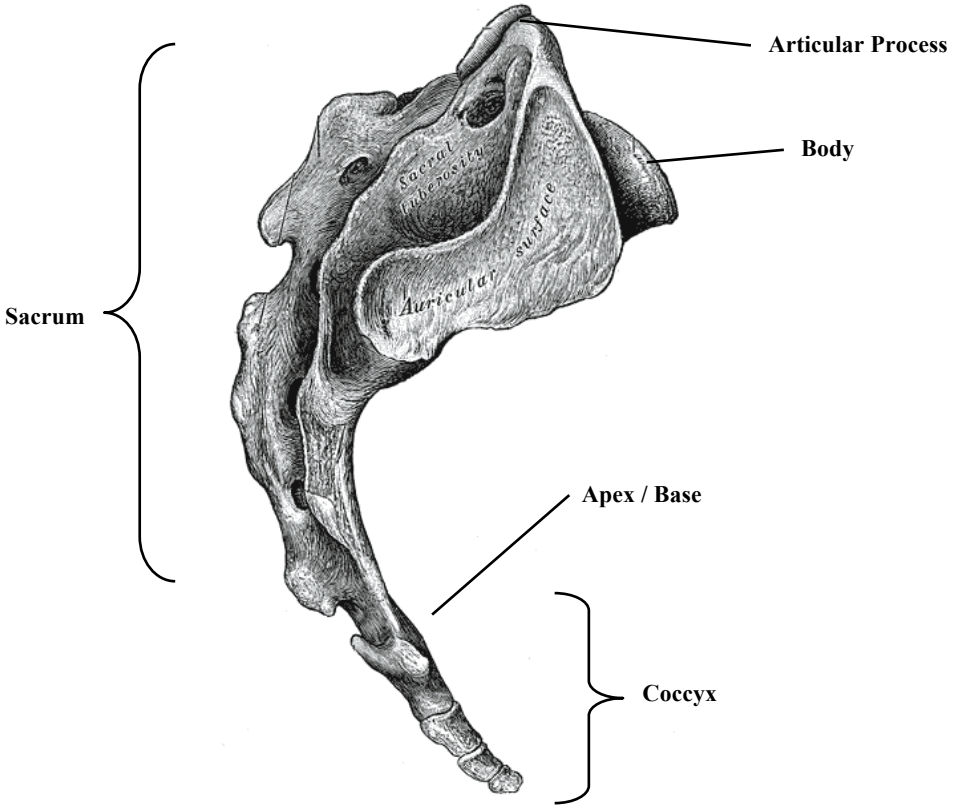


(Adapted from Gray, 1918)

**Figure 2-15: Lateral surfaces of sacrum and coccyx**

The sacrum is a large triangular bone located at the inferior end of the vertebral column near the pelvic cavity where it acts as a wedge between the two hip bones. The base of the sacrum articulates with the last lumbar vertebra and its apex interacts with the coccyx. The coccyx (or tail bone) is usually formed of four basic vertebrae of which are lacking pedicles, laminae and spinous processes. The first is the largest and often exists as a separate piece from the last three that are typically fused together.

### 2.1.2 Vertebral Physiology

The principal biomechanical role of the vertebral body is to support the compressive loads of the spine due both in part to body weight and muscle forces. As a result the size of the vertebral bodies increase moving downward from the cervical to the lumbar spine as the corresponding mass of the body above the spinal segment increases and thus the vertebra is subjected to increased loads.

The bony architecture of the vertebral body is comprised mainly of cancellous bone in the interior covered by a thin shell of dense cortical bone that has an average thickness of only 0.35 – 0.5 mm (Silva *et al*, 1994). The cancellous bone bears the majority of vertical compressive loading while the outer shell forms a reinforcement which in addition can bear some of the applied torsion and shear loads. Surprisingly McBroom *et al* (1985) have shown that removal of the thin layer of cortical bone from the vertebral body results in an overall decrease in vertebral strength of only about 10%. The predominantly vertical orientation of the cancellous structure in the vertebral body also shows the physiologic role of the vertebrae in supporting the vertical loading that acts between the superior and inferior endplate. It is also important to note that while the majority of cancellous structure is aligned with the primary loading direction, there is also the presence of horizontal structures which link together the vertical structures to prevent buckling of the columnar forms. Therefore bone loss associated with either the vertical or horizontal structures is expected to have a significant impact on the load carrying capacity of the vertebrae.

The vertebral endplates form a boundary between the intervertebral disc and the cancellous bone of the vertebra and are comprised of a thin layer of semi-porous subchondral bone having an approximate thickness of 0.5 mm. The main function of the endplates is to prevent the intervertebral disc from extruding into the vertebral body as well as to evenly distribute the load from the disc to the vertebral body. The endplate is porous to allow the passage of water and nutrients but does not allow for large proteoglycan molecules to leave from the disc space. The material properties of the endplates vary by location and combined with the trabecular bone allow for some shock absorption; with the non-rigid system providing up to 0.5 mm of compression under load (Grant *et al*, 2001; Brinckmann *et al*, 1983). Failure of the endplate can occur via pressurization of the intervertebral disc which results in extrusion of the disc material into the vertebral body following fracture. Failure can occur more easily in subjects with reduced bone mineral density (Grant *et al*, 2002) thereby establishing a potential pain source from increased intraosseous pressure (Yoganandan *et al*, 1994).

Vertebral strengths have been measured in-vitro to range from 0.8 – 15.0 kN (Hutton *et al*, 1979; White & Panjabi, 1990). The wide range of results can be attributed to the natural variation in geometry, bone density and architecture. While both vertebral geometry and structure have been shown to be equally important factors in

vertebral strength (Burklein *et al*, 2001), a strong correlation between volumetric bone density and strength has been observed (Crawford, Cann & Keavney, 2003) The strength of vertebrae increase caudally, which can be attributed to the increase in size since the bone density is fairly constant between the individual vertebral levels.

## 2.2 Facet Joints of the Spine

The posterior elements of the spine are responsible for guiding the motion of adjacent spinal segments as well as limiting the extent of torsion and anterior-posterior shear developed during motion and spinal loading. In addition, they are also an important attachment point for many spinal ligaments and muscles.

The facet joints are responsible, to varying extents, for limiting inter-segmental motion. The orientation of the facet joints determines their effect on spinal kinematics. Since the orientation and geometry of the facets varies in each spinal region, their role and influence on overall spinal motion is unique in cervical, thoracic and lumbar spine.

### 2.2.1 Anatomy of the Facet Joints

The facet joints are the only synovial joints of the spine. The mobility of a cartilaginous joint such as the disc is relatively restrictive compared with a synovial joint which employs compliant surface layers of articular cartilage (on trabecular subchondral bone) that slide over each other in the presence of synovial fluid (Figure 2-16). The synovial fluid is held within the articular capsule, a sac-like structure that ensures synovial fluid is available to be entrained into the contact zone or pulled into the articular cartilage as it recovers from deformation. The articular capsule has a fibrous outer layer and is surrounded by ligaments. However, to maintain mobility the articular capsule only causes a slightly elevated pressure in the synovial fluid, just enough to prevent lubricant starvation.

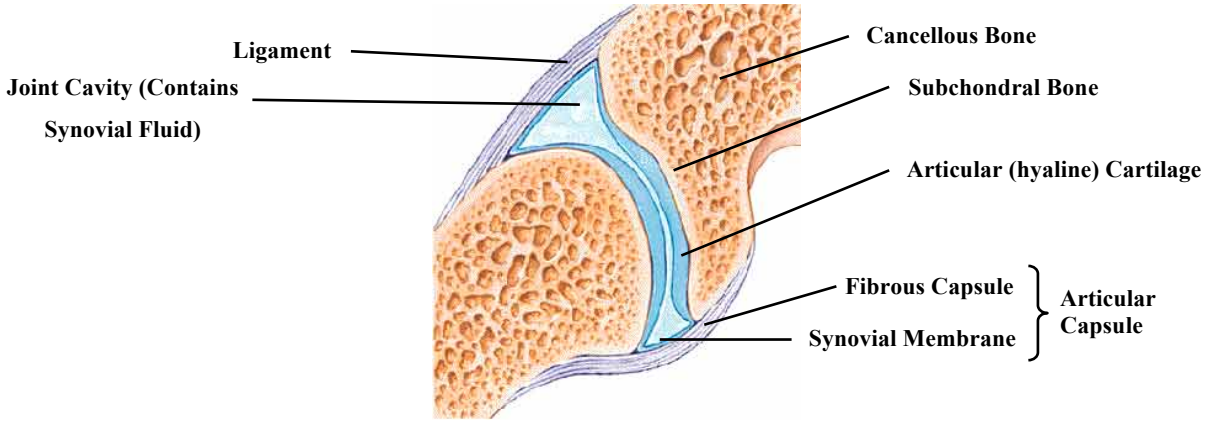


(Adapted from www.umm.edu)

**Figure 2-16: Anatomy of a typical synovial joint**

The facet joints are attached to the vertebral body via the transverse process and undergo a marked change in orientation, shape and location moving from the head down to the sacrum (Panjabi *et al*, 1993; Boos and Aebi, 2008) (Figure 2-17). The facets of the atlas and axis are oriented parallel to the transverse plane.

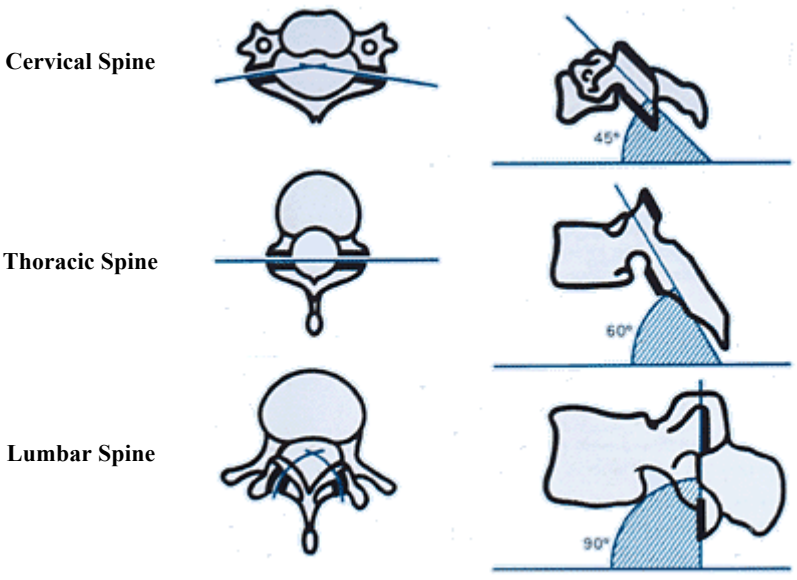


(Adapted from www.maitrise-orthop.com)

**Figure 2-17: Facet joint orientation of different regions of the spine**

In the cervical spine the facets slope in the posterior direction at an angle approximately 45° to the transverse plane and are located along a line somewhere between 0° and 20° to the frontal plane (Figure 2-18).

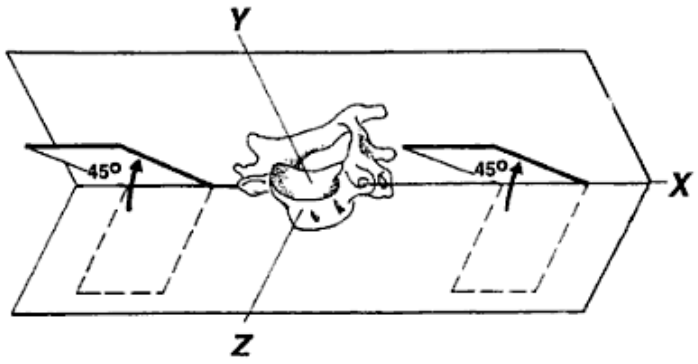


(Reproduced from Clark, 2005)

**Figure 2-18: Orientation of the articular processes of the lower cervical spine in the frontal plane**

The facet joints of the thoracic spine are oriented approximately 60° to the transverse plane and are located along a line that is somewhere between 0° and 20° to the frontal plane in the axial view. The lumbar facets exhibit a vertical posterior slope and are typically located along a line that is approximately 45° to the frontal plane.

White and Panjabi (1990) have proposed that facet asymmetry of approximately 10° between facets is observed in approximately 25% of the population. This tropism can generate rotation towards the oblique facet under compression and shear loading of the spinal segment.

The articular capsules form a bridge between the circumferences of the articular cartilage of the superior and inferior facet and are comprised of the fibrous, ligament-like fibrous capsule and the synovial membrane. While the cartilage can only support compressive loading, the articular capsule can be stretched in tension when separation or shearing motion of the facets occurs. The capsules of the cervical spine exhibit the loosest condition thereby allowing significant separation and shear motion of the adjacent articular surfaces. The capsules of the lumbar spine are not as loose as those in the cervical spine but provide significantly more freedom than the thoracic spine capsules. The laxity of the facet capsules seem to be linked to the degree of motion provided by the associated region of the spine since more motion will require more inter-facet motion.

It is important to note that the facet capsules are important to spinal stability especially in extreme flexion and lateral bending when the capsules oppose hyper extension and separation of the adjacent vertebral bodies.

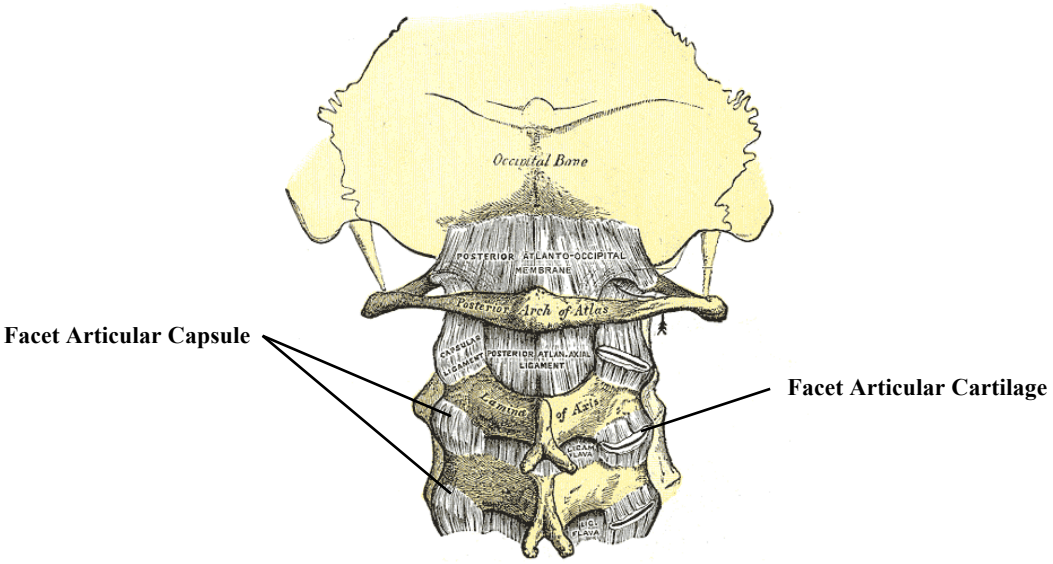


(Adapted from Gray, 1918)

**Figure 2-19: Posterior view of upper cervical spine showing the articular capsules**

The articular cartilage is not innervated and therefore direct contact is not pain generating, the facet capsules are innervated and thus are a potential source of neck and back pain.

### 2.2.2 Facet Joint Physiology

The facets are involved in spinal segment kinematics in several different modes of motion, with their geometry heavily influencing the resulting motion patterns. In all motions of the spine except some ranges of pure flexion and segment shear in the posterior direction that tend "distract" them, the facet joints share the applied loads and torques with the disc and the various spinal ligaments. The facets have been most commonly studied in the lumbar spine, with less data available in the cervical spine and even less data available in the thoracic spine.

In the C1-C2 spinal segment the facets are practically horizontal which results in the accommodation of substantial rotation as well as significant load sharing of applied axial loading. This orientation does not

accommodate rotational constraint by the articular surfaces, which in this case are accomplished by the facet capsules and other spinal ligaments.

In the cervical spine the facets are oriented at approximately 45° to the vertical direction and therefore the facets accommodate flexion, extension and rotation and are capable in providing constraint in extension, shear and rotation. The orientation of the facets also results in significant motion coupling of rotation and lateral bending (Figure 2-20). When the cervical spinal segment is rotated about the axial direction, after the contralateral facets make contact, the superior facet tends to continue to move in the anterior direction (due to the rotation) but also shifts upwards in the superior direction due to the 45° inclination of the facet contact surfaces. This causes coupled lateral bending motion to accompany the applied axial rotation. In the corollary, if the cervical spinal segment is subjected to lateral bending, when the lateral facet joints make contact, the superior facet continues to move downward in the inferior direction but also moves towards the posterior down the slope of the facet contact surfaces thus adding rotation to the initially applied lateral bending.

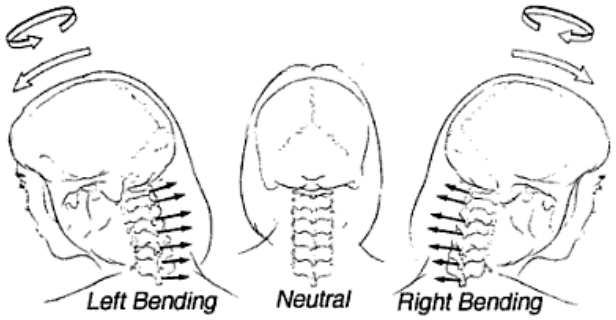


(Reproduced from White and Panjabi, 1990)

**Figure 2-20: Coupled axial rotation and lateral bending of the cervical spine**

In the thoracic spine the facets are oriented more vertically than in the cervical spine making an angle of 60° to the transverse plane which results in the allowance of significant lateral bending and rotation with some flexion and extension. There is some motion coupling in the thoracic spine but it is not as pronounced as in the cervical spine due to the significantly reduced range of motion compared to the cervical spine.

The facets of the lumbar spine have an almost vertical orientation and are approximately parallel to the sagittal plane and thus provide flexion, extension, lateral bending but constrain rotational motion. Since the facets are parallel there is little to no motion coupling in the lumbar spine since rotation and lateral bending cause motion that is either in plane or parallel with the facet contact planes.

In the cervical spine the load sharing of the disc and facets have been studied with the use of finite element methods by Goel *et al* (1998). The application of an axial compressive load resulted in the facets transmitting 12% of the total load equally shared between both left and right structures. Under compression with some applied flexion the facets did not carry any of the applied loading since they were not in contact and were separated due to the flexion motion. Combined compression and extension resulted in the loading of each facet with 51% of the applied compressive load with the disc observing 14% of the axial loading. Compression combined with rotation

resulted in the unloading of the lateral facet and loading of the contralateral facet with 37% of the applied compressive loading with the disc carrying 75% of the loading.

In the lumbar spine load sharing between the disc and facets has been measured directly (el Bohy et al, 1989; Lorenz *et al*, 1983) or with the aid of numerical finite element models (Miller *et al*, 1983; Shirazi-Adl et al, 1986; Yang and King, 1984). In the normal upright standing position approximately 10-20% of the vertical compressive load is carried by the facets of the lumbar spine compared to 30% of the load when in hyperextension. This is because in hyperextension the facets are in direct contact and are responsible for limiting the amount of extension as well as preventing the anterior shear of the superior vertebra of the motion segment. It has also been found that the facet joints resist up to 50% of the anterior shear (up to 2000N of force) developed in forward flexion (Cyron, Hutton & Troup, 1976). During torsional loading due to rotational motion the contralateral facet (the one opposite to the direction of motion) is heavily loaded.

The contact pressures observed in the facet joints is also heavily interdependent with the biomechanics of the intervertebral disc where a 1 mm decrease in disc height has shown to increase the facet contact pressure by 61% (Dunlop, Adams & Hutton, 1984). All of the articulating components of the spinal segment are heavily interdependent where degeneration or damage to one component will typically alter the segmental kinematics thus modifying the motion observed by the other component(s). This may promote accelerated degeneration of all the articulation in the spinal segment.

## 2.3 Intervertebral Discs of the Spine

The soft tissues of the spinal motion segment include the intervertebral discs which separate adjacent vertebrae, the attaching ligaments which control the motion of the spine, and the spinal cord which is protected within the spine and is not designed to support any loading. The discs (Figure 2-21) provide soft tissue support between each of the vertebral bodies of the spine and allow motion in the anterior-posterior, medial-lateral and axial rotation planes. The disc is also responsible for transferring and distributing the loading through the vertebral column and must withstand significant compressive loads from body weight and muscle forces as well as bending and twisting loads over the range of spinal motion.

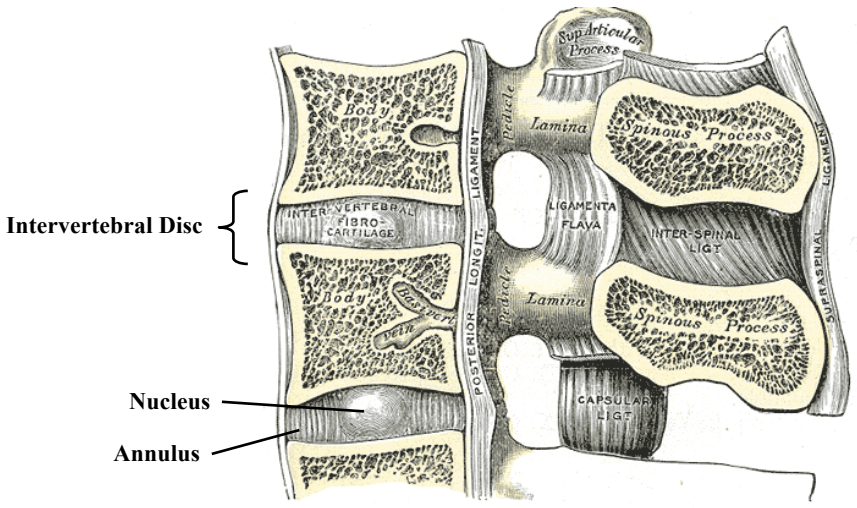


(Adapted from Gray, 1918)

**Figure 2-21: Median sagittal section of two lumbar vertebrae showing the intervertebral disc**

The intervertebral discs in each region of the spine are shaped to accommodate the geometry of the vertebral endplate to which the disc is attached to each vertebral body. The thickness of the discs is also varied at each different level of the spine and is generally linked to the overall size of the disc; larger discs are thicker and vice versa.

### 2.3.1 Anatomy of the Intervertebral Disc

The disc is a fibro-cartilagenous joint and is mostly anneural meaning that there are few nerve endings within its structure. The disc has a low cell density and is the largest avascular structure in the body and is comprised mainly of collagen fibers embedded in a hydrated extra-cellular matrix. There are three main components that make up the heterogeneous structure of the disc; the nucleus pulposus, the annulus fibrosis and the end plates situated between the disc and the mating vertebrae (Figure 2-22). Water and nutrients can move across the end plates thus allowing various levels of "hydration" of the disc.

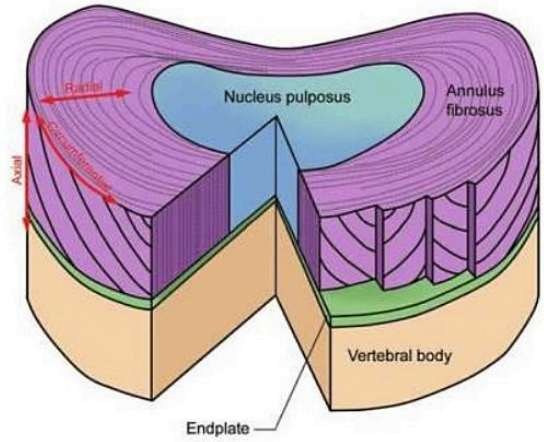


(Reproduced from Kurtz and Edidin, 2006)

**Figure 2-22: Structure of the typical intervertebral disc**

The nucleus pulposus is a semi-solid structure, the dry weight of which is 20% collagen and 30-50% proteoglycans. When hydrated, the nucleus pulposus is 70-80% water. The bulk of the pulposus is made up of helically organized proteins (or Type II collagens) which are hydrophilic and attract water to create osmotic pressure. In the reclined position, the osmotic pressure is approximately 0.1-0.2 MPa increasing to 1-3 MPa when standing unloaded (Kurtz and Edidin, 2006). Loads are carried by some combination of osmotic pressure along with the physical pressure from the restrictions to fluid motion caused by the small pore size of the collagen/proteoglycan matrix and the endplates. Also loads are carried by the electrostatic repulsion as fixed negatively charged elements within the matrix are forced into close proximity as the nucleus becomes less hydrated and by tensile resistance of the collagen fibres. This makes the nucleus pulposus a viscoelastic material but it is often approximated as an elastic material within certain frequency ranges with a compressive elastic modulus of 1.0 - 3.4 MPa (Panzer and Cronin, 2009).

The annulus is comprised of approximately 15-40 distinct layers of organized fibro-cartilage oriented at alternating angles within a proteoglycan matrix (Marchand, 1990; Kurtz and Edidin, 2006). Fibres are oriented at 30° from the mid-disc plane and are 120° between adjacent fibre layers. It is anchored to the adjacent vertebral bones and is understood to be anisotropic in tension but not to the same extent in compression. In terms of dry weight, 60-70% of the annulus is collagen and 10% is proteoglycans. The annulus is typically loaded in tension as axial loading causes the vertebral bodies to be forced together and the disc attempts to deform in the radial direction outwards from the spine. Type I collagen which is well suited for tensile loading is heavily distributed at the radial edge of the annulus while Type II collagen is more prevalent at the inside edge because it can better withstand the increased deformation associated with compressive loading than Type 1 collagen (Eyre and Muir, 1976). Therefore the material properties of the annulus fibrosis are heavily location dependant (Best et al, 1994; Skaggs *et al*, 1994). It is relevant to note that even in a region subjected to compressive loading most of the collagen fibres in this composite material develop tensile stresses.

The cartilaginous end plates are approximately 0.6 mm in thickness (Kurtz and Edidin, 2006) and constrain the discs helping prevent their extrusion from between the vertebra. The end plates are strongly connected to the vertebrae in the annual region with a weaker connection in the central, nucleus region (Clark, 2005). They provide structural support and tend to spread the loads across the disc to reduce the possibility of disc damage due to herniation and/or impingement. Also, an important function of the end plates is to allow water and nutrients to move across them into the disc. In particular, the water can move both in and out of the disc, thus allowing various levels of hydration. Both the nucleus and annulus are hydrated and the level of hydration influences the load carriage by the disc; the nucleus in particular loses water during the day when the spine observes an almost constant compressive load, rehydrating at night during horizontal resting.

In modeling the response of the human spine to loads and motions using finite element analysis (FEA), material properties for the various components of the spine are needed. The key component with regards to this response is the disc. Although in reality each of these entities is an anisotropic, non-linear viscoelastic material, they have been approximated as linear elastic materials in several studies with an elastic modulus and Poisson's ratio that can apply over a range of strain frequencies and amplitudes (Table 2-1 and Table 2-2).

**Table 2-1: Nucleus pulposus material properties**

| Study | Elastic Modulus (MPa) | Poisson's Ratio |
|---|---|---|
| Yoganandan *et al* (2000) | 3.4 | 0.49 |
| Natarajan *et al* (2000) | 3.4 | 0.499 |
| Ng and Teo (2001) | 1.0 | 0.499 |
| Average | **2.60** | **0.496** |

**Table 2-2: Annulus fibrosis material properties**

| Study | Elastic Modulus (MPa) | Poisson's Ratio |
|---|---|---|
| Yoganandan *et al* (2000) | 3.4 | 0.4 |
| Natarajan *et al* (2000) | 4.2 | 0.45 |
| Ng and Teo (2001) | 3.4 | 0.4 |
| Clausen *et al* (1993) | 4.2 | 0.45 |
| Kumaresan *et al* (1999) | 4.7 | 0.45 |
| Average | **3.98** | **0.430** |

### 2.3.2 Intervertebral Disc Physiology

During normal physiological motion the intervertebral disc is subjected to a combination of compression, bending, shear and torsional loading. In the healthy disc axial loading is supported by the hydrostatic pressure of the nucleus pulposus which is contained by the woven matrix of the annulus (Nachemson, 1963) (Figure 2-23).

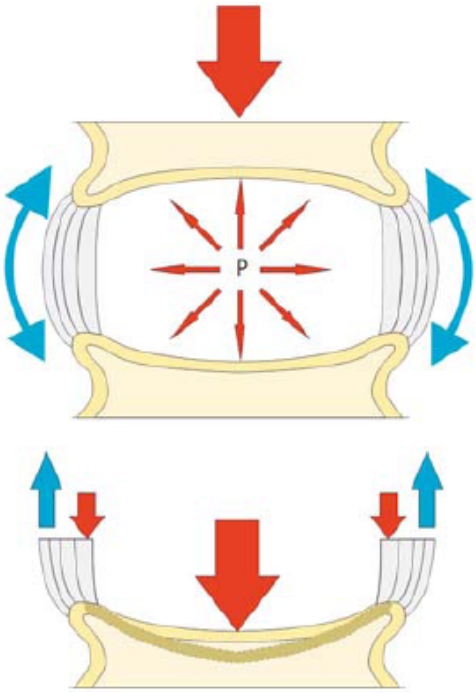


(Adapted from Boos and Aebi, 2008)

**Figure 2-23: Axial loading of the healthy intervertebral disc**

The outer fibres of the annulus are loaded in tension as the internal pressure developed in the nucleus attempts to extrude the inner disc material out though the radial edge. The resulting internal pressure causes deformation of the endplate at the point where the disc mates the vertebra. The inner annulus is put into compression due to the adjacent nucleus and vertical loading between the two endplates. The outer fibres of the annulus support bending and torsional loading.

The pressure generated within the nucleus is approximately 1.5 times the externally applied load, and since the nucleus is an incompressible substance, this causes bulging under load of approximately 1 mm for physiological forces (Stokes, 1988). The stress in the annulus fibres is approximately 4-5 times the applied stress in the nucleus (Nachemson, 1960; Nachemson, 1963; Galante, 1967) with the fibres elongating by up to 9% during torsional loading. The ultimate elongation at failure is over 25% for fibres of the annuli (Stokes, 1987).

The presence of disc degeneration has a significant effect on the load transfer through the disc due to dehydration of the disc. With aging the elastic modulus and visco-elasticity of the disc is reduced resulting in less capability to absorb shock loading, as well as a shift in loading from the nucleus to the annulus which may lead to pain or rupture of the annulus.

The motion response of the disc in a spinal segment has been studied by White and Panjabi (1990) to show that it exhibits flexibility at low loading and increasing stiffness at higher loads, which is similar to the non linear response in torsion (Farfan, 1973). Very little resistance to torque is observed in approximately the first 3° of rotation, a linear response between 3°-12° and failure of the outer annular fibres occurs at 20° of rotation.

Bulging of the annulus is most prevalent during extension and is least during flexion (Figure 2-24).

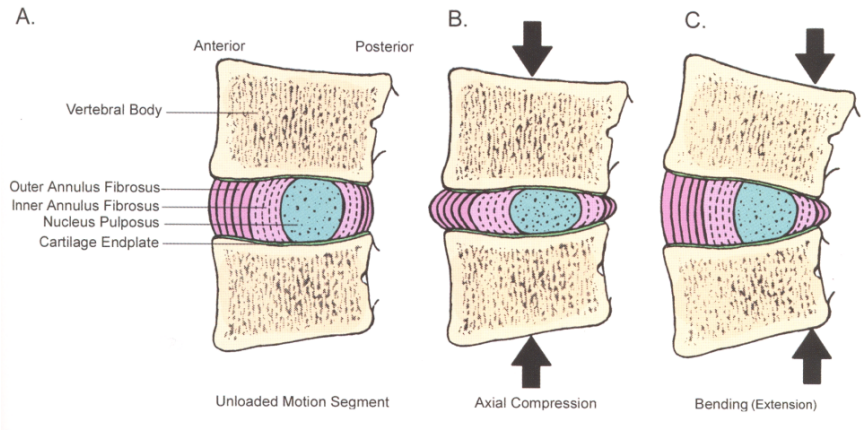


(Reproduced from Kurtz and Edidin, 2006)

**Figure 2-24: Intervertebral disc loading states (A-no load, B-axial, C-bending)**

Failure of the annulus through extrusion of the nucleus most commonly occurs in the posterolateral direction that can directly result in the compression and impingement of the dura or spinal nerve root. Failure of the annulus has been postulated to be due to fatigue of the outer annular fibres (Adams and Hutton, 1982; Adams and Hutton, 1985) mainly under combined loading of the spinal segment as pure compressive loading does not cause herniation.

## 2.4 Ligaments of the Spine

The ligaments of the spine complement the various other spinal structures to aid in the overall stability as well as to guide and control the segmental motion at each spinal level. Typically ligamentous structures can only support tensile loading in the axial direction between the two attachment points. Spinal ligaments are often only begin to contribute to spinal stability near the ends of the ranges of motion and act as constraints to prevent hyper mobility of the spine in any physiological directions. Thus they are termed passive components as they are not directly responsible for motion, like muscles are, but act as restraints at the limits of the motion.

### 2.4.1 Spinal Ligament Anatomy

The ligamentous structures are divided into two primary groups; the intrasegmental and the intersegmental ligament systems. As described by their names, the intrasegmental system of ligaments holds the individual vertebrae together and the intersegmental system of ligaments are responsible for holding many vertebrae together. The intrasegmental system of ligaments includes the ligamentum flavum, the facet capsule, and the interspinous and the intertransverse ligaments. The intersegmental system includes the anterior and posterior longitudinal ligaments, as well as the supraspinous ligaments. All ligaments except for the ligamentum flavum have a high collagen content which has a high concentration of elastin to ensure that it is always under tension to pre-stress the disc even in the neutral position (Evans and Nachemson, 1969).

The ligamenta flava connect the laminae of adjacent vertebrae and is present from the axis to the first section of the sacrum and are most easily viewed from the interior of the spinal canal (Figure 2-25). The ligament

starts on either side of the roots of the articular processes and continue to the point where the laminae meet at the spinous process. The ligamenta flava are comprised mainly of elastin, the tissue of which is yellow in colour, and serve to maintain the upright posture as well as return the spinal segment to the neutral position after periods of flexion. The ligaments are thin and broad in the cervical spinal region and increase in thickness moving down the spine in the inferior direction to the lumbar region.

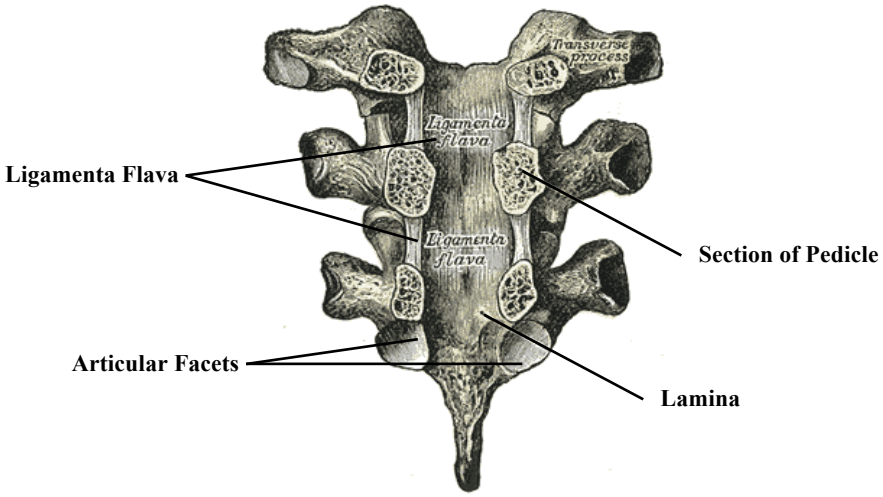


(Adapted from Gray, 1918)

**Figure 2-25: Anterior view of vertebral arches of thoracic vertebra**

The capsular ligaments (Figure 2-26) are of thin geometry and loosely attach the margins of adjacent vertebral articular processes. The laxities of the capsule ligaments is largest in the cervical spine to accommodate the wide range of motion in this region, are tighter in the lumbar spine and exhibit even less laxity in the thoracic spine. The laxity of the capsular ligaments seems to show a strong correlation to the intersegmental range of motion in each region of the spine.

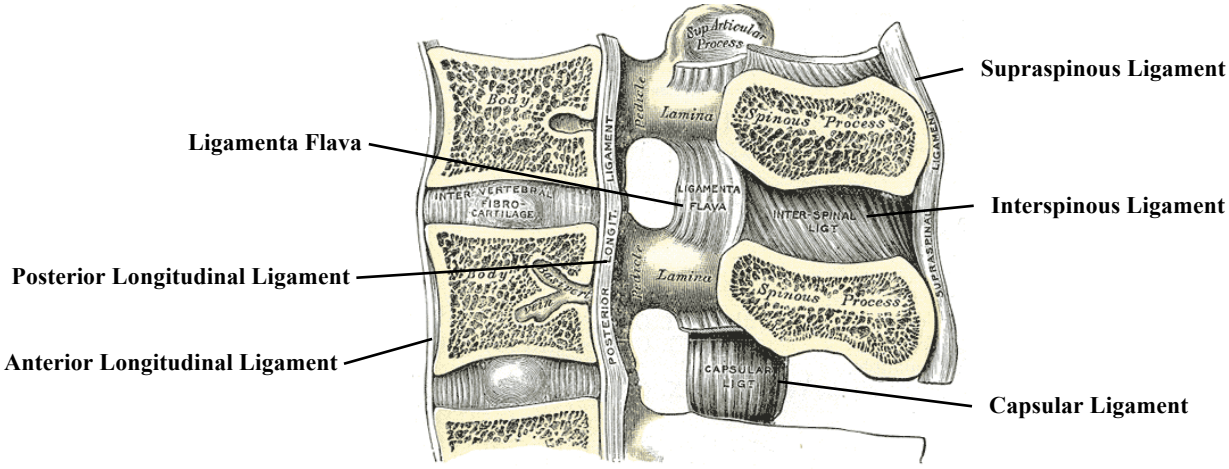


(Adapted from Gray, 1918)

**Figure 2-26: Median section of lumbar vertebrae showing ligamentous structures**

The interspinous ligaments (Figure 2-26) connect the adjacent spinous processes of vertebrae extending from the root to the apex of each process. They are thin and membrane-like and move from a narrow, elongated morphology in the thoracic spine to a broader, thicker geometry in the lumbar spine and are almost non-existent in the neck.

The intertransverse ligaments are positioned between the transverse processes. In the cervical spine they are comprised of irregular, scattered fibres, in the thoracic spine they are rounded cords that are interconnected with the musculature of the back and in the lumbar region they are thin and membrane-like.

The anterior longitudinal ligament (ALL) (Figure 2-26) is a strong grouping of fibres that extends along the anterior surface of the vertebral bodies from the axis to the sacrum. The ALL is the thickest in the thoracic spine and tends to be thicker at the point of attachment to the vertebral bodies than in the span adjacent the intervertebral disc. It exhibits a strong connection to the anterior of the disc as well as the anterior lip of the vertebral bodies but it not well attached to the vertebral bodies in between the endplates. It is comprised of several layers of fibres which vary in length; some spanning only one vertebra to the next with the longest spanning four or five vertebral levels.

The posterior longitudinal ligament (PLL) also seen in Figure 2-26 is positioned along the border of the vertebral canal and the posterior faces of both the vertebral body and the intervertebral disc and extends from the axis to the sacrum. Like the ALL, the PLL is thicker in the thoracic region than in the lumbar or cervical spine and is narrow and thick when passing over the centres of the vertebral bodies. The PLL is comprised of smooth, shining, longitudinal fibres that are denser and more compact than that of the ALL and consist of superficial fibres which span three to four vertebral levels and deeper layers which extend between adjacent vertebrae.

The supraspinous ligament (Figure 2-26) can be described as a strong fibrous cord that spans the spinous processes from the seventh cervical vertebra to the sacrum. It is thicker in the lumbar spine than in the thoracic spine, with the most superficial fibres spanning three or four vertebrae and deeper fibres pass between two to three vertebral bodies. Between the spinous processes it is continuous with the interspinous ligaments.

A detailed layout of the ligaments in the lower cervical spine can be seen in Figure 2-27.

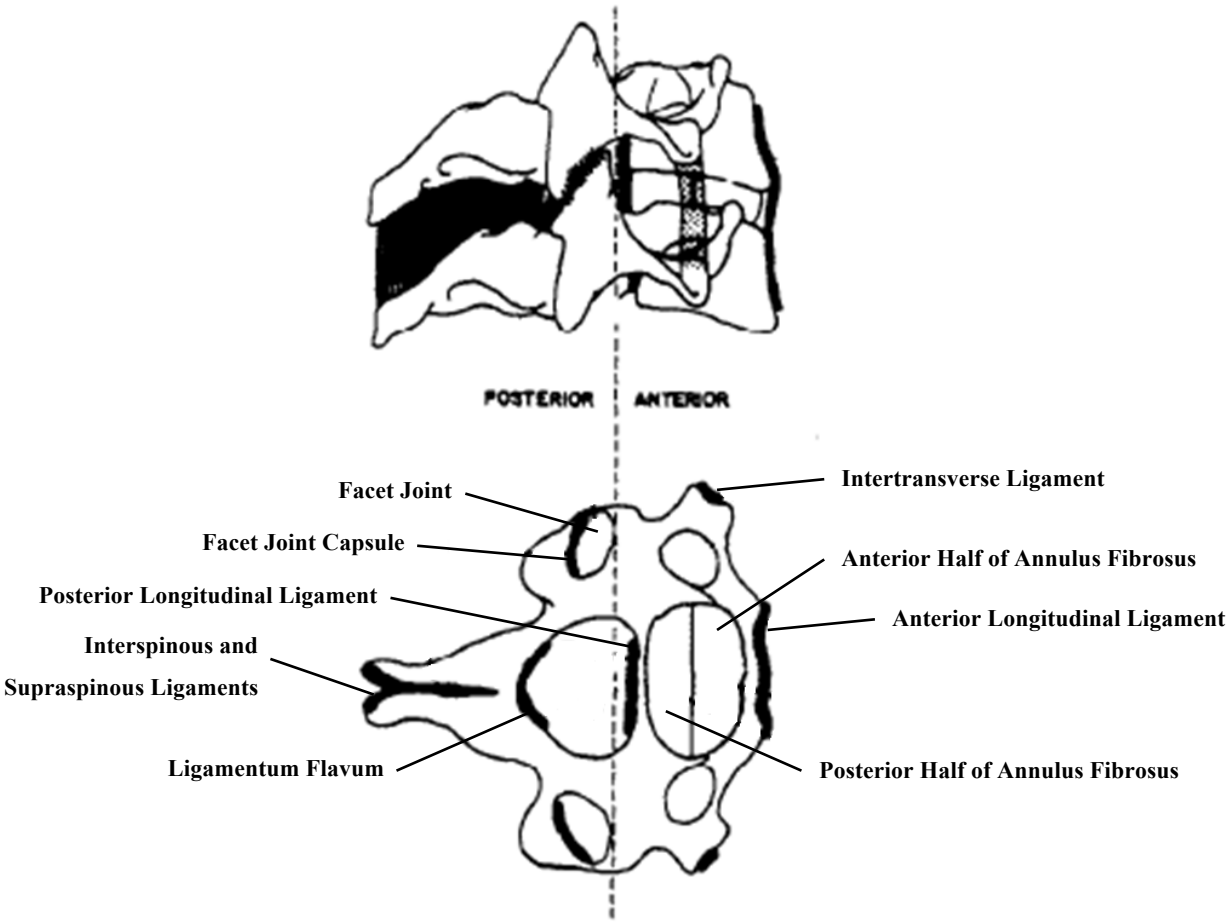


(Adapted from Panjabi *et al*, 1978)

**Figure 2-27: Superior view of the ligaments of the lower cervical spine**

## 2.4.2 Spinal Ligament Physiology

The ligaments of the spine limit the intervertebral motion by constraining the separation between the attachment points of each individual component. They become axially loaded in tension near the limits of the range of motion and exhibit some viscoelastic properties based on strain and loading rates. The functional role of each individual ligament and the resulting contribution to overall spinal motion can be determined *in vitro* by repetitive loading following the sequential removal of each anatomical structure (White, Panjabi and Johnson, 1975).

During flexion the ligamentum flavum, capsular ligaments and interspinous ligaments are highly strained. This is due to the fact that these elements are located on the posterior of the vertebral bodies and thus when flexion motion is observed the attachment points of the posterior elements separate thereby generating tensile strain and the anterior parts move together which does not generate loading of the ligaments as they can only support tension and not compressive loading.

During extension motion the anterior longitudinal ligament is loaded, again since during extension the anterior components move apart causing strain in the ALL which is on the anterior face of the vertebral bodies. The posterior components move towards one another and therefore the ligaments do not observe loading.

Lateral bending results in the contralateral loading of the intertransverse ligaments, the ligamentum flavum and capsular ligaments. This is because in leftward bending the right side of the vertebral bodies separate and thereby generate an increase in length between the attachment points of the ligaments thus causing them to observe tensile strain.

Rotational motion in the lumbar spine is typically resisted by the capsular ligaments that acts in addition to the annulus of the intervertebral disc (Panjabi, Goel and Takata, 1982) since this type of motion results in separation of the contralateral facet joint surfaces.

It is important to note that the larger the distance between the centre of rotation of a particular type of motion and the constraining ligament, the greater the stabilizing potential due to the increased moment arm and resulting lower forces required to arrest and balance the applied forces.

The properties of the ligaments of the lumbar spine have been studied in higher prevalence than those in the cervical spine, with the tensile properties being reported for the ligamentum flavum (Evans and Nachemson, 1969), the ALL and PLL (Tkaczuk, 1968), inter and supraspinous (Waters and Morris, 1973), and intertransverse ligaments (Chazal *et al*, 1985). The response of the ligaments is generally non-linear with an initial neutral zone, an elastic zone with a somewhat linear response between load and displacement and finally a plastic zone which proceeds non-linearly to material failure. The physiologic range of the ligament resides in the neutral and elastic regions since entering the plastic region is typically the point of initiation of injury. Physiologic strain levels for the ligaments in the lumbar spine have been reported by Panjabi, Goel and Takata (1976) using *in vivo* radiographic measurements. In flexion the supraspinous observes 30%; the interspinous, 27%; and the PLL 13% of strain. In extension the ALL observes a strain of 14% and in rotation the capsular ligaments endure 17% of strain.

The typical loads and strain to failure of the ligaments of the lumbar spine have been studied by Farfan (1975) and White and Panjabi (1990) as listed in Table 2-3.

**Table 2-3: Typical loads and strains to failure of lumbar ligaments**

| Ligament | Failure Load (N) | Failure Strain (% elongation) |
|---|---|---|
| ALL | 450 | 26% |
| PLL | 324 | 26% |
| Ligamentum Flavum | 285 | 26% |
| Interspinous | 125 | 13% |
| Supraspinous | 150 | 32% |

(Data adapted from Farfan,1975; and White & Panjabi, 1990)

It can be seen that the ALL and PLL are the strongest ligaments which constitutes their roles as two of the main stabilizing systems of the spine. The supraspinous ligament exhibits the highest strain to failure which is probably a result of the posterior position of this ligament and the resulting large range of motion it observes.

It has been also observed that during aging the spinal column increases in stiffness due to physiological changes in the passive subsystem (osteophytes formation, articular hypertrophy, etc.). It has been thought that these changes are the body's natural response to compensate for the reduced ability of the active stabilizing systems to provide adequate support (Panjabi *et al*, 1978). It is important to note that this increase in stiffness is often not sufficient and surgical intervention in the form of bracing and or fusion is required in some cases.

## 2.5 Musculature of the Spine

The points of attachment of a muscle typically describe its function since they provide tensile axial force between the point(s) of affixation to the structure of the body. The moment arm created by the combination of the contractile muscle and the rigid, typically jointed, structure of the body is what determines the direction and resulting reaction force generated by the anatomical component.

The muscles of the torso can be divided into function subgroups known as the extensors and the flexors, with the prior providing extension motion and the latter generating a flexion motion. The main extensors can be found in the abdominal region; these include the rectus abdominis, the internal and external oblique, and the transverse abdominal muscles, as well as the non-abdominal psoas muscles. The main extensors include the sacrospinalis, transversospinal and short back muscle groups. Vertebral muscle is comprised of 50-60% type 1 muscle which is commonly referred to as 'slow twich' muscle that is fatigue resistant. This is the same type of muscle that is found in most postural muscles which allows the body to maintain adequate upright posture for extended periods of time (Bagnall *et al*, 1984).

### 2.5.1 Spinal Musculature Anatomy

The muscles (and attaching tendons) of the neck can be seen in Figure 2-28. The main flexors are located on the anterior side of the spine in order to provide forward flexion (Figure 2-29). The muscles that provide extension are located on the posterior side of the spine and include the deep muscles (Figure 2-30), and the superficial muscles of the back (Figure 2-31). The deep muscles of the back are subdivided into the sacrospinalis group, the transversospinal group and the short back muscle group.

It should also be mentioned that the tendons, which are the element that attaches the muscles to the skeletal system, have built in force transducers that provide feedback to the neural system regarding the forces generated by the muscle.

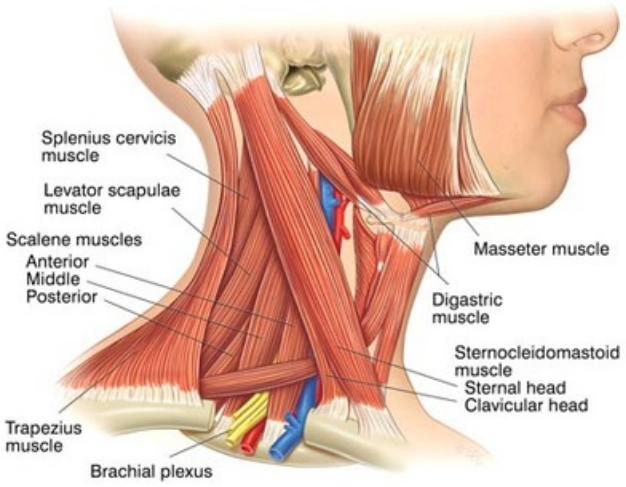


(Adapted from www.neckpainsupport.com)

**Figure 2-28: Muscles of the neck**

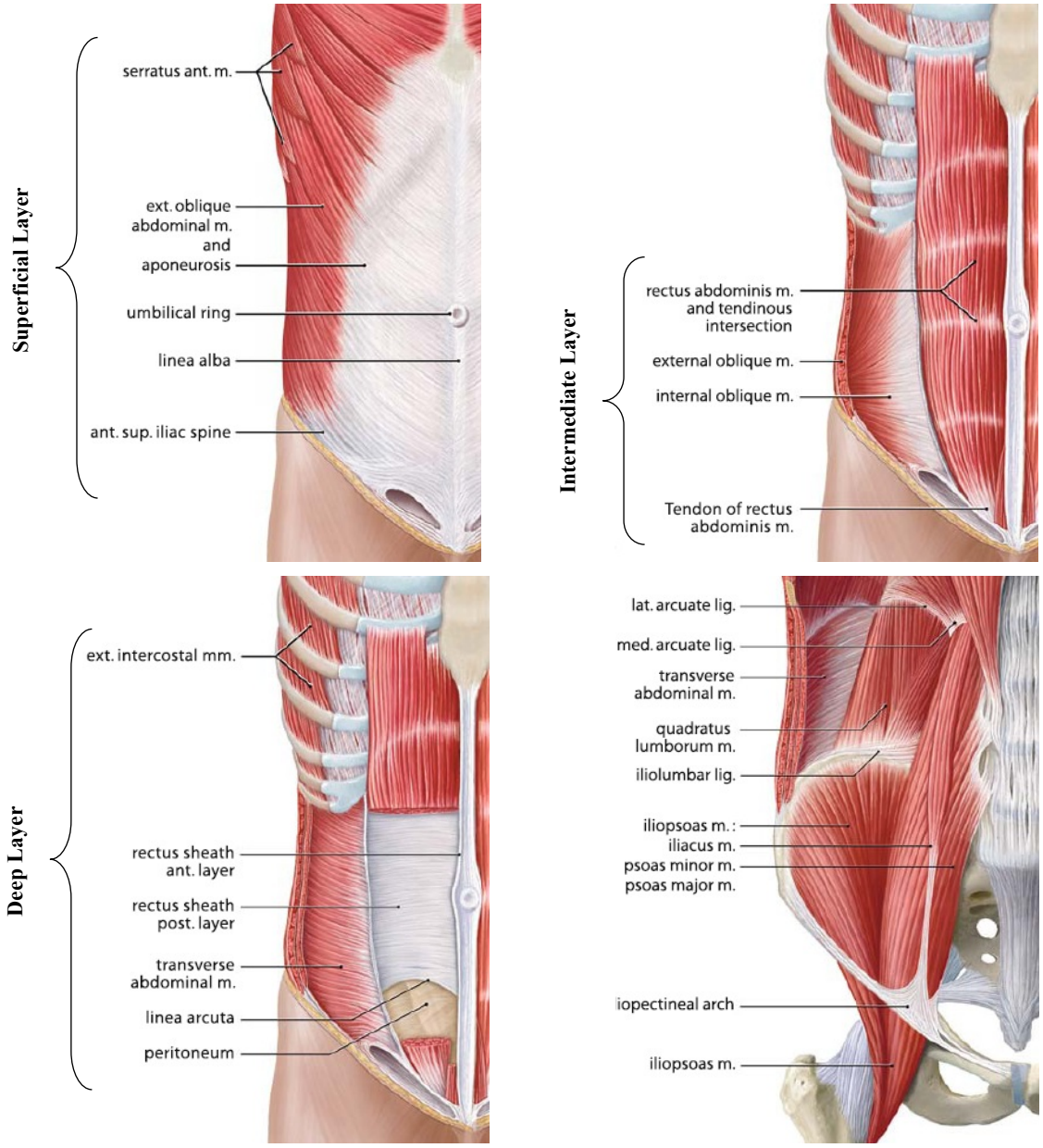


(Adapted from Boos and Aebi, 2008)

**Figure 2-29: Anterior muscles of the spine**

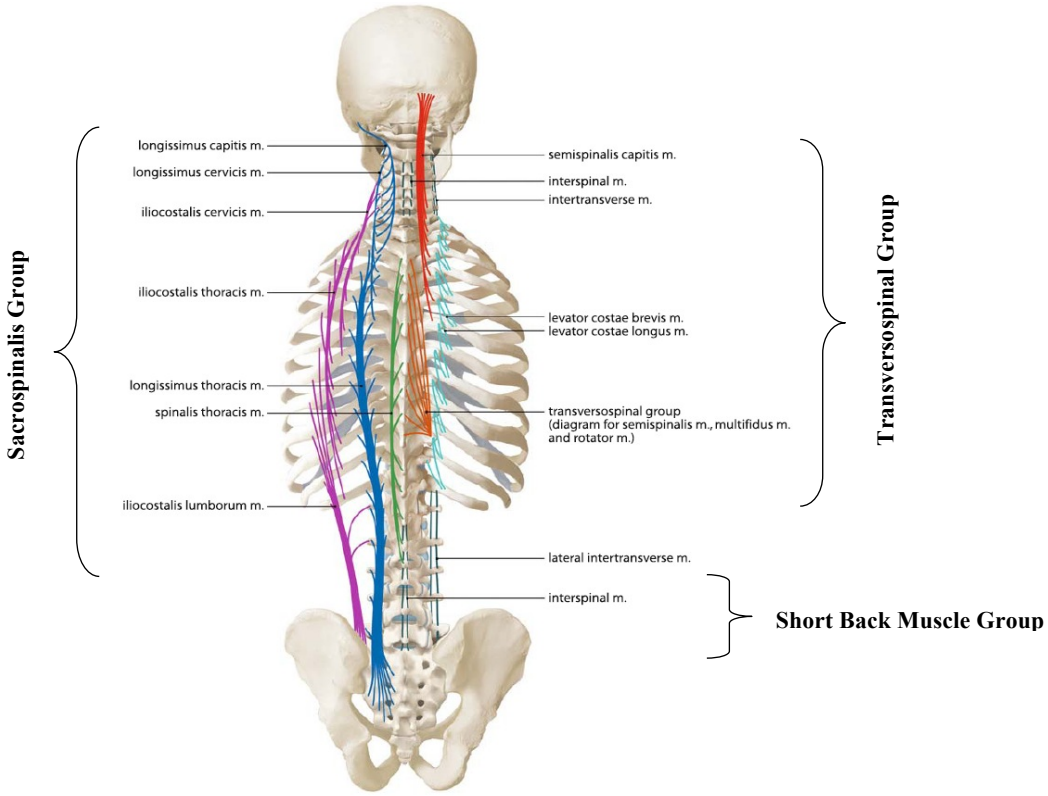


(Adapted from Boos and Aebi, 2008)

**Figure 2-30: Deep muscles of the back**

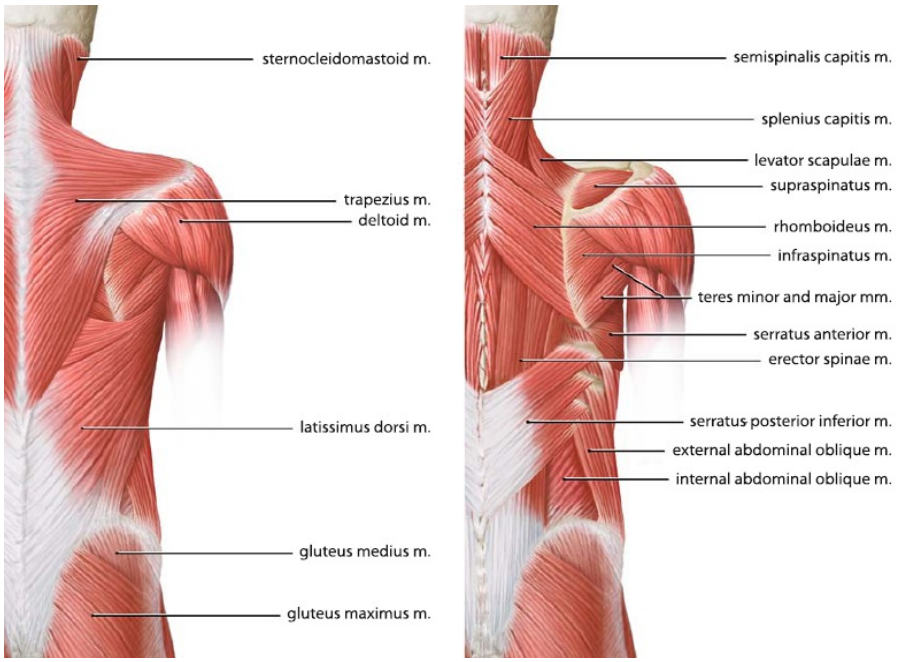


(Reproduced from Boos and Aebi, 2008)

**Figure 2-31: Superficial muscles of the back**

### 2.5.2 Spinal Musculature Physiology

Muscle activity can be directly measured using electromyography or indirectly using mathematical computer models which interpret external loading and attempt to predict the internal reactions required to support the applied loads. These models require a significant amount of information regarding the geometry of the muscle and attaching structure include the insertion points, the origin, cross sectional area (to estimate the strength) and the muscle type and length. The relationship between the line of action of the muscle and the center of rotation of the joint determines the maximum torque available which is dependent on the moment arm created by the structure. Moment arms for muscles in both the cervical and lumbar spine have been studied and determined from MRI and CT images (McGill, Sataguida and Stevens, 1993; Nemeth and Ohlsen, 1986; Tracy *et al*, 1989; Tsuang *et al*, 1993), but the inherent redundancy of the spinal musculature, potential for simultaneous contraction and complex geometry make the numerical modeling of actual muscle force difficult and therefore models often determine the optimal muscle force for the required load accommodation and may represent lower forces than actually observed *in vivo*.

It is important to note that the stability of the spine is dependant to some extent and enhanced by the activity of the various spinal muscles. Bergmark (1989) has divided the spinal muscular system into three functional groups; the local stabilizers, the global stabilizers and the global mobilizers (Figure 2-32).

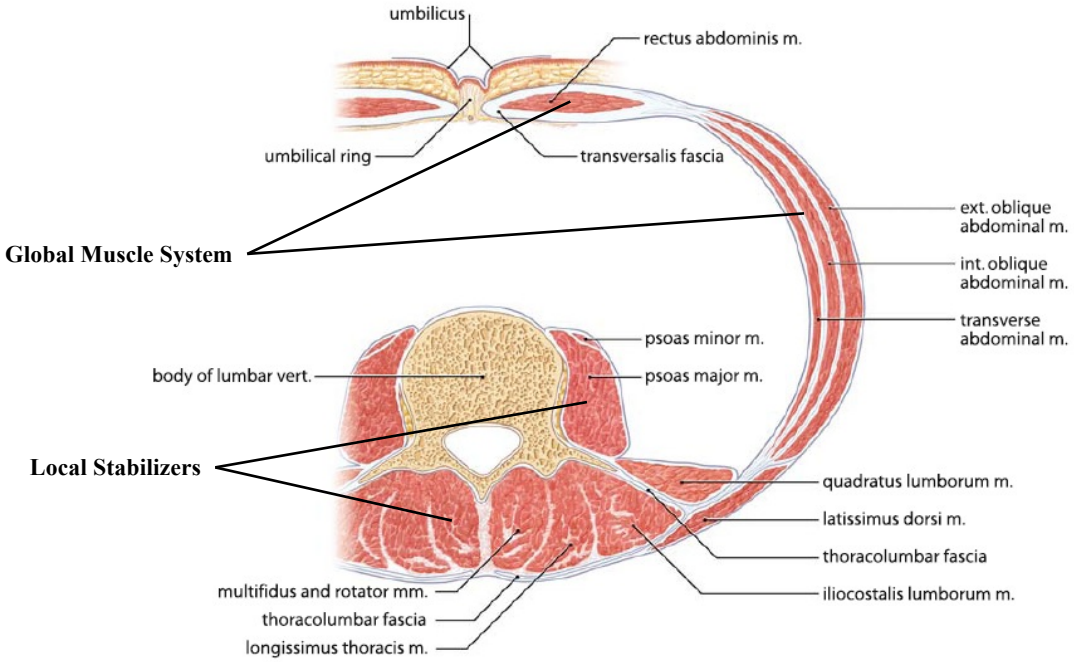


(Adapted from Boos and Aebi, 2008)

**Figure 2-32: Inter-Dependence of anterior and posterior spinal muscles of the lumbar spine**

The local stabilizers are directly connected to the spine, typically spanning single spinal segments. They are responsible for the control of the neutral position of the intervertebral joint, whereas the ligaments typically are active at the end limits of the range of motion. The local stabilizers operate a low speeds and are not directly

responsible for motion; their main role is to stiffen the spinal segment and control motion in transient applied loading. As aging occurs the ability of the active system to provide stability is degenerated which often results in the inability to produce coordinated motion. This may place increased stress on the passive system as the limits of motion may be encountered more often as the active system is unable to counteract applied loads. The result of this may be poor segmental control and pain when non-physiologic motion is encountered.

The global muscle system is comprised of the global stabilizers and the global mobilizers which include the larger torque generating muscles that are further away from the vertebral bodies and thus have a larger moment arm which acts on the spine. Contraction of these muscles can both generate motion as well as enhance spinal stability. Although global muscles are most commonly targeted for low back pain, it is the local stability system which results show may contribute more to spinal stability and thus would be more advantageous to target during rehabilitation. Clinical instability has been defined by Panjabi (1992) as a significant decrease in the ability to maintain the intervertebral neutral zone within the prescribed physiological limits. As mentioned previously, the main anatomical structure responsible for maintaining the neutral zone of the spinal motion segment is the stabilizing musculature of the spine.

Most of the motion provided by the spine in both flexion and extension is accommodated in the lumbar and cervical spine due to the constraining geometry of the thoracic spine and stiffness of the ribcage. Flexion of the spine is initiated by the anterior spinal musculature which is augmented by the anterior weight shift of the upper body which provides an increasing forward bending moment. Flexion is controlled by the co-contraction of the posterior extensor muscles. At the location of full flexion, Farfan (1975) and Andersson *et al* (1996) have proposed that the forward bending moment is counteracted both passively by both the elasticity of the posterior muscles and ligaments which are initially slack but tighten as flexion occurs, and actively by the deep muscles of the spine. During extension motion the posterior muscles initiate motion which is accommodated by a rearward bending moment created by the posterior shift of body weight at which point the anterior abdominal musculature becomes active to modulate the extension motion.

Lateral bending of the spine occurs in both the lumbar and cervical spine, during which the spinotransversal, transversospinal and the abdominal muscles are active. The motion is initiated by ipsilateral contraction of the muscles in the direction of motion. At the same time contralateral contractions control the progression of bending (Andersson, 1997). Axial rotation is generated by both the back and abdominal musculature including both ipsilateral and contralateral contractions, during which large amounts of co-contraction have been observed (Lavender, Tsuang and Andersson, 1992) which may be due to the poorly situated muscle lines of action during this type of motion.

# Chapter 3

# Physiological Motion and Loading

The spine is the anatomical structure which provides mobility to the trunk as well as relative motion between the torso and neck. The overall range of motion of the spine is relatively large to accommodate daily human activities. This large range of motion is provided by the sum of many much smaller movements between each of the twenty four individual vertebral bodies which combine to provide spinal mobility in all anatomical planes. The sharing of motion is not consistent between all levels of the spine; with the variation due to differences such as vertebral and disc geometry, position and condition of spinal ligaments and musculature.

The spine is also responsible for supporting the loads applied to the upper body and transferring the applied forces to the lower extremities which transfer the body forces to the ground. The loads incurred by the spine increase as the point of interest is moved from the head down to the sacrum due to the increased amount of body mass above the plane section. The spinal response to loading is also dependant on the material properties of each anatomical components as well as the interaction between components. The load sharing between spinal structures is also a function of position and therefore varies significantly for different activities.

In order to define the range of motion and kinematics of the spine, the standard medical terminology is used as previously described.

## 3.1 Spinal Kinematics

Motion at the intervertebral joint exhibits six degrees of freedom which includes rotation and translation about all three physiologic axes (Figure 3-1).

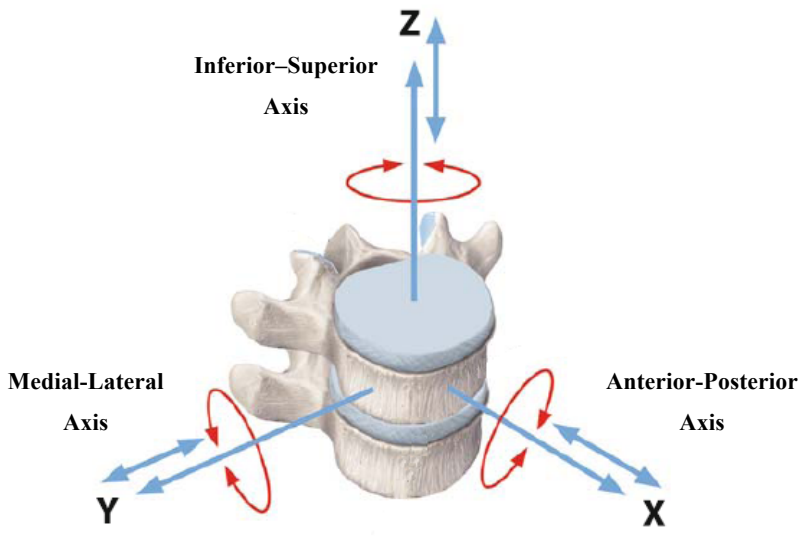


(Adapted from Boos and Aebi, 2008)

**Figure 3-1: Motion characteristics of the spinal segment**

The six degrees of freedom is provided by a complex interaction between the intervertebral disc, the posterior elements, the muscles and the ligaments of the spine. It is important to note that different structures provided varying degrees of motion; for example the intervertebral disc provides 6 degrees of freedom while the facet joints limit motion in the direction perpendicular to the plane of contact. Therefore spinal motion is typically a combination of simultaneous flexion or extension, lateral bending and rotation, provided by the combined interactions of all the components of the spine.

### 3.1.1 Range of Motion

The overall motion of the spine can be determined clinically by digitizing the locations of surface markers mounted on the skin of participants. This method provides an accurate representation of the posture of participants, but does not have the accuracy or resolution required for measurement of intersegmental motion.

In order to obtain direct measurement of motion at each individual level, a combination of *in vivo* radiographic and *in vitro* cadaveric measurements have been performed for the different levels of the spine. In particular, White and Panjabi (1990) studied the range of motion of the human spine in the flexion-extension, lateral bending and axial rotation. The results of that study can be seen in Figure 3-2, where it is clear that the lumbar and cervical spine experiences the largest amount of motion while the thoracic spine observes the smallest amount of intersegmental motion. The spine can also provide small amounts of translation motion in the three anatomical axes as well. The intersegmental range of motion is determined by the local spinal geometry and functional demands.

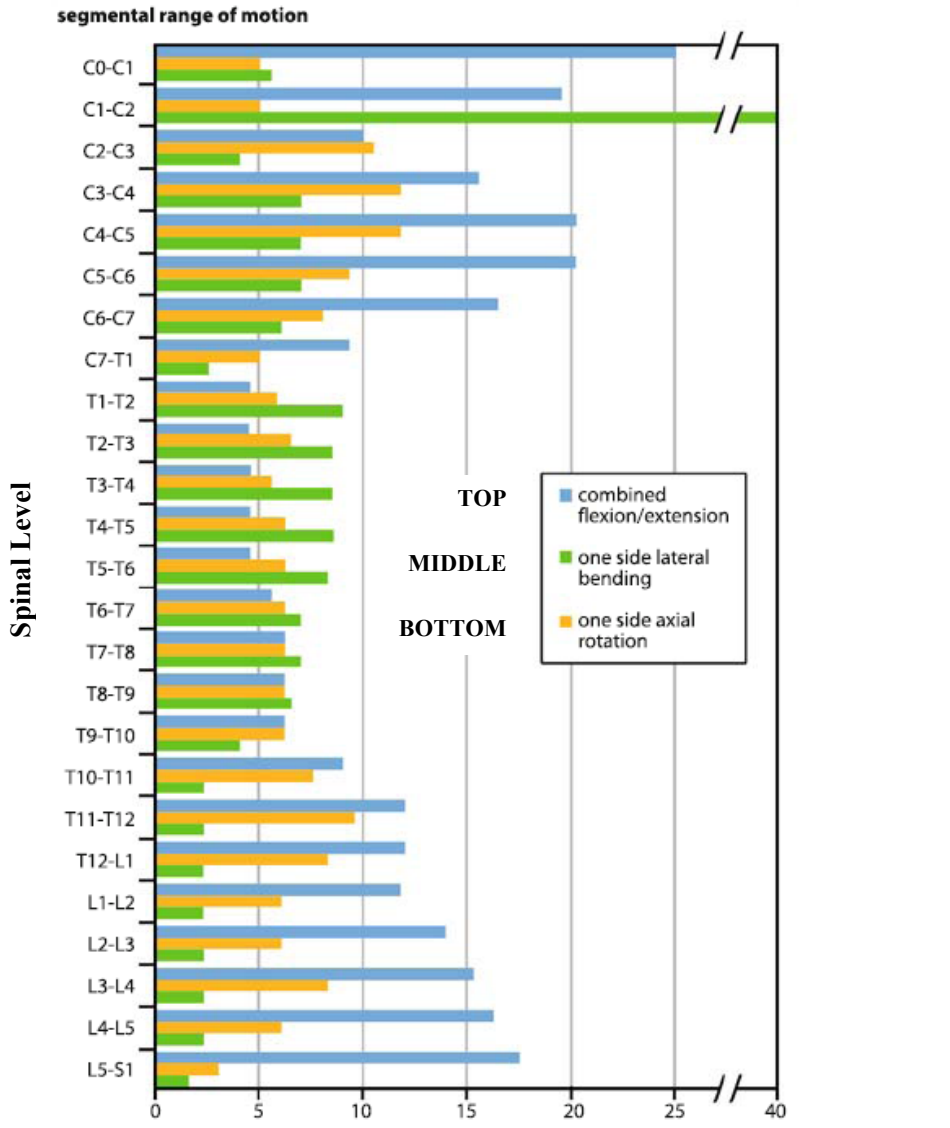


(Adapted from Boos and Aebi, 2008)

**Figure 3-2: Range of motion of the human spine**

The extent and type of the movements provided are influenced by the shape and direction of the articular surfaces, particularly the intervertebral disc and facet joints.

In the cervical region the upward inclination of the facet surfaces accommodates free flexion and extension. The average total rotations in flexion and extension can be seen in Table 3-1, with more rotation permitted in extension than flexion. At the end of extension motion the posterior edges of the facets contact and limit further progression of motion. Maximum flexion is controlled by the interaction between the projecting lower lips and the upper shelving surfaces of the vertebral bodies of the adjacent vertebrae. Both lateral bending and axial rotation are widely permitted in the cervical spine but are always combined due to the upward and medial inclinations of the contact plane of the facets. Pure lateral bending is accommodated by axial rotation as

the ipsilateral facet slides posteriorly, and pure axial rotation is accompanied by lateral bending as the contralateral facet is forced upwards in the superior direction during motion.

**Table 3-1: Average total flexion-extension rotations (in degrees) in the cervical spine**

| Region | Dvorak *et al*, 1988a & 1988b | | White and Panjabi, 1990 | Penning, 1978; *In vivo*, active |
|---|---|---|---|---|
| | *In vivo*, active | *In vivo*, passive | | |
| C2-C3 | 10 | 12 | 10 | 12 |
| C3-C4 | 15 | 17 | 15 | 18 |
| C4-C5 | 19 | 21 | 20 | 20 |
| C5-C6 | 20 | 23 | 20 | 20 |
| C6-C7 | 19 | 21 | 17 | 15 |
| C7-T1 | - | - | 9 | - |

A more detailed study by White and Panjabi (1990) outlining the range of motion of each cervical spinal segment in multidirectional bending can be seen in Table 3-2.

**Table 3-2: Range of motion of cervical spinal segments in degrees (White & Panjabi, 1990)**

| | C0-C1 | C1-C2 | C2-C3 | C3-C4 | C4-C5 | C5-C6 | C6-C7 |
|---|---|---|---|---|---|---|---|
| Flexion | 7.2 ± 2.5 | 12.3 ± 2.0 | 3.5 ± 1.3 | 4.3 ± 2.9 | 5.3 ± 3.0 | 5.5 ± 2.6 | 3.7 ± 2.1 |
| Extension | 20.2 ± 4.6 | 12.1 ± 6.5 | 2.7 ± 1.0 | 3.4 ± 2.1 | 4.8 ± 1.9 | 4.4 ± 2.8 | 3.4 ± 1.9 |
| Axial rotation | 9.9 ± 3.0 | 56.7 ± 4.8 | 3.3 ± 0.8 | 5.1 ± 1.2 | 6.8 ± 1.3 | 5.0 ± 1.0 | 2.9 ± 0.8 |
| Lateral bending | 9.1 ± 1.5 | 6.6 ± 2.3 | 8.6 ± 1.8 | 9.0 ± 1.9 | 9.3 ± 1.7 | 6.5 ± 1.5 | 5.4 ± 1.5 |

Values are mean ± standard deviations. Values for axial rotation and lateral bending sum both right and left sides.

There are significant differences in the motion provided by the upper and lower cervical spine, this is clearly evident in Figure 3-3 where the average motion in flexion, extension, one side axial rotation and one side lateral bending is plotted for each cervical spinal level.

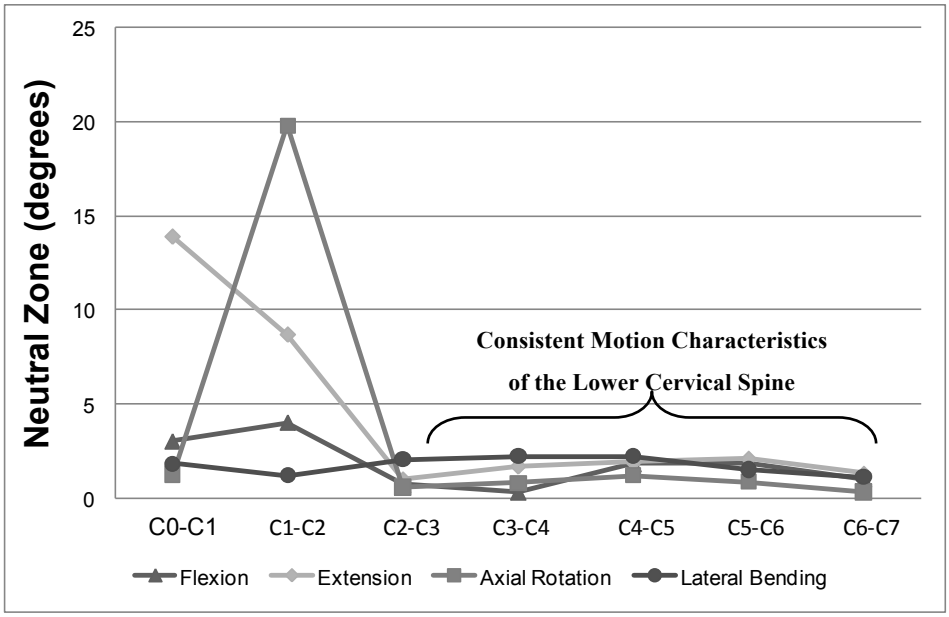


**Figure 3-3: Segmental ranges of motion in the cervical spine**

The total average range of motion of the cervical spine not including the C7-T1 segment is approximately 40° in flexion, 50° in extension, a total of 50° of lateral flexion and a total of 90° of axial rotation. The most superior level (C0-C1) is responsible for a significant amount of extension motion; over 40% of the total extension motion provided by the cervical spine is accommodated at this level. The C1-C2 level accommodates a significant amount of flexion, extension and axial rotation, providing over 63% of the total rotation of the cervical spine. The remaining cervical motion segments from C2 to C7 all exhibit the same characteristics of motion as shown by the almost horizontal trend lines existing from C2 through to C7. These motion segments provide an average of 4.5° of flexion, 3.75° of extension, 2.3° of axial rotation to each side and 3.9° of lateral bending to each side (Table 3-3).

**Table 3-3: Segmental motion of the lower cervical spine (White & Panjabi, 1990)**

| Type of Spinal Motion | Average Lower Cervical Spine Segmental Motion | Total Cervical Spine Motion | % of Total Motion Provided by Lower Cervical Segments |
|---|---|---|---|
| Flexion | 4.5 | 41.8 | 10.7% |
| Extension | 3.75 | 51 | 7.3% |
| Axial Rotation | 2.3 (one side) | 44.9 | 5.2% |
| Lateral Bending | 3.9 (one side) | 27.3 | 14.2% |

While the upper cervical spine provides a significant amount of motion at one or two levels, the lower cervical spine must consistently provide intersegmental motion with each segment responsible for approximately 9% of the overall motion in flexion and extension, 5% of global motion in rotation and 15% of the overall motion

in lateral bending. It is interesting to note that this region of the spine provides a similar amount of rotation in all physiologic directions; forward bending, rearward bending and lateral bending.

In the thoracic spine all movements are limited in order to minimize the interference of motion with normal breathing, respiration and to prevent significant compression and motion of the internal organs. Flexion is prevented by the nearly complete absence of an upward inclination on the facet contact surfaces. Extension is permitted and limited by contact of the facet articular surfaces with the adjacent laminae, as well as contact of the spinous processes. The discontinuity in motion provision between the cervical and thoracic spine is accommodated by the C7-T1 spinal level which limits extension of the C7 vertebra and flexion of the T1 vertebral body to allow for spinal continuity and integration of these two spinal levels with distinct motion characteristics. Rotation is permitted in the thoracic region and there is only limited motion coupling observed. Lateral bending would is permitted by the spinal segments but this motion is prohibited, especially in the upper region by the resistance provided by the ribs and sternum.

In the lumbar region both flexion and extension are free with more rotation being permitted in flexion motion. There is considerable separation of the inferior and superior articular facet surfaces and therefore a considerable about of lateral bending can also be accommodated in the lumbar spine. Some rotation is permitted in the lumbar region but is limited to an almost negligible amount due to the interlocking of the adjacent facet joints.

The prevalence of motion in the lumbar and cervical spine suggests that injuries would be more common in these regions compared with the thoracic spine which observes significantly less intersegmental motion. It must also be noted that all of the above motions of the spine can occur simultaneously. Also, the spine can have small amounts of displacement in the x, y and z directions. While this does not influence the overall motion much, these displacements can influence loading of the various joints and ligaments.

### 3.1.2 Motion Contribution of Cervical Anatomic Structures

In an attempt to determine the contribution of each individual spinal element on the overall kinematics and stability of the spine, *in vitro* testing of spinal segments with consequent removal of anatomical structures has been performed.

Goel *et al* (1988) performed a three dimensional load-displacement study on the C4-C5 and C5-C6 segments while sequentially removing ligamentous structures from the latter segment. Removal of elements was progressed as follows; transaction of supraspinous and interspinous ligaments, ligamentum flavum, and finally the capsular ligaments. The bilateral removal of the capsular ligaments at the C5-C6 level resulted in a significant increase in motion in extension, lateral bending and axial rotation showing the importance of these posterior ligamentous structures in the cervical spine. Removal of the ligamentum flavum resulted in a significant increase in flexion. Surprisingly the motion observed at the superior C4-C5 level also increased in the post-injury state. The results of this study are similar when compared to work performed by Zdeblick *et al* (1994).

The intervertebral disc plays an integral role in the transfer of loading between adjacent vertebrae as well as providing prescribed and controlled intersegmental motion. The disc is commonly injured via herniation of the

nuclear elements and is often the focus of degeneration which results in stiffening of the disc material. The results of this damage can be accompanied by the formation of osteophytes which can be described as bony ingrowths that is an attempt by the body to increase the contact area of the articulation thus reducing the observed contact stresses, the relative misalignment of vertebral bodies and potential changes in the facet joints (Lipson and Muir, 1981). Schulte *et al* (1989) performed a study on the effects of total discectomy on the motion characteristics of the C5-C6 spinal segment. At the C5-C6 level, motion increased in flexion by 66.6%, extension motion increased 69.5%, lateral bending increased 41.6% and axial rotation observed an increase of 37.9%. Surprisingly the results of this study are contradicted by Martins (1976) and Wilson and Campbell (1977) who did not observe any significant increases in motion, however the experimental methods for these studies were significantly different and may be the cause of discrepancy.

The laminae of the cervical spine are also responsible for some load transmission and motion constraint. Goel *et al* (1988) removed the laminae of cervical spines at the C5-C6 level and observed an increase in flexion-extension motion of approximately 10%. This increase is due to the loss of the posterior ligaments which observe tension in flexion and the lack of laminar contact in hyper extension.

The facet joints are also an integral component of the spinal segment. Cusick, Yoganandan and Pintar (1988) found that a total removal of one facet resulted in a decrease in compression-flexion strength of 31.6%, if both facets were removed the reduction of strength increased to 53.1%. The removal of the facet joints also results in the migration of the instantaneous centre of rotation in the anterior direction which resulting in the increased compression of the vertebral body and disc. This may cause accelerated degeneration of the remaining elements of the spinal segment. Raynor *et al* (1987) and Raynor, Pugh and Shapiro (1985) found that the effects of facet removal started to become significant after removal of more than 50% of the facet contact surfaces, with 75% resection producing a large decrease in shear strength. Also, facet capsule resection of more than 50% may result in post operative hyper-mobility which may require segment stabilization. Others have recommended that total facetectomy of more than 25% is accompanied by arthrodesis (spinal fusion) to prevent spinal instability.

### 3.1.3 Mechanical Response of the Spine

Since the motion and load response of the spinal segment is a function of the anatomical elements it is comprised of as well as the type of motion or loading applied, three dimensional flexibility testing is often used to characterize the overall structural properties of the spine. Flexibility is simply the response of a non-rigid body to an applied load which results in some degree of deformation. For the spine, the flexibility is measured by applying a load or series of loads which include axial loading, shear loading and bending moments about the three anatomical axes, and then measuring the mechanical response of the spinal segment in terms of displacement and rotation. The result is often a complex combination of motion in all three planes. It is this form of testing which is most closely related to the *in vivo* response of the spine since it is anatomically in-tact as it would be in the human body. The only difference would be the method of load application where in the body motion would be generated by the skeletal musculature whereas in the laboratory the motion is applied at the end of the motion segment(s) via translation and bending moments.

The load-displacement curve that is obtained is typically non-linear due to the incorporation of several non-linear anatomical components that comprise the spinal segment. For small loads the observed displacement is relatively large due to the presence of what is known as the neutral zone. Under larger applied loads the resistance to motion increases significantly as the laxity in the disc and ligaments is taken up and their structures begin to observe deformation that is proportional to the increase in distance between their points of attachment. This area of motion is called the elastic zone as it involves elastic deformation of the components of the spinal segment. The total range of motion is the sum of the motion observed in the neutral and elastic zones.

The presence of the neutral zone is due to the inherent laxity of the intervertebral disc and spinal ligaments in the vicinity of the neutral position and can be compared to a ball in a bowl with an ellipsoidal curvature (Figure 3-4).

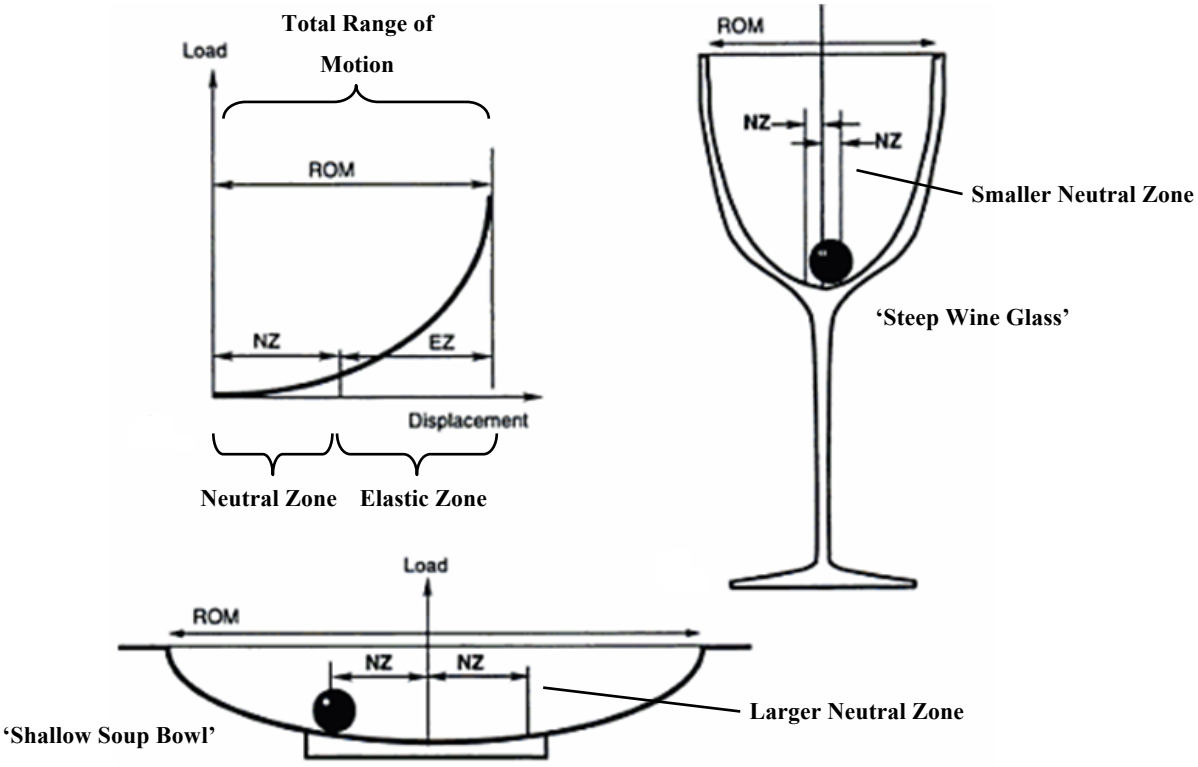


(Adapted from Clark, 2005)

**Figure 3-4: Typical load displacement curve of a spinal segment**

The proportion of motion observed in each region is dependent on the rate of change of the slope of the load displacement curve at low loadings. When using the ball analogy one can imagine applying a force to the ball that will result in the ball climbing the incline until the force applied to the ball equals the component of gravity that is trying to roll the ball towards the centre of the bowl. The point of equilibrium will depend on the angle of incline and therefore it can be seen for a bowl with a lower positive rate of change of slope the ball will move

further in the horizontal direction than a ball would in a wine glass which exhibits a larger positive rate of change of slope. The ball will stop in both cases at the same angle of inclination; the angle which will create equilibrium and equal the force applied to the ball. In the spine the size of the neutral zone will depend on the inherent laxity of the disc and ligaments of the individual under examination. The laxity, and thus the extent of the neutral zone of these structures will depend on various factors such as age, level of spinal degeneration, activity levels, repetitive cyclic loading and the presence of high speed trauma.

White and Panjabi (1990) presented the neutral zones of the cervical spine in multidirectional loading (Table 3-4). The neutral zone of each spinal segment shows a strong correlation to the total motion provided by the segment; if the segment provides a significant range of motion, the neutral zone is also larger. The opposite is also true. In order to provide larger ranges of motion the disc and ligaments must accommodate larger distances between points of attachment and therefore the neutral zone is inherently larger since it takes more motion before the laxity of the structures are taken up.

**Table 3-4: Neutral zones of the cervical spine under multidirectional loading (White & Panjabi, 1990)**

| | C0-C1 | C1-C2 | C2-C3 | C3-C4 | C4-C5 | C5-C6 | C6-C7 |
|---|---|---|---|---|---|---|---|
| Flexion | 3.0 ± 1.0 | 4.0 ± 2.4 | 0.7 ± 0.6 | 0.3 ± 0.5 | 1.8 ± 1.3 | 1.8 ± 1.3 | 1.0 ± 0.7 |
| Extension | 13.9 ± 4.1 | 8.7 ± 6.7 | 1.0 ± 0.7 | 1.7 ± 1.7 | 1.9 ± 1.8 | 2.1 ± 2.0 | 1.3 ± 1.0 |
| Axial rotation | 2.5 ± 1.6 | 39.6 ± 7.5 | 1.1 ± 0.5 | 1.6 ± 0.5 | 2.4 ± 0.6 | 1.7 ± 0.5 | 0.6 ± 0.3 |
| Lateral bending | 3.6 ± 1.5 | 2.4 ± 1.2 | 4.1 ± 1.1 | 4.4 ± 1.2 | 4.4 ± 1.1 | 3.0 ± 1.1 | 2.2 ± 1.0 |

Values are mean ± standard deviations. Values for axial rotation and lateral bending sum both right and left sides.

It can also be seen that the neutral zones of the cervical spine are distinct for both the upper and lower cervical spine. This difference can be clearly seen in Figure 3-5.

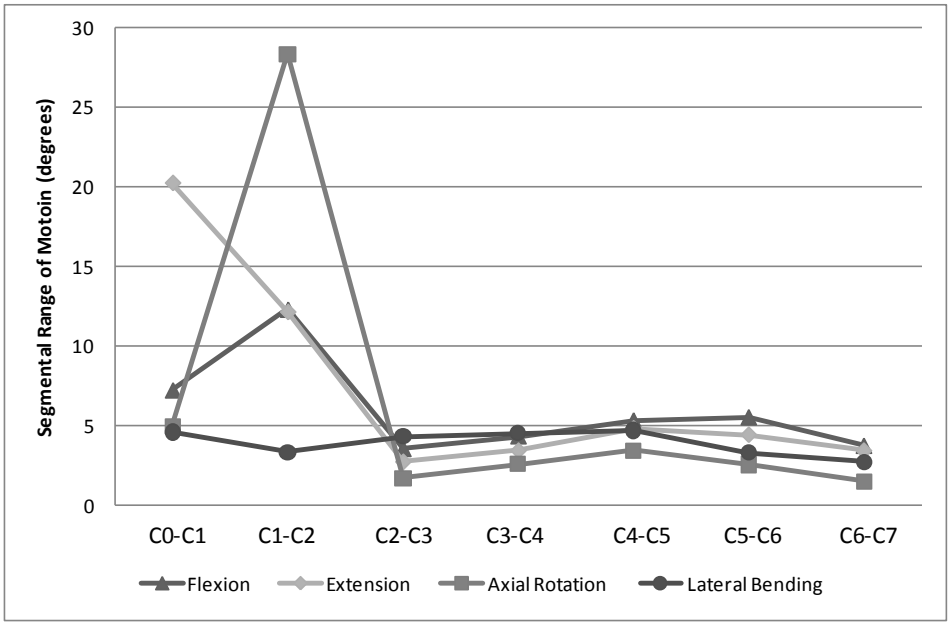


**Figure 3-5: Neutral zones of the motion segments of the cervical spine**

The spatial characteristics of the neutral zone closely mimic those observed in the overall ranges of motion. It is apparent that the range of motion and neutral zone are interdependent due to the physical characteristics of both high mobility and low mobility joints. It is important to note that the motion segments of the lower cervical spine (C2-C7) all exhibit similar ranges of motion and neutral zones.

Oxland & Panjabi (1992) studied the relation between the magnitude of the neutral zone and injury of the spinal motion segment. Porcine spinal segments were subjected to sequential amounts of soft tissue injury while the neutral zone, elastic zone and overall range of motion were monitored. It was found that the size of the neutral zone was the first parameter to exhibit significant differences even with only a few observable anatomic lesions on the specimens. After this onset of spinal injury it was again the neutral zone which observed an increase when the intersegmental motion again increased due to subsequent injury. The neutral zone was the most sensitive parameter in the definition of the onset and progression of spinal injury and thus may be of interest in the diagnosis of spinal segment damage and degeneration.

The stiffness of spinal segments is often expressed in terms of a flexibility coefficient which defines the amount of flexion of the spinal segment in degrees in response to the application of a bending moment. The unit of this coefficient is °/Nm. Several studies (Berkson *et al*, 1979; McGlashen *et al*, 1987; Moroney *et al*, 1988; Panjabi, Brand & White, 1976; Schultz *et al*, 1979; Tencer *et al*, 1981; Tencer *et al*, 1982) have included the calculation of this parameter for all regions of the spine; a summary of the data can be seen in Table 3-5.

**Table 3-5: Average flexibility coefficients of the motion segments of the spine**

| Spinal Region | Flexion | Extension | Lateral Bending | Axial Rotation |
|---|---|---|---|---|
| Cervical | 2.33 | 1.37 | 1.47 | 0.86 |
| Thoracic | 0.45 | 0.36 | 0.36 | 0.40 |
| Lumbar | 0.74 | 0.48 | 0.57 | 0.20 |

(Note: The units are degrees of rotation per Nm applied [°/Nm])

It can be seen that the cervical spine exhibits the largest flexibility coefficients, followed by the lumbar spine, with the thoracic spine having the lowest flexibility coefficients. Again the distribution of the flexibility coefficients are dependent on the range of motion of the spine, with the region of the spine providing the largest amount of motion also having the largest flexibility coefficient which represents the lowest stiffness. Again this can be related to the anatomical laxity of the spinal segments in the region with those having to provide larger ranges of motion having higher laxity and thus a larger neutral zone and therefore less resistance to separation of the attachment points of these structures. In addition, typical spinal motion is a combination of one or more of these individual motion components and thus these flexibility coefficients will also interact during such motions.

### 3.1.4 Instantaneous Centre of Rotation

The instantaneous centre of rotation (ICR), also known as finite axes of rotation, or instantaneous axis of rotation, represents the centre of the arc upon which the movement of each vertebra occurs about. A generic representation of the ICR of a generic vertebral body can be seen in Figure 3-6. In the physical sense the ICR represents the unique location where the body that is undergoing rotation could be pinned and still observe the same overall motion.

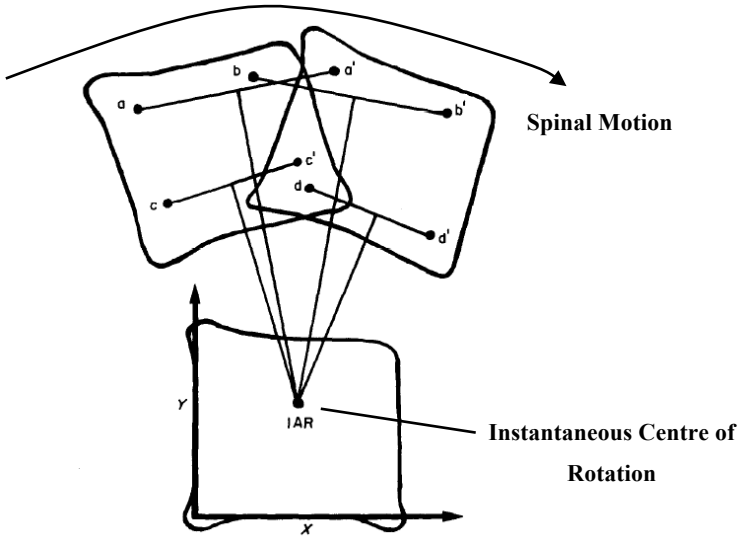


(Adapted from Galbusera *et al*, 2008)

**Figure 3-6: Instantaneous centre of rotation of the vertebrae**

The intervertebral motion of the spine occurs in all three planes and thus there exist three ICR; one in flexion-extension, one in lateral bending and one in axial rotation. At the present time there is less information regarding the instantaneous centers of rotation in lateral bending or axial rotation, with most of the motion studies focusing on flexion-extension motion. Since most natural spinal motion is a combination of one of more of these motions, a more complex three dimensional description of the relative motion between two vertebrae can be provided by the helical axis of motion. The helical axis (Figure 3-7) includes a simple screw motion which is described by a rotation about and a translation along a single unique axis in a three dimensional space. The compilation of the helical axis for complex spinal motion requires significant accuracy in motion measurement and is typically obtained using cadaveric studies where accurate placement of the motion markers can be accomplished.

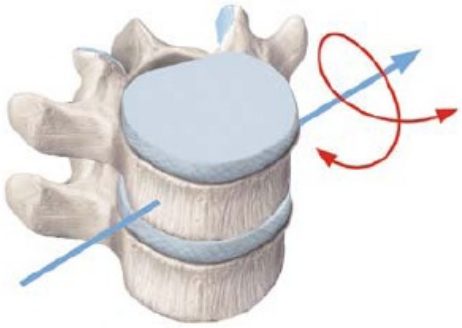

(Reproduced from Boos and Aebi, 2008)

**Figure 3-7: Representation of the helical axis**

The ICR is also load dependent and is therefore a transient parameter due to the interaction of the posterior elements including the facet joints as well as the various spinal ligaments. Since these components only interact at higher levels of extension, lateral bending and rotation, their effect on the ICR varies greatly.

It is also known that spinal degeneration can significantly alter the location of the ICR (Boos & Aebi, 2008). Knowledge of the location of the ICR of spinal segments in each region of the spine is of importance for the design of future spinal implants, as this parameter describes the motion observed at each level. The accommodation of the natural ICR is important to maintain natural load sharing and to prevent the accelerated degeneration of the other articulations of the spinal segment.

### 3.1.5 Cervical Spine

In the cervical spine the ICR in flexion-extension is generally located below the respective vertebral bodies (Figure 3-8). Moving inferiorly from the superior direction, the axis of rotation in flexion-extension is located higher and closer to the intervertebral disc of the vertebrae.

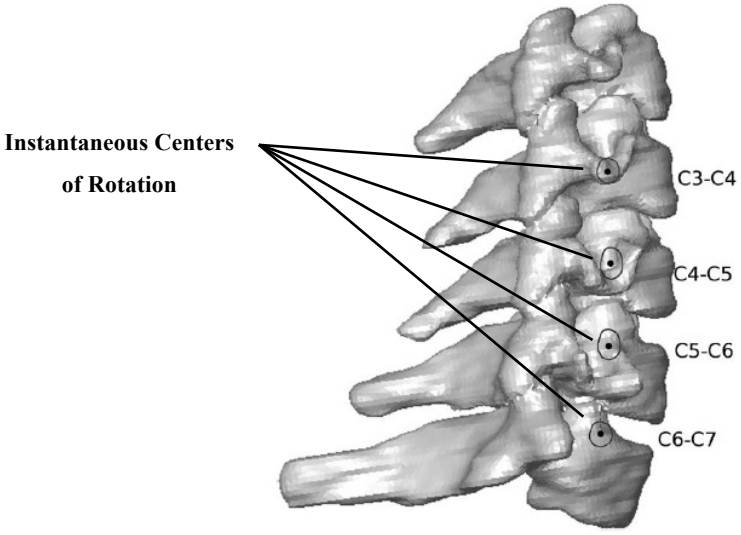


(Adapted from Amevo *et al*, 1991)

**Figure 3-8: Instantaneous centers of rotation of cervical vertebrae in flexion-extension**

Penning (1978) was one of the first to study the approximate normal movements of the cervical spine using tracings of the cervical spine using the end positions of flexion extension movements. Amevo, Worth and Bogduk (1991) further studied this motion using a series of radiographs during motion to determine the distribution of the location of the ICR in the cervical spine using radiographs of 40 normal subjects in flexion and extension. The results (Figure 3-9), allowed for the formal definition of the mean ICR location as seen as a white dot as well as the normal physiological range of locations for the ICR as seen in black shaded areas. The results of this study also show that the ICR location tends to migrate towards superior end plate of the inferior vertebral body moving from the upper cervical spine to the lower cervical spine. At the C5-C6 level the ICR is located just under the superior endplate of the C6 vertebral body.

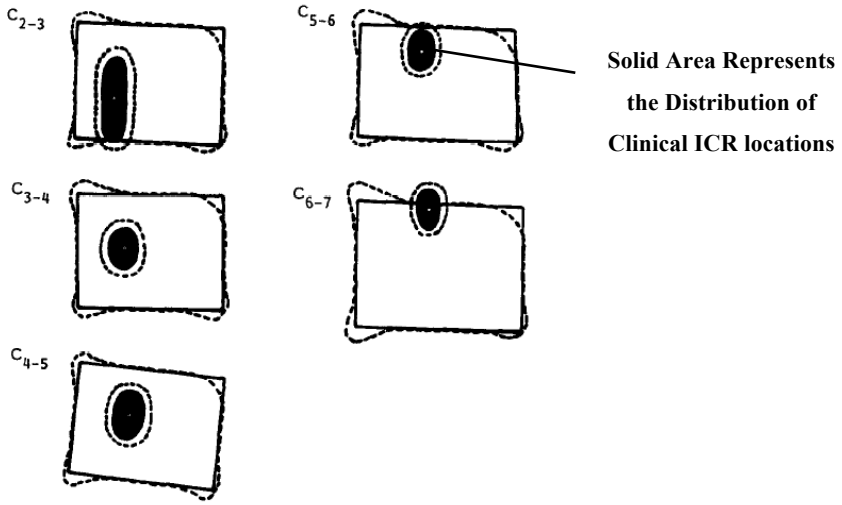


(Adapted from Amevo, Worth and Bogduk, 1991)

**Figure 3-9: Distribution of ICRs in the cervical spine**

The influence of the loading on the location of the ICR was studied by Galbusera *et al* (2006) for a healthy intact C5-C6 segment. The polar coordinate system used to identify the location of the ICR (Figure 3-12) includes a vector length ρ and an angle θ which reference the origin P which is positioned at the centre of the superior vertebral endplate defined at a distance L/2 from the posterior margin of the vertebral body. The results of the study can be seen in Table 3-6.

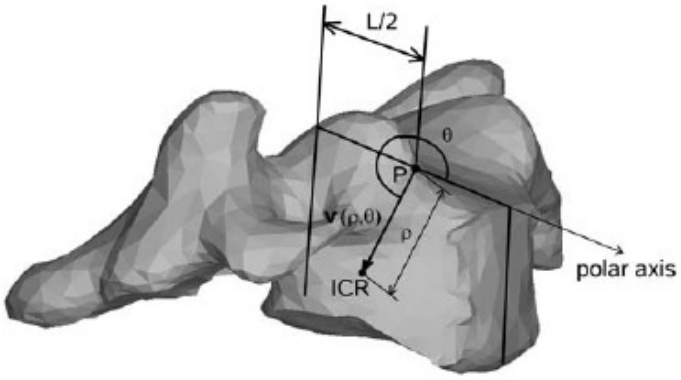


(Adapted from Galbusera *et al*, 2006)

**Figure 3-10: Method to quantify the position of the ICR of cervical vertebra**

**Table 3-6: ICR locations of the C5-C6 intact disc motion segment under flexion-extension loading**

| | Applied Moment (Nm) | P (mm) | ϴ (°) |
|---|---|---|---|
| Extension | -1.8 to -1.35 | 3.8 | 320 |
| | -1.35 to -0.9 | 3.5 | 300 |
| | -0.9 to -0.45 | 3.5 | 280 |
| | -0.45 to 0 | 3.2 | 260 |
| | Extension Mean | 3.5 | - |
| Flexion | 0 to 0.45 | 3.0 | 250 |
| | 0.45 to 0.9 | 3.2 | 250 |
| | 0.9 to 1.35 | 3.3 | 250 |
| | 1.35 to 1.8 | 3.3 | 250 |
| | Flexion Mean | 3.2 | - |
| | Overall Mean | 3.3 | - |
| | Overall Std. Deviation | 0.24 | - |

(Data Summarized from Galbusera *et al*, 2006)

The average location of the ICR in flexion and extension is found at ρ =3.2 mm and ρ =3.5 mm at angles ϴ=250° and ϴ=290° respectively. The ICR exhibits more migration in extension than in flexion (Figure 3-11); low applied extensive bending moments result in an anterior location of the ICR which progressively moves towards the posterior as the moment is applied. The ICR in flexion is much more consistent with the average location in flexion being located very closely to the individual data points.

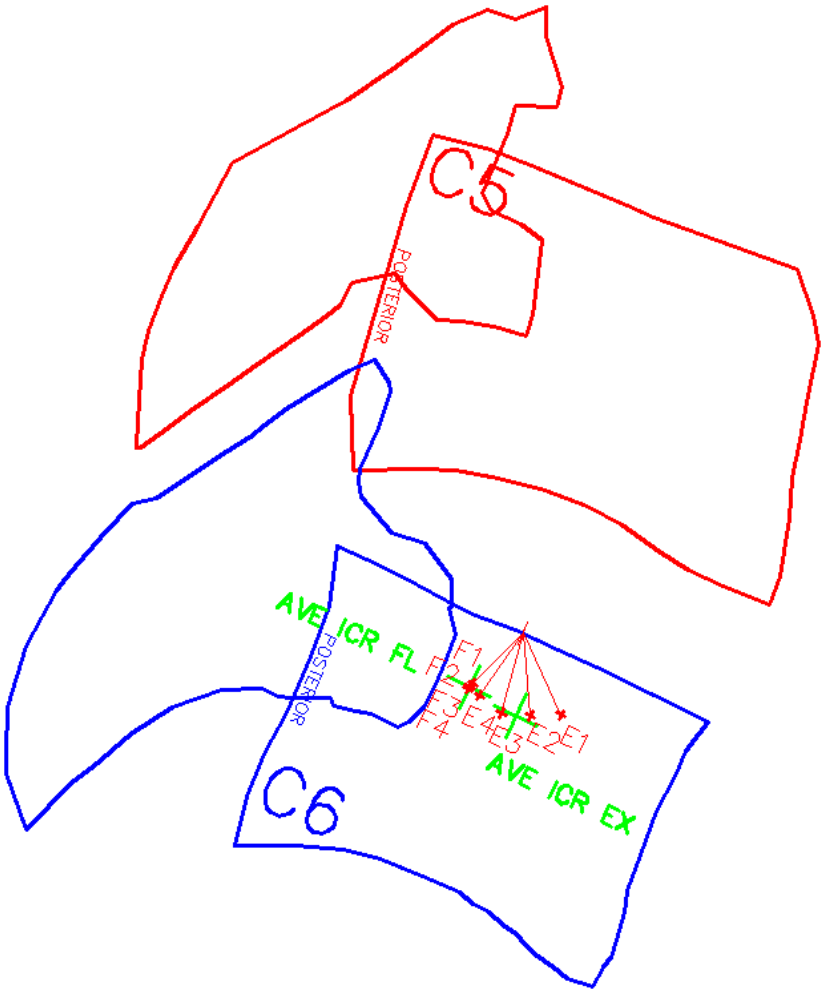


(E1-E4 and F1-F4 represent the movement of the ICR in progressive extension and flexion respectively, AVE denotes average location)

**Figure 3-11: Transition of the ICR of the cervical spine in flexion and extension**

The increased migration of the ICR in extension is expected since the posterior elements play more significant role in extension than flexion that will result in a modification of the centre of rotation. The contact of these elements will only allow translation in the plane of contact. For small levels of extensive loading the centre of rotation is towards the anterior because the only motion controlling structure is the disc which is positioned towards the anterior of the motion segment. As the loading increases and the posterior elements begin to make contact and influence motion the ICR moves towards the posterior as the motion is controlled by both the anterior disc and the posterior elements and thus the motion is more posteriorly centered.

The ICR of the cervical spine in pure lateral bending is located within the superior, moving vertebral body. It is important to note that the uncovertebral joints are both located on the radius of a circle centered on the ICR thus revealing the physiologic importance of these joints and their ability to provide some translation at their point of interaction.

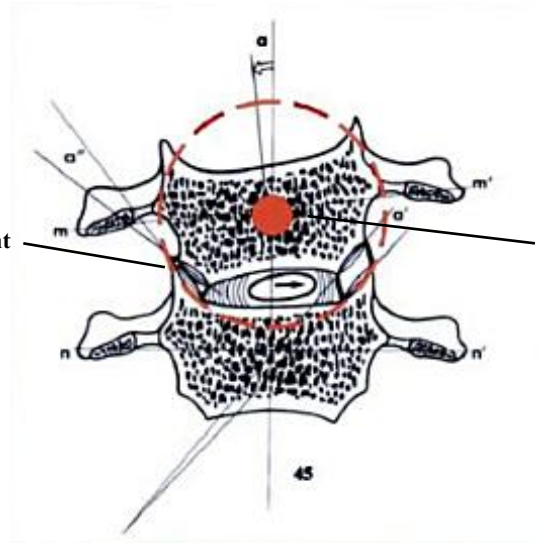


(Adapted from Kim *et al*, 2006)

**Figure 3-12: Instantaneous centre of rotation of cervical vertebrae in pure lateral bending**

In pure axial rotation of the cervical spine the ICR is estimated to occur along the sagittal plane somewhere along the midline of the intervertebral disc (Figure 3-13).

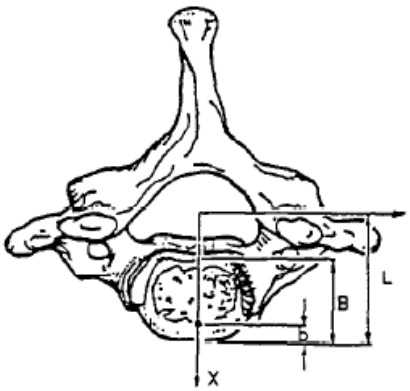


(Reproduced from Myers *et al*, 1989)

**Figure 3-13: Location of the ICR (b) for the cervical spine in axial rotation**

The mean center of rotation was found by Myers *et al* (1989) using cadaver studies to be located at a point approximately 1/5 the length of the vertebral body from the anterior edge (i.e. b/B=0.20). It is important to note that large flexion-extension moments and anterior posterior shear forces were also observed simultaneously during axial rotation.

Due to the inherent motion coupling of lateral bending and axial rotation motion that is observed in the cervical spine that is a direct result of the inclination of the facet joints, the validity of the ICR locations in pure lateral bending and axial rotation are of arguable validity. Since lateral bending and axial rotation always occur simultaneously in the cervical spine, the use of a helical axis to describe this type of motion is necessary for the accurate representation of these motions.

Recent developments in three dimensional coordinate measurement systems have allowed for much more detailed data acquisition on the coupled motion of the cervical spine rather than relying on the combination of two dimensional data to infer results. This improved method allows for the complete description of the composite motion as a rotation about, and translation along, the helical axis in three dimensional coordinates. Penning and Wilmink (1987) postulated that the axis of composite motion is approximately perpendicular to the plane of the facet joints, and therefore used computed tomograms of the articulating bodies along this proposed axis to construct the location of the composite axis. This resulted in an axis which passed obliquely through the superior vertebral body of the motion segment from the anterior edge of the inferior endplate to the posterior corner of the superior endplate in the sagittal plane.

In order to define the location of the composite axis, the relationship to physiological landmarks must be used. The parameters used to describe the locations (Figure 3-14) include the axis to mid-sagittal angle (E), the axis to mid-sagittal position (A), the axis to disc angle (ADA), the axis to disc position (ADP), the axis to facet angle (AFA) and the anterior disc height (IVDA).

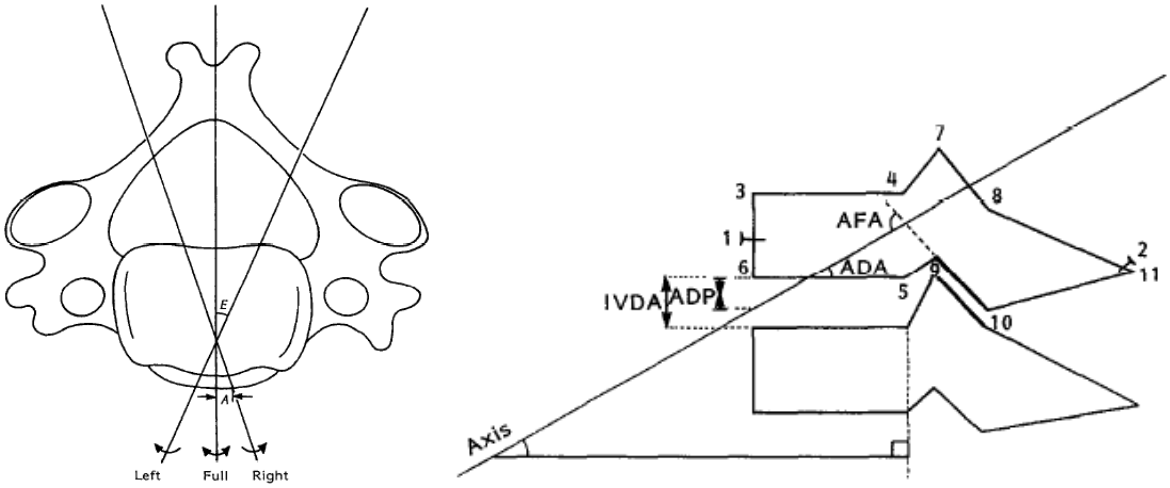


(Reproduced from Milne, 1993)

**Figure 3-14: Composite (or helical) axis in transverse plane (left) and sagittal plane (right)**

The results of the study showed that the helical axis lies very close to the sagittal plane when the radiographs from the extreme left and right positions were analyzed. For unilateral motion to one side only, and thus comparison of the extreme left or right position with the neutral position, the composition axis was found to pass on the opposite side of the mid-line of the anterior edge as the direction of motion. The angle was dependant on whether the primary motion was axial rotation or lateral bending. Therefore motion to the right resulted in the axis passing through the anterior edge of the vertebral body on the left side of the sagittal mid line.

In the lateral projection the location and angle of the composite axis was also found to depend on the type of primary motion with lateral bending resulting in shallower axis to disc angles than axial rotation (Figure 3-15).

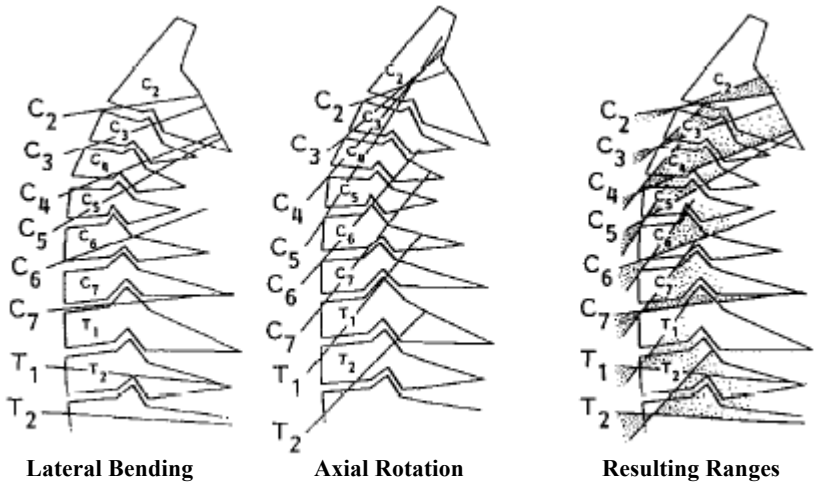


(Adapted from Milne, 1993)

**Figure 3-15: Lateral view of the axes of composite motion**

The composite helical axis of the C5-C6 spinal level in particular can be seen in Figure 3-16 in both the lateral (left) and axial (right) planes. Note that the axis passes through the right side of the anterior edge of the disc for both axial rotation and lateral bending to the left.

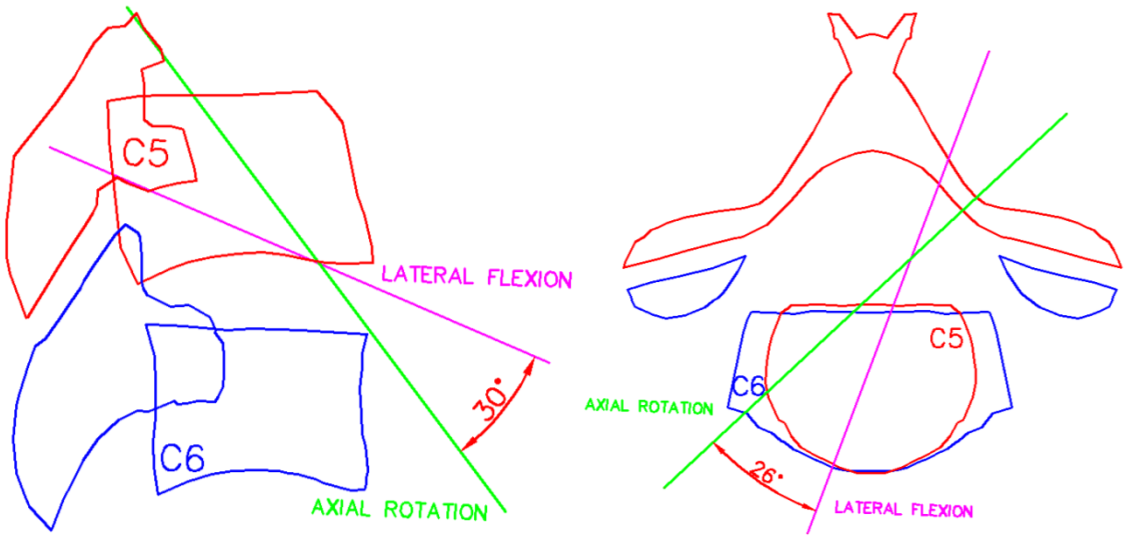


**Figure 3-16: C5-C6 helical axis for leftward axial rotation and lateral bending**

The angle of inclination from the anterior-posterior direction in the lateral view and the sagittal plane in the axial view is greater for primary axial rotation motion than for lateral flexion. Thus the motion coupling ratio for axial rotation is greater than the motion coupling ratio for lateral bending. The axis also passes through the anterior part of the intervertebral disc and not through the inferior intervertebral body and projects up through the posterior edge of the superior intervertebral body. The fact that the axis passes through the disc may signify that the rolling like motion occurs about the helical axis in the hollow, bowl-like structure formed by the uncinate

processes and uncovertebral joints which function as a socket in which the superior vertebra rolls. It is also interesting to note that the anterior annulus of the cervical vertebra typically remains intact while the posterior region of the disc is universally fissured in adults. This may be because the anterior portion of the disc would observe relatively small amounts of intervertebral motion while the posterior section would observe more significant motions as the superior vertebral body pivots about the anterior of the inferior vertebral body as shown by the results of this study.

The angle between the helical axis and the facet joint contact plane (Figure 3-17) was close to 90° in the upper to middle cervical spine, with divergence from perpendicular occurring in levels below the C7 vertebra. The angle generated in axial rotation was larger than 90° and the angle during lateral bending was less than 90°. Surprisingly the average angle observed when both motions are taken into consideration is 90° and thus the average helical axis at the C5-C6 level is indeed perpendicular to the facet contact plane.

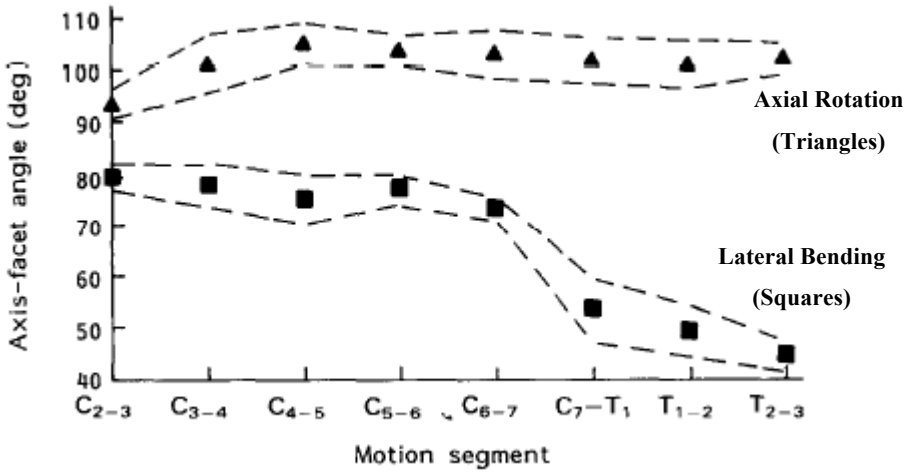


(Adapted from Milne, 1993)

**Figure 3-17: Helical axis - facet contact plane relative angles of the cervical spine**

Surprisingly there were no consistent sex differences in the location of the helical axis with the only age related parameter being the overall range of motion observed, with specimens over 50 years of age exhibiting a smaller range of motion than specimens from younger donors.

### 3.1.6 Thoracic & Lumbar Spine

In the thoracic and lumbar spinal regions motion coupling is not present due to the primarily vertical orientation of the facet joints and thus the ICR locations can be expressed for planar motion in flexion-extension, lateral bending and axial rotation (Figure 3-18).

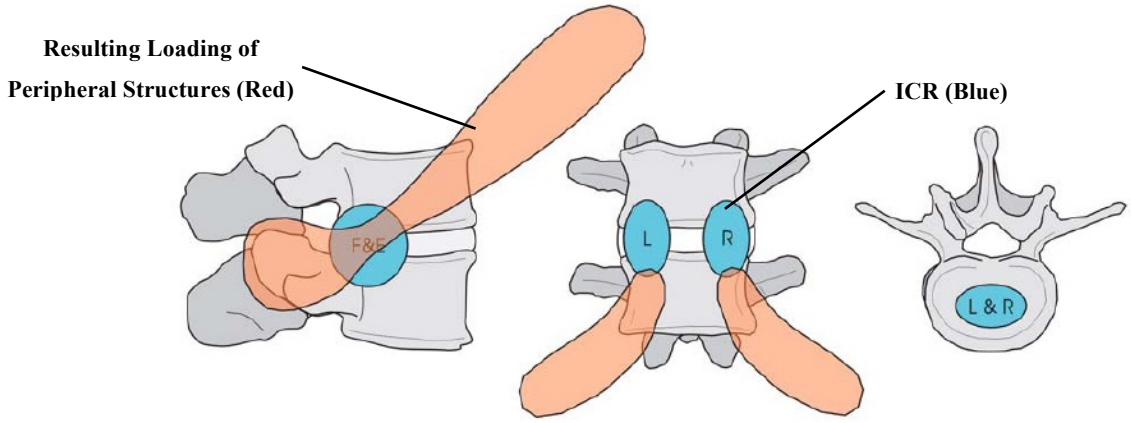


(Adapted from Boos and Aebi, 2008)

**Figure 3-18: Typical instantaneous centers of rotation for the thoracic and lumbar spine**

In the thoracic and lumbar spinal regions the ICR typically lies within the disc space for a healthy motion segment. The location migrates with progression of spinal degeneration as the flexibility of the motion segment is reduced and the stiffness increases. The location of the ICR in these regions is similar for pure axial rotation, but varies significantly for flexion-extension motion with the ICR being located much more superiorly and towards the posterior of the intervertebral end plate. Lateral bending occurs about the ICR, which is located in the disc space and not in the superior intervertebral body as in the cervical spine, thus the lumbar and thoracic spine does not tend to rotate within a socket (like in the bowl created by the uncovertebral joints) as in the cervical spine.

There are significant differences in motion between the cervical spine and the lower regions of the spine due mainly in part to the orientation of the facet joints as well as the presence of the uncovertebral joints in the cervical region.

## 3.2 Physiological Loading of the Spine

The loading of the spine is produced both by gravitational forces acting on the elements that are supported by the spine and the muscle forces which actuate the motion thereby further increasing the applied loading of the spine. Loading of the ligaments at the end limits of motion can also contribute significantly to the loads observed in the spine. The type of deformation observed in the disc depends on the loading state. For example, axial loading may be symmetric causing the disc to be compressed somewhat uniformly in the vertical direction or asymmetric which can cause tension on one side and compression on the other side of the disc. While it is common for the disc to experience loading in several states simultaneously, experimental data is typically obtained independently for each loading state and therefore will also be investigated separately in the present proposal.

Direct measurement of spinal loading is not possible due to the associated difficulty in the insertion of force metering devices. Therefore the loads of the spine are often estimated by recording the internal disc pressure Nachemson (1960b) or the forces acting on internally mounted spinal fusion hardware (Rohlmann *et al*, 2000). Spinal loading can also be estimated using computer models which incorporate the electromyographic activity of the spinal and trunk muscles and applying the resulting muscle forces to a three dimensional model for a variety

of different physical activities. This method can introduce error due to variability in geometry and muscle forces and thus provides an estimation of the spinal forces.

The magnitude of the applied loading to the spine increases in the caudal direction as the distance from the cranial aspect increases; this is mainly due to the increased gravitational body forces and the higher muscle loading that accompanies these body forces. The lumbar spine observes the highest applied loading and the highest incidence of damage and degradation. Thus, it has been subjected to the most extensive scrutiny and as a result the prevalence of spinal loading data is greatest for the lumbar spine.

Motion during loading increases the local muscle activity thereby increasing the spinal loads in comparison to static loading scenarios. During walking, loads in the lumbar spine can exceed 2.5 times the body weight (Cappozzo, 1984), which is a direct result of the inertial forces acting on the mass of the body above the lumbar spinal region.

It should be noted that the behavior of the lumbar spine under load is expected to be somewhat similar to that of the thoracic or cervical spine except that the loads are decreased in those regions and the dimensions of the discs will also be reduced proportionately. Therefore the results of this investigation are expected to be somewhat applicable to the entire spine due to the similar geometries and loading conditions. Shultz et al (1982) have studied the loads at L3 in the lumbar spine (Table 3-7) as a result of several different positions and activities. The range of physiological loads is estimated to vary between 340 and 2350 N.

**Table 3-7: Compressive loading at the L3 level of the lumbar spine**

| Activity | Load (N) |
|---|---|
| Standing | |
| Relaxed | 440 |
| Resisting horizontal forces | |
| Flexion | 1190 |
| Right lateral bending | 710 |
| Extension | 470 |
| Right twisting | 620 |
| Upright, arms in, holding 8 kg | 650 |
| Upright, arms out | 460 |
| Upright, arms out, holding 8 kg | 1170 |
| Flexed 30°, arms out | 1400 |
| Flexed 30°, arms out, holding 8 kg | 2350 |
| Sitting | |
| Relaxed | 380 |
| Resisting horizontal forces | |
| Flexion | 1130 |
| Right lateral bending | 730 |
| Extension | 530 |
| Right twisting | 590 |
| Weight-holding with right hand | |
| Position A, holding 0 kg | 340 |
| Position A, holding 4 kg | 700 |
| Position B, holding 0 kg | 370 |
| Position B, holding 4 kg | 670 |
| Position C, holding 0 kg | 340 |
| Position C, holding 4 kg | 750 |
| Position G, holding 0 kg | 340 |
| Position G, holding 4 kg | 640 |
| Position I, holding 0 kg | 350 |
| Position I, holding 4 kg | 530 |

(Reproduced from Shultz *et al* (1982)

The highest loads are observed by the spine during lifting due to both the increased mass that must be carries by the spine, but also the increased muscle forces that must accommodate the bending moment of the object being lifted since it is typically not directly above the spine but is located in front of the torso. Loads during lifting are proportional to the mass of the object being lifted and can be extremely high; potentially approaching the failure load of a single vertebrae which has been estimated to be somewhere between 5000 and 8000 N in the lumbar spine. The vertebral endplate is the weak link and thus will often fail before the intervertebral disc. Micro-damage of the endplate may occur during heavy loading; this damage can potentially be repaired whereas damage to the disc would be generally irreversible. Therefore initial damage to the bony endplate is desired due to the ability of the body to repair the damage in between loading (Hasegawa *et al*, 1993).

Physiological loading of the cervical spine for were presented by White and Panjabi (1990) as a function of intradiscal pressures by incorporating the cross sectional area of the intervertebral discs and the applied compressive force (Figure 3-19). The intradiscal pressures for this data were obtained from Hattori *et al* (1981) who postulated that the standard upright position imposes 75 N of loading on each level of the cervical spine and Moroney *et al* (1998).

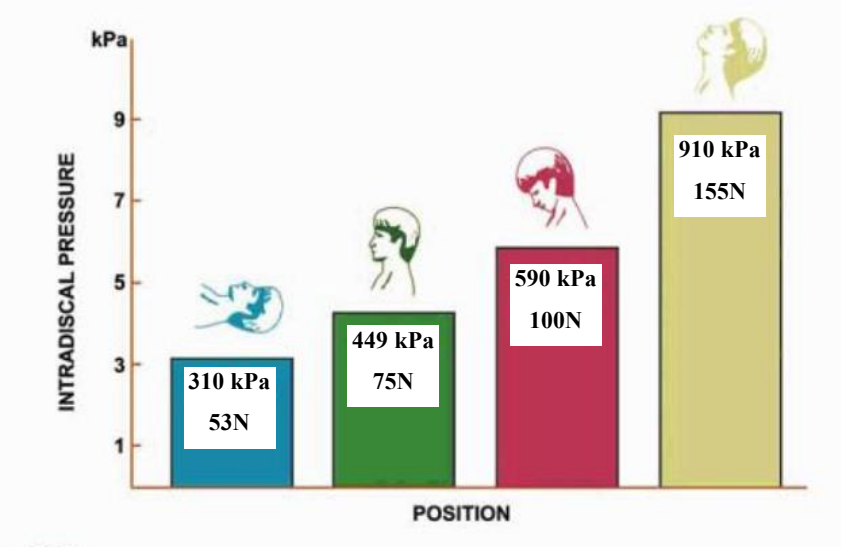


(Adampted from Panjabi and White, 1990)

**Figure 3-19: Cervical intradiscal pressures and estimated forces for physiological positions**

For the cervical spine, a somewhat similar study by Moroney *et al* (1998) estimated the loads acting on a seated person when moving to their motion limits (Table 3-8). It is expected that the normal loadings observed during daily activities involving smaller motions would be significantly lower. The loading of the cervical spine is somewhat lower than that of the lumbar spine with the compressive load varying between 122 and 1164 N.

**Table 3-8: Mean loads of motion segment at motion limits under maximum voluntary loading**

| Activity | Lateral Shear (N) | Anteroposterior Shear (N) | Compression (N) |
|---|---|---|---|
| Relaxed | 0 (0) | -2 (1) | 122 (36) |
| Left Axial Rotation | 33 (8) | 70 (24) | 778 (228) |
| Extension | 0 ( 0) | 135 (69) | 1164 (494) |
| Flexion | 0 ( 0) | 31 (63) | 558 (375) |
| Left Lateral Bending | 125 (58) | 93 (59) | 758 (422) |

(Standard deviation in parenthesis; Data from Moroney *et al*, 1998)

It is important to note that these values represent the total loading observed by the spinal motion segment and that these loads are resisted in tandem by all of the articulating joints of the spine. Compressive loads are resisted by both the intervertebral disc and the facet joints. Goel *et al* (1998) studied the load sharing between the disc and facets of a C5-C6 motion segment using finite element methods; the results of which can be seen in Table 3-9.

**Table 3-9: Predicted loads transmitted through the disc and facets of C5-C6 motion segment**

| **Structure** | **Comp. 73.6 N** *Compression* | **Comp. & 1.8 Nm** *Flexion* | **Comp. & 1.8 Nm** *Ext.* | **Comp. & 1.8 Nm** *Left Axial Rot.* | **Comp. & 1.8 Nm** *Right Axial Rot.* |
|---|---|---|---|---|---|
| R. Facet Force (N) | 4.2 | 0 | 37.6 | 27.6 | 29.9 |
| L. Facet Force (N) | 4.2 | 0 | 37.6 | 0 | 0 |
| Disc Force (N) | 65.2 | 83.3 | 10.4 | 54.9 | 50.1 |
| Intradiscal Pressure (MPa) | 0.19 | 0.32 | 0.08 | 0.19 | 0.15 |

(Disc force includes the compressive forces in the nucleus, ground substance and uncinate processes)

(Data adapted from Goel et al., 1998)

The results of the load sharing study can be presented as a percentage of the applied loading that each component is subjected (

Table 3-10). This allows for the application of the data for other applied spinal loads in similar modes of motion.

**Table 3-10: Compressive load sharing of articular facets and disc of C5-C6 motion segment**

| Structure | Compression | Comp. & Flexion | Comp. & Ext. | Comp. & L. Axial Rot. | Comp. & R. Axial Rot. |
|---|---|---|---|---|---|
| R. Facet (%) | 6 | 0 | 51 | 37 | 41 |
| L. Facet (%) | 6 | 0 | 51 | 0 | 0 |
| Disc (%) | 88 | 113 | 14 | 75 | 68 |

(Data adapted from Goel et al., 1998)

Panzer and Cronin (2009) studied the load sharing of the C4-C5 motion segment as a function of angular displacement also using a finite element model (Figure 3-20). The results showed that in axial rotation the facets carried less than 10% of the applied loading even under significant rotations, with the intervertebral disc responsible for most of the load transmission. In lateral bending the facets again carried a relatively small proportion; less than 12%. Under small rotations in flexion the disc carried most of the load, until after approximately 3 degrees of rotation after which the ligaments become the predominant load carrying structure. The facets did not observe any loading in flexion. In extension however the facets were the main load carrying structure for all degrees of rotation, and at higher levels of extension he disc transitioned from compressive to tensile loading.

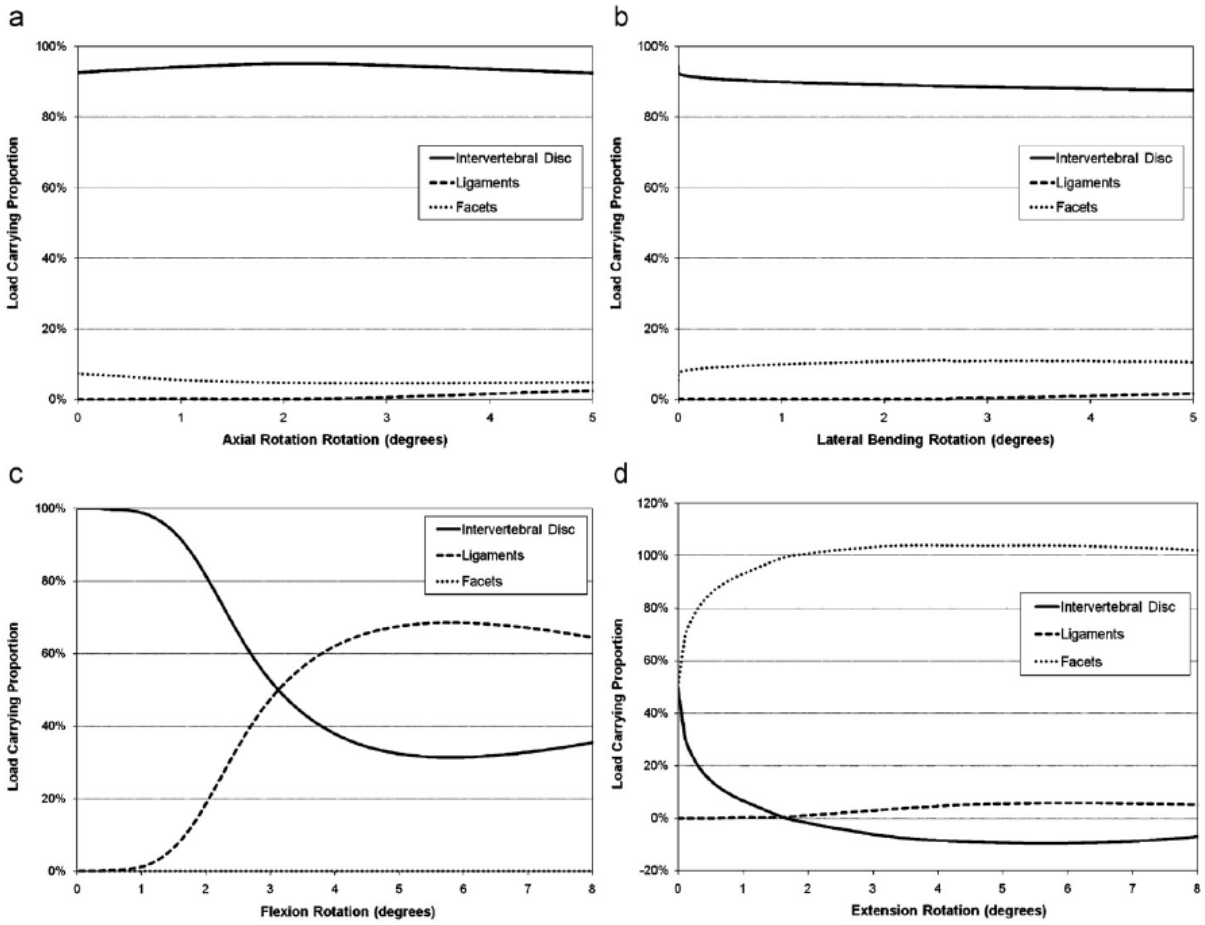


(a) Axial rotation, (b) lateral bending, (c) flexion, and (d) extension

(Reproduced from Panzer and Cronin, 2009)

**Figure 3-20: Load carrying proportion of the intervertebral disc, ligaments and facets**

In all cases the ligaments were generally not significantly loaded, with small amounts of forces being observed only near the end limits of motion. The results of this study show that the facets are important in load transfer primarily in extension and make a small contribution in axial rotation and lateral bending. In the other cases the disc remains the primary structure for load transfer in the cervical spine.

The deformation that results from loading of the cervical spinal motion segments has also been measured *in vitro*. Panjabi *et al* (1986) found that the anterior-posterior translation of a C5-C6 motion segment under a 50 N compressive load was 3.5 mm. Moroney *et al* (1998) observed a total translation of 0.52 mm under a 19 N compressive load.

# Chapter 4
# Degenerative Disorders

Degeneration of the spine typically includes degenerative disc disease, which can also include facet joint degeneration, disc herniation, nerve impingement and stiffening of the spinal motion segment. The results of spinal degeneration can include loss of normal disc mechanical function, severe tissue damage, pain and/or loss of sensation in the extremities, back/neck pain and paralysis to varying extents. The degenerative process is not necessarily a pathogenic process since spinal degeneration is almost universal in the adult population.

The degeneration of the spinal structures is commonly referred to as spondylosis which represents damage to the intervertebral discs, vertebrae as well as the other associated spinal joints including the facets. The results of spinal spondylosis can include central or foraminal stenosis which affects the nerve roots or spinal cord. These are termed spondylotic radiculopathy for impairment of the nerve roots and spondylotic myelopathy for the spinal cord.

## 4.1 Disc Degeneration

Most of the population over the age of 30 shows some signs of degeneration in the discs which may include a reduction in its height and/or a loss of osmotic pressure of the nucleus pulposus (Rohlmann *et al*, 2006). Additional changes that occur during the degeneration process include a loss of demarcation between the nucleus and annulus, a reduction of the nucleus rehydration ability as well as altered loading of the facet joints. The exact causes of disc degradation are currently unknown. Attempts to attribute this degradation to the normal loadings observed in the workplace and daily activities have typically been inconclusive but there has been some evidence to suggest that smoking and obesity may increase the rate of degeneration (Kurtz and Edidin, 2006). Genetic and environmental factors may also affect the rate of onset and the amount of disc degeneration that occurs. Also, poor blood flow and low cellular density of the disc can be considered contributing factors to the degradation process because the disc is unable to regenerate at a rate equal than or greater than the rate at which damage occurs.

Since an implant to replace the disc must withstand the *in vivo* conditions as well as mimic the natural structures, it is useful to consider the degradation of the individual components of the disc.

### 4.1.1 Nucleus Pulposus Degradation

The proteoglycans (Figure 4-1) of the nucleus pulposus are thought to be the first spinal component to be affected by the degradation process. The proteoglycans (PG) contribute to the generation of pressure within the nucleus by trapping water molecules within the Type II collagen fiber mesh in the long fibrous structure. When this structure is damaged or its presence is reduced, the ability of the nucleus to exert osmotic pressure is also reduced.

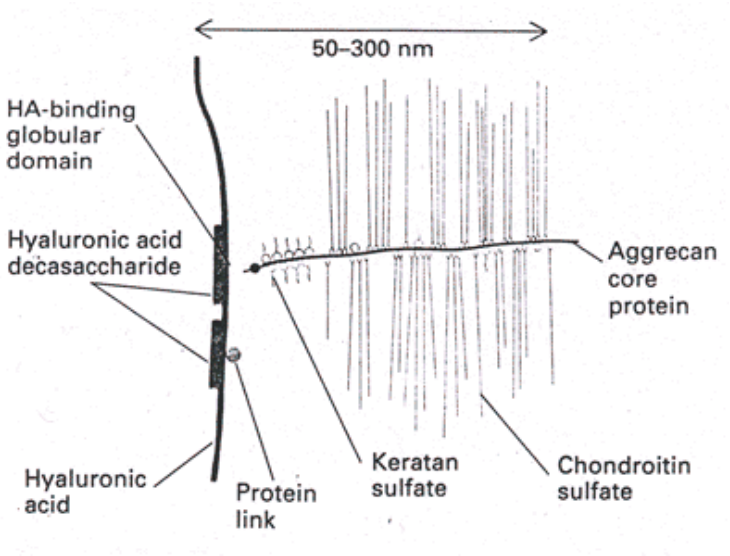


(Reproduced from Yogandan et al, 2000)

**Figure 4-1: Proteoglycan structure**

An investigation in the water content of the disc in both healthy and degraded nuclei has shown values of 90% for a healthy disc as compared to 70% for a degraded disc (Kurtz and Edidin, 2006). This reduction is expected to be a direct result of a decrease in PG content since as the disc ages the balance between synthesis and degradation is lost resulting in a net loss of PG within the disc. Analysis of degraded nuclei has also shown the presence of matrix metalloproteinase which are enzymes which are known to degrade proteins such as PG.

The reduced pressure of the nucleus modifies the loading pattern of the annulus (Figure 4-2) resulting in a bulging pattern on both the interior and exterior radial walls of the annulus fibrosis as well as an overall increase of the stress in the annular region.

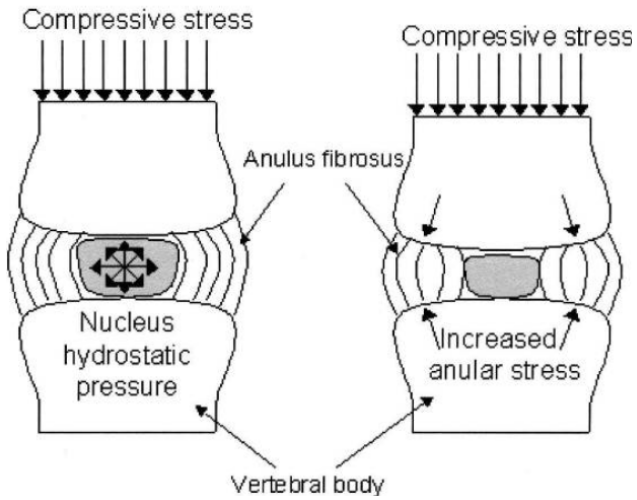


(Reproduced from Rohlmann *et al*, 2006)

**Figure 4-2: Modified loading pattern of the annulus due to decreased nucleus pressure**

Empirical evidence also shows a reduction in Type II collagen which explains a loss in compressive stiffness of about 0.4-1 MPa. In addition, the swelling pressure that can be exerted by the nucleus decreases from 1-2 MPa to approximately 0.03 MPa as a result of the reduced PG content of the nucleus (Kurtz and Edidin, 2006).

### 4.1.2 Annulus Fibrosis Degradation

As mentioned above, the annulus fibrosis of a degraded disc has been found to carry higher stress due to the reduced pressure of the nucleus, the typically organized structure of the annulus is also observed to become somewhat disorganized in the degraded state which may be a result of the increased stress. Furthermore, the presence of Type I collagen drops from 50% of the dry weight to 40% resulting in a loss of tensile loading capability and a reduction in the failure strain. It has also been observed that the Poisson's ratio of the annulus decreases by 50% from the healthy to degraded state which is expected to significantly alter the observed deformation of the annulus under applied loading (Kurtz and Edidin, 2006).

### 4.1.3 End Plate Degradation

In the post degeneration state the end plates have been observed to have reduced cartilage thickness and the presence of occlusion of the marrow canals which result in the inhibition of the migration of nutrients to the entire disc. Although the effects of this degradation on the mechanical response of the disc are not currently known, it is expected that the more significant influence of end plate degradation is the reduction in the pathway of nutrients and water through them to the disc.

### 4.1.4 Clinical Implications of Spinal Disc Degradation

The combined effects of disc degeneration result in an inability to differentiate the disc structural components and a loss in disc height (Figure 4-3).

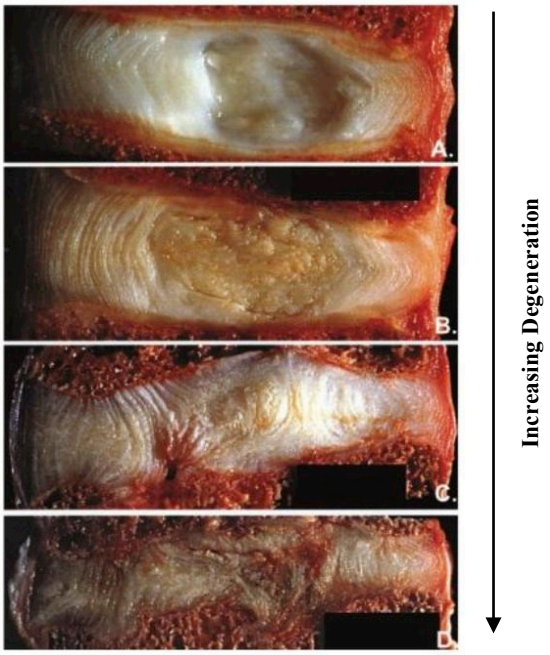


(Adapted from Kurtz and Edidin, 2006)

**Figure 4-3: Images of different grades of disc degeneration (A=healthy, D=degenerated)**

The net loss of disc height often causes the radial outer edge of the disc to bulge from between the adjacent vertebrae. Consequently, the nucleus pulposus may be extruded through the weakened annulus fibrosis and this is known as disc herniation. The loss of height and the bulging of the extruded nucleus pulposus often cause an impingement on nerves causing pain or numbness in the patient's extremities (Figure 4-4).

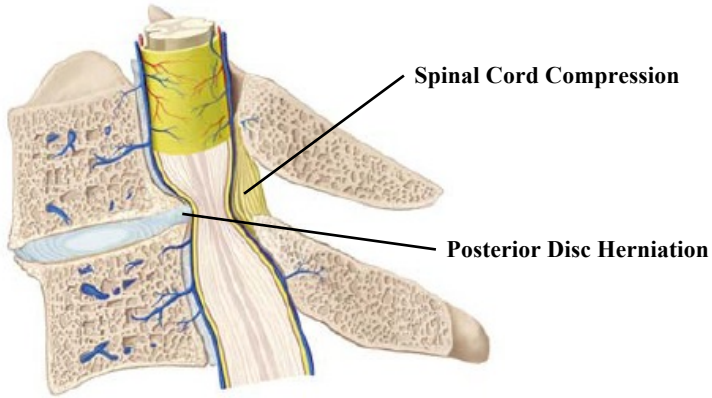


(Adapted from Boos and Aebi, 2008)

**Figure 4-4: Compression of the spinal cord in the cervical spine due to posterior disc herniation**

All of these conditions can occur in the cervical, thoracic, and lumbar regions of the spine and often include some level of damage to the spinal cord itself. Myelopathy initially shows itself as muscle weakness and or numbness and can progress to more severe disability including loss of muscle function and/or sensation.

In addition, the reduced vertebral spacing causes the increased loading and stressing of the facet joints which over time may progress to develop osteoarthritis. It has been estimated that a 1-mm decrease in disc height results

in a 36% increase in facet pressure, increasing to a 4-mm loss of disc height results in a 61% increase in facet pressure (Boos and Aebi, 2008). Due to the innervations of the facet joints, if the articular cartilage of the facet joints wears away due to increased loading there may be associated facet pain.

Some of the common forms of disc degeneration (Figure 4-5) include bulging, herniation, thinning and eventually the formation of osteophytes on the vertebrae adjacent to the damaged disc. Similar failure modes are known to occur in the cervical spine as well. The formation of osteophytes is the body's response to the joint damage as it attempts to strengthen the trabecular bone of the vertebra via increased bone formation. These osteophytes may also cause further nerve impingement giving both pain and dysfunction. Therefore, the osteophytes unwanted byproducts of the disc degeneration process.

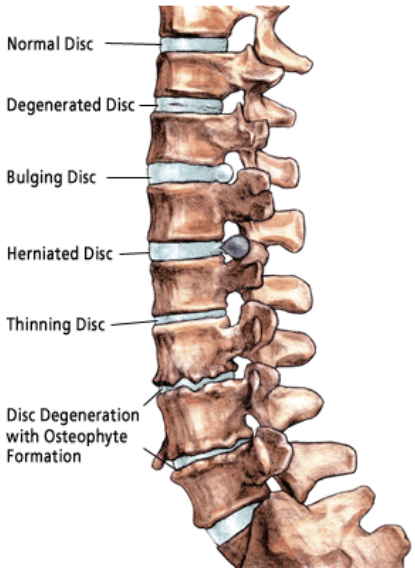


(Adapted from Orthopedics International, 2009)

**Figure 4-5: Examples of disc degeneration as shown in the lumbar spine**

It can be seen that disc degeneration has a significant impact on several aspects of spinal health. In Figure 4-6, a flow chart summarizing the overall disc degeneration process is taken from Phillips *et al* (2002). However, it should be mentioned that the starting point in the disc degeneration process is not likely to be simply abnormal stress. At a certain stage, abnormal stress does indeed occur, and so the flow chart does give the end part of the sequence, but there may be a number of types of initiators. These initiators may include impairment of nutritional pathways, fatigue, wear of facet joint surfaces, ligament laxity, various types of trauma and impaired muscle coordination.

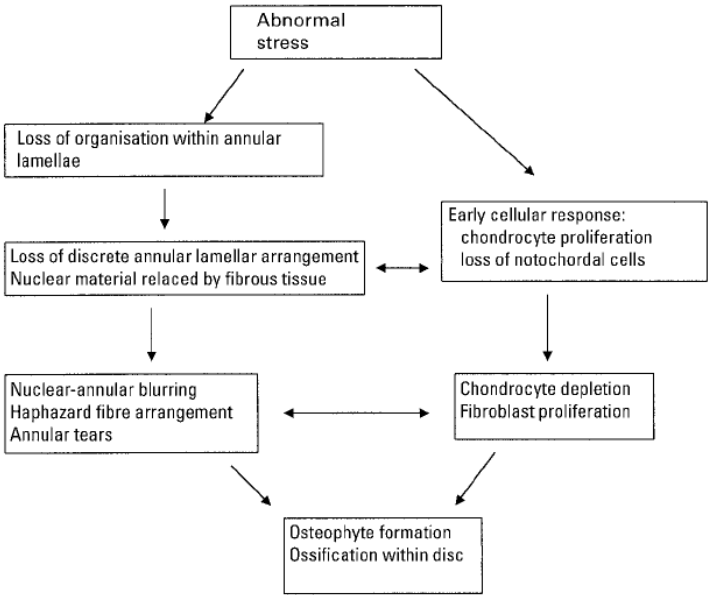


(Reproduced from Phillips *et al*, 2002)

**Figure 4-6: Disc degeneration flowchart**

## 4.2 Facet Joint Degeneration

The prevalence of back pain being related to and/or accompanying facet joint degradation is also significant in that approximately 70-75% of back pain sufferers are afflicted with problems of these joints (Kalichman and Hunter, 2007). It is estimated that in the cervical spine the facet joints are responsible for up to 62% of neck pain cases (Clark, 2005). The loads carried by the facet joints have been studied by several authors including Shirazi and Drouin (1987) and analysis of the relationship between disc degradation and facet joint damage have been performed (Fujiwara et al, 1999) to show that it is expected that in general disc degeneration precedes facet degeneration. Other studies (Kirkady-Willis *et al*, 1978) however have shown that the osteoarthritic changes in the facets occur simultaneously to degenerative changes in the intervertebral disc, which results in progressive modification of the functional spinal motion segment. A biomechanical study performed by Dunlop, Adams and Hutton (1984) in the lumbar spine showed that pressure between the facets increased significantly when the intervertebral disc space was reduced.

The morphological changes observed in the facet joints include varying levels of joint space narrowing, the formation of osteophytes (bony spurs at the edge of the cartilage surfaces), loss of cartilage and hardening of the joint structures including the cartilage and capsular ligaments. Four grades of lumbar facet joint degeneration can be seen in Figure 4-7.

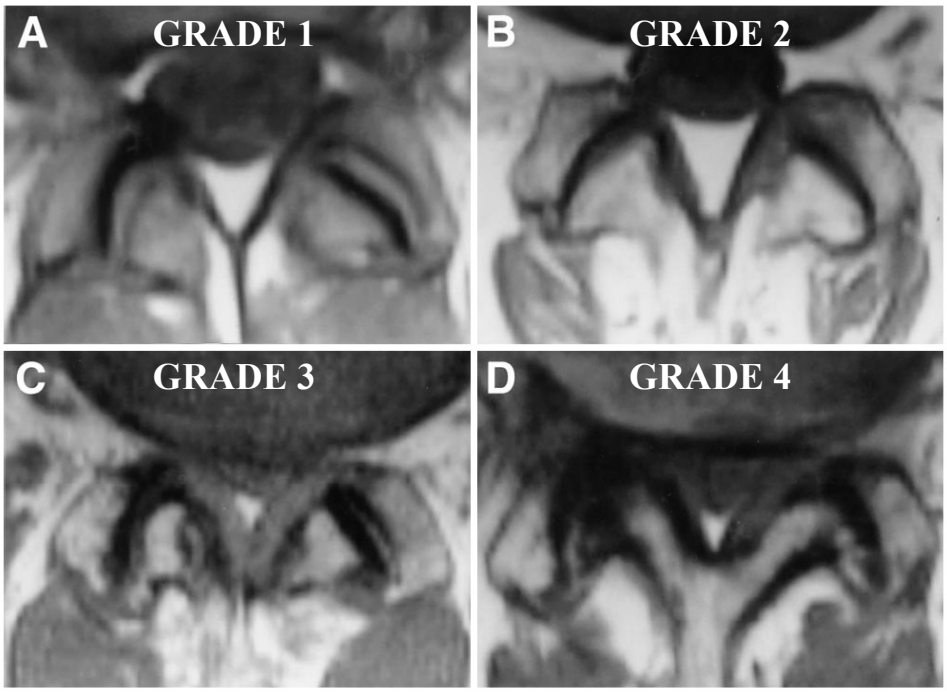


(Adapted from Fujiwara *et al*, 1999)

**Figure 4-7: Four grades of facet joint osteoarthritis**

Grade 1 represents normal facet joints showing not significant degenerative changes. Grade 2 represents mild facet joint degeneration and can include some joint space narrowing which may be accompanied by mild osteophyte formation. Grade 3 is moderate degeneration of the facets with the presence of sclerosis and/or moderate osteophyte formation around the articular surfaces. Severe degeneration of the facets is included in the Grade 4 assessment and includes marked osteophytes (Figure 4-8).

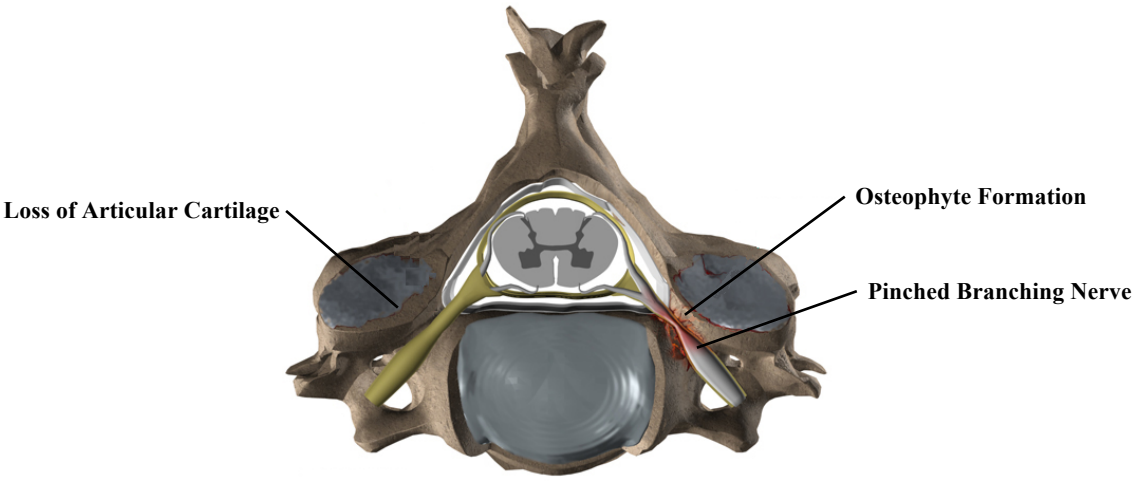


(Adapted from www.eorthopod.com)

**Figure 4-8: Morphology of grade 4 degenerated facet joints in the cervical spine**

The degeneration of facets also seems to have a strong correlation with age (Table 4-1). It seems that facet joints only show minor chondral changes before the age of 45 and experimental observations tend to support the postulation that, in most cases, the disc degenerates prior to the facets.

**Table 4-1: Mean age vs. prevalence of facet joint osteoarthritis (OA)**

| Study | Mean Age (yrs.) | Prevalence of Facet OA |
|---|---|---|
| Butler *et al* (1990) | 41.8 | 21% |
| Fujiwara *et al* (1999) | 46.8 | 38% |
| Pathria *et al* (1987) | 52.8 | 65% |

Since the disc clearly affects the biomechanics of the facets, the change in disc geometry causes the loads on the facets joints to increase. It is plausible to assume that the increased loads cause facet joint degeneration (Butler et al, 1990). However, the motion of the facet joints also changes as the disc degenerates and this may also cause or contribute to facet joint degeneration.

Although the general consensus in published data is that the facets tend to fail after the disc degenerates, the facets can become damaged prior to the disc due to trauma observed during a sporting event or a collision. In this case it is possible that one or more of the facets become damaged without severely affecting the disc. This may be accentuated at younger ages when the disc has not observed any degeneration and is therefore resilient enough to be subjected to the forces and range of motion required to damage the facet joints without sustaining any significant damage itself. However, in time, the disc may degenerate prematurely due to the loss of facet joint support and/or constraint. Several studies described by Clark (2005) implicate the facet joint as a site of painful injury in the neck with as many as 62% of neck pain cases arising from the facet joint. Although neck pain may not indicate irreversible disc or facet degeneration, there is the suggestion that facet joints are susceptible to trauma.

## 4.3 Stability of the Cervical Spine

The health of the cervical spinal column is closely related to the stability in the sense that degeneration or dysfunction of one or more structures of the spine can result in reduced control of overall motion of the spine. The spinal stability system has been postulated to consist of three separate but functionally interdependent subsystems; the passive and active musculoskeletal systems, and the neural feedback system (Figure 4-9).

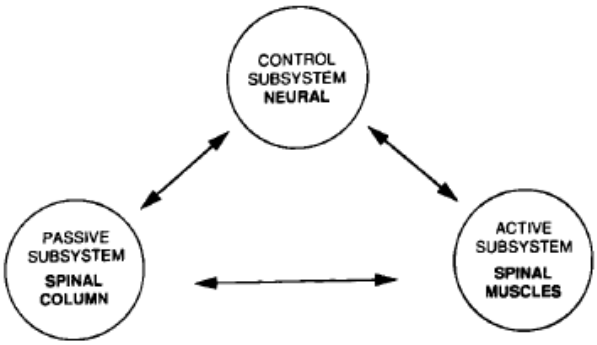


(Reproduced from Panjabi, 1992)

**Figure 4-9: The spinal stability unit as postulated by Panjabi**

The normal function and purpose of the stability system is to accommodate the constantly changing demands of the spine due to transient posture and loading in both static and dynamic loading scenarios.

### 4.3.1 The Neural Control Subsystem

The neural subsystem interprets input from various transducers and then commands the active systems to achieve stability. This requires a significant amount of bandwidth and processing to accomplish and may also degrade with age resulting in application of muscle loads that are too low or too high for the required application. Muscle forces that are too low may result in overloading of the passive systems as the motion limits are reached under heavy loads that are not accommodated. Muscle forces that are too high may cause overloading of the active systems as well as passive systems if the applied loadings are excessive for the required task.

### 4.3.2 Dysfunction of the Spinal Stability System

Panjabi *et al* (1978) have postulated a flowchart (Figure 4-10) in an attempt to describe the dependence spinal stability on each sub-system.

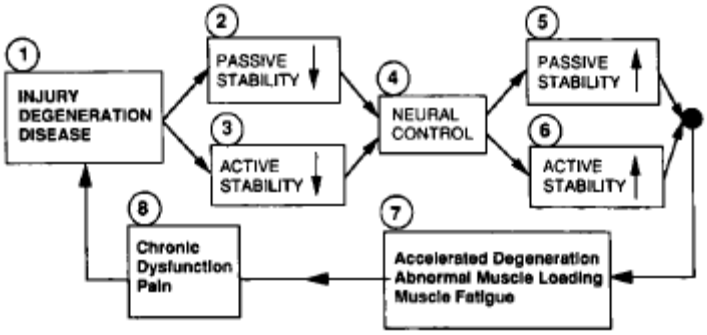


(Reproduced from Panjabi *et al*, 1978)

**Figure 4-10: Dysfunction flowchart of the spinal stability system**

The process is initiated by injury, degeneration or disease (1) which then may result in a decrease in the passive stability (2) and/or active stability (3). In an effort to mitigate the resulting loss of stability the neural

control unit (4) increases the stabilizing function of the remaining spinal components; either passive (5) or active (6). This may lead to accelerated degeneration, abnormal muscle loading and fatigue (7). If this mitigation attempt fails the result may be chronic dysfunction and/or pain (8).

Failure of the spinal stability system could result in clinical instability of the spine which is defined as a significant decrease in the capacity of the stabilizing system of the spine to maintain the intervertebral neutral zones within the physiological limits so that there is no neurological dysfunction, no major deformity and no incapacitating pain (Panjabi, 1992b).

White *et al* (1976) have proposed that the adult lower cervical spine to be destabilized if the following two conditions are met;

- There is > 3.5mm of horizontal displacement of one vertebra in relation to the vertebra below, measured at the posterior walls, on a neutral-position or a flexion view, at a tube-to-film distance of 183cm.
- The disc angle measured between two adjacent vertebral bodies is 11° greater than the disc angles of the levels above and below.

White and Panjabi have also proposed a numerical deficiency based guideline for cervical spine instability where each structural deficiency is given a weighting and the sum of all deficiencies determines the stability (<5) or structural instability (>5) of the cervical spine (Table 4-2).

**Table 4-2: White & Panjabi cervical spine instability criteria**

| **Structural Deficiency** | **Numerical Penalty** |
|---|---|
| Anterior element damage | 2 |
| Posterior element damage | 2 |
| Sagittal translation > 3.5 mm or 20% or vertebra | 2 |
| Sagittal rotation > 11 degrees | 2 |
| Positive stretch test (abnormal separation of elements under applied load) | 2 |
| Cord damage | 2 |
| Nerve root damage | 1 |
| Abnormal disc narrowing | 1 |
| Dangerous loads anticipated | 1 |
| **Unstable if Total Score Sum is >** | **5** |

The condition based criteria is a slightly more conservative definition of instability with the two criterion ranking only a score of 4 using the above numerical approach (abnormal separation of elements=2, sagittal rotation > 11 degrees=2, Total =4).

## 4.4 Pathogenesis of Cervical Spinal Degeneration

Age related changes to one or more spinal structure in the cervical spine initiates the degenerative process which progressively deteriorates the articulations of the spinal motion segment. Commonly a reduction in disc height due to degeneration of the extracellular matrix of the disc results in bulging of the disc at the annulus. Even small amounts of instability due to increased disc bulging initiates the formation of osteophytes around the circumference of the vertebral endplates as the body attempts to increase stability and surface area to reduce contact pressure. These protrusions can penetrate into the spinal canal and inhibit the spinal cord and spinal branching nerves. The formation of osteophytes on the vertebral endplates and facet joints results in a reduced range of motion.

### 4.4.1 Neck Pain

Pain that presents in the neck is most commonly caused by muscular and ligamentous factors which can be related to poor posture and ergonomics and muscle fatigue (Rao *et al*, 2007). The intervertebral disc and facets are significantly innervated and therefore degeneration can lead to pain generation (Chen *et al*, 2006; Ferlic, 1963; McLain, 1994).

### 4.4.2 Cervical Spondylosis

The main causes of cervical disc herniation are age related changes of the intervertebral disc which makes the annulus prone to tearing and fissuring. Cervical radiculopathy (mechanical nerve impairment) due to disc herniation typically occurs in the early stages of motion segment degeneration most commonly affecting patients in the $4^{th}$ and $5^{th}$ decades of life (Radhakrishnan *et al*, 1994). Extrusion of the disc through the tears and fissures of the annulus is called soft herniation. In some cases the extruded disc can spontaneously recede back within the disc but this occurrence is dependent on the location of the herniation (Mochida *et al*, 1998).

Spondylotic syndrome presents as a combination of recurrent episodes of neck pain that occur with motion in the arm and shoulder, vertigo and dizziness as well as headaches.

### 4.4.3 Cervical Spondylotic Radiculopathy

Further progression of deterioration after the initial soft herniation includes the formation of osteophytes on the vertebral endplates, facet joints and uncovertebral joints. This results in the narrowing of both the spinal canal and the spinal foramen through which the spinal branching nerve pass. These hard herniations cause a condition known as spondylotic radiculopathy which is observed via the marked reduction in foraminal heights, widths and areas which impairs the function of the spinal branching nerves. The reduction in size of the foramen, also known as foraminal stenosis, can cause permanent (or transient) mechanical irritation of the nerve roots which can lead to local oxygen starvation of the nerve root and dorsal root ganglion. Radiculopathy incorporates mechanical deformation of the nerves due to disc extrusion as well as chemical irritation of the nerves due to the release of pro-inflammatory cytokines and nerve growth factor (NGF) at the point of injury (Rydevik and Garfin, 1989; Van Zundert *et al*, 2006).

The symptoms of cervical spondylotic radiculopathy include radicular pain, sensory disturbances, motor weakness and deficits of the reflexes.

### 4.4.4 Cervical Spondylotic Myelopathy

Impingement of the spinal canal by disc herniation or osseous spurs can have a significant impact in the cervical spine and lead to severe neurological deficits known clinically as myelopathy. Acute myelopathy can be a result of a large disc herniation or trauma induced narrowing of the spinal canal. More chronic cases are typically the results of degeneration (spondylosis) or the ossification of the posterior longitudinal ligament which results in direct compression of the spinal cord. Cervical spinal myelopathy (CSM) can result in a variety of neurological deficits including impairment of the senses, motor function, gait, etc. The severity of CSM is dependent on several factors which include both static and dynamic factors.

The normal diameter of the spinal canal ranges from 14 to 22 mm (Hayashi *et al*, 1987; Edwards and LaRocca, 1983; Burrows, 1963) which provides adequate space for the neural elements (which occupy 75% of the total space), ligaments and adipose tissue. A spinal canal having a diameter of less than 13 mm constitutes a congenitally narrow spinal canal and thus there is a significantly higher risk to the development of myelopathy. Penning *et al* (1986) found that neurological deficit was observed only after a 30% reduction in the cross sectional area of the spinal cord. These results coincided with Teresi *et al* (1987) who found that asymptomatic patients exhibited an average of 7% of area reduction, with a maximum of 16% reduction in area observed without deficit.

Flexion motion results in the lengthening of the spinal cord, which in the presence of posterior spondylosis may inflict damage as it is pinched between posterior disc bulges and/or osteophytes. An advanced state of spinal motion segment degeneration may also permit significant anterior-posterior translation which can result in a reduction in the spinal canal space of approximately 2-3 mm as the adjacent vertebral bodies move relative to one another. This combined with hyper mobility of the motion segment can place increased shear loads on the spinal cord (Baptiste and Fehlings, 2006).

Cervical myelopathy presents with reduced function and senses of the hands, reduced fine motor skills, difficulty walking, symptoms of tetraparesis and bowel and/or bladder dysfunction in the late stages of myelopathy.

## 4.5 Prevalence of Cervical Spinal Degeneration

In a study of 1100 randomly selected Saskatchewan adults it was found that the annual incidence of neck pain was 14.6%, of which 0.6% of the population developed disabling neck pain. It was also found that women were more likely to develop neck pain than men (Cote *et al*, 2004). A similar study performed on a Swedish population of 4415 subjects found a neck pain prevalence rate of 17%, and surprisingly 51% of the neck pain reporters also had chronic back pain (Guez *et al*, 2006). Approximately 25% of neck pain sufferers attributed the condition to injury.

The prevalence of cervical radiculopathy, which is the compression of spinal nerve structures, is less prevalent than the occurrence of neck pain affecting 3.3 per 1000 people and occurs most frequently in the 4$^{th}$ and

5th decades of life (Winner and Gill, 2000). The age specific prevalence was most pronounced in Women and surprisingly only about 15% of cases were accompanied by a history of physical exertion or trauma. A confirmed disc protrusion was only observed in 21.9% of cervical radiculopathy patients with the main cause of the remaining 68.4% of patients being attributed to general degeneration of the spinal motion segment.

# Chapter 5

# Treatment for Spinal Joint Degeneration

There are several approaches that attempt to accommodate the damage caused by disc degeneration. Physiotherapy, spinal massage, chiropractic manipulation and taking analgesics can all help control the effects of the damage. However, more permanent treatment often requires surgical intervention. There are various approaches, some of which are in clinical practice and others that are in the experimental stage.

## 5.1 Conservative Treatments

The early stages of spondylosis in the form of non-specific neck pain are best managed with non-invasive treatment because most often a correlation of structural deficit to the cause of pain is not clearly identifiable. Minimally invasive surgical techniques are marked by the low impact of these procedures on the patient and a relatively short recovery period. These procedures are typically performed via endoscope such that very little exposure of the surgical site is required, which is a major cause of long recovery times and damage to adjacent sites.

The first step in conservative treatments is often the administration of oral medications which may include analgesics (painkillers) and muscle relaxants in an attempt to mitigate the presented symptoms. Manipulative therapy, traction in particular, has been reported to provide short term relief of radiculopathy (Cleland et al, 2005). There is moderate evidence to support the use of long term dynamic and isometric resistance exercises of the neck and shoulder musculature for chronic or frequent neck disorders. This attempts to improve the active musculature of the spine to increase the overall stability. The administration of transforaminal injections can result in instant pain relief in patients suffering from cervical radiculopathy. The safety of this method is under scrutiny for the concerns of subsequent spinal cord injury post injection.

Radiofrequency denervation of the facet joints can be performed to remove the nerves that innervate the facet joints. Remove of the nerves eliminate the generation of pain in the facets, although it is possible for the damaged nerve to repair itself and regain the capacity to generate pain. The efficacy of this procedure is unproven with some studies showing positive results (Shin *et al*, 2006), however these results are limited and more clinical experience is required.

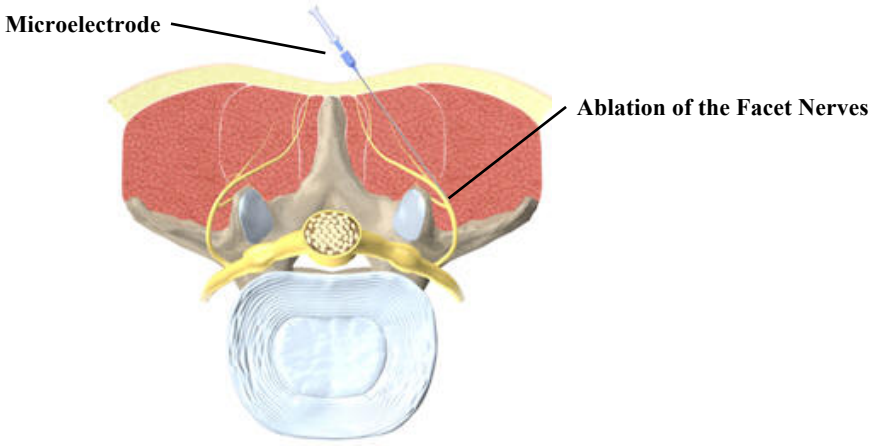


(Adapted from www.back.com)

**Figure 5-1: Radiofrequency denervation of the facet joints**

After the failed application of these conservative treatments potential surgical intervention should be explored.

## 5.2 Surgical Treatments

Surgical intervention is typically indicated only after the non-responsive application of conservative therapy. While surgery for non-specific neck pain is typically not supported, evidence supports that patients with CSR and CSM benefit from surgical intervention after non-operative care has failed (Yonenobu, 2000; Fountas *et al*, 2002). The indications for CSR and CSM as presented by can be seen in Table 5-1.

**Table 5-1: Indications for Surgery**

| Cervical Spondylotic Radiculopathy | Cervical Spondylotic Myelopathy |
|---|---|
| • Progressive, functionally important motor deficit<br>• Definitive nerve root compression<br>• Symptoms of radiculopathy<br>• 6-12 weeks of persistent pain | • Progressive, functionally important motor deficit<br>• Acute onset and progression of neurological deficits<br>• Evidence of spinal cord compression with myelopathic symptoms<br>• Progressive kyphosis with neurological deficits |

The primary goal of surgery for CSM is the prevention of further progression of neurological symptoms because improvement of established myelopathic changes is extremely rare (LaRocca, 1988). Therefore the patient must be aware of this pre-operatively to ensure reasonable goals and expectations are understood.

There are two main surgical approached that are used in the cervical spine; the anterior (frontal) and the posterior (rear) approach, the choice of which is dependent on the location of the presentation of the pathology. An anterior deficit is best treated from the front and vice versa.

### 5.2.1 Spinal Arthodesis (Discectomy and Fusion)

Spinal arthodesis (or fusion) is one of the most common spine surgical techniques and involves the rigid attachment of the vertebrae adjacent to the degenerated disc (Figure 5-2). It is commonly referred to as the 'gold standard' for the treatment of disc herniations and cervical spondylotic radiculopathy. Fusion surgery focuses on restricting the mobility of the damaged regions thereby reducing pain and nerve impingement. In addition, it restores the original disc height and stabilizes the damaged spinal segment. Fusion can be performed using either an anterior or posterior approach, or a combination of both approaches.

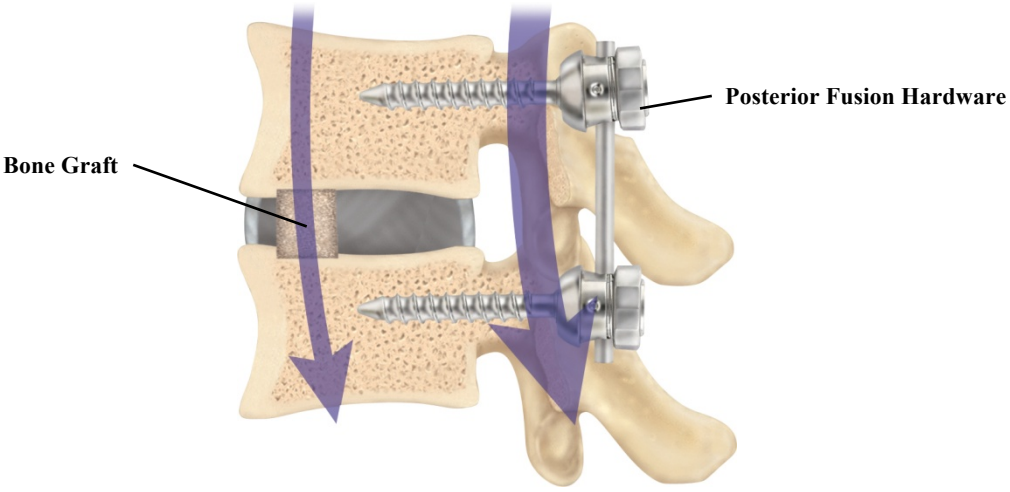


(Adapted from www.back.com)

**Figure 5-2: Fusion of a spinal motion segment with a bone graft and posterior hardware**

The radiological fusion rate is dependent on the number of levels to be fused; Bohlmann *et al* (1993) reported successful fusions for one, two and multilevel fusions of 89%, 73% and 67% respectively. Clinical results vary with some studies reporting single level fusion rates of 88%, with values typically ranging from 50-100% (Emery *et al*, 1997, Kurtz and Edidin, 2006; Deyo *et al*, 2004). There is a significant correlation between non fusion and the present of post operative neck and arm pain suggesting that obtaining fusion is critical to clinical success. Clinical outcome of fusion is a function of the decompression of the compromised nerve root and/or spinal cord and has been reported as excellent in 70-90% of fusion recipients (Rao *et al*, 2007).

The radiographs of a 56 year old male exhibiting degeneration of the $5^{th}$, $6^{th}$ and $7^{th}$ cervical levels that produced compression of the spinal cord resulting in the development of pain and neurological deficit can be seen in Figure 5-3. Post operatively the patient was fully functional with occasional episodes of neck pain.

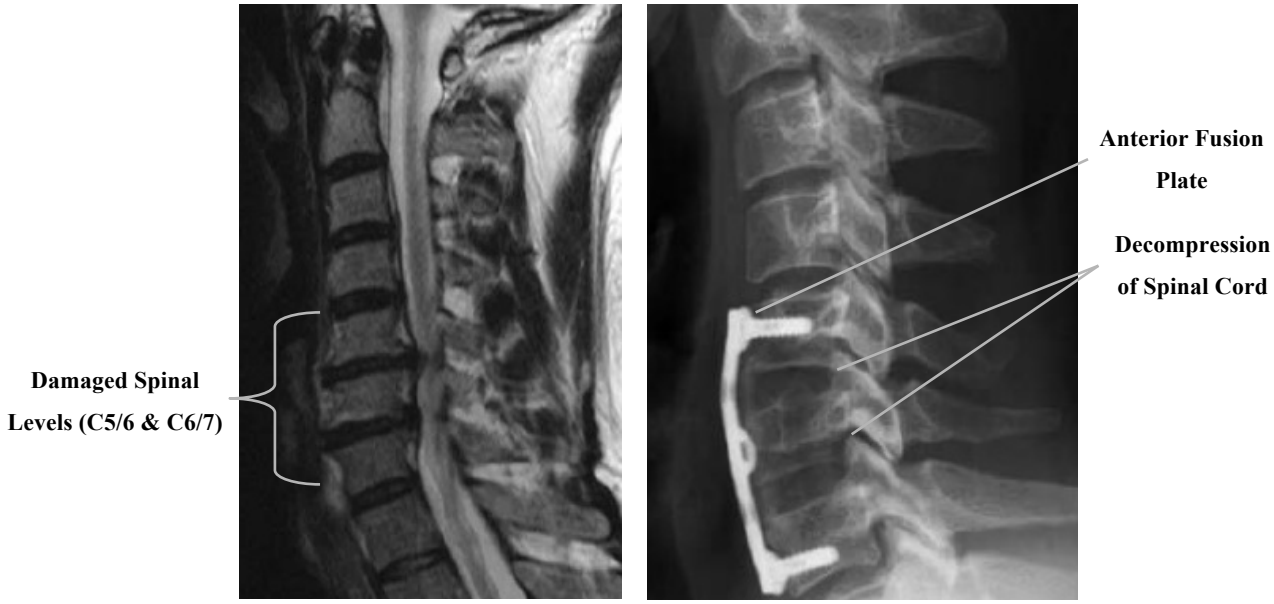


(Adapted from Boos and Aebi, 2008)

**Figure 5-3: Multilevel C5/6 & C6/7 anterior fusion with bone plate**

While the rigid fixation of the adjacent vertebrae does stabilize the damaged joints (facets and disc), it also causes increased stress and motion of the discs above and below the fusion site which may lead to adjacent level degeneration. There is also the possibility that the spinal fusion cage or screw fixation may fail requiring a second revision surgery to correct the problem.

Adjacent segment degeneration has been the main argument against spinal fusion. Hilibrand *et al* (1999) studied 374 patients who underwent anterior cervical fusions for a total of 20 years post-operatively and found that about one quarter of patients were at risk of developing symptomatic adjacent segment disease within 10 years post-operatively.


(Adapted from Boos and Aebi, 2008)

**Figure 5-4: Adjacent segment degeneration at 6 years follow-up**

A single level fusion involving C5/6 or C6/7 accompanied by preexisting degeneration was found to be the greatest risk factors for the development of new disease. The main point of argument is whether the new degeneration is a result of the progression of pre-existing degeneration or of the presence of the fusion (Cherubino *et al*, 1990).

### 5.2.2 Spinal Disc Arthroplasty (Replacement)

Total spinal disc arthroplasty (TDA) involves the removal of the damaged disc and replacing it with an articulating implant (Figure 5-5) which restores the original disc height, the load carrying capacity and the normal *in vivo* kinematics of the spine. More than 15 different designs are currently under pre-clinical and clinical investigation. Current devices use either metal-on-metal or metal-on-polymer articulations.

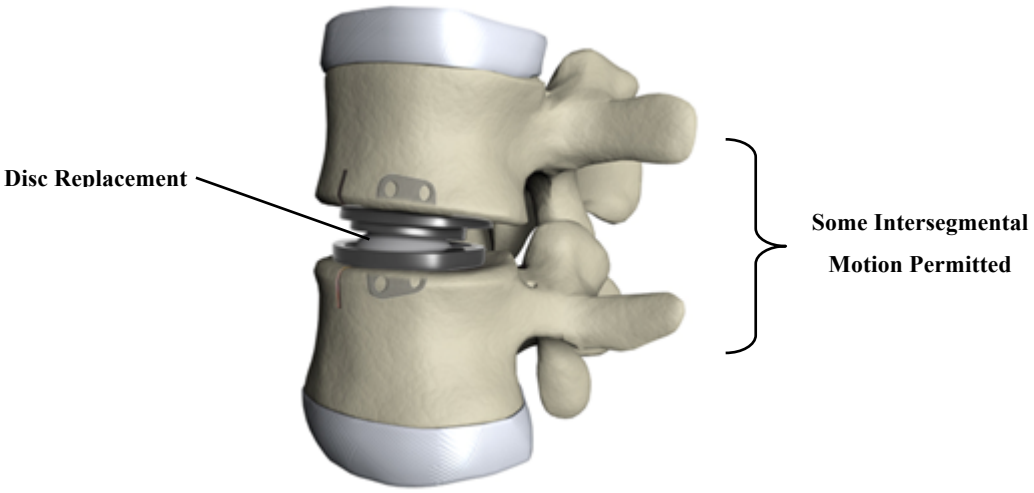


(Adapted from EOrthopod, 2009)

**Figure 5-5: Spinal disc arthroplasty**

Lumbar disc replacement implants are physically larger and typically employ a ball-in-socket configuration to provide some intersegmental motion. FDA approved implants include the Charite® (sold by DePuy Spine since 2003), the Prodisc II® (from Syntheses Inc.) and the Maverick® (from Medtronic Spine & Biologics).

Cervical disc replacement implants (Figure 5-6) are smaller than lumbar disc replacement implants because they carry smaller loads. They too often employ a ball-in-socket configuration however some include some anterior-posterior sliding motion. The three FDA approved implants are the Prestige® and the Bryan® (both from Medtronic Spine & Biologics) and the Prodisc-C® (from Syntheses Inc.). In general, clinical trials comparing arthroplasty to fusion of the lumbar spine have shown that disc replacement patients reported significantly less pain and disability compared to those who received a fusion procedure (Delamater *et al*, 2003).

(Adapted from Boos and Aebi, 2008)

**Figure 5-6: Total disc arthroplasty at C5/6**

Current indications and contraindications for total disc arthroplasty can be seen in Table 5-2.

**Table 5-2: Indications and contraindications for total disc arthoplasty**

| Indications | Contraindications |
|---|---|
| • symptomatic cervical disc disease | • >3 damaged levels |
| • up to two level involvement | • cervical instability |
| • visible structural deficit (disc herniation) | • adjacent cervical fusion |
| • > 6 wks failed conservative therapy | • previous surgery/fracture at level |
| • 20 yrs < Age < 70 yrs | • allergy to implant material |
| • no contraindications | • severe spondylosis (osteophytes, facet joint OA) |
| | • axial neck pain as the only symptom |
| | • systemic and metabolic diseases |

There is the possibility of complications in total disc replacement as was the case with the lumbar disc replacement known as the Charite. This prosthesis had a poor design configuration which subjected the interior polyethylene component to tensile stresses that led to its gross failure if the implant was subjected to motions only slightly outside its intended limits. Also, an adverse immune reaction to the wear particles occurred for some Charite implants that led to implant loosening. The resulting revision surgeries were costly in terms of the surgery itself and the lost work time for many of these patients as well as being stressful for the patients (Punt et al, 2008).

Studies of the preliminary performance of TDA has shown that segmental motion can be preserved in the short term and compares well with fusion in terms of clinical performance (Bertagnoli *et al*, 1993; Chang *et al*, 2007; Nabhan *et al*, 2007; Sasso *et al*, 2007). Whether or not TDA will prevent adjacent segment degeneration is currently not known due to the lack of long-term clinical data.

### 5.2.3 Nucleus Replacement Technologies

Nucleus replacement procedures are intended to restore the original disc height and spinal kinematics through the removal of the failed nucleus and the implantation of a device which mimics the original properties of the healthy component. Recent developments in hydrogels have allowed for the development of a gel that can be injected into the disc nucleus to assist in carrying the applied spinal loading. This technique has the advantage of not requiring full surgical access; however the technology is still relatively new and therefore is currently under pre-clinical investigation.

A polymer on polymer articulation known as the NUBAC™ (Figure 5-7) that is offered by Pioneer Surgical Technologies is a prosthesis that has been proposed for use in treatment of lumbar disc degeneration. The device is designed for patients with low back pain due to degenerative disc disease. The device uses a ball in socket design to provide some intersegmental motion and surprisingly can be implanted using a posterior, lateral or anterolateral approach. The device does not incorporate any type of fixation and is self locating within the annulus which is retained in this approach. The device is currently in cadaver investigational studies in the United States, preliminary results have shown that the NUBAC™ is able to restore disc height and provide some intersegmental motion and stability.

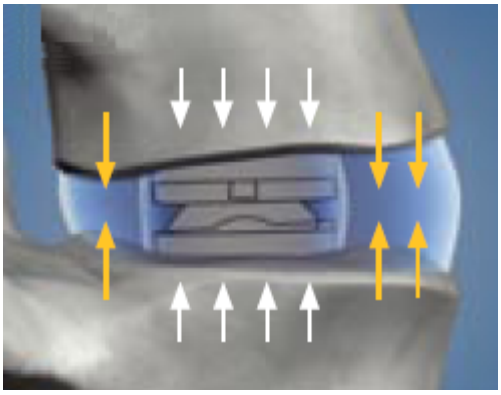

(Adapted from www.pioneersurgical.eu)

**Figure 5-7: NUBAC(TM) lumbar nucleus replacement device**

The success of nucleus replacement requires that the annulus be intact in order to constrain the replacement and therefore this technique is most effective in early cases of disc degeneration. Furthermore, degeneration of the annulus must stop after the nucleus replacement is inserted and the nucleus replacement cannot sustain significant creep or fatigue over time. At present, no nucleus replacement device is FDA approved.

### 5.2.4 Intervertebral Disc Regeneration

Recent work in the area of cell based therapies has allowed for the generation of non-invasive disc regeneration techniques which eliminate the risks associated with the aforementioned treatments. Recent work by Mochida (2005) has shown that the implantation of nucleus pulposus cells into a damaged disc slowed further degeneration since the existing nucleus cavity was observed to be able to retain the cells. It must be noted however that in their present state, these therapies have only been found to be effective in patients exhibiting early signs of disc degeneration.

In intermediate and advanced stages of disc degeneration, the injection of growth factors such as OP-1 has been found to induce the regeneration of the disc, and recent work with the injection of cells carrying specific genes has shown that this can also aid in the restoration of a damaged disc.

The implantation of cell-seeded collagen based scaffolds in the disc space to regenerate the nucleus has also shown somewhat encouraging results (Long *et al*, 2005). It has been suggested that further studies must be performed to optimize the cell growth within the scaffold that include growth factors and hydrostatic loading and conditioning of the implanted collagen scaffolds. This is because the *in vivo* performance of these constructs has been disappointing in terms of longevity and fatigue resistance. It is expected that the scaffold grown cells need to be preconditioned with applied loadings in-vitro prior to being implanted in order to obtain the desired mechanical properties which will resist fatigue and provide required tough flexible connection.

### 5.2.5 Further Development of Minimally Invasive Therapies

It is possible that minimally invasive therapies can be developed. These therapies might consist of some sort of cell-based or pharmaceutical intervention to prevent and/or mitigate spinal disc degeneration.

Recent work (Hunter *et al*, 2003) on the role of notochordal cells in the development of the nucleus pulposus has been performed in an effort to determine their usefulness in the tissue engineering of a nucleus replacement. The notochord is a rod of tissue which forms at the center of the embryo and guides the development of the neural tube and the vertebral columns. Around day 20 of development the ectoderm folds over the notochord to form the neural tube after which at day 30 mesenchymal cells begin to migrate to this location and become trapped. The exact role of these trapped cells is unknown but they are thought to take part in the formation of the nucleus pulposus. The notochordal cells gradually disappear during maturation and interestingly the onset of disc degeneration seems to coincide with the loss of these cells, which may represent a significant link between IVD health and notochord cells (Hunter *et al*, 2003). Further research into the exact role and improving the retention of these cells is ongoing.

The injection of mesenchymal stem cells, the process of which is shown in Figure 5-8, has shown to have the capability to differentiate into nucleus pulposus like cells which are capable of synthesizing a physiological, proteoglycan rich extracellular matrix characteristic of healthy IVDs (Acosta *et al*, 2005). It should be noted that this however only generates a soft tissue having similar properties to that of a healthy IVD and is not a biological replacement.

Unfortunately, these cell-based disc degeneration therapies involve techniques that are in their infancy. As yet, efficacious therapies have not been developed.

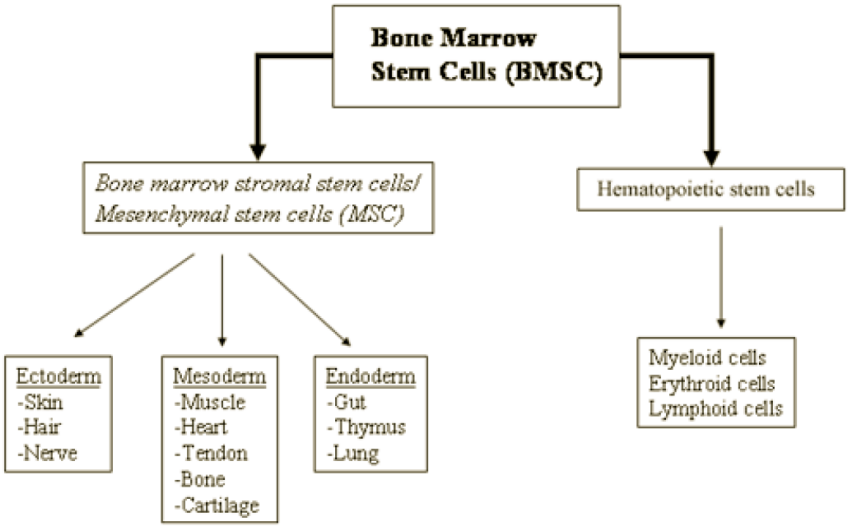


(Adapted from Acosta *et al*, 2005)

**Figure 5-8: Mesenchymal stem cell therapy flowchart**

## 5.3 Cervical Disc Replacement Designs

The concept of joint replacement (arthrodesis) has been successfully applied to several human joints including the hip and knee and is now currently in widespread clinical use. Failure of the hip or knee joint is typically associated with a loss of function and pain. The symptoms associated with failure of the cervical intervertebral disc are more subdued with pain and dysfunction typically presenting in the later stages of degeneration. In order to accommodate the neurological deficits of disc failure it is imperative that the natural vertebral spacing be recovered to achieve decompression of the posterior neural elements. Cervical disc arthroplasty aims to preserve motion and provide stability after neural decompression.

The field of cervical arthroplasty has been active since the 1950s, with much advancement having occurred in the late 1990s to the present time. Early attempts at cervical disc replacement did not succeed; the first implant was described by Fernstrom in 1966 (Fernstrom, 1966) as a metal ball bearing that had been implanted in both the lumbar and cervical regions. The cervical prosthesis was 6 to 10 mm in diameter. The majority of patients exhibited segmental hyper mobility and implant migration and subsidence into the vertebral endplates due to excessive contact stress between at the bone-implant interface.

More recently the Charite lumbar prosthesis design was introduced in 1982 and consisted of metallic endplates which were separated by a mobile polymeric core. Good results in more than 70% of patients have been reported. The Charite design however suffered a large list of complications including excessive wear resulting in complications *in vivo* (Link, 2002; Van Ooij et al, 2003). The Acroflex lumbar disc was also introduced in the 1980s, however it never reached the clinical trial stage due to potential carcinogenic and fatigue concerns over its rubber core (Szpalski, Gunzberg and Mayer, 2003). A metal on metal prosthesis named the ProDisc was introduced in the late 1980s.

A cervical arthroplasty device known as the Cummins-Bristol device was introduced around 1990 and consisted of a stainless steel, metal on metal, ball in socket configuration (Figure 5-9). Early results of clinical trial revealed several mechanical failures of the device including screw pull-out and fracture.

(Reproduced from Le et al, 2004)

**Figure 5-9: The Cummins-Bristol Disc (Currently known as Prestige®)**

The design was modified to allow more physiological motion that would be restrained by the natural facet joints and was termed the Frenchay cervical disc replacement. The result of a 2 year pilot study showed that of

fifteen patients, motion was preserved in all but one (Wigfield, Gill and Nelson, 2002). Further work compared the adjacent segment degeneration observed in patients that received the disc arthroplasty and those that received spinal fusion. The fusion group experienced an increase in adjacent segmental motion by 5% at 6 months and 15% at 1 year while the adjacent segment motion for the Frenchay disc was relatively unchanged. The Frenchay disc is now known as the Prestige® cervical disc.

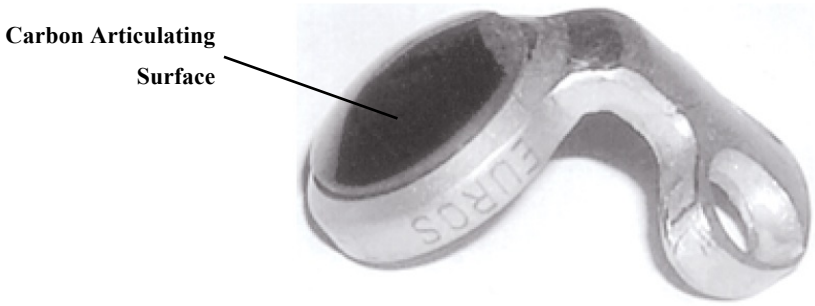


(Adapted from Le *et al*, 2004)

**Figure 5-10: The Pointillart Cervical Disc Prosthesis**

A more simple design was proposed by Pointillart (2001) which mimicked a unipolar hip replacement (Figure 5-10). The design used a carbon sliding surface that would articulate with the adjacent vertebral body. Early trials of the device showed that mobility was not maintained in patients, with fusion occurring between the adjacent vertebrae.

There are three cervical disc implants that have been FDA approved since 2007 (FDA, 2009); the Prestige® cervical disc, the Bryan® cervical disc and the Prodisc-C total disc replacement.

### 5.3.1 Prestige® Cervical Disc

The Prestige® cervical disc implant (formerly known as the Frenchay disc) is manufactured and sold by Medtronic Spine & Biologics (Memphis, TN). It is a two-piece ball-and-trough configuration and features a metal-on-metal stainless steel articulation (Figure 5-11). The Prestige® replaces a damaged and/or diseased cervical spinal disc while maintaining some motion at the treated segment. The ball articulating component is located on the superior side and the trough on the inferior side. The device is implanted via an open anterior approach in the disc space between vertebrae after the damaged disc has been removed.

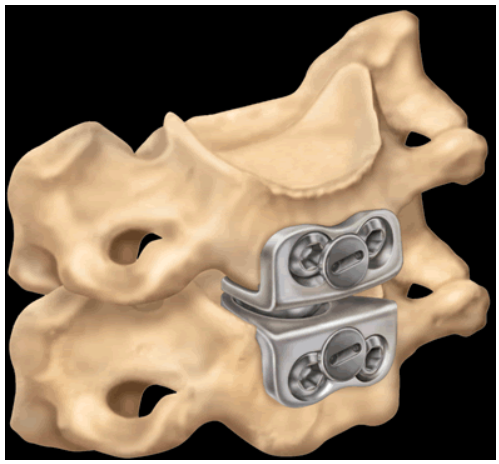

(Adapted from Medtronic Inc., 2009; eSpine, 2009))

**Figure 5-11: Prestige® cervical disc implant from Medtronic Spine & Biologics**

The Prestige® implant was designed to allow for the natural motions provided by the intervertebral disc including flexion, extension, side bending and rotation and is available in a variety of sizes to allow surgeons to closely match patient anatomy.

The Prestige is indicated in skeletally mature patients for the purpose of reconstructing the intervertebral disc from levels C3-C7 following a single level discectomy for intractable radiculopathy and/or myelopathy. The patient should present with at least one of the following items producing symptomatic nerve root and/or spinal cord decompression which is documented in patient history (neck and/or arm pain, functional deficit, and/or neurological deficit), and radiographic studies: 1) herniated disc and/or 2) osteophytes formation.

The safety and efficacy of the device has not been established in patients with certain pre-existing conditions. These include an active infection, an allergy to stainless steel, more than one cervical level with degenerative disc disease, not skeletally mature, clinically significant cervical instability, prior fusion at adjacent cervical level, severe facet joint pathology of the involved bodies, prior surgery at the treated level and bone mass loss (osteopenia) which can be caused by osteomalacia or osteoporosis (Medtronic Inc., 2009).

To avoid excessive wear a titanium ceramic composite (TCC) was developed, and a new "low profile" design was implemented (Powell *et al*, 2005). The resulting design is known as the Prestige LP® (Figure 5-12). This device is currently being implanted in Europe but is not FDA approved.

(Adapted from www.medtronic.co.uk)

**Figure 5-12: Prestige LP cervical disc implant from Medtronic Spinal & Biologics**

The Prestige® cervical disc replacement received United States FDA approval on July 16, 2007 for reconstruction of the disc from the C3 to C7 spinal levels for intractable radiculopathy and/or myelopathy (FDA, 2009).

### 5.3.2 Bryan® Implant

The Bryan® disc implant (Figure 20) is FDA approved for use in patients with single level degenerative disease or disc herniation between spinal levels C3-C7, intractable radiculopathy and a failure to respond to 6 weeks of conservative therapy (FDA, 2009). It replaces the natural spinal disc (Figure 5-13) and is designed to maintain the range of motion of the natural cervical spine including flexion/extension, lateral bending, axial rotation and translation.

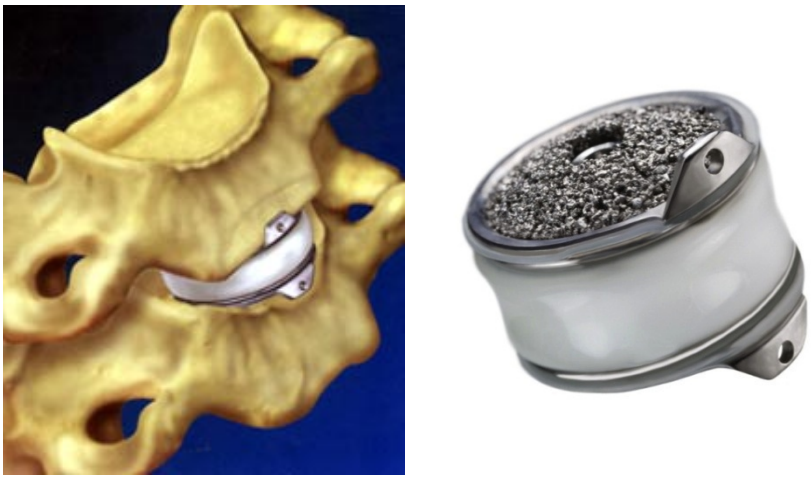

(Adapted from Le *et al*, 2004; www.medtronic.com)

**Figure 5-13: Bryan cervical disc implant from Medtronic Spine & Biologics**

The Bryan® disc consists of titanium alloy endplates separated by a dense polyurethane central "cushion" that is wrapped with a more flexible polyurethane membrane. The endplates include convex porous surfaces that accommodate bone in-growth. The device is not rotationally constrained and allows 11° of motion in flexion, extension and lateral bending as well as 2mm of translation (Bryan, 2002).

The Bryan implant was conceived by neurosurgeon Dr. Vincent Bryan in 1993 after which pre-clinical testing began in 1998. Since then more than 20,000 Bryan implants have been sold worldwide. The Bryan implant has been used quite extensively in Europe. At two year follow-up, the overall success and neck disability indices are superior to fusion patients (Le et al, 2004). Goffin *et al* (2002) have reported clinical success rates of 86% of patients at 6 months and 90% of patients at 1 year with motion being preserved in all patients, averaging more than 7° per level for the range of flexion and extension at one year.

Galbusera *et al* (2006) used finite element models of the intact spine and Bryan® implanted levels to compare the location of the instantaneous centers of rotation (ICR) at the C5-C6 spinal level. The Bryan® disc was found to reproduce the location of the ICR relatively well; however the observed location at the implanted

level exhibited higher variability than the intact model which may show that some motion control is lost at the level of implantation.

At the present time no significant complications associated with the Bryan® disc have been reported.

### 5.3.3 ProDisc™-C Implant

The Prodisc-C cervical disc implant (Figure 5-14) is offered by Synthes Spine and is a ball and socket design. The prosthesis is comprised of three components; two metal endplates made from cobalt-chromium-molybdenum alloy separated by a core made from medical grade ultra high molecular weight polyethylene.

(Adapted from Synthes Interational, 2009)

**Figure 5-14: ProDisc™-C cervical disc implant**

The device was attained by reducing the size of the already successful ProDisc lumbar disc replacement. The ProDisc-C employs a rough surface coating of pure titanium that allows bony in-growth within a few months. The ball and socket design attempts to permit a physiological range of motion. Loading of the facets is controlled by the motion limits implemented by the geometry of the implant's endplates. The centre of rotation at the surgical level is located just below the superior end plate (Synthes International, 2009).

The ProDisc-C was approved by the United States FDA on December 17, 2007 for use in reconstruction of the disc from the C3-C7 spinal levels following removal of the disc at one level (FDA, 2009). The intended use of the device is to stabilize the operated spinal level and allow some motion.

### 5.3.4 PCM Prosthesis

The Porous Coated Motion (PCM) prosthesis (Figure 5-15) employs a metal on UHMWPE (polyethylene) articulation. The endplates are coated with a TiCaP porous coating for enhanced bone in-growth and long term fixation.

(Reproduced from Traynelis, 2006)

**Figure 5-15: PCM Prosthesis from Cervitech Inc.**

The PCM is currently undergoing an FDA-approved 2 year IDE study of its use in patients with single level disc degeneration accompanied by radiculopathy or myelopathy. Motion of the PCM disc relies on sliding of the superior endplate on the polyethylene core in the flexion-extension, lateral bending and axial rotation motions.

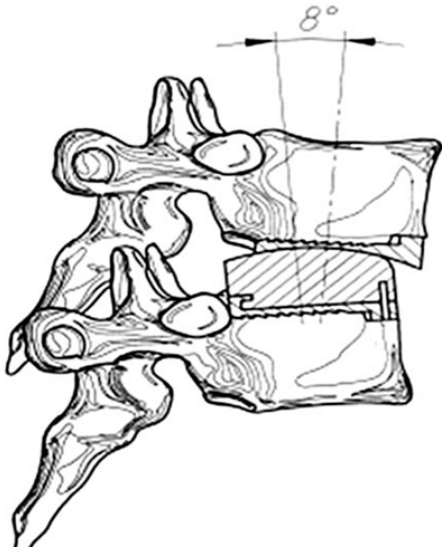


(Adapted from Vaccaro, 2004)

**Figure 5-16: Motion Pattern of the PCM Prosthesis in flexion-extension**

The geometry of the PCM prosthesis is claimed to be more suited to high loading due to increased contact area compared to typical ball in socket designs which provide more mobility but have less contact area.

### 5.3.5 Kineflex C Disc

The Kineflex C prosthetic disc (Figure 5-17) was developed in South Africa and is currently offered by Spinal Motion Inc. It is currently an investigational device in the United States with some clinical trials of the artificial disc for treatment of degenerative disc disease.

(Adapted from Vaccaro, 2004)

**Figure 5-17: The Kineflex C Disc**

The Kineflex C utilizes a captured mobile bearing core which articulates on two endplates. Both contacts are spherical in geometry.

### 5.3.6 CerviCore Disc

The CerviCore disc (Figure 5-18) is a total cervical disc replacement constructed of cobalt-chromium alloy offered by Stryker Spine.

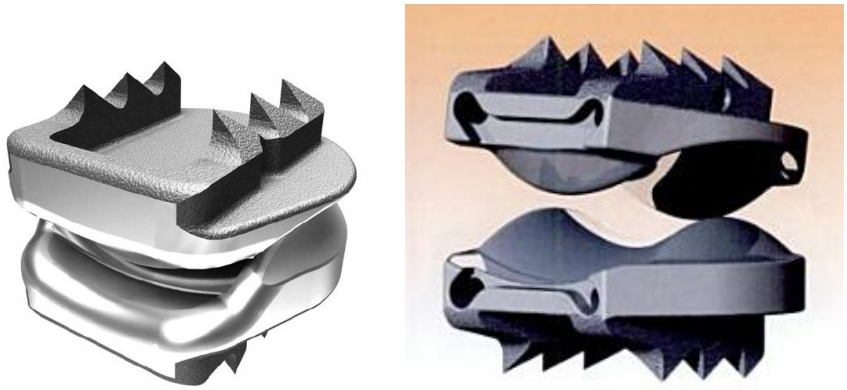

(Adapted from Vaccaro, 2004)

**Figure 5-18: The CerviCore Total Cervical Replacement**

The CerviCore uses a innovative metal-on-metal saddle articulation that provides 10 degrees of motion in flexion-extension and 11 and 7 degrees in lateral bending and axial rotation respectively. The saddle design allows the centre of rotation in lateral bending to be located in the superior vertebra while in flexion-extension the centre of rotation is found in the inferior vertebra which more closely represents the natural spinal segment. Axial rotation of the device beyond +/- 3° is coupled with a distraction motion (separation of the endplates and thus vertebrae) because of the unique saddle shaped articulation. In axial rotation the articulation contact occurs about

two points which is suspected to be the cause of wear markings being present on tested prosthesis, however total wear volume is reported to be not significant (Kim *et al*, 2006).

The device is coated with a titanium plasma spray to promote bone in-growth and augment the teeth which anchor into the subchondrial bone. The CerviCore is currently undergoing pre-clinical testing.

### 5.3.7 Mobi-C Cervical Disc

The Mobi-C® cervical disc prosthesis (Figure 5-19) is a semi-constrained device with a mobile UHMWPE insert between two chrome cobalt plates. The device is not currently available in the North America but is in the process of clinical trials in France.


(Adapted from Kim *et al*, 2006)

**Figure 5-19: The Mobi-C® cervical disc prosthesis**

The device allows 5 degrees of freedom and provides mean flexion-extension and lateral bending rotation of 10° and mean rotation of 8° (Vital et al, 2008).

### 5.3.8 Nunec/Nubac Nucleus Replacement

The Nunec™ and the Nubac™ are nucleus replacement devices for use in the cervical and lumbar spine respectively. Both devices uniquely allow for only the replacement of the nucleus (or the central section) of the intervertebral disc (Figure 5-20). Because only the nucleus (and not the annulus) is replaced, the devices cannot be classified as a total disc replacement and are termed nucleus replacement devices.

(Adapted from www.pioneersurgical.eu)

**Figure 5-20: The Nubac$^{TM}$ Nucleus Replacement**

Both the Nubac and Nunec devices are constructed completely of PEEK Optima and employ an all-polymer articulation to provide motion to adjacent spinal segments through the replacement of the nucleus. The annulus must be healthy and remains intact to limit implant migration and provide some stability to the spinal segment.

## 5.4 Cervical Disc Replacement vs. Spinal Fusion

Spinal fusion is an effective and popular surgical technique in the treatment of back and neck pain related to severe degeneration of the disc and/or facet joints. The fusion procedure restores disc height, stabilizes the spine and provides a strong mechanical link between the vertebrae. However, because it prevents or significantly restrains the motion of the spine at the level of the surgery, this change induces increased levels of stress and range of motion (ROM) of the adjacent (inferior and superior) segments (Figure 5-21). The change in ROM has been suggested by several studies in both the cervical and lumbar spine with the occurrence of accelerated disc degeneration and facet joint arthritis at the adjacent levels (Chen et al, 2009; Chang et al, 2007). The reduction in motion at the operated level was coincident with higher ROM, annulus stress and facet joint pressure in both flexion and extension at the adjacent levels. Fusion is also thought to increase the pressures within the adjacent discs (perhaps due to more bending strains these levels) which inhibit the diffusion of nutrients from the endplate thus contributing to an overall degeneration of the disc. This effect was observed most prominently at the superior level.

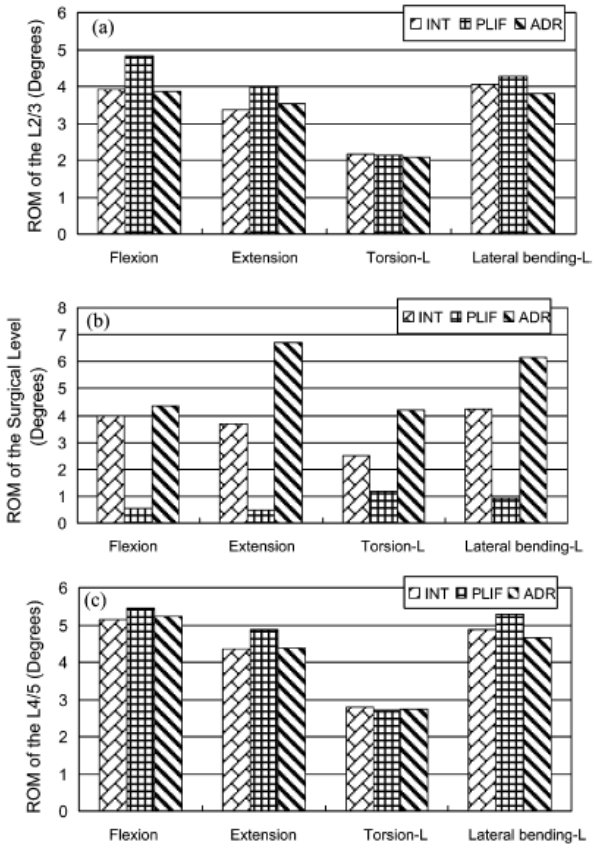


(INT-intact, PLIF-fusion, ADR-after disc replacement)

(Reproduced from Chang *et al*, 2007)

**Figure 5-21: Range of motion of operated and adjacent levels**

Although fusion has produced somewhat acceptable results, total disc arthroplasty (TDA) can be performed to maintain ROM at the surgical level in an effort to minimize the increase in both stress and ROM observed at the adjacent levels. There are several published biomechanical studies that show evidence that TDA in both the lumbar and cervical spine can preserve varying levels of motion when compared to the intact spine at the surgical level (Chen et al, 2009; Chang et al, 2007) while leaving the motion of the adjacent segments relatively unchanged. However, cadaveric studies have shown that the facets observe significantly higher forces at the surgical level (Figure 5-22), with the greatest changes noted in extension. Conflicting results have been observed regarding the change in facet contact forces at adjacent levels after TDA. Some authors (Chang et al, 2007) show increased facet contact pressures while others report only minor changes (Chen *et al* 2007). It has also been noted that the superior portion of the facet joint capsule is subject to extensive stretching during heavy loadings. Therefore, it appears that TDA prevents an increased ROM at the adjacent levels but increases the facet joint forces (and thus contact stresses) at the surgical level and perhaps at the adjacent levels.

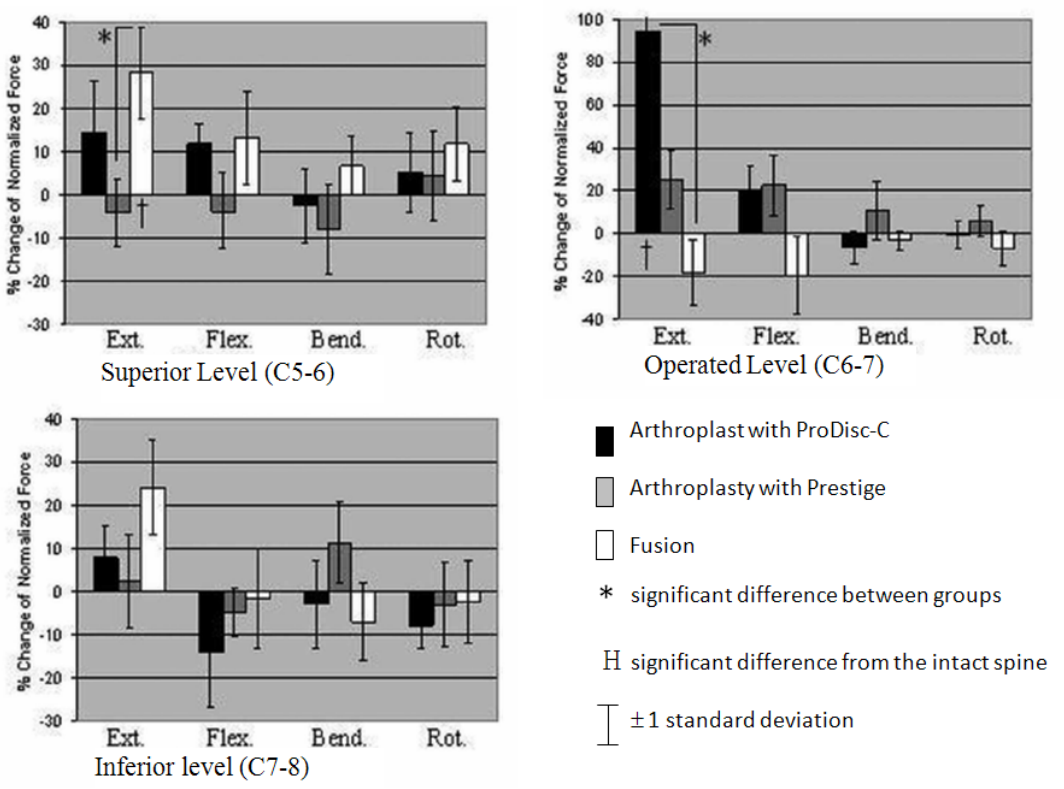


(Adapted from Chang *et al*, 2007)

**Figure 5-22: Cervical facet contact forces at different levels after total disc arthroplasty**

Finally, cadaveric studies (Chang *et al*, 2007) of TDA have also shown that the pressures within the adjacent discs remains relatively unchanged when compared to the significant increases observed with spinal fusion.

It is also possible that the modified range of motion and kinematics at the operated level in some TDA devices may *reduce* the forces on the facet joints in some activities and this may cause some atrophy at specific regions of the facet joint surfaces. Thus, both higher and lower forces may act on the facet joints and both may cause damage. Progressive damage to the facet joints may require that the TDA be revised to a fusion.

From an overall perspective TDA represents a significant improvement over spinal fusion with regards to the reduction in adjacent level ROM and stresses. This, however, comes at the risk of abnormal facet joint forces at both the surgical and adjacent levels especially in extension when the facets are most engaged and carry the highest proportion of applied spinal load. Therefore, there is still some possibility of improvement in TDA. Efforts should be made to reduce the effects of the procedure on facet joint forces and to plan for the possibility of replacing the facet joints. This suggests that TDA devices should re-designed to achieve both a minimal influence on the facet joint forces and to accommodate a subsequent facet joint replacement and thus an integrated technology of total level arthroplasty system (TLAS).

## 5.5 Spinal Device Market Analysis

Spinal fusion is a standard treatment for herniated spinal discs. However, it has been shown by Galbusera *et al* (2008b) that this may lead to adjacent level degradation due to the abnormal kinematics and load transfer patterns induced by the fusion. Nation-wide survey data from the United States estimates that the annual numbers of hip arthroplasty, knee arthroplasty and spinal fusion procedures have all increased since 1993 but at different rates (Figure 5-23). Interestingly, the annual number of spinal fusions increased by 77% between 1996 and 2001, while over the same time period hip and knee arthroplasty increased only about 14% (Deyo *et al*, 2004). This surge in spinal fusions slowed after 2001 but they kept pace with hip and knee arthroplasties. The rates are influenced by a number of factors, including the number of revision surgeries for wear particle-induced osteolysis, patient and surgeon perceptions regarding long term outcomes and policies of both medical insurance providers and governments.

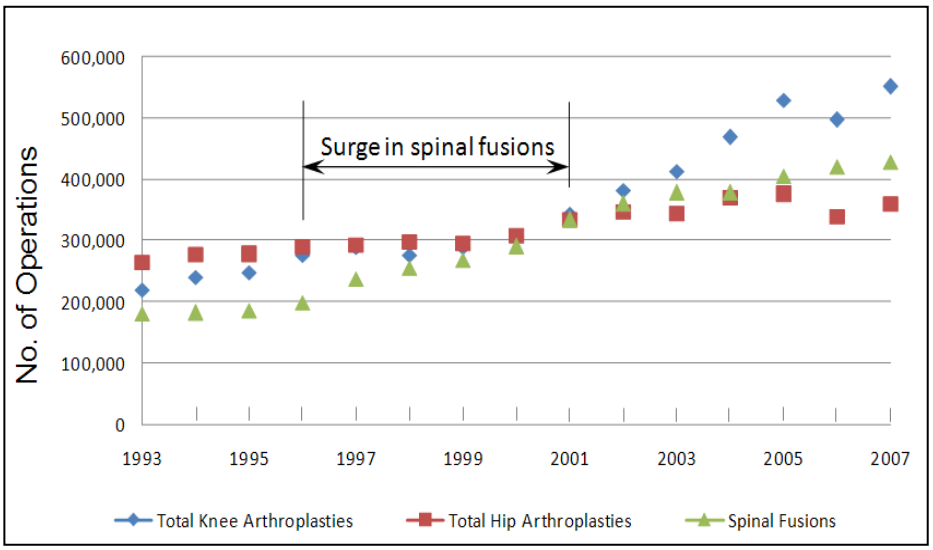


(Data obtained from AHRQ, 2009)

**Figure 5-23: Estimated annual hip and knee replacements compared to spinal fusions in the U.S.**

Approximately 75% of spinal fusions in 2004 were performed for spondylosis (spinal degenerative changes), disc disorders and spinal stenosis. At the same time, it was also estimated that the market for spinal implants, including spinal fixation devices and bone graft substitutes, was $2 billion a year with an annual growth rate of 18 to 20 percent (Deyo *et al*, 2004). Both lumbar and cervical spinal fusions increased fairly steadily since 1993, presumably reflecting the willingness of patients and surgeons to seek a surgical solution for back pain, neurological deficits and disability (Figure 5-24). This trend also suggests that there is significant growth in the target market for the facet replacement device since facet damage is often found in patients after disc degeneration and prior to spinal fusion.

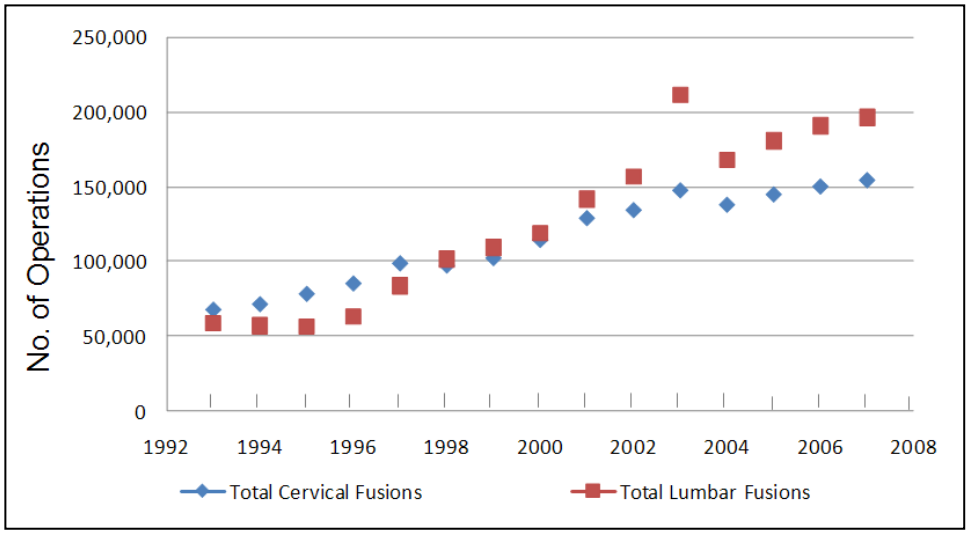


(Data obtained from AHRQ, 2009)

**Figure 5-24: Annual number of lumbar and cervical spinal fusions in the U.S.**

In 2009, a survey of practicing spine surgeons performed by Whang *et al* (2004) showed that 42% had performed lumbar TDA while 30% had performed cervical spine TDA. Some 81% of the respondents stated that they were 'more likely' to perform cervical TDA now compared to 1 year ago.

There are two main diagnosis categories when a patient presents with a spinal disorder; spondylosis (the degeneration of spinal joint tissues) and stenosis (the narrowing of the spinal cord canal), the latter of which can often lead to myelopathy which is damage to the spinal cord itself. Spinal joint damage typically presents first which them commonly leads to narrowing of the spinal canal as tissue encroaches on the spinal cord. Each of these conditions can present in the cervical, thoracic and lumbar spine. Estimates of combined spinal diagnoses (splondylosis and stenosis) in the United States show significant increases from 1997 to 2007 for each region of the spine can be seen in Table 5-3.

**Table 5-3: Trends of combined spinal spondylosis and/or stenosis diagnoses**

| Spinal Region | Year | | % Change |
|---|---|---|---|
| | 1997 | 2007 | |
| Cervical Spine | 94,227 | 151,550 | +60.8 |
| Thoracic Spine | 13,816 | 16,617 | +20.3 |
| Lumbar Spine | 230,915 | 365,481 | +58.3 |
| **Total Spine** | **338,958** | **533,649** | **+57.4** |

(Data obtained from AHRQ, 2009)

It is from this patient population that the target market for a facet replacement system would be obtained because facet joint damage commonly accompanies cervical spondylosis and stenosis. Facet degeneration has been estimated to represent up to 97% of contraindications to total disc arthroplasty in the lumbar spine (Wong *et*

*al*, 2007). The cervical region of the spine exhibited the highest increase in diagnoses (60.8%) form 1997 to 2007. It is possible that TDA with a facet joint replacement (either shortly after or somewhat later) may become the preferred strategy for treating spinal stenosis and spondylosis. The current market for TDA of the spine in both the cervical and lumbar regions is still in its infancy with only an estimated 2500 lumbar and 1500 cervical TDA performed in 2007 in the United States (Figure 5-25). The drop in lumbar TDA from 2005 to 2007 may have been caused by the emergence of problems with the Charite TDA. The wear problems associated with this device have since been resolved in current lumbar replacement designs and the use of the Charite disc has declined significantly. It is expected that the number of operations in the lumbar spine has be climbing since 2007 (Punt *et al*, 2008).

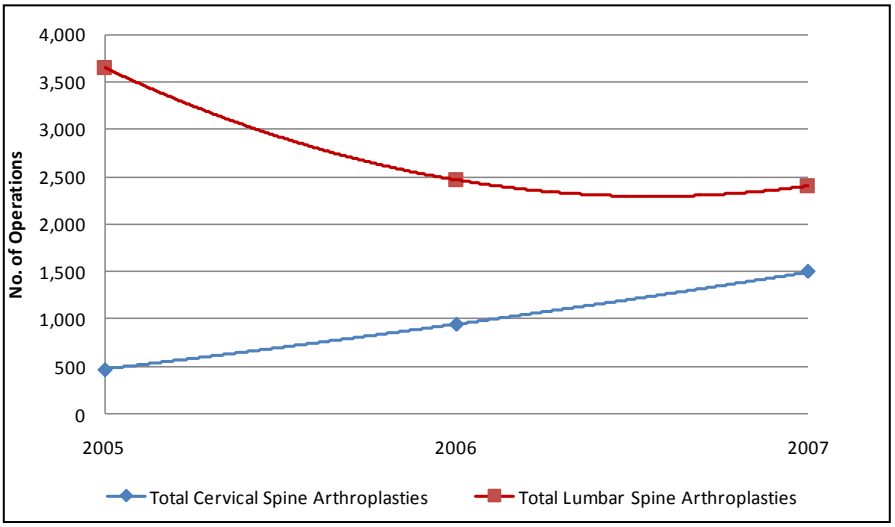


(Data obtained from AHRQ, 2009)

**Figure 5-25: Annual number of lumbar and cervical spine arthroplasties in the U.S.**

If TDA is a better choice than fusion for spinal degeneration (both stenosis and spondylosis) that does not involve facet degeneration, then a total level arthroplasty system (TLAS) which consists of a TDA with a facet joint replacement, may be able to completely displace fusion as the most common surgical treatment. Furthermore, the number of diagnosis of both stenosis and spondylosis along with the number of fusions and TDA are all increasing.

The spinal implant and orthobiologic technology market in the United States (Figure 5-26) has observed steady increases in recent years and is approaching the size of total hip and knee arthroplasty an annual sales (Orr er al., 2007). The spinal fusion market commands much of the market share for spinal implant devices but the emergence of TDA as an effective alternative to fusion is expected to divert some of the fusion market to it. This effect would be enhanced by the introduction of a TLAS.

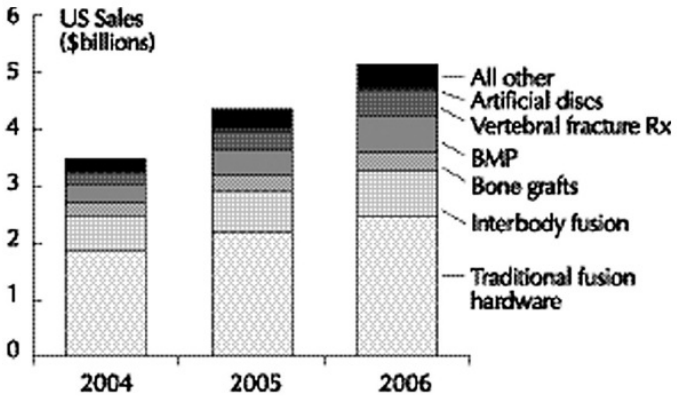


(Reproduced from Orr *et al*, 2007)

**Figure 5-26: Spinal device sales in the United States (BMP=bone morphogenic protein)**

Unfortunately, the extent of a future market for a cervical TLAS cannot be determined with certainty based on the data presented so far. Problems such as wear particle-induced osteolysis or structural fatigue could discourage the application of TLAS. Furthermore, advances in tissue engineering might provide a better alternative to TLAS. However, at the present time, there does appear to be a strong potential market for TLAS.

The application of the engineering design process to the development of such a device combined with adequate research and development could mitigate the risk of implant failure after long-term clinical implantation.

## 5.6 Facet Joint Implant Designs

There are a number of conceptual designs for the replacement of facet joints in the lumbar spine but there is currently no FDA approved device on the market and all are classified as investigational devices in the United States. For the cervical spine, in particular, the present author has not found any conceptual designs in the mainstream media or in the academic literature.

### 5.6.1 Patent by Fitz (2000)

An early patent for a facet joint replacement implant was obtained by Fitz (2000). The patent was issued in 1996 and re-issued in 2000. The proposed implant design could be classified as a surface replacement device that consisted of separate components that would be placed on both the superior and inferior surfaces of the facet joint. The implant was presented (Figure 5-27) in an article by Zigler (2009). The patent suggested that the inferior component might have a surface made of a polished medical grade cobalt chromium molybdenum alloy or a medical grade ultra high molecular weight polyethylene. This implant apparently relied upon the fibrous capsule of the facet joint and other spinal ligaments to maintain alignment and stability.

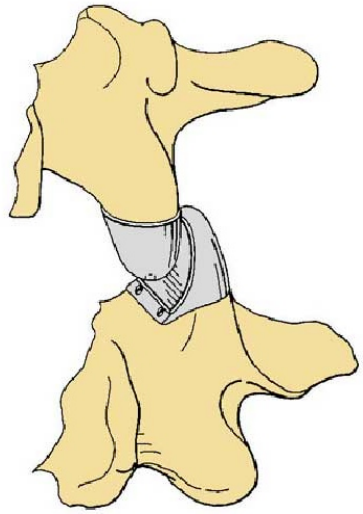

(Adapted from Spine-Health, 2009)

**Figure 5-27: Facet joint replacement implant**

By covering the affected bony structures with a metallic cap, the pain associated with the facet degeneration would probably be eliminated. Somewhat similar implants have been used successfully in hip arthroplasty. However, in order for this design to maintain stability, the fibrous capsule of the facet joint and the surrounding spinal ligaments would have to be functional and preserved after surgery. However, in severe cases of spinal degradation, the joint capsule and surrounding ligaments might not be intact (or could be significantly damaged) and therefore this device might be subject to misalignment and instability. The lack of geometric conformity of the natural facet joint would exacerbate this potential problem. Also there might be complications associated with stress shielding if the loading is not transferred to the underlying pedicle bone uniformly which could result in implant loosening and the need for revision surgery.

### 5.6.2 ACADIA™ Facet Replacement System

The ACADIA™ facet replacement system (Figure 5-28) was developed by Facet Solutions Inc. (Facet Solutions, 2009). It was developed based on studies of intact facet joints to mimic the natural kinematics and range of motion. The implant was machined from a cobalt alloy with a plasma sprayed titanium plus hydroxyapatite coating on its bone-contacting surfaces to promote bone in-growth. Further fixation was achieved by titanium alloy pedicle screws. The articulating surfaces seemed to be ball joints made from highly polished cobalt alloy.

(Adapted from Facet Solutions, 2009)

**Figure 5-28: Two views of the ACADIA™ Facet Replacement System**

The ACADIA™ implant replaces the damaged natural facets with metallic components after removal of the entire facet and pedicle structures. The original motion of the natural facets is produced by the articulating metallic components. There appear to be a stabilization link that connects the adjacent balls of the superior components of the implant. This may be an effort to reduce the moment generated on the superior fixation that is caused by the articulating ball being at the end of a cantilever beam.

### 5.6.3 Total Facet Arthroplasty System (TFAS)

The TFAS® (Figure 5-29) was developed by Archus® Orthopedics. The device is secured to the vertebral bodies via pedicle screws and articulation is achieved and controlled using two caudal socket type bearings as articulating surfaces. The superior component is fixed in the pedicles using bone cements. The two inferior components are fixed in the same way, each in its own pedicle. Initial cadaveric studies of the TFAS system have shown encouraging results following facetectomy without disc removal and/or replacement (Phillips *et al*, 2009).

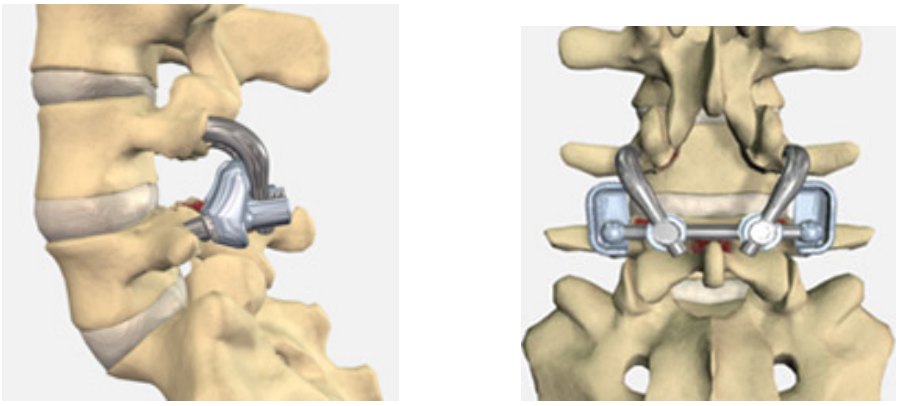

(Adapted from www.archususa.com)

**Figure 5-29: Two views of the TFAS facet joint replacement**

The TFAS implant is somewhat similar to the ACADIA implant described in the previous section. However, it permits more motion because the ball is not contained within a ball joint but rather it can slide is an open-ended box. Thus, this implant does not provide much resistance to flexion unless the ball encounters the end of the box. Compared with the ACADIA, the reduction in constraint may or may not be advantageous but the wear is likely to be higher due to the sliding with a smaller contact area. Also, the cement fixation is questionable and may eventually suffer fatigue damage.

### 5.6.4 Total Posterior System (TOPS)

The TOPS lumbar facet replacement system (Figure 5-30) was developed by Impliant, Inc. to replace degenerated facet joints and thus alleviate persistent leg and low back pain associated with moderate to severe spinal stenosis of the lumbar spine between L3 and L5. The design consists of superior and inferior titanium alloy components that are fixed to the vertebral bodies using titanium alloy pedicle screws. The superior and inferior components are connected by load transfer system which is hidden by an elastomeric casing (colored green in Figure 5-30). The load transfer system consists of polycarbonate urethane "bumpers" that apparently provide rotation and extension within certain limits while providing support, stability and perhaps shock absorption (in parallel with the intervertebral disc).

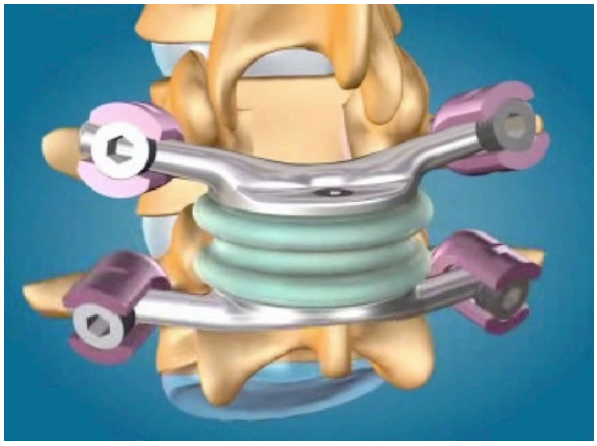

(Adapted from Impliant Inc., 2009)

**Figure 5-30: TOPS lumbar facet replacement system by Impliant Inc.**

The compliant core introduce some shock absorption which may mitigate the shock loading observed by the device at the bone-implant interface and may reduce the chance of overloading and/or loosening of the device and perhaps share shock absorption with the intervertebral disc. The contraindications for the device include a primary diagnosis of degenerative disc disease and therefore the device is intended mainly for facet joint degradation and not for patients exhibiting disc damage (Impliant Inc., 2009).

# Chapter 6
# Design of a Cervical Total Level Arthroplasty System

The previous sections have provided a detailed background to our design problem and the current state of spinal arthroplasty and commercially available prosthesis. The design method that has been adopted to allow for the improvement of the field to accommodate the replacement of both the cervical disc and facet joints now requires specifications of the analysis of need, problem definition, constraints to provide boundaries for the problem and criteria to judge the alternative designs. While other formats can be used to present our design approach, in our opinion, the chosen one provides the greatest clarity.

There are three clinical situations in which facet replacement may serve as an adjunct to total disc replacement: (1) concurrent facetogenic and discogenic lower back pain, (2) asymptomatic facet degeneration and discogenic lower back pain, and (3) facetogenic pain associated with a previous total disc replacement. The occurrence of simultaneous facet and disc based pain is a relatively rare situation with only 3% of a study population who underwent both disc and double facet blocks showing positive indications on both tests. Thus this population would be a rare indication for a total level arthroplasty procedure. Facet degeneration frequently accommodates disc degeneration especially in elderly patients exhibiting collapsed discs. The availability of a total level arthroplasty device would widely expand the indications for total disc replacement to include this patient population (Kim et al, 2006). Degenerated facet joints tend to limit segmental motion after total disc replacement and are therefore a common contraindication to the procedure. A recent study of patients with the Maverick disc prosthesis showed that patients with severe facet degeneration exhibited significantly smaller range of motion of the devices.

## 6.1 Analysis of Need

Patients, that exhibit both disc and facet joint degeneration in the cervical spine, are surgically limited to spinal fusion since facet damage is typically a contraindication for total disc arthroplasty (TDA). Fusion causes an increase in the loads and motions of the adjacent discs and facet joints which may lead to their degeneration. TDA is also somewhat limited in that the implant causes small modifications in the natural kinematics and in the natural facet contact pressures at the operative level. This may eventually lead to atrophy and/or accelerated facet joint degradation. Also, the current TDA designs are not specifically designed to function in conjunction with facet replacement implants and thus the performance of both devices if applied in tandem would be questionable.

This suggests that a cervical total level arthroplasty system (CTLAS) for the cervical spine should consist of both TDA and facet joint replacement implants that could operate alone or together and could be implanted almost simultaneously (within months of each other) or in a longer sequence (within years of each other). This CTLAS implant system must produce very similar load distribution and kinematics at both the operative and the adjacent level discs and facet joints. Furthermore, all components must be very resistant to structural fatigue to avoid *in situ* collapse, fixation fatigue to avoid mechanical loosening and wear to avoid wear particle-induced osteolysis.

The development of a CTLAS implant system that actually satisfies all these needs would be a remarkable achievement and would take many years. It would allow the selective or combined treatment many of the severe spinal joint (disc and facet) degeneration problems in a manner that discourages the progressive sequence of spinal degeneration. However, the many other spinal diseases and abnormalities (such as vertebral osteoporosis, scoliosis, rheumatoid arthritis of the facet joints and so on) would continue to be very challenging to treat.

## 6.2 Problem Definition

The design of a CTLAS implant system is probably an inevitable development in spinal surgery. The development is likely to happen in a graduate rather haphazard way. For example, severe curvature of the spine was first treated with Harrington rods, then Luque rods and finally the complex rod and fixture systems that now distract, align and de-rotate an abnormally curved spine. This process took some 40 years and continues to evolve. However, if some bold, integrative, well-engineered efforts can be made in the mechanical design of the implant hardware early on, the development of effective surgical treatments may be accelerated.

The design problem can therefore be defined as follows:
*In order to provide patients exhibiting both disc and facet degeneration in the cervical spine a surgical alterative to spinal fusion, the means by which to restore the natural kinematics, load sharing and range of motion of the spinal segment via the replacement of both the disc and facet joints is required to be investigated and designed.*

The scope of this problem includes the design of the mechanical means by which to facilitate the total level replacement of the cervical spinal motion components in their entirety. Accordingly, our problem is to develop a conceptual design for a CTLAS implant system. To accomplish this objective, we must apply some design constraints to limit the scope of the problem. Otherwise, the problem becomes intractable. To this end, we have considered important design criteria that govern the selection of our final design from a number of choices (alternative designs).

## 6.3 Design Objectives

The objectives of the current investigation include the investigation and design of an implant for use in cervical total level arthroplasty to accommodate the replacement of both the intervertebral disc and facet joints.

## 6.4 Design Specifications

Further investigation is required in order to allow for the application of the engineering design process for the development of a cervical spinal arthroplasty.

### 6.4.1 Targeted Spinal Level

The facet joints of the cervical spine (Figure 6-1) are oriented more horizontally than in other regions of the spine. The upper facet joints make an angle of approximately 45 degrees superiorly in the transverse plane and

gradually assume a more vertical position as they move towards the thoracic region. The facet widths increase from C3 to T1 with the interfacet distance varying from 9 to 16 mm (Kurtz and Edidin, 2006).

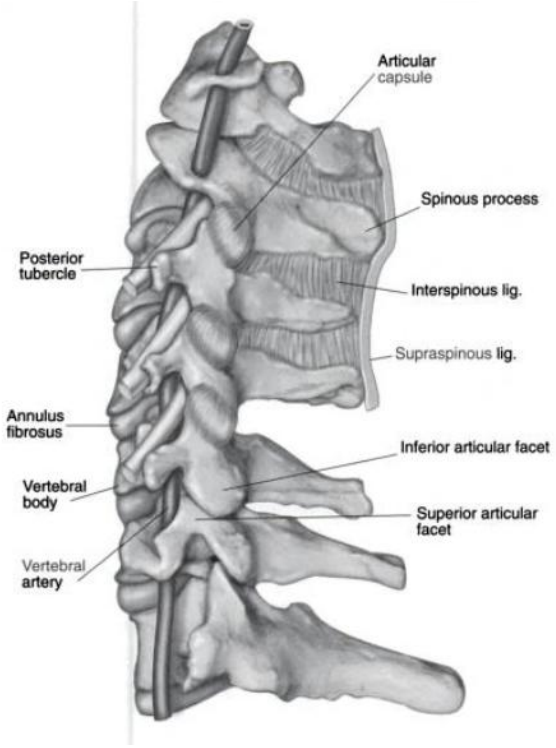


(Reproduced from Clark, 2005)

**Figure 6-1: Lateral view of the cervical spine**

The varying geometry of the facets and relative position to the intervertebral disc would require that any potential prosthesis design for use in the cervical spine be available in different sizes to accommodate implementation at different spinal levels. In order to simplify the current design investigation, a single level will be selected so that the mean dimensions of the selected level can be used in the process.

Injuries due to flexion-extension motion are the most common type of damage observed in the cervical spine. The C5-C6 spinal level is the most commonly injured level observing the highest proportion of flexion-extension, compression, and rotation injuries incurred in the cervical spine (Tjandra, 2006). The main weight-bearing role of the cervical spine is to support the mass of the head. When the natural curvature of the spine is combined with any flexion or extension motion the moment arm created from the downward acting head weight force is maximum at the C5/C6 level (Figure 6-2).

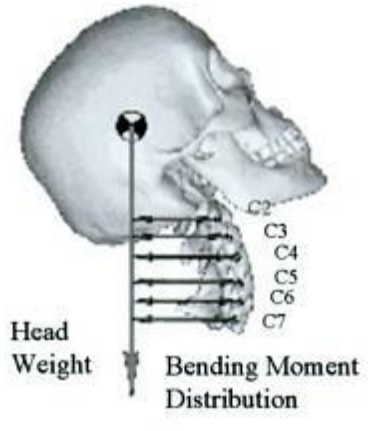


(Reproduced from Kim *et al*, 2006)

**Figure 6-2: The caudally increasing bending moment distribution in the cervical spine from**

This generates the highest applied moment at the C5/C6 level, as seen above, and as a result of this the highest axial force and disc pressures result. The facets are also loaded as the spine attempts to buckle under load and migrate to the anterior (or to the right in the case of the given loading pattern).

Therefore in order to accommodate the design process the C5-C6 level will be analyzed since this is the most commonly injured level in most injury modes. After the initial development of the design it is expected that the device can be adapted to other cervical spinal levels by scaling the dimensions and or spatial relationships of components that would then allow the design to be applied to a broader range of spinal segments.

### 6.4.2 Range of motion and Instantaneous Centers

As discussed in previous sections the motion of the disc and facets is heavily interdependent and modification of the motion characteristics of one is likely to change the loading and contact of the other. Therefore each potential design must attempt to mimic the natural range of motion and instantaneous centers such that the supplied motion is as close to the natural kinematic motion of the spine as possible. This will ensure that the impact to the remaining biological features is minimized post-operatively.

## 6.5 Needs Assessment

The need to accommodate degeneration of the cervical spine is well known and can be accommodated using a variety of methods ranging from physiotherapy and pain management to more invasive surgical techniques including spinal fusion or disc replacement. The application of each individual technique must be carefully judged by both the suffering patient and his/her medical practitioner to select the most advantageous therapy on an individual basis. As technology has progressed the complexity (and arguably efficiency) of the available treatments has also progressed from motion therapy through to some of the more recent techniques including total disc replacement. These advancements have allowed for the improvement in the areas of motion

preservation, pain management, adjacent level degradation and post operative quality of life. Therefore the present need for a disc replacement technology is currently known.

However the present state of disc arthroplasty technology does fall short of the biologic spinal segment in terms of the ability to repair damaged facet joints, particularly in the cervical spine where the facets assist in most spinal loading conditions. At the present time damage to the facet joints can be accommodated with removal of the facet joints which leaves the spinal segment more likely to be damaged by overloading because some (or all) of the facets have been removed and thus more of the load has to be carried by the remaining intervertebral disc. If facet damage accompanies disc damage then disc replacement is prohibited and fusion of the segment is typically performed if the resulting pain is severe enough. This severely limits the motion of the fused segment and results in increased stresses in the adjacent segments as they attempt to make up for the loss of motion at the fused level.

While fusion is a much simpler procedure, the advantages of joint replacement and the resulting motion preservation, makes spinal arthroplasty a more favorable option for many patients. This option is currently not available for those with facet damage and thus this represents a current shortfall in spinal arthroplasty technology.

However, in order to compete with the more simple fusion procedure any potential disc and facet replacement must have a simple surgical procedure that the surgeons will favor. Most patients will want to select the motion preserving joint replacement option compared to fusion due to the potential for long-term motion restoration and to reduce the chances of subsequent adjacent level degeneration that can occur after fusion. The healthcare provider is also a customer of the design, and therefore the cost of both the device and the procedure should also be minimized.

If the needs of all the key customers can be adequately addressed, then a cervical total level arthroplasty system would be suitable for implementation in the spinal arthroplasty market.

## 6.6 Design Constraints

### 6.6.1 Cervical Spine

While a total level arthroplasty system for the lumbar spine might also be useful, we have chosen to restrict our design to the cervical spine. The loads on the cervical spine are lower than in the lumbar spine, but the kinematics are much more complicated, especially with the spinal cord nearby and the facet joints carrying significant normal load. Fusion also introduces quite serious problems in the cervical spine due to the increased range of segmental motion required in this region.

The cervical spine was also selected due to the increased need for clear post-operative medical imaging because of the proximity of the disc and facets to the spinal cord, surrounding this essential neurological structure on three sides.

### 6.6.2 Avoid Fixation Issues

The design of the bone-implant interface would be a challenging problem and would probably involve pedicle screws and bone in-growth surfaces. Innovation here would be risky and ultimately

clinical trials would establish whether the fixation was adequate. This is not included in the scope of the current design project. At this stage, we will assume an adequate fixation design can be developed without significantly changing our proposed mechanical design of a CTLAS implant system. Thus, we will avoid designing the fixation but our design will be judged to some extent by controlling the stress at the bone-implant interface as explained subsequently in the Design Criteria section.

### 6.6.3 Material Selection Emphasizing Minimizing Image Distortion

The design of improved materials will not be attempted in our CTLAS design. However, we do intend to make extensive use of materials that have minimal effect on the performance of post-operative medical imaging. The rationale for this constraint is our judgment regarding the importance of medical imaging in the cervical spine. It should be noted that the selected material must have adequate structural strength, fatigue resistance, virtually no medical image distortion, bulk biocompatibility and, in most contacts, wear resistance.

### 6.6.4 Mechanical Design Only

The proposed CTLAS design will be constrained to include only a mechanical design with a focus on obtaining the kinematics and range of motion required by the spinal segment. Subsequent stress analysis and development and manufacture of prototypes for initial creep, fatigue and wear testing are to be the focus of future studies. Thus, we will produce a conceptual design with some supporting experimental data. Cadaveric studies, surgical investigations with animals and clinical trials would all be performed after our conceptual design has been developed. It is recognized that some modifications might have to be made based on the results of subsequent more clinical studies but we hope to avoid the need for extensive modifications by having a good mechanical design for CTLAS.

### 6.6.5 Modularity

The implants in the CTLAS system should be modular meaning that they can be implanted individually or as a group. This constraint is required because while the spinal degradation may initially only include one structure (disc or facet), subsequent degeneration of the remaining natural component(s) may need to be addressed by the system. Failure of both the disc and facets could simply be addressed by the concurrent application of both the disc and facet replacement devices. This constraint has some important implications. Since the first surgery could replace either one of the facet joints or the intervertebral disc, only the second surgery can have mechanical links to the implant of the first surgery and, finally, only the third surgery can have mechanical links to one or both of the first and second surgeries. Now, it might be possible to design three implants (one for each facet joint and one for the intervertebral disc) that do not have any mechanical links between them. However, to avoid abnormal loading or motion on the remaining natural joints, the implants would have to mimic the natural spine closely.

## 6.7 Design Criteria

The following design criteria will be used to judge the alternative designs and lead to the selection of a "chosen" optimal design. The basis for judgment will be mostly qualitative and thus the final chosen design will require extensive evaluation to justify its continued implementation. While we will initiate this evaluation, the full assessment is beyond the scope of our proposed design efforts.

### 6.7.1 Kinematics (Geometry and Motion)

The CTLAS should have a minimally intrusive geometry, replacing as little bone as possible and staying within the confines of the motion segment (2 vertebral bodies and processes, disc and facet joints). The CTLAS implant system must stay as far as possible from the spinal cord and any branching nerves and prevent migration to such structures. The CTLAS should produce, as close as possible, the motion and motion limits of a healthy natural spine in order to avoid damage to the remaining joints and tissues at the replacement level and to discourage adjacent segment degeneration. Reproduction or accommodation of the helical axis and inherent coupling of axial rotation and lateral bending that occurs in the cervical spinal must also be addressed in the CTLAS in order to maintain, as closely as possible, the natural load sharing of the spinal elements.

### 6.7.2 Stress (Load Sharing)

The stress within the implants, at the implant-bone interfaces and in the articulating contacts should be evenly distributed. This is particularly important in the contact because stress peaks can cause higher wear with associated wear particle-induced osteolysis and at the bone-implant interface because it can lead to a breakdown at the interface. In both cases, loosening of the implants can occur and revision surgery would then be required. Also, regions of low stress should be avoided at the bone-implant interface because they can cause stress/strain shielding and a deleterious resorption of the bone.

As for the motion, the stress within the remaining tissues should stay as close as possible to that of a healthy natural spine to avoid damage to the remaining joints and tissues at the replacement level and to discourage adjacent segment degeneration.

### 6.7.3 Shock Absorption

The CTLAS should passively provide an appropriate range of shock absorption, if possible. The target range of shock absorption is somewhat difficult to define because the natural amounts of spinal shock absorption decline quite dramatically with age. The benefits of shock absorption may be observed at the implant level and at more remote locations such as junctions of branching nerves at adjacent levels or even at other sections of the spine.

### 6.7.4 Creep, Fatigue and Wear Resistance

The CTLAS design should be creep resistant to maintain its geometric integrity, fatigue resistant to avoid component fracture and wear resistant to avoid wear particle-induced osteolysis. Since our design constraints have removed the fixation design from consideration, the fatigue of the bone-implant interface will not be considered. However, we will assume a bone in-growth fixation in some regions and try to control the overall bone-implant interface stress as discussed above.

### 6.7.5 Medical Imaging

The CTLAS should be comprised of a material that minimizes post-operative image distortion through the use of material that is radio-translucent to some extent. It may be necessary to use a small amount of titanium alloy (perhaps for pedicle screws used in the fixation) in one or more of the alternative designs and, if so, the effect on medical imaging will be considered during judging.

### 6.7.6 Surgical Procedures

Efforts will be made to design a CTLAS system that is easy to place surgically. This may be accomplished with a design that is as simple as possible and can possibly accommodate some degree of misalignment. While it may be somewhat difficult to anticipate the extent of the surgical complexity without cadaver studies and clinical trials, some attempt to judge this characteristic will be made.

### 6.7.7 Manufacturing and Total Cost

Some efforts will also be made to consider ease of manufacture and low total cost in the design a CTLAS system. The complexity of the design and dimensional tolerances will be the main contributors to the cost of the design.

## 6.8 Abstraction and Synthesis

In order to develop several different CTLAS design options that will satisfy all of the design constraints, a morphological table can be developed and used. The first column of the table will be populated with design aspets that will need to be specified to define a particular concept. To the left of each design aspect, all possible design options that fall within the respective aspect will be listed. Each design option represents a unique design option and if one design option is selected from each listed design aspect, then a unique design concept will be formulated. Each concept formulated using the morphological table will meet the design constraints because each design option listed under each design aspect meets the criteria.

### 6.8.1 Selected Design Aspects

*Material:* The material specified for construction of the design could include one or more types if, for example, an insert in back plate style configuration is suggested. The material design options are somewhat limited because all materials that significantly degrade medical imaging cannot be included.

*Level of Disc Constraint:* The amount of constraint provided by the disc prosthesis is considered and ranges from no constraint (such as a spherical contact on a flat plate) to constrained (which could be a tightly fitted ball-in-socket configuration). Current disc prostheses exhibit varying levels on constraint depending on the stability the device must provide and the share of load that the remaining natural stabilizing structures are to carry post-operatively.

*Type of Disc Replacement:* The type of articulation that is employed by the disc replacement design is considered. A ball-in-socket and spherical contact types are sliding articulations while a gear style represents a gear like articulation where slipping is controlled with ridges. A rolling element articulation employs rolling rather than sliding to allow relative motion between the surfaces. A deformable design mimics the natural disc with the use of a low modulus material but may suffer from fatigue issues.

*Facet Constraint Location:* The facet joints constrain motion to some extent and are responsible for coupling axial rotation and lateral bending. The CTLAS can recreate this motion constraint after removal of the facets at two possible locations, at the location of the original facet joints or at the disc.

*Shock Absorption:* The design may not provide any shock absorption, or could provide it to the articulation via a leaf, coil or cantilever spring, or with the use of some low modulus and deformable material.

*Device Interconnection:* This aspect specifies whether or not the individual components (if any) are interconnected. All the components (disc and facet) can be interconnected; just the facets joint replacements, or all could be individually applied to the spinal segment without any physical bridging.

*Type of Facet Replacement:* The type of facet replacement includes consideration of the case where the facets are simply removed and the motion and constraints are applied at the disc prosthesis, where a surface style replacement replaces the facet surfaces at the physiological location or where there are hardware 'outriggers' mounted on the anterior or posterior of the intervertebral body.

### 6.8.2 Morphological Table

A morphological table was constructed using the design aspects listed above with various choices for each design aspect. However, the overall design must satisfy all of the design constraints (Table 6-1).

**Table 6-1: Morphological Table**

| **Design Aspect** | **Design Options** | | | | |
|---|---|---|---|---|---|
| **Material** | **polyethylene** | PEEK | **titanium** | ceramic | |
| **Level of Disc Constraint** | constrained | **semi-constrained** | **unconstrained** | | |
| **Type of Disc Replacement** | **ball-in-socket** | rolling element | **spherical contact** | gear | deformable |
| **Facet Constraint Location** | none | **at the facets** | at the disc | | |
| **Shock Absorption** | none | **leaf spring** | coil spring | cantilever spring | deformable |
| **Device Interconnection** | **none** | facets only | disc and facets | | |
| **Type of Facet Replacement** | none – remove & constrain at disc | surface style | **posterior hardware** | lateral hardware | |
| Concept #1 design selections | | Concept #2 design selections | | **Concept #3 design selections** | |

The selection of one or more design option for each aspect results in the generation of a design concept. Care must be taken during this process to select design options that are compatible. For example, if the 'none' or 'at the disc' facet constraint location is selected, then the 'posterior hardware' type of facet replacement cannot be chosen because we have already decided to provide the facet constraints at the disc. This process was completed three times to generate three unique design concepts that all meet the design constraints defined earlier in this document.

Design concept 1 uses a titanium and polyethylene, semi-constrained disc replacement with a combination spherical and gear contact to support and control applied loading and resulting motion. The facet constraints are applied at the disc to eliminate the need for separate facet replacement devices. No shock absorption is accommodated with concept 1 because the combination articulation will not be supportive of the surface deformation required to provide compliance.

Design concept 2 comprises an all-PEEK semi-constrained disc replacement that uses a combination ball-on-socket and spherical contact articulation. The facets are replaced at the physiological location using a surface style replacement with no device interconnection. The design provides no shock absorption due to the complexity of the articulations used.

Design concept 3 uses titanium and polyethylene to comprise a combination ball-in-socket and spherical contact disc replacement. The facet constraints are applied at the facets and shock absorption is to be provided using a leaf spring style motion stops. The facets will be replaced using posteriorly mounted hardware that will not be interconnected to the disc replacement component due to the presence of the spinal branching nerves that are located between the disc and facets in the cervical spine.

These design concepts can then be judged and ranked using the design criteria to select the most suitable design solution. This allows for a number of designs to be generated and ranked relatively early in the process so that little effort is wasted on non-ideal designs.

### 6.8.3 Design Concept #1 – Fluted Rotationally Constrained Disc

The design option selections for design concept 1 can be seen as boxes outlined in a thick blue border in the morphological table. This design consists of a two-piece prosthesis that occupies the disc spaces that applies the rotational constraints of the facet joints at the disc (Figure 6-3). The superior component is concave to interact with the convex inferior component and it fluted with teeth of a constant thickness along the anterior-posterior dimension. These teeth interact with corresponding depressions in the inferior component that is flared moving outwards from the centre of the prosthesis to allow the normal physiological range of axial rotation. The superior component is manufactured using a titanium alloy because of the strength needed to resist the axial torsion applied to the relatively small teeth ridges (a polymer would probably not be strong enough for the required teeth dimension). The inferior component is comprised of polyethylene because the larger groove dimensions permit a weaker base material to be used.

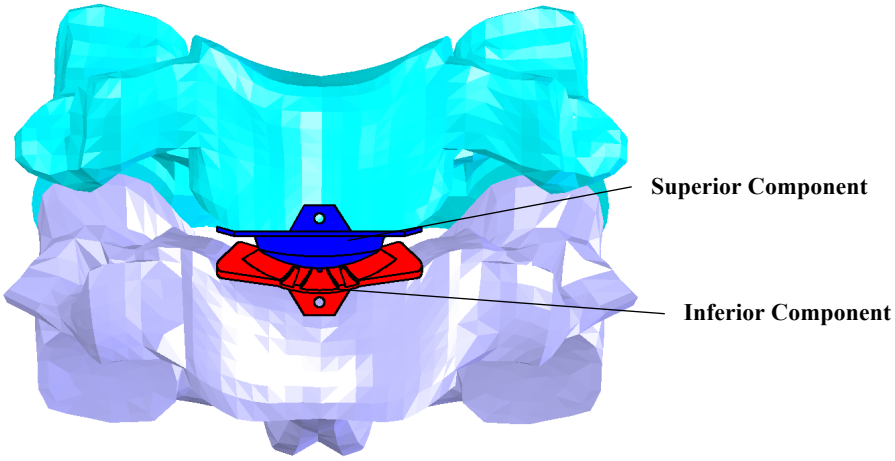


**Figure 6-3: Concept #1 - Fluted rotationally constrained disc**

The instantaneous centre of rotation in both flexion-extension and lateral bending is located near the superior surface of the inferior vertebral body. This mimics the natural location of the ICR in F-E but not in lateral bending where it occurs near the centre of the superior vertebral body. The titanium/polyethylene material pairing was selected since this combination is commonly used in commercially available total disc replacements at the present time. While it doesn't represent a significant improvement in medical imaging (due to the inclusion of titanium in the superior endplate), the expected loading of the fluted components justifies the use of a metallic superior component.

The type of contact employed for the disc is a spherical contact with a geared element that controls the amount of axial rotation permitted between adjacent intervertebral bodies (Figure 6-4). This is done to reproduce the rotation constraints of the natural facet joints at the disc. If the facets are intact the device will assist the

natural facets in limiting rotation in an attempt to reduce the potential for post-operative facet overloading. If the facets are damaged they are removed via a facetectomy at the time of insertion of the disc prosthesis and the disc prosthesis provides all resistance to over-rotation. If the facet capsules are healthy enough they are maintained to provide some stability in extreme flexion when they normally enter a state of tension.

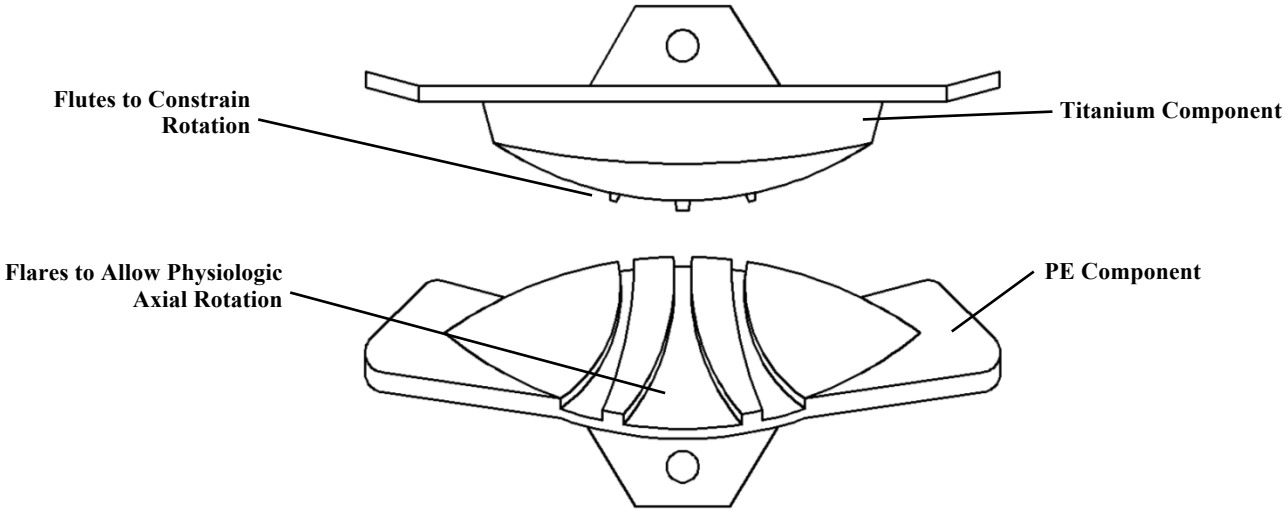


**Figure 6-4: Detailed view of design concept #1**

There is no shock absorption included in this design. There is also no need for device interconnection in this case since the kinematics and constraints of both the disc and facets are accommodated with a single device located in the disc space.

### 6.8.4 Design Concept #2 – Helical Axis Disc with Facet Surface Replacements

The design option selections for design concept 2 can be seen as boxes shaded in light grey in the morphological table. This design concept consists of both a disc and facet replacement system which are designed to operate individually or in unison, depending on the needs of the patient (Figure 6-5). The disc replacement is ramped on the posterior edge to mimic the natural helical axis of the cervical spine and motion coupling of axial rotation and lateral bending. As the superior vertebral body is rotated, lateral bending is imparted as the posterior edge of the superior component ramps up the inferior component. The ratio of motion coupling is tuned via geometry to match the natural motion coupling of the human cervical spine.

The facet joints are replaced using a surface style design which allows the facet joint capsule to remain if it is healthy at the time of implantation. This will allow the capsules to continue to provide stabilization in cases of extreme flexion when the capsules are under tension and prevent hyper-flexion.

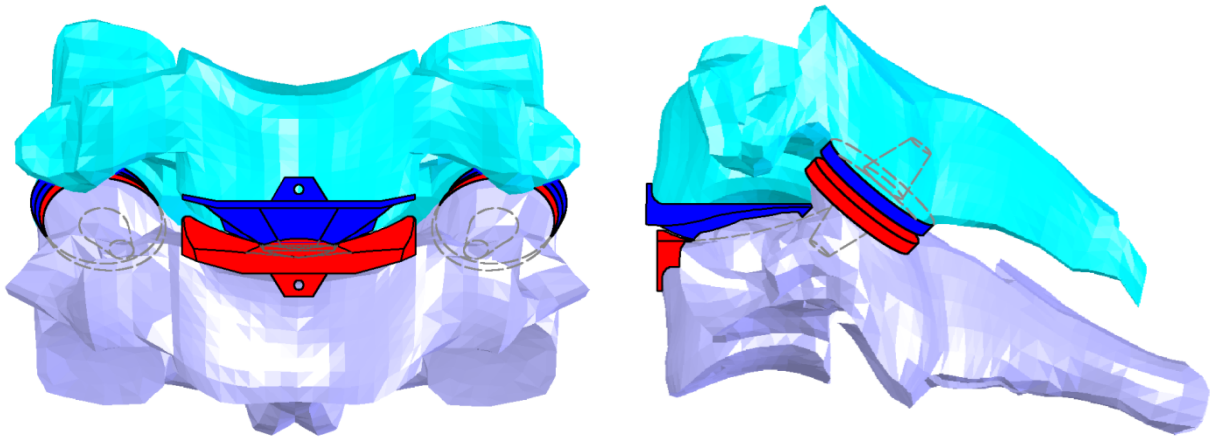

**Figure 6-5: Concept #2 – Helical axis disc with facet surface replacements**

All-polymer PEEK articulations were selected for the design of both the disc and facet joint replacements because the geometry provided large contact areas which is suitable for the (softer) polymeric bearings. In the disc replacement component, loads are transmitted through both the spherical contact (which also acts as a pivot in combined axial rotation and lateral bending) and the posterior ramp surfaces, which when combined, represent a relatively large area of contact thus mitigating the contact stresses observed at the contact. The facet joint replacements also observe low contact stress since, like the natural facet joints, are conforming and are thus going to observe large contact areas. The inclusion of only non-metallic components in this design means that impacts to post-operative imaging will be minimized.

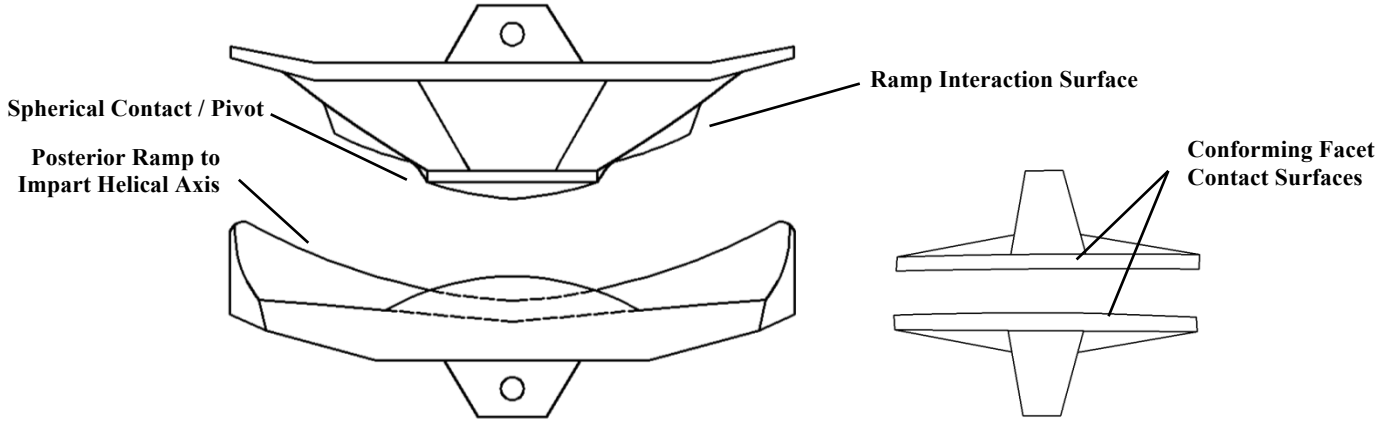


**Figure 6-6: Detailed view of design concept #2**

The disc replacement employs a semi-constrained geometry that limits anterior-posterior shear which is an attempt to limit the potential for overloading of the facet joints (natural or artificial) post-operatively. The device also constrains and couples axial rotation and lateral bending to mimic the natural motion of the cervical spine, which again is provided by the facet joints. This was done to mitigate the potential overloading of the facet joints

that is thought to occur when a disc replacement is unaccommodating to this kinematic characteristic unique to the cervical spine.

The majority of the facet constraint forces remain at the facet joint with some of the loading shared with the disc prosthesis in certain motions including hyperextension. It is important to note that the design intends to maintain the natural load sharing between the disc and facets to prevent atrophy of natural structures. The disc prosthesis attempts to accommodate the natural helical axis by carefully guiding motion much like the way the outer annular fibers are thought to guide motion in axial rotation and modes of anterior-posterior shear.

No shock absorption is provided in this design, although this difference is only apparent in the disc where some compliance is observed in the natural disc. There is also no device interconnection in this design, mainly because of the delicate nerve branches that are present in the space between the disc and facet prostheses, which pose significant neurologic risks.

### 6.8.5 Design Concept #3 – Shock Absorbing PE wafer with Posterior Facet Hardware

The design option selections for design concept 3 can be identified as boxes with bold red text in the morphological table. This concept uses two different prostheses to accommodate the replacement of the disc and facet joints (Figure 6-7). The disc is replaced with a three-piece design that provides a unique center of rotation for flexion-extension motion and lateral bending motion in an effort to mimic the natural ICR locations.

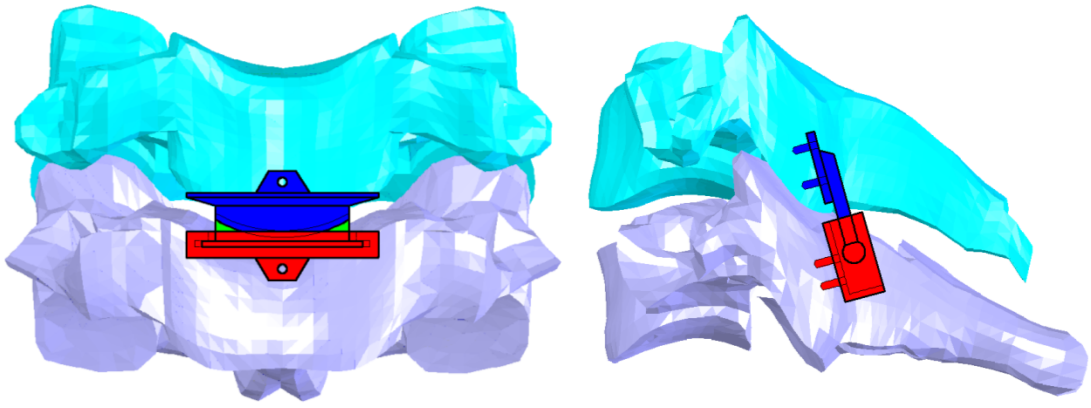

**Figure 6-7: Concept #3 – Shock absorbing PE wafer with posterior facet hardware**

This is accomplished using a saddle design that permits rotation in flexion extension (shown in blue) about the inferior vertebral body, and rotation in lateral bending (shown in red) about the superior vertebral body (Figure 6-8). Axial rotation is accommodated by rotational sliding of the central ‘wafer’ in the lower component and occurs about the centre of the device to mimic the natural centre of rotation that occurs near the front of the endplate of the lower vertebral body.

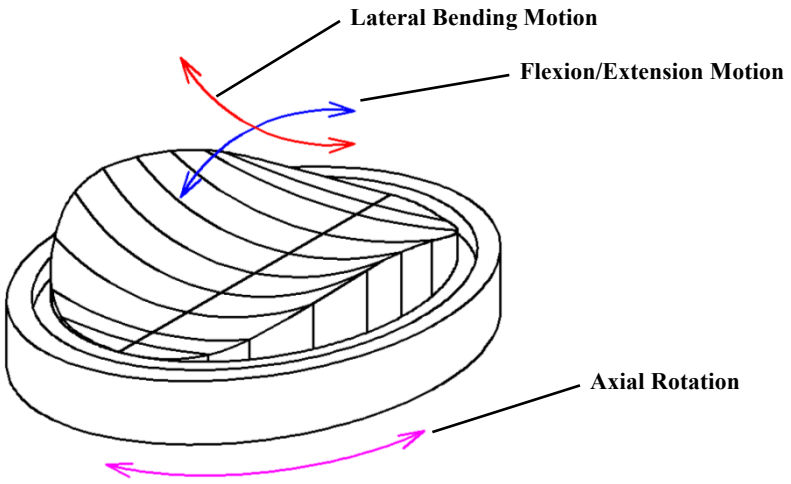


**Figure 6-8: Detailed view of 'saddle type' articulation used in Concept #3**

The design attempts to restore the natural modes of motion to the intervertebral segment about the natural anatomical centre of rotation. This will minimize the effect of the device(s) on the natural kinematics of the spine and thus reduce the possibility of post-operative facet overloading and/or degeneration of other natural structures. The facet joints are accommodated using a two-piece design that is mounted to the posterior surfaces of the vertebral bodies after the damaged facets have been removed (the joint capsule can remain if it is intact to provide some stability in extreme flexion).

The endplates in design concept 3 are made of titanium and the central core is constructed of polyethylene (PE) with a hollow core to provide some shock absorption in the axial direction (Figure 6-9). Titanium was selected as the endplate material because this material has sufficient strength to provide the required stability and strength to support the device and accommodate bone in growth, with appropriate surface characteristics. Specifically an ultra high weight polyethylene (UHMWPE) would be used in the central core for its known wear resistance articulating with metallic components.

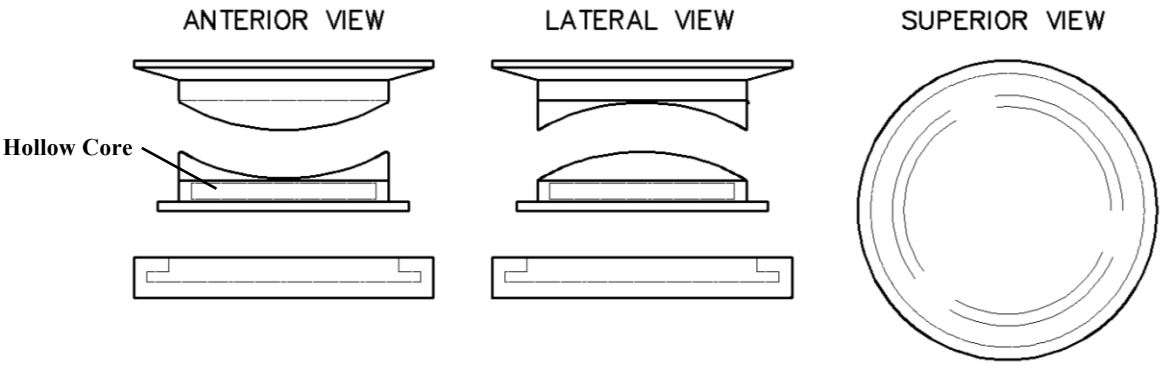


**Figure 6-9: Detailed view of the disc replacement of Concept #3**

The disc is semi-constrained and provides motion about all the natural physiological axes; however the motion is limited to the natural ranges of motion by physical stops in flexion/extension and lateral bending. The

disc replacement includes both a ball-in-socket articulation between the central core and the superior endplate, and a flat planar sliding articulation between the central core and the inferior endplate. It is important to note however that the facet joints provide all constraints in axial rotation because the disc core is free to rotate in the lower endplate. This is slightly different than the natural scenario where the disc provides some resistance to rotation, especially near the end of the range of motion as the annular fibers become loaded in tension.

The facets are replaced with hardware mounted on the posterior surfaces of the intervertebral bodies (on the pedicle surfaces) and thus the facet forces are thus transmitted in a similar fashion as the natural intact segment (Figure 6-10). Shock absorption is included in both the disc and facet replacement, with the disc employing a leaf spring style of suspension via a void in the centre of the PE core that accommodates approximately 1 mm of compression. The facet joint replacement provides shock absorption in flexion as the superior facet moves away from the surface of the inferior facet (shown as a green arrow) causing spreading of the sides of the inferior component. This force increases as the distance moved in the upward direction increases.

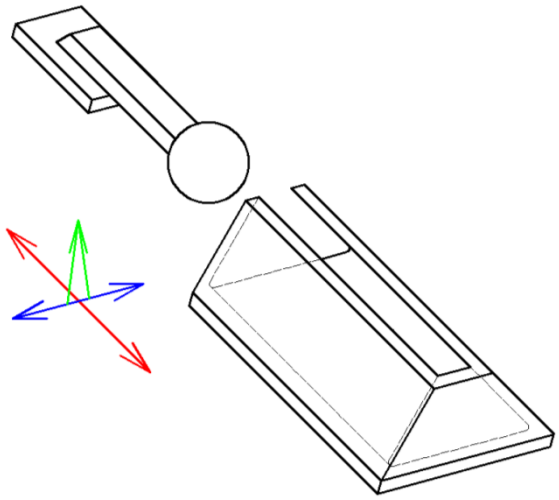

**Figure 6-10: Detailed view of the facet replacement of Concept #3**

The superior component of the facet joint replacement consists of a sphere that articulates within the pocket of the inferior component. The superior detail is manufactured from titanium due to the relatively small dimensions and the loads that it must support during normal operation.

## 6.9 Decision Matrix

In order to evaluate the three design concepts produced with the help of the morphological table, a decision matrix is used. Weighting are applied to each of the previously specified design criteria that reflects the relative importance of each criteria to the success of the overall design (Table 6-2).

**Table 6-2: Decision matrix weighting**

| Design Criteria | Weighting |
|---|---|
| 1. Kinematics | 0.25 |
| 2. Stress (Load Sharing) | 0.15 |
| 3. Shock Absorption | 0.05 |
| 4. Creep, Fatigue, Wear | 0.25 |
| 5. Imaging | 0.20 |
| 6. Surgical Procedure | 0.05 |
| 7. Manufacturing Cost | 0.05 |
| Total | 1.0 |

Design criteria weightings were applied based on the relative importance of each parameter as identified by the present author in terms of their affects on the overall clinical performance of the implant system. The kinematics and bearing characteristics of the design are easily identifiable as the most important contributors to the clinical performance of the design and are therefore raked highest of all the design criteria. Medical imaging was identified by the present author as a major contributor to the improvement of the design of spinal arthroplasty devices and as such was given the second highest ranking. The load sharing of the device, or the degree to which is accurately reproduces the stresses applied to the disc and facets, was also identified as an important criterion. The shock absorption, surgical procedure and manufacturing cost are all important in ranking each design, but are not as important as the previously described parameters and as such are given equally small, albeit not negligible, weightings.

The three design concepts are judged regarding how effectively they address each design criterion and given a score that is multiplied by the weighting for that criterion to generate a numerical representation of the overall effectiveness of each design (Table 6-3). Depending on the fidelity of the author's judgment regarding the scoring and weighting, this decision procedure allows the selection of the best design concept.

In terms of kinematics, design concept 2 is clearly the best option because it best preserves and re-creates the natural helical axis of the cervical spine and thus was given the highest score for this design criterion. The fluted design with rotational constraint is most unlike the natural disc; with the facet constraint applied at the disc space, and thus was scored the poorest.

The degree to which the design accurately mimics the natural load sharing between the disc and facet joints is closely linked to the kinematic accuracy of the design and at the concept stage must be estimated using the degree to which the design applies the physiological loading to the natural anatomical structures of the spine. If the location of load application and distribution is varied significantly from the natural layout, then a low score will be observed whereas if loads are applied in a similar manner then a higher score will be achieved. These

scores will be coarse since the difference between a 5 and 6 is nor discernable with an estimate at this stage in the design. Concept 2 was ranked the highest because the natural locations of constraint are maintained, and the degree of load sharing between the disc and facets is maintained similar to the healthy state by accommodating the natural helical axis. Concept 3 maintains the natural locations of constraint (rotation is constrained at the facets) and was ranked 2nd. Concept 1 was ranked poorest because the rotation is constrained at the disc and not at the facets, this may cause some degree of atrophy.

At the concept stage, quantifying the shock absorption of each design is difficult because an actual device has not been manufactured and tested. Therefore in order to judge each design, the expected shock absorption and ability to approach the natural force-displacement response of the spine will be estimated. The values given to these parameters will likely be coarse since deciphering between a rank of 5 and 6 is impossible with an estimate, and thus a low rank will represent an unaccommodating design and a high number will represent a design that could potentially reproduce the shock absorption of the disc. Shock absorption is only provided by design concept 3 and therefore is ranked first in this design criterion, although the degree to which the design accurately represents the natural disc is currently unknown. It is expected that the deformation would be able to be tuned during kinematic testing to accurately represent the force-displacement characteristics of the natural intervertebral disc. Design concepts 1 and 2 only provide passive compliance and shock absorption through deformation of the polymeric components and therefore are ranked equally poorly. They will still provide some compliance due to their use of polymeric components so there will be some displacement realized with this system, however it is unlikely that they will achieve anything near the shock absorption of the natural disc.

Creep, fatigue and wear are difficult parameters to estimate without actual simulator testing of each design and its corresponding unique geometry. This amount of testing would require significant effort and time to complete and thus this was judged for each design based on the type of articulation and the wear performance that is known and/or expected for the specified material pairing. Concept 2 scored poorest due to the unusual polymer-on-polymer articulation that presents some tribological risks (that were deemed acceptable for the enhanced image clarity). Concepts 1 and 3 were ranked equally higher because of the more common metal-on-poly articulations that are more widely accepted in articulating medical implants.

Medical imaging is based solely on the type(s) of material used in each design concept. Concept 2 is ranked highest because it uses PEEK for the entire design and the radiolucency of PEEK can be tailored from completely radiolucent to opaque if desired. Concepts 1 and 3 contain, by necessity of design, metallic components that distort medical imaging and thus are ranked lower than concept 2 for this design criterion.

The simplicity of the surgical procedure used to insert the device(s) is also difficult to judge, however the current approach simplified this analysis to include whether or not the implant system required an anterior, posterior, or combined anterior & posterior approach to implement the entire system. The requirement of two approaches significantly increases complexity, cost and risk to the patient and thus was ranked poorer than one that required a single anterior or posterior approach. Concept 1 ranked highest in this regard since the disc prosthesis accommodates both the damaged disc and facet joints with one (anterior) approach. Concept 3 ranked

next highest because although it requires two surgical approaches to implement, the posterior facet hardware would be easier to implement than the surface style replacement of design 2 that was ranked poorest.

Manufacturing cost was also estimated through analysis of the overall design complexity and all designs were ranked relatively poorly in this regard since all include complex surfaces with small dimensions and tolerances. Designs 1 and 3 were given a slightly higher ranking due to the complexity of the surfaces required or the disc replacement in design 2 to achieve reproduction of the helical axis.

**Table 6-3: Design concept decision matrix**

| Concept | Design Criteria (*weighting*) | | | | | | | Concept Total |
|---|---|---|---|---|---|---|---|---|
| | 1 *(0.25)* | 2 *(0.15)* | 3 *(0.05)* | 4 *(0.25)* | 5 *(0.20)* | 6 *(0.05)* | 7 *(0.05)* | |
| 1. Fluted rotationally constrained disc | 4 | 2 | 2 | **8** | 4 | **8** | **5** | 4.9 |
| 2. Helical axis disc, surface style facets | **8** | **9** | 2 | 5 | **10** | 6 | 4 | **7.2** |
| 3. PE wafer, posterior facet hardware | 6 | 6 | **8** | **8** | 5 | 7 | **5** | 6.4 |

The decision matrix identifies concept 2 as the best design with a concept total score of 7.2, with concepts 3 and 1 following with 6.4 and 4.9, respectively. In order for a clear leading design to be identified the difference between the highest ranking design and the next best design must be significant; in this case it is deemed that the ranking difference between concept 2 and 3 is viewed to be acceptably large and thus concept 2 is selected as the best design.

## 6.10 Design Process Summary

The previous sections outlined a design process that was used to generate potential design solutions to allow for the replacement of the intervertebral disc and facet joints in the cervical spine. This design process is a customizable tool that, when applied correctly, can be used to solve a wide range of engineering design problems. The first step in utilizing this tool is to define the problem and the need for a solution. In this case, the problem was that current spinal arthroplasty devices modified the natural kinematics of the spine, did not accommodate facet joint replacement, and were constructed of metallic materials that interfered with post-operative imaging to varying extents. There was a need for a solution to this problem because facet forces were increased after spinal disc arthroplasty; and patients with facet degeneration were limited to spinal fusion, a procedure viewed by some as inferior to arthroplasty. After the design problem was clearly defined, the objectives and specifications of the design were defined to outline the general goals and requirements of the concepts. In order to further describe the design, the design constraints and criteria were then explicitly defined. The design constraints identified what each potential design solution must include and/or perform, and the design criteria specified what constitutes a good design and allowed for the judging of different design concepts. In this case one of the design constraints identified that the design must accommodate the replacement of both the disc and facet joints in the cervical spine,

and one of the criteria identified that an effective design is one that will accurately replicate the natural kinematics of the cervical spine after it is implanted. Thus, all of the concepts produced by the customized design process will satisfy the design constraints, but will be judged by the design criteria to varying extents based on their effectiveness.

Accurate definition of the design problem, constraints and criteria allow the design process to produce design concepts through the abstraction and synthesis process using a morphological box. The morphological box encompasses the different design options that may be selected while still satisfying the design constraints. In this case the morphological box included selections such as the type of articulation, material, and location of facet constraints. Selection of one or more design aspect for each design aspect outlined in the morphological box was performed three times to develop three unique design concepts. All three of the design concepts satisfied the design constraints, and were thus valid designs. The best design was selected by judging them based on the aforementioned design criteria. A numerical value (out of ten) was given to each design concept by weighting each design criteria based on their significance to the clinical performance of the design, and then multiplying this weighting by the design's score for each criteria. This was then summed and used to select the best overall design concept.

It is important to note that while the design process used in the present study is an effective tool to aid in the formulation of design solutions, it cannot be applied blindly and requires a great deal of input to ensure that the resulting concepts are novel and effective solutions for the design problem at hand. Therefore it is simply one method to provide a means by which to organize the problem, define the requirements, and produce unique and documented design solutions.

## 6.11 Detailed Discussion of Proposed CTLAS Design

The design process as described above yielded a novel CTLAS to treat both disc and facet degeneration individually or in unison (Figure 6-11). Polyetheretherketone (PEEK) made by Invibio Ltd. (Thornton Cleveleys, Lancashire, UK) was the selected material since it would give clear, radiolucent post-operative imaging, but it also introduced a tribologically unusual all-polymer bearing and this had many implications, as discussed in the next section that outlines the wear testing of PEEK-on-PEEK material pairings. Replacement of the damaged disc is addressed by a semi-constrained bearing geometry that was specifically designed to mimic, with great precision, the *in vivo* motion and load sharing of the disc and facets joints of the cervical spine. The facet joints are treated (if necessary) using a surface replacement design, potentially allowing the facet capsule and synovial membrane to remain if healthy or perhaps re-generate, as could occur in the post-arthroplasty hip. The retention of the facet capsules was considered necessary to contain and replenish the lubricant and to help maintain spinal stability, especially in flexion (Zdeblick *et al*, 1993).

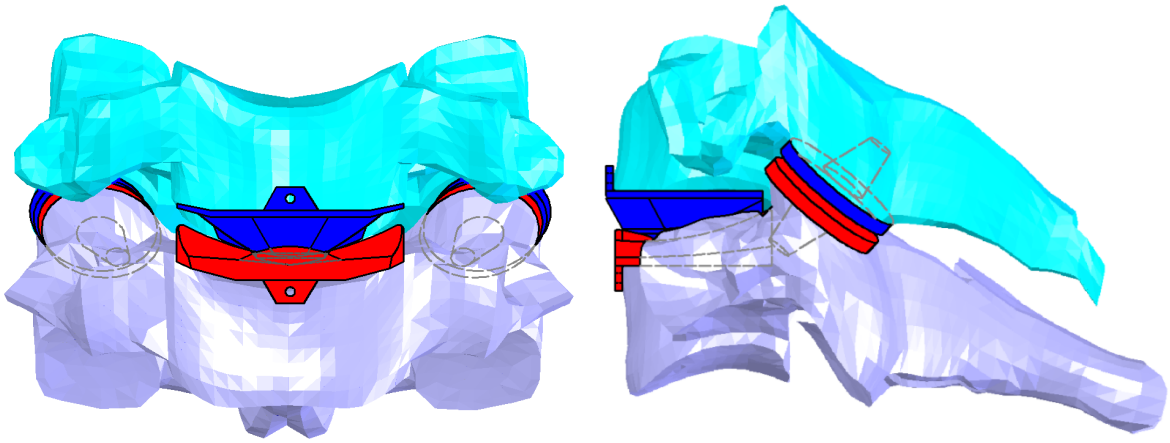

**Figure 6-11: Proposed CTLAS design *in vivo***

To mimic the natural motion, the design pays particular attention to the inherent coupling of axial rotation and lateral bending in the natural cervical spine. This coupling is facilitated by the interaction of the facet joints and creates a motion pattern in the cervical spine in which it rotates about a locus of points that forms a helical (or screw) axis in three-dimensional space (White and Panjabi, 1990). This characteristic of cervical spinal motion could not be accommodated with a fixed centre of rotation. The CTLAS achieved this complex motion with a saddle-shaped inferior surface that was concave in the lateral profile but convex in the anterior profile thus imparting axial rotation during pure lateral bending and vice-versa. The instantaneous center of rotation in axial rotation occurred about the anterior section of the disc space, in lateral bending about the superior vertebral body and in flexion-extension near the surface of the inferior vertebral endplate. These locations are close to the natural locations of these instantaneous centers of rotation (Kim *et al*, 2006; Myers *et al*, 2004; Galbusera *et al*, 2006). Also, some anterior posterior translation is permitted, as occurs in the natural spine.

The facet joint surface replacements are shaped such that all of the natural cartilage (if any remains) including the osteochondral surface is removed prior to insertion (Figure 6-12). This will ensure adequate exposure of underlying bone to promote osseointegration of the device.

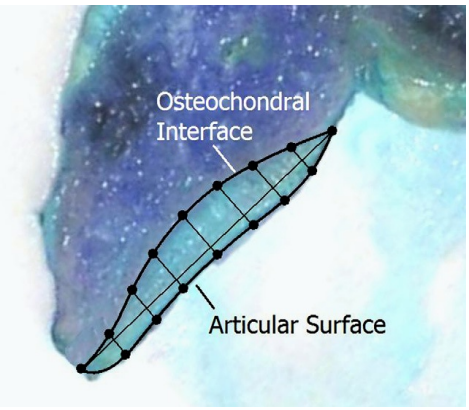


(Reproduced from Womack *et al*, 2008)

**Figure 6-12: Typical facet cartilage thickness**

In order to accommodate the range of natural facet perimeter shapes the facet replacement will target the mean perimeter shape (Figure 6-13). One possible advantage of the all-polymer articulation surface might be that the device could be shaped by the surgeon in the operating room prior to insertion if the natural facet is much smaller than the mean. This means that a fewer number of different sizes would have to be produced at the point of manufacture while still providing a better, more custom fit for each patient. There are concerns that would have to addressed, such as potential damage from the cutting tools during sizing as well as cleaning procedures post-sizing to ensure that the amount of polymeric debris is minimized prior to insertion.

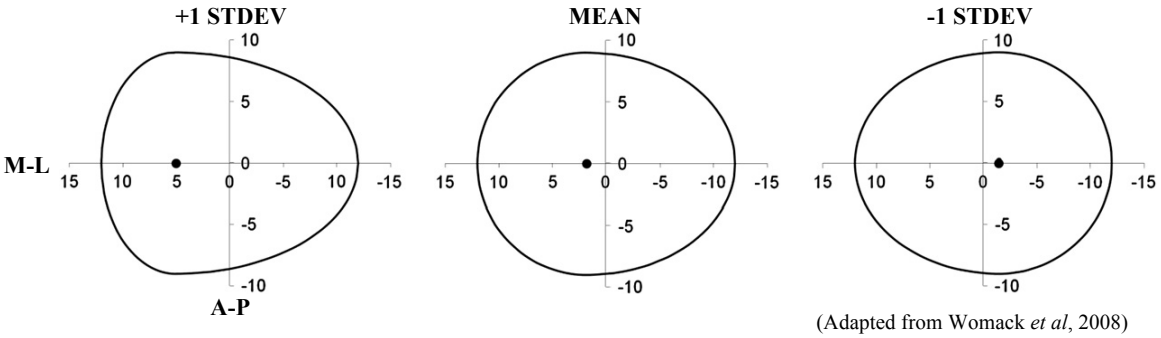


(Adapted from Womack *et al*, 2008)

**Figure 6-13: Range of perimeter shapes of facets**

The contact surfaces of the cervical facet vary significantly by spinal level and between different individuals. Studies of surface topography have found a wide range of surface shapes and curvatures, but in general the superior facet tends to have a convex surface with a large radius and the inferior surface a concave surface with a large radius (Figure 6-14). In order to simplify the design of the facet surface replacement, the design incorporates concomitant surfaces having a large radius of curvature (R=8000 mm) to mimic the natural facets. The superior facet replacement is convex and the inferior facet is concave to mimic the natural geometry.

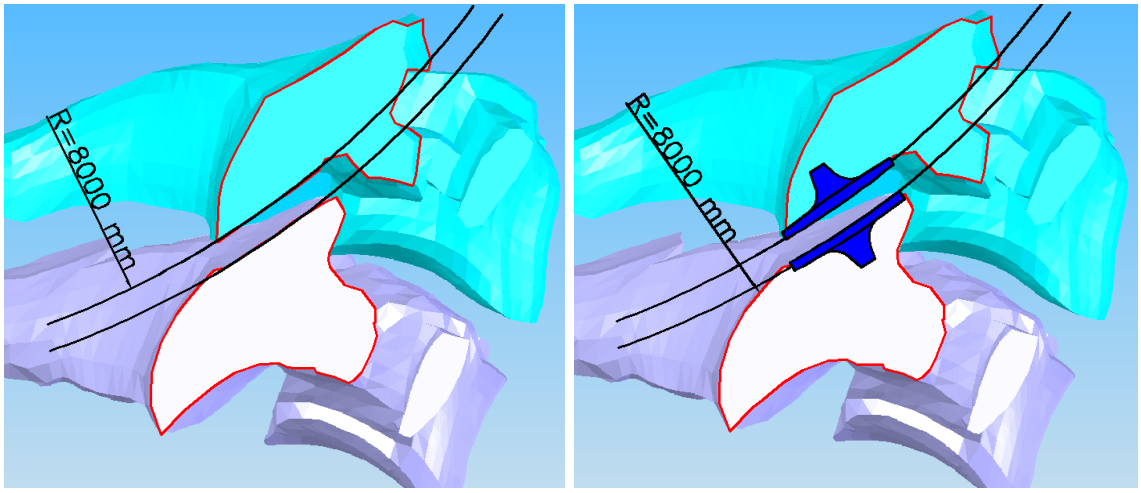


**Figure 6-14: Natural (left) and replaced (right) facet surface curvature**

The facet replacement provides a contact similar to the natural facet and mimics the radius of curvature and convexity/concavity of each facet. Replacing the natural cartilaginous facet surfaces with PEEK components of the same geometry should minimize the impact of the procedure on the natural facet kinematics. The retention of the natural facet capsule and overall contact essentially leaves the facet joint complex unchanged from the natural state. The only difference between the natural and replaced systems is that the PEEK components will be stiffer than the natural cartilaginous structure and therefore may affect the load distribution of the underlying cancellous bone structure.

## 6.12 CTLAS Design Concluding Remarks

The previous section outlined a design process through which a cervical total level arthroplasty system (CTLAS) was developed. This process was assisted with the definition of the design problem, identification of the design constraints and criteria. The selected 'best design' includes both disc and facet replacement implant systems that attempt to mimic the natural kinematics of the human cervical spine. The disc replacement promotes motion about the natural helical axis of the cervical spine, motion that is normally provided by the interaction between the natural disc and facet structures. Implantation of the disc replacement requires the resection of much of the annular fibers that surround the disc space and thus the provisioning of the helical axis is provided by the artificial disc replacement post-operatively. The facet replacement mimics the anatomy of the natural facet joints and attempts to allow the facet capsules to remain after implantation and therefore it is expected that the replacement facet joints will not have a significant impact on the kinematics of the cervical spine or the load sharing between the disc and facets.

It is important to note that there is still significant work required to develop the detailed geometry of the interacting surfaces of the disc replacement to perfect the implant system to produce the natural kinematics and motion of the natural cervical spine. This process could include extensive use of finite element modeling to incorporate the physiologic loads and motion of the cervical spine to develop and validate the geometry of the disc

replacement. Accurate end loads and moments could be applied to the adjacent intervertebral bodies and the resulting displacements and rotations could be compared to a model of the natural spinal segment.

The facet joint replacement geometry is expected to be fairly accurate but individual fitting of the implant remains a concern since the facets vary significantly between patients and spinal levels. Significant variation can also be observed between each facet pair at each spinal level and thus it is important to provide a wide range of sizes to accommodate this variation. Furthermore, it is expected that the PEEK material would be accommodating to device sizing by the Surgeon at the time of implantation where the prosthesis could be shaped in the operating room to suit the observed geometry after the facetectomy procedure. Some investigation would be required to determine whether this could be performed without damaging the implant and whether wear debris would be generated and possibly removed via a cleaning process.

Implant fixation also needs to be addressed and could include the use of porous or titanium coated PEEK in tandem with screw fixation to provide the initial stability required to promote bone ingrowth (Kurtz, 2007). It is recommended that the implants to not rely only on screw fixation but incorporate some level of bone ingrowth as this is known to provide superior fixation. This is especially important in the cervical spine where implant loosening and subsequent migration could have serious neurological implications if the spinal canal is breached.

The implementation of the implant system has three distinct treatment paths depending on the type of deterioration presented initially by the patient (Figure 6-15). If the patient exhibits disc and facet pain then the both the disc and facet replacement system will be implanted to provide a total level replacement. If the patient presents either disc or facet pain individually only the damaged component will be replaced. If future deterioration of the other spinal structure(s) occurs, future replacement can be accommodated with the present design. This allows the replacement solution to be tailored to the individual patient's needs such that the procedure is as minimally invasive as possible, but can still accommodate future degradation with a future procedure if required.

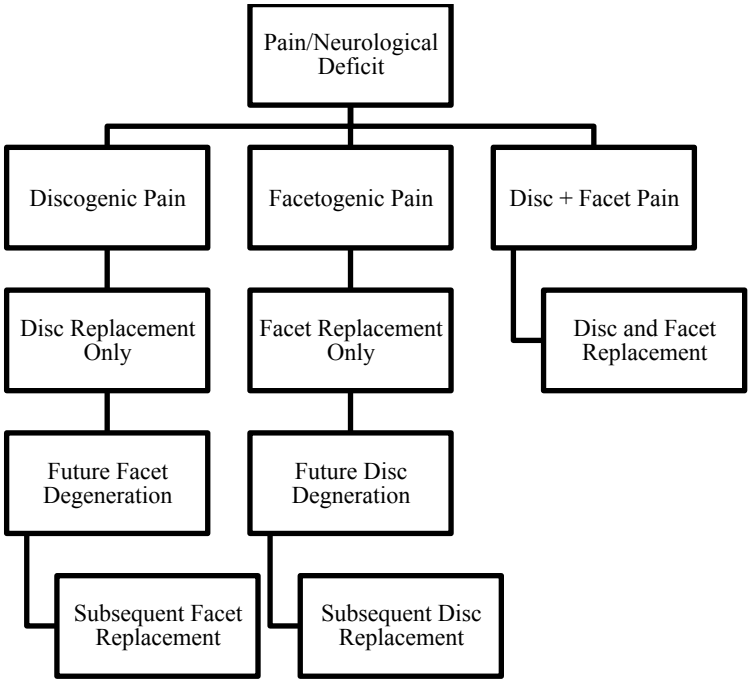


**Figure 6-15: CTLAS implant system treatment flowchart**

The selected design represents a significant advancement in spinal disc arthroplasty and introduces a cervical total level spinal arthroplasty system (CTLAS) that includes a cervical disc replacement that better replicates the kinematics of the cervical spine, and a facet replacement that allows for the removal of damaged facets while preserving segmental motion (where fusion was required in the past).

# Chapter 7
# Wear Testing of PEEK-on-PEEK

As previously discussed, medical grade PEEK is a polymer that has adequate structural strength to be a load-bearing implant and the stiffness to provide a stable bone-implant interface, in addition to being radiolucent and non-distorting to MRI images (Austin, 2008). PEEK has already gained acceptance as material for spinal fusion implants (cages and rods) in the lumbar, and more recently, the cervical spine (Kurtz, 2007). Various groups have considered the use of PEEK in self-mating bearing configurations.

## 7.1 Previous Wear Testing

The use of PEEK-OPTIMA (OPT) from Invibio Ltd. (Thornton Cleveleys, Lancashire, UK) in an all-polymer PEEK-on-PEEK bearing configuration was proposed for the NUBAC™ nucleus replacement device in the lumbar spine (Bao *et al*, 2007) which employs a ball-and-socket type articulation (Schwenke *et al*, 2007; Wimmer *et al*, 2008; Brown *et al*, 2008; Brown *et al*, 2009; Brown *et al*, 2010). Schwenke et al (2007) performed spine simulator testing of six NUBAC™ devices, subjected the implant devices to cyclic loading of up to approximately 1.3 kN about the normal physiologic motions of the lumbar spine for a total of 10 Mc in newborn calf serum. Run-in type wear was observed for all six specimens during the first 1 Mc, after which a constant average wear rate was observed. The contact surfaces of the articulations became highly polished with some signs of light surface scratching. No signs of severe surface adhesion or surface fatigue were observed with all implants surviving the 10 Mc of testing. The authors concluded that the wear performance of the self-mating PEEK Optima wear couple was acceptable and comparable to other disc arthroplasty devices that use established material combinations.

A second set of testing of two groups of six NUBAC™ devices investigated the effects of gamma sterilization in air and simulating aging on wear and was performed by Wimmer et al (2008). Surprisingly the aged devices did not seem to show run-in wear during the initial 1 Mc as was observed with the un-aged specimens that had been gamma sterilized in air. This suggested that the wear properties of PEEK are not susceptible to excessive gamma radiation and accelerated oxidative aging, which was thought by the authors to support the bio-durability of PEEK for disc arthroplasty applications.

Brown et al (2008, 2009, 2010) also performed spine simulator wear testing of the NUBAC™ over 10 Mc and observed an increased wear rate when multidirectional motion was imparted on the implants compared to unidirectional motion. Surprisingly, artificially aged components in this study showed more wear during the initial 5 Mc and less wear that was statistically significant over the final 5 Mc. This opposes the findings of Wimmer et al (2008) where aged components did not exhibit and run-in wear and thus produced less wear early in the wear test as opposed to late in the test. Light, elliptical surface scratching was observed in the implants testing multidirectional motion, while heavier cross hatching wear patterns were observed in those subjected to the frequency shifted motion which provides an increased cross shear effect on the surfaces.

The total wear of the NUBAC™ lumbar replacement, as assessed by pre-clinical wear testing, was deemed acceptably low and clinical trials have been initiated (Coric *et al*, 2010; Yuan *et al*, 2010).

Grupp et al (2010) studied PEEK-on-PEEK wear for application in a cervical disc replacement implant that employed a ball-in-socket geometry. Wear testing was performed using a six station spinal wear simulator (made by Endolab GmBh, Thansau, Germany) for four differenct material pairings; CoCr-on-UHMWPE, PEEK-on-PEEK, CFR-PEEK-on-CFR-PEEK and PEK-on-PEK, that were molded in the geometry of the active® C cervical total disc arthroplasty (TDA) device. Cyclic loading of up to 150 N was applied to the implants over the physiological range of motion observed in the cervical spine to produce multidirectional motion of the articulating surfaces. It was found that the wear of the CoCr-on-UHMWPE was similar to the PEK-on-PEK devices. The CoCr-UHMWPE devices showed significant run-in wear while the PEEK and PEK material pairings showed less wear during the first 1 Mc that had similar wear rates to what was observed in the remainder of the test. The natural PEEK-on-PEEK devices exhibited a tri-modal wear trend with different rate observed from 0-2, 2-4, and 4-10 Mc. The PEEK OPT material pairs also showed severe pitting and delamination while the CFR-PEEK pairings exhibited an excellent wear behavior with minimal surface damage and a reduction in wear rate by one order of magnitude. Therefore the authors suggested that CFR-PEEK is the most suitable of all materials tested for potential future use in spinal arthroplasty.

At the same time as the above studies were conducted, two sets of fundamental wear studies of the PEEK-on-PEEK bearing configuration were also being conducted, one at the University of Waterloo and the other at Durham University, each using somewhat similar crossing-path pin-on-plate type wear test devices (Austin *et al*, 2008; Scholes and Unsworth, 2008; Austin, 2008; Austin *et al*, 2010; Scholes and Unsworth, 2010). Various types of PEEK were tested including the above defined OPT and CFR and, in the Waterloo studies, the load was progressively increased until gross surface damage was observed in a "test to failure scenario". Typical wear results of these previous studies were compared with the wear results of the present study in a subsequent section. However, there were some differences in the pin-on-plate test protocols of the two sets of tests as discussed below. The protocols of the present study were essentially the same as those employed by Austin et al (2008).

One set of studies (Austin *et al*, 2008; Austin, 2008; Austin *et al*, 2010) consisted of wear tests on specimen pairs of OPT, CFR and a carbon nano-fibre reinforced (CNF) PEEK. The contact consisted of a pin with a spherical tip radius of about 100 mm moving in reciprocating rotation (± $87^{o}$ at 1 Hz) against a flat plate in a reciprocating almost linear arc motion (± 8.5 mm at 1 Hz) having a stroke length of 17 mm all in the presence of a lubricant held at 37 $^{o}$C and consisting of alpha calf fraction serum diluted to 12 g $L^{-1}$ protein concentration using a phosphate buffer solution (PBS). First loads of 80 N were imposed for 2 million cycles (*Mc*) and then progressively increasing "adverse" load conditions (120 – 400 N) were imposed for a total of 1.05 *Mc*.

During the first 2 Mc the CFR specimens showed almost no wear and had lower overall wear than the OPT and CNF. The results of the current study correspond with findings indicating carbon fibers improve the wear of PEEK. Surprisingly the wear studies found carbon nano-fibres to be detrimental to the wear rate. The CFR pin exhibited on average only 4.2% of the total wear of the material pair while the OPT and CNF pins represented 50.0% and 47.1% respectively. Under the increasing loads, 3/4 OPT specimen pairs experienced a sharp increase

in wear between 2.45-2.75 Mc while both the fiber reinforced specimens exhibited steady increase in wear. Interestingly, when the density of OPT (1.265 mg/mm$^3$) was considered, the wear amounts at 2 Mc were very similar to those found by Schwenke et al (2007) during the testing of an all-polymer bearing made from OPT in a spinal wear simulator. Overall, it was found that both OPT and CNF showed significantly higher wear than the CFR, with the OPT specimen showing damaged regions consisting of depressions with torn and shredded surfaces which may have been caused by an adhesive/fatigue wear mechanism perhaps enhanced by elevated surface temperatures. Under the increasing loads, CFR wear remained remarkably low. Examination of 2 of the 4 CFR specimen pairs that showed slightly higher levels of wear than the other specimens showed damaged regions consisting of depressions exhibiting intact fibers at the surface suggesting delamination due to sub-surface fatigue. It is apparent that the carbon fibers assisted the PEEK matrix in resisting the surface adhesion/abrasion.

Overall, the CFR PEEK was found to be a suitable material with the lowest (and most predictable) wear. The wear amounts of OPT at 2 Mc (80N) were similar to published spine simulation results which suggests clinical relevance of the current test parameters. Severe damage was observed at higher loading for both OPT and CNF specimen pairs; however the *in vivo* occurrence of such conditions is unknown.

The other set of studies (Scholes and Unsworth, 2008; Scholes and Unsworth, 2010) consisted of extensive wear testing of specimen pairs of OPT and CFR PEEK (with either pitch or PAN type carbon fibres), as well as specimen pairs of polyetherketoneetherketoneketone (PEKEKK) and polyetherketone (PEK). The wear tests were performed using a four station pin-on-plate machine that applied reciprocation and rotation to create cross-shearing motion that is observed in many joints of the body. The contact consisted of flat-ended 5 mm diameter pins in continuous rotation (at 1 Hz) on flat plates in linear reciprocating motion (±25 mm at 1 Hz) in the presence of a lubricant held at 37$^o$ C and consisting of new born calf serum diluted to 15 g L$^{-1}$ protein concentration using distilled water. The applied load was 40 N and the test duration was either 2 or 5 *Mc*.

The wear results of the PEEK optima showed several different wear regions including some run-in wear during the initial 0.2 Mc followed by a period of reduced wear which is interrupted by a region of higher wear that eventually returns to a lower rate of wear. The wear of the CFR PEEK exhibit run-in wear during the first 0.2-0.4 Mc followed by relatively constant wear for the remainder of the testing that is significantly lower than the OPT material pairs. When the wear of pitch and PAN based CFR PEEK is compared it is apparent that the PAN based material pairs observed only about one-third the wear the pitch CFR PEEK observed.

Overall, the authors concluded that both the CFR PEEK (pitch and PAN based) and the PEK material pairings exhibited better wear performance than the PEEK Optima specimen pairs. The PAN based CFR PEEK provided the lower wear, although both versions of the CFR PEEK exhibited very low wear throughout testing.

## 7.2 Apparatus

In order to evaluate the wear performance of a self-mating PEEK-on-PEEK articulation, pin on plate wear testing was performed using an OrthoPOD™ wear apparatus. Pin-on-plate wear testing applies similar sliding speeds and contact stresses to the material in question but does not replicate the actual implant geometry and *in vivo* kinematics. A true simulator study is often completed prior to clinical trials to evaluate the design in conditions as close to actual *in vivo* as possible, but is often costly and requires a significant time frame to complete. Pin-on-plate wear testing is a useful tool for the initial evaluation of material combinations prior to simulator studies provided testing conditions such as contact stress and sliding distance are similar to what is expected *in vivo*. However, pin-on-plate devices and even joint simulators struggle to provide an exact representation of the *in vivo* wear that occurs under a wide range of conditions that vary from patient to patient.

The present study examines the pin-on-plate wear performance of an unconventional PEEK polymer-on-polymer material pair. Literature of polymer-on-polymer wear testing is limited and thus further research in this area is of interest.

### 7.2.1 OrthoPOD™ Pin-on-Disc Apparatus

The OrthoPOD™ friction and wear testing apparatus is a six-station pin-on-disc machine produced by AMTI (Watertown, MA) that was developed for orthopedic material screening tests. The OrthoPOD™ was strictly speaking a pin-on-disc rather than a pin-on-plate device. The lower surface was a large disc that had a small angle reciprocating rotation about its vertically oriented central axis. The much smaller circular plate specimens were mounted on this disc (also with their axes vertically oriented) and the resulting wear paths on them followed a large radius arc so that they were almost linear, thus being very close to the characteristic linear reciprocating motion of pin-on-plate devices. The same load was applied to each specimen pair at any given time during the wear tests.

As previously noted, the wear test apparatus applied crossing-path motion to the contact. Such motion was used in the present study because it was expected to be more clinically realistic and, for metal-polyethylene hip implants, it had produced more clinically relevant wear results (McKellop and Clarke, 1984; Bragdon *et al*, 1996). The apparatus used in the present study applied a reciprocating rotation (± 4.5°) to the central axis of the lower disc and a reciprocating rotation (± 87°) to the central axes of the pins. The lower disc motion gave wear paths on the specimen plates along 0.108 m radius arcs to cause the pin centre to have a 17 mm sliding distance per cycle. However, the total sliding distances imposed on general points of the bearing surfaces in the contact zone were the sum of the sliding distances along the path of the plate arcs and the lateral sliding distances due to the rotations of the pins. The sliding distances due to the pin rotation were a function of the radial location of the point of interest from the central axis of the pin and were small (but not negligible) compared with the sliding distances along the large arcs of the lower disc.

Conventional pin-on-disc machines typically provide rotary and/or reciprocating motions that do not provide adequate wear paths for testing polymeric materials. The OrthoPOD™ can provide suitable crossing path

motions as well as an environment to produce results as accurate as possible to those expected with actual joint simulator wear tests.

The apparatus (Figure 7-1) consists of two basic assemblies; the top head and the base. The top head includes six independent pin actuators located at a 52 mm radius from the center of the base disc drive. The base assembly includes a single disc drive axis with a mounting plate having a diameter of 189 mm allowing for the attachment of plate specimens. The machine has three independent servo-controlled motions that control the pin rotational motion, the plate rotational motion and the individual normal loading of the six pins.

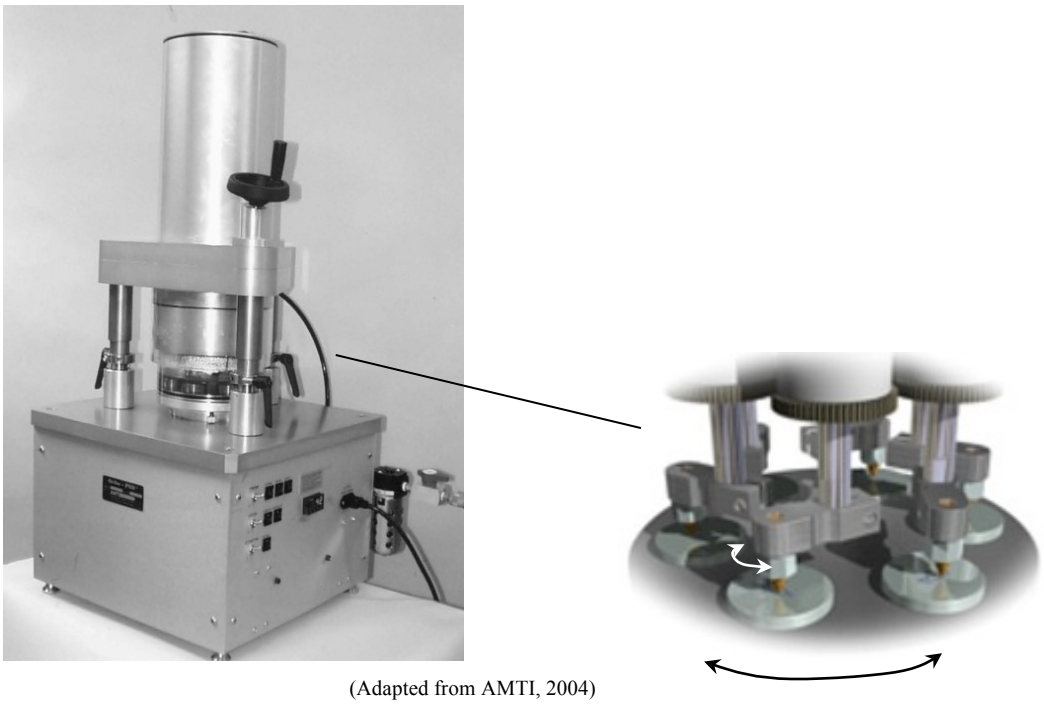

(Adapted from AMTI, 2004)

**Figure 7-1: OrthoPOD® pin on disc wear testing apparatus**

Each of the six pins drive axes is centered on a planet gear that is driven by a single sun gear through a backlash free harmonic drive gear head. A brushless DC motor drives the gear head and therefore all the pins therefore observe the same rotational motion. Each of the individual pin load actuators also provides an identical load with each pin can having the capability of being individually activated.

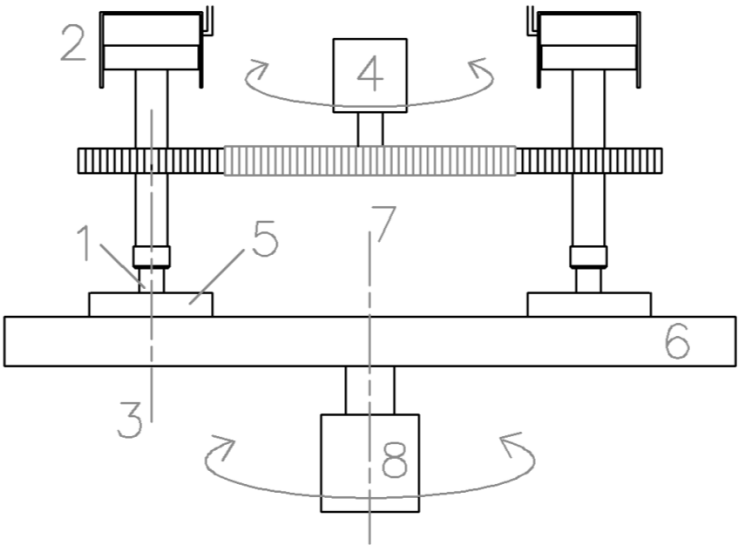


(1: pin, 2: pin load cylinder, 3: centre of rotation of pin, 4: pin drive, 5: plate, 6: lower disc, 7: centre of rotation of lower disc, 8: lower disc drive)

**Figure 7-2: Cross-section schematic of the OrthoPOD(TM) pin-on-disc wear apparatus**

The pin is loaded by applying air pressure to a precision piston at the top of the shaft assembly (Figure 7-3), the force on each pin is continually monitored via a closed loop control system that uses pressure transducers which measure the force applied to the cylinders. Each individual pin can be loaded dynamically from 0-450 N (1-100 lb.).

The main disc drive is located on the base and is mounted on high capacity tapered roller bearings. The disc can be driven in rotary or reciprocating motion at a speed of up to 0.5 revolutions per minute. The maximum torque that can be provided by the disc drive is 6.7 Nm. The disc provides mounting surfaces for six specimen discs at various radial positions. An external circulating temperature control unit provides thermal control via heat transfer passages located in both the top head and base of the apparatus.

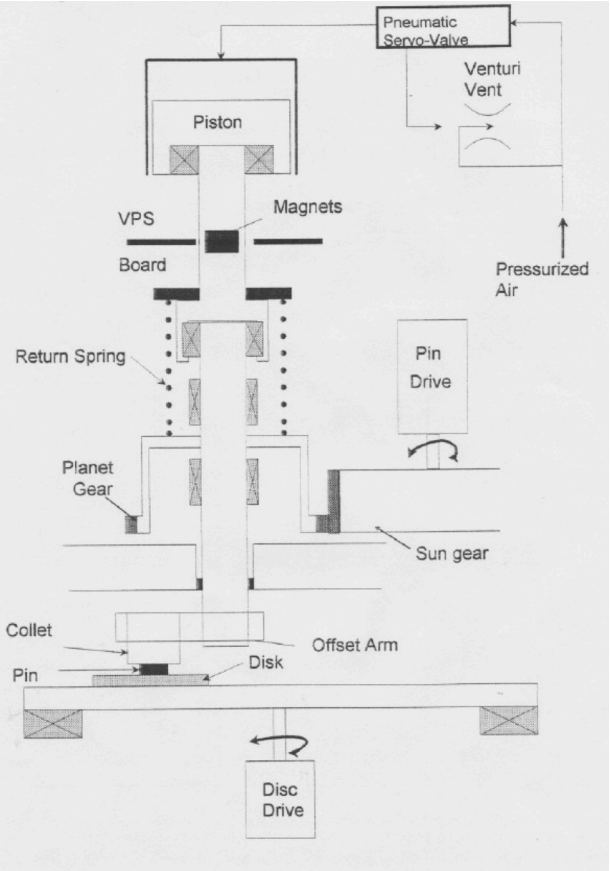


(Reproduced from AMTI, 2004)

**Figure 7-3: OrthoPOD™ pin and disc drive schematic**

Multi component force sensors are also included in each of the three vertical legs of the top head unit which provide 3 directional force measurements. A total of nine force components are mathematically summed by the control system software to provide the total $F_x$, $F_y$, and $F_z$ forces as well as the $M_x$, $M_y$ and $M_z$ moments acting on the top head unit due to specimen contact reactions. The resulting normal force of the contact between the pin(s) and plate(s) is equal to the computed $F_z$, and the force of friction can be resolved using the two horizontal force components; $F_x$ and $F_y$. The friction force of each individual material pair is determined by actuating only one pin with a vertical load and then measuring the reaction forces at the legs. This is performed for each material pair to obtain individual friction forces and the resulting coefficient of friction.

The OrthoPOD™ is controlled using an internal embedded microprocessor which dynamically directs the pin rotation, plate rotation and load. A PC is used to program the desired waveform which is then downloaded to the waveform board in the machine via an RS-232 interface. Data acquisition is performed at user specified intervals during the testing process, for the current tests this was performed at the start and finish of each test sample.

### 7.2.2 Load Soak Apparatus

For the current study material wear is measured by the change in mass of the specimens over the course of the investigation. The mass can be converted to volumetric wear by dividing by the density of the material. Polymeric materials are capable of fluid absorption and PEEK is known to absorb water until saturation is reached. The level of water absorption is a function of temperature, pressure, applied loading and exposed surface area. Net water absorption results in an increase in specimen mass and thus can affect the wear results that are a function of mass.

In order to accommodate for the fluid absorption of the specimens during the wear test, a load soak apparatus (Figure 7-4) was used which subjects specimens to similar temperature and loading conditions, however these specimens do not observe any wear and thus the fluid absorbed by these specimens can be used to estimate the fluid absorption of the specimens in the pin on disc wear simulator.

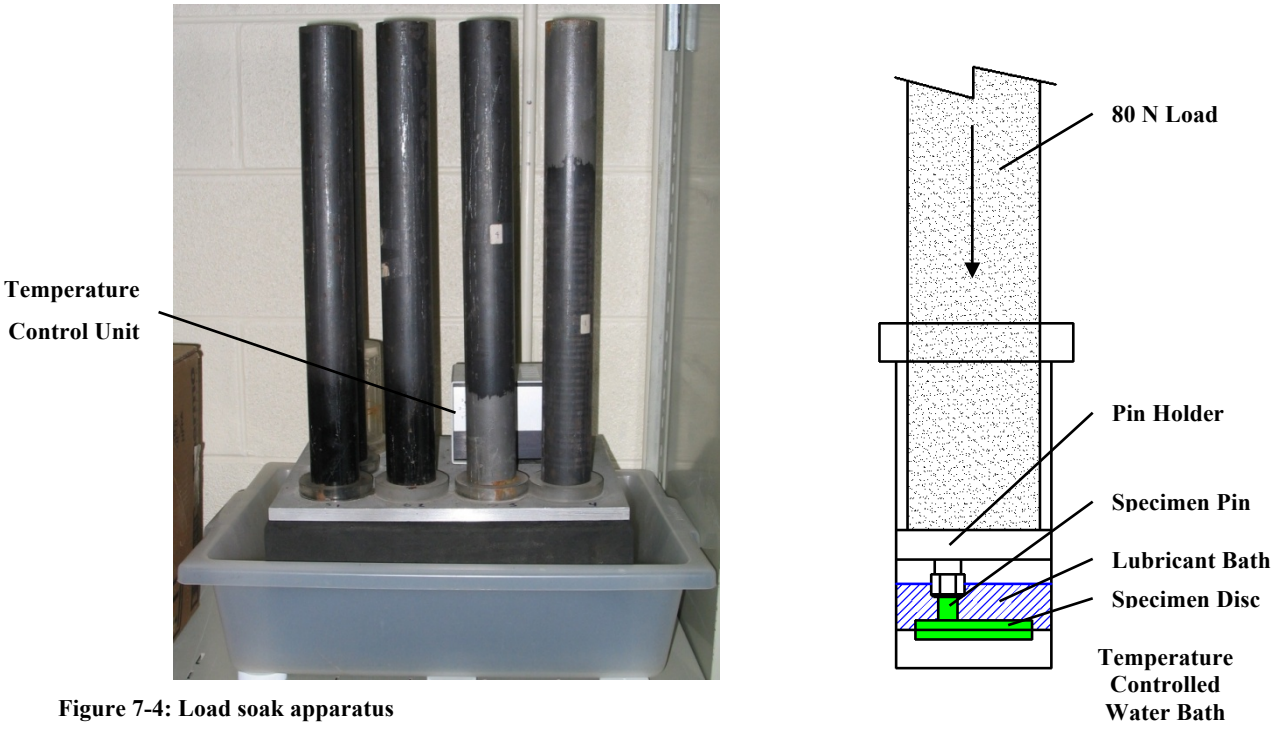


**Figure 7-4: Load soak apparatus**

The specimens in the load soak apparatus are mounted in the same specimen holders that are used in the OrthoPOD™. The specimens are maintained at 37° C in a bath of the same lubricant used in the wear test apparatus and are loaded with 80 N of compressive force to mimic the applied loading conditions.

One significant difference between the wear test and the load soak apparatus is that the motion, and resulting friction & heat, is not observed in the load soak. Therefore any transient motion effects on the fluid absorption of the specimens is not accounted for in the load soak, nor is the results of any temperature elevation observed due to friction generation in the wear tester. These effects can be minimized by allowing the specimens to reach equilibrium by observing a 'rest period' after testing and prior to cleaning and weighing. When the wear

tester finishes the prescribed number of cycles the machine halts motion and applies a steady load of 80 N; these conditions are identical to the load soak apparatus. As a result any excess heat and transient motion effects on the fluid absorption will be mitigated and both specimens in the OrthoPOD™ and the load soak will have observed identical conditions for a period of time prior to mass measurement.

During compilation of the data the change in specimen mass observed in the load soak apparatus is subtracted from the change in mass observed in the specimens undergoing the wear test. This allows for some correction of fluid absorption to be accomplished and relies on similar fluid uptake between the OrthoPOD™ and the load soak. Austin (2008) showed that the fluid uptake observed in the load soak was very similar to that observed in the OrthoPOD™, and that fluid uptake did not vary significantly between stations in both the load soak and the wear test apparatus.

## 7.3 Materials and Methods

### 7.3.1 Wear Path

For the present wear tests a crossing path motion was used which consists of reciprocating motion of both the pin and the disc. The pin rotated through an angle of 87° and the disc through an angle of 4.5°. The resulting wear path on the pin and disc can be seen in Figure 7-5.

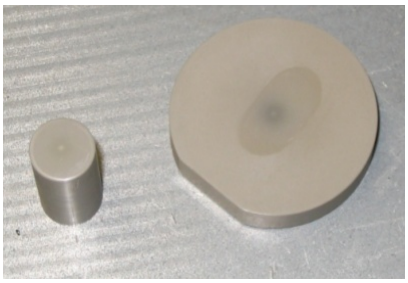

**Figure 7-5: Wear path as observed on pin and disc**

Analysis of explanted devices has shown that crossing-path motion is observed *in vivo* and is of particular importance in the wear testing of polymeric materials (Scholes and Unsworth, 2001). When the intervertebral disc is replaced with a sliding contact crossing path motion is observed due to the combination of the natural motion of the spine that includes flexion, extension, lateral bending and axial rotation. Different implant geometries will incur varying levels of crossing path motion. The current wear path selection is expected to be an exaggeration of the motion observed by a spinal implant due to the relatively low amount of intersegmental motion between adjacent vertebral bodies.

The total sliding distance of the wear path is 17 mm (reciprocation through 8.5 mm each cycle) based on the motion of the centre of the pin. It is important to note that the sliding distance observed by locations on the pin not located directly at the centre of the pin will vary due to the combination of rotation and translation. This effect increases with increasing radius since the radial displacement of a point on a cylinder is proportional to the radius at which the point is located.

### 7.3.2 Load

The present study incorporates two marked loading regimes that consist of normal and adverse conditions to which each material pair is subjected. The normal loading condition involves the application of an 80 N compressive load that represents the mass of the head on each level of the cervical spine which has been reported to be 73.6 N by Hattori et al (1981). The adverse loading condition includes the application of successively larger loading starting at 120 N and progressing to an ultimate load of 400 N. Previous studies (Austin, 2008) have also investigated similar loading conditions with the adverse conditions following the application of normal loading conditions.

The normal loading condition of 80 N was selected to allow for analysis of material wear under the expected physiologic loading conditions of the natural human spine. This load may represent the mean compressive load that the implant(s) would be subjected to over the course of the day with increased loading observed during strenuous activities and decreased loading during periods of rest.

The adverse loading condition of 120 N increasing to 400 N was selected to explore the extreme limits of the material pair performance and the response to increased and potentially non-physiologic applied loads. This loading is expected to be significantly higher than what would be observed *in vivo*. These loads are significantly larger than the loads suggested by ASTM and ISO standards for the investigation of wear performance of spinal implants.

### 7.3.3 Temperature

For the present wear test the temperature of the specimen environment was maintained at 37° C in both the wear test and load soak apparatuses. This was done to mimic the *in vivo* environment in which the current materials are proposed for use in. An external bath of de-ionized water is heated to 41° C by a heating unit which is then circulated through the OrthoPOD™ to produce a resulting temperature of 37° C at the specimen locations due to heat energy loss through the heating passages and to the environment. The load soak apparatus is continually bathed in a temperature controlled de-ionized water bath maintained at 37° C to match the wear test apparatus conditions.

It is crucial to mimic the actual conditions in which the material has been proposed for use in. The material properties, interface temperature and fluid uptake are just some of the properties that are affected by temperature. Maintaining identical temperature between the wear test and load soak apparatuses is also important since fluid uptake is temperature dependent.

### 7.3.4 Lubricant

The lubricant used in the present study consisted of non-iron supplemented alpha calf fraction serum (Fisher Scientific, Whitby, Ontario) diluted with phosphate buffer solution (PBS) or blood blank saline (VWR International, Mississauga, Ontario) to a specific protein concentration in g/L. In order to control bacterial growth in the lubricant during testing a general Antimycotic antibiotic was added (Invitrogen Canada Inc., Burlington, Ontario).

Two different protein concentrations were used to emulate different lubricating properties. A concentration of 12 g/L was used to simulate the lubricating properties of typical synovial fluid that is found in synovial joints. This protein concentration is commonly used in wear simulator studies that test material pairings for use in total joint replacements including the hip and knee. The facet joints are synovial joints and are therefore lubricated by synovial fluid.

The fluid that would lubricate a total disc replacement would not be synovial fluid as the intervertebral disc is a cartilaginous and not a synovial joint. Therefore the fluid surrounding a total disc replacement device would not be synovial fluid but would be more of an interstitial fluid. This interstitial fluid would likely contain a lower protein concentration and thus a second lubricant having a protein concentration of 6 g/L was also used for some of the test intervals to determine if a change in lubricant properties resulted in significant differences in the observed wear. This lower protein lubricant represents the expected conditions found in the intervertebral disc space and allows for the examination of the effects of protein concentration on the wear of the material pairs.

Preparation of the lubricant was performed using a simple calculation that allowed for the required final protein concentration. Each lot of alpha calf fraction contained different amounts of protein and therefore different amounts of PBS had to be added for each bath of lubricant. The total protein in the serum was obtained from the certificate of analysis provided by Fisher Scientific. Sample volumes of each lubricant constituent to provide a total protein concentration of 12 g/L for a lot of alpha calf fraction having an initial protein concentration of 36 g/L can be seen in Table 7-1.

**Table 7-1: Sample lubricant constituent volumes**

| Constituent | Volume |
|---|---|
| Alpha Calf Fraction (36 g/L protein) | 500 ml |
| PBS | 995 ml |
| Antimycotic Antibiotic | 5 ml |

The total volume produced in this mixture is 1.5 L. The total amount of protein in the solution is 18 g (since there is 0.5 L of 36 g/L alpha calf fraction serum). Therefore the total protein concentration in the final solution is 12 g/l (18 g of total protein into 1.5 L of solution). The alpha calf fraction and antibiotic are thawed and then mixed to the desired final protein concentration and then separated into 250 ml containers. The individual containers contain enough lubricant for one filling of the specimen chambers in both the wear test and load soak apparatuses.

Total protein concentrations of 12 g/L and 6 g/L differ from the recommendation of 20 g/L (ASTM, 2006) and 30 g/L (ISO, 2005) that is suggested as standard values for testing of intervertebral disc prosthesis. The lower protein concentration is postulated to better represent the non-synovial environment of the intervertebral space.

### 7.3.5 Specimens

In the present study, pin-on-plate wear testing was performed using OPT and CFR (30 wt% PAN fibers) PEEK specimen pairs that were provided by Invibio Ltd. (Thornton-Cleveleys, Lancashire, UK). The specimen pairs had a fairly simple geometry (Figure 7-6). The pins were cylindrical having a diameter of 9.5 mm and a length of 19 mm with a spherical contact surface on one end having a radius of either 60 or 100 mm. This spherical surface was fabricated to avoid developing high contact stresses at the pin edges during the wear testing which could cause a sort of cutting/tearing action that was unlikely to occur in a well-designed arthroplasty implant. Two different radii were used to investigate the effects of this parameter. Also, the pins having a radius of 100 mm were found to be rather shallow and thus the wear scar progressed near the edge of the pin. Therefore in order to prevent any possible edge effects if the wear did progress right to the edge of the pin to develop a sharp edge, a radius of 60 mm was used in some wear tests. The plates were also cylindrical having a diameter of 32 mm and a thickness of 6.5 mm. A flat notch allowed for radial alignment in the plate holders. The carbon fiber orientation was prescribed in the CFR specimens. The plates were manufactured with a contact surface that was as smooth and flat as possible. Care was taken during manufacturing to ensure that inter-specimen variation was minimized.

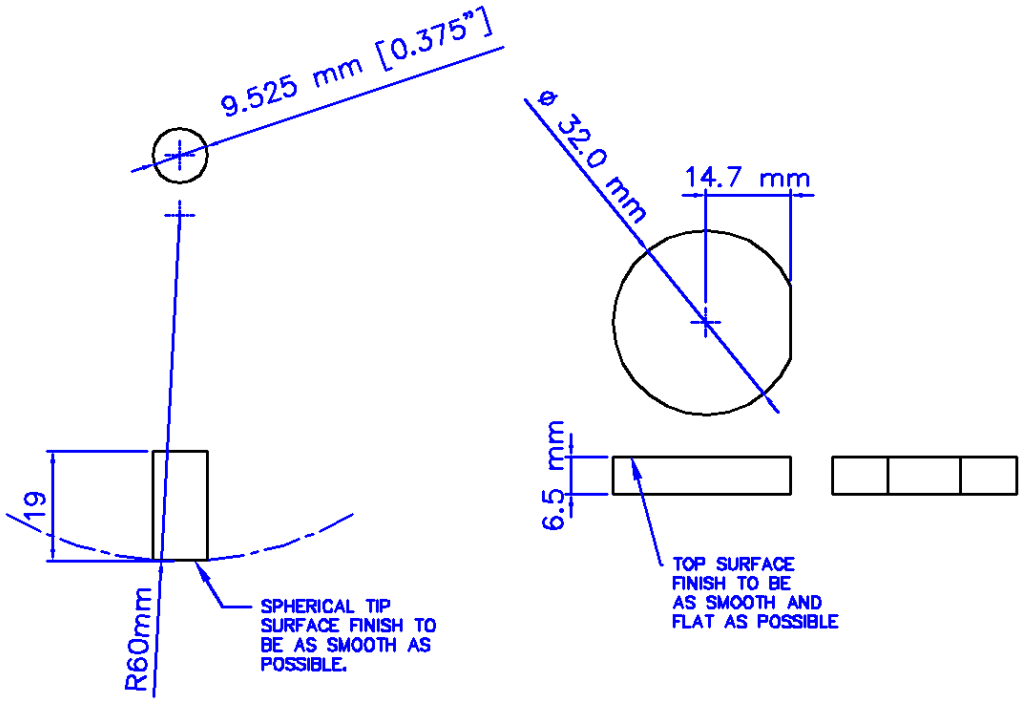


**Figure 7-6: Pin and plate specimen dimensions**

Both unfilled PEEK Optima and filled carbon fiber reinforced formulations of PEEK were tested in the present study. The material properties of each formulation can be seen below in Table 7-2 as obtained from Kurtz and Devine (2007), Invibio Biomaterial Solutions (2009), Green (2005), and Jones, Leach & Moore (1985).

**Table 7-2: PEEK material properties**

| Property | PEEK Optima | PAN-CFR PEEK (30%) | MOTIS-G PEEK |
|---|---|---|---|
| Density [mg/mm$^3$] | 1.265 | 1.4 | 1.42 |
| Tensile Strength [MPa] | 93 | 230 | 155 |
| Elastic Modulus [GPa] | 4 | 20 | 15 |
| Tensile Elongation [%] | 30-40 | 1-2 | 2.2 |
| Melting Point [°C] | 334-335 | 400 | 343 |
| Poisson's Ratio | 0.36 | 0.40 | 0.41 |

The orientation of the carbon fiber reinforcements in the filled PEEK was controlled in both the pin and plate. The fiber orientation in the plate was maintained as parallel to the contact surface as possible to provide a wear resistant mesh of carbon fibers on which the pin could articulate (Figure 7-7).

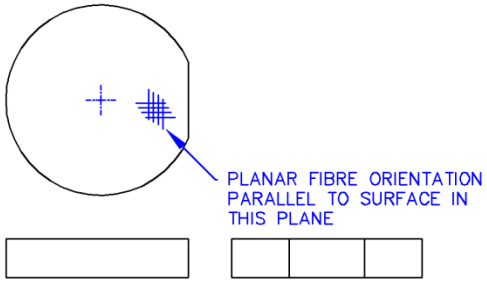


**Figure 7-7: Fiber orientation in filled PEEK plates**

In the pin two different fiber orientations were investigated. One set of specimens was machined with an axial orientation of the reinforcing fibers and another set was produced with a random radial orientation (Figure 7-8).

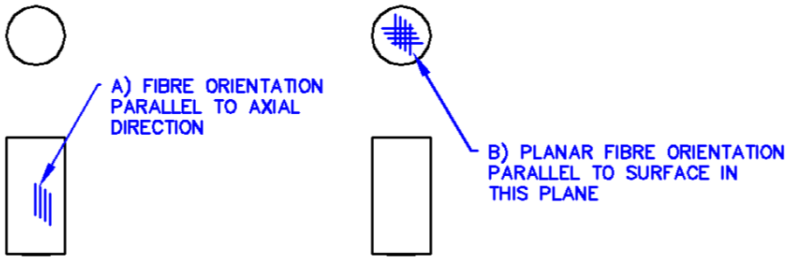


**Figure 7-8: Fiber orientation in filled PEEK pins**

The axial orientation provides a pin contact surface that consisted of the ends of fibers that would then articulate against the flat mesh of fibers on the plate contact surface. The planar surface orientation provides a pin contact surface with a mesh of reinforcing carbon fibers that would then articulate against a similar fiber mesh on the plate contact surface.

### 7.3.6 Assembly and Disassembly Protocol

In order to minimize variability in the wear results due to the disassembly and assembly of the specimens into the wear test apparatus protocols regarding the removal and installation of the specimens to allow for gravimetric weight measurement were followed. Both pin and plate specimens remained in the same machine station for the duration of each individual study.

The pin specimens are symmetrical about the cylindrical length and therefore this represents a potential source of variability, as there is no positive locating feature for the radial orientation of the pins in the pin holders. Prior to obtaining the baseline weight the pin specimens were marked using a vibration impact marker with a line on the outer diameter of the cylinder near the spherical contact tip. This was then used to align the pins in the same orientation with respect to the pin holders every time the specimens were re-installed in the apparatus. This ensured that the relationship between the motion of the pin and the plate remained constant throughout each individual wear test study.

The plate specimens are manufactured such that they are radially located in the plate holder by the flat surface machined along one edge that interacts with the plate holders. This ensures that the plates are always in the same radial orientation with respect to the plate specimen holder and removes any variability in the removal and installation process. Any motion between the plates and the specimen holders was removed through the insertion of thin plastic shims at the location of the flat surface on the side of the plate. This reduced the majority of the motion that could occur if the plate was slightly smaller than the recess in the plate holder that could introduce variability in the motion between the pin and plate.

A few drops of clear bath algaecide was placed in the deionized water bath used to transmit thermal energy from the temperature controlled base plate in the wear test apparatus to prevent any unwanted contaminant growth.

### 7.3.7 Specimen Cleaning and Drying Protocol

Potential adhesion of proteins from the lubricant generated the need for a specific procedure to ensure that all specimens received an aggressive enough cleaning while minimizing the any effects on the wear performance of the material pairs. The fluid absorption characteristics of PEEK also required a specific drying procedure to ensure that all specimens observed a similar amount of fluid extraction.

Previous wear studies have included a period of vacuum drying of the specimens in an effort to reduce mass variation due to different amounts of fluid uptake. This process may help eliminate the fluid found at the surface but may also introduce a vacuum environment that would not be observed *in vivo*. This may affect the wear performance of the specimens. Scholes and Unsworth (2009) performed pin-on-plate, crossing path motion wear testing of OPT and CFR PEEK against CoCrMo plates using both load soak and vacuum oven drying techniques to accommodate for fluid absorption in the polymeric component. Of four specimen sets tested, the wear of all four was determined using load soak controls (method 1), and in addition the wear of specimen pairs 1 and 2 was determined by subtracting the dry mass at the end of the wear test from the dry mass at the start of the wear test (method 2). The dry mass of the specimens was obtained using a vacuum oven drying technique which

employed two control specimens which ensured that the specimens were dried to the same amount in both the pre and post-wear states. The wear factors for each measurement method were compared by the present author (Table 7-3).

**Table 7-3: Load soak vs. vacuum drying wear factors**

| Description | k avg for pairs 1 and 2 [10-6 mm3/ (N m)] | | k for pairs 1, 2, 3 and 4 [10-6 mm3/ (N m)] | |
|---|---|---|---|---|
| | method (1) | method (2) | method (1) | |
| | | | avg | range |
| OPT pin / LC CoCrMo plate | 8.19 | 8.26 | 7.37 | 4.83 – 8.60 |
| CFR pin / LC CoCrMo plate | 0.0671 | 0.0583 | 0.209 | 0.0403 – 0.685 |
| CFR pin / LC CoCrMo plate (again) | 0.0983 | 0.0906 | 0.0793 | 0.044 – 0.161 |
| CFR pin / HC CoCrMo | 0.294 | 0.299 | 0.176 | 0.0325 – 0.400 |
| CFR (PITCH) pin / HC CoCrMo | 0.225 | 0.235 | 0.123 | 0.0785 – 0.620 |

(Data adapted from Scholes and Unsworth, 2009)

When the wear factors obtained for specimens 1 and 2 using the two different wear assessment methods are compared, the differences appear to be negligible compared the to the range of k values obtained from the other specimen pairs in the test. Thus the use of a vacuum drying technique was thought to be an unnecessary procedure and did not seem to increase accuracy of wear test results and was therefore not employed in the present study.

To minimize the effects of varied fluid uptake and wear debris and protein adhesion on the surface a regimented cleaning and drying procedure was used at the end of each wear trial prior to specimen weighing (Table 7-4). Loosely attached debris was removed initially with the aid of a soft bristled brush and deionized water. An ultrasonicating bath was then used to remove more firmly attached debris with a cleaning solution comprised of 2% liquid-NOX. The specimens were then subjected to the ultrasonicating bath submerged in deionized water to remove any residual cleaning solution. Finally the specimens were soaked in iso-propanol alcohol to remove any residual surface water and dried in a stream of high purity nitrogen gas. Each step was performed for a specified amount of time to ensure repeatability between each wear trial and associated cleaning and drying procedure.

**Table 7-4: Mass measurement protocol for load-soak and wear test specimens**

| Step | Procedure |
|---|---|
| 1 | Rinse all of the specimens (pins and plates) with de-ionized water to remove loose contaminants |
| 2 | Scrub specimens with a soft bristled brush to remove more strongly attached contaminants and rinse specimens again with de-ionized water |
| 3 | Clean specimens in an ultrasonic cleaner in individual containers in a solution of 2% Liqui-NOX® detergent (Alconox, Inc., White Plains, NY, U.S.A.) for 10 min |
| 4 | Rinse specimens with de-ionized water |
| 5 | Clean specimens again in an ultrasonic cleaner in individual containers in de-ionized water for 5 min |

| | |
|---|---|
| 6 | Soak specimens in isopropyl alcohol for 5 min. to remove residual surface water and then dry specimens in a stream of nitrogen gas |
| 7 | Allow specimens to air dry and acclimatize next to the balance for 10 minutes under a cover to prevent dust settling |
| 8 | Calibrate the balance using the automatic calibration feature and set its zero value |
| 9 | Measure the mass of a manual calibration "weight" (a backup for the automatic calibration) |
| 10 | Successively measure the masses of each specimen once, re-setting the zero value for each measurement if needed |
| 11 | Repeat the preceding protocol item twice more to obtain three measurements for each specimen |
| 12 | Average the three mass measurements for each specimen. If all three measured values of a particular specimen were not in the range of 0.2 mg, repeat steps 8 – 12. (This rarely occurred in the present study) |
| 13 | Measure the mass of the manual calibration "weight" to ensure that it is within 0.2 mg of the value determined in step 9. If not, the whole mass measurement procedure would have to be repeated. In the present study this did not occur |

### 7.3.8 Weighing Protocol

Every 0.15 *Mc* (except once when the controller malfunctioned as described in subsequent sections), during the adverse conditions, and every 0.25 *Mc* during the testing under the load of 80 N, the specimens were removed from the machine and then cleaned and weighed. Gravimetric weight measurement was performed with a Denver Instrument M-310 analytical balance with a precision of 0.1 mg. The balance was calibrated prior to each weighing interval and trial weights of 1 g and 10 g were tested to verify the correct operation of the balance prior to and after the weight measurement of the specimens was performed.

Mass measurements were obtained for each specimen three times and the average was calculated. After a reading for each specimen had been obtained the process was repeated twice to provide a total of three mass measurements for each specimen (pin and plate). If a difference of greater than 0.1 mg was observed for each successive measurement of a specimen the mass was measured again to eliminate the possibility for erroneous values.

### 7.3.9 Wear Measurement

The volumetric wear was estimated by taking the change in mass of the specimen and dividing it by the density of the specimen material. Fluid absorption of the specimens was determined from the load-soak specimen pairs that had been subjected to the same loading, temperature and lubricant as the wear specimen pairs.

For each wear specimen, the average mass at the end of a test interval was subtracted from its average mass at the very beginning of the wear test to determine the *apparent* mass loss caused by wear for that specimen. Then, for each load-soak specimen, the average mass at the end of the test interval had the average mass at the very beginning of the wear test subtracted from it to get the mass gain (caused by fluid absorption). Since the apparent mass loss had been falsely reduced by fluid absorption that occurred during the wear test intervals, it had to be corrected to give the *real* mass loss due to wear ($\Delta m_W$). Thus, for each *wear test* specimen, the average of the mass gains (caused by fluid absorption) of all the *load-soak* specimens of the same geometry (either pin or plate)

and the same material (either OPT or CFR) was added to the apparent mass loss of the wear test specimen to give $\Delta m_W$ which was then used to calculate the volumetric wear ($V$) in $mm^3$ using the following equation:

$$V = \frac{\Delta m_W}{\rho}$$

where $\rho$ is the material density in $mg\,mm^{-3}$ (Table 7-2). For each specimen pair, the wear in $mm^3$ was plotted against number of cycles in *Mc* to describe its wear performance.

### 7.3.10 Wear factor

Following many previous studies (Austin *et al*, 2008; Scholes and Unsworth, 2008; Austin, 2008; Austin *et al*, 2010; Scholes and Unsworth, 2010), classic wear factors ($k$) were calculated based on the following equation:

$$k = \frac{V}{F \cdot x}$$

where $V$ is the volumetric wear in $mm^{-3}$, $F$ is the load in N and $x$ is the sliding distance in m.

The classic wear factor was developed to represent wear that occurred in a linearly proportional manner from the beginning of the wear test. In the wear of the present study, run-in wear occurred, to varying extents, at the beginning and whenever the load was changed. Thus, a wear factor was developed only to represent the wear that occurred *for each specimen* pair under a load of 80 N in the regions where it seemed to be increasing in a linearly proportional manner. This approach required the following adaptation to the wear factor equation:

($V/x$) = slope of the least squares curve fit of the $V$ versus *Mc* data
divided by the approximate sliding distance of $17 \times 10^3$ m $Mc^{-1}$

The wear factor contained the wear rate and facilitated comparison of wear results with those of other studies with different sliding distances and/or loads. However, it assumed that wear would be proportional to the product of load and sliding distance. If the friction force was proportional to load, then the product of load and sliding distance was itself proportional to the work done on an individual surface, which suggested that the wear would be proportional to the work done by the friction force and might even be considered as a material property.

Unfortunately, wear is a much more complex function of the entire Tribology of the contact and thus a wear factor is not a material property of the individual surfaces and does not often remain constant for a particular specimen pairing when even moderate variations in load or sliding distance occur.

### 7.3.11 Contact Stress Measurement

The stress at the point of contact between the material pairs was monitored throughout the wear tests by measuring the contact area that was denoted by the wear scar on the pin using a ruler. The force applied to the material pair is known and is controlled by the OrthoPOD™. Contact stress is defined by the following formula;

$$\sigma_c = \frac{F}{A}$$

The actual contact stress throughout the wear test can be determined and is a function of the contact area, which is a transient value that changes as the materials experience wear. The initial contact stress can be estimated using Hertzian Contact Theory for a circular contact that incorporates the elastic modulus of both materials and the contact radius of the two contact surfaces using the following formula (Williams, 1994);

$$\sigma_{hertzian} = \frac{F}{a}$$

$$where \quad a = \left(\frac{3FR}{4E^*}\right)^{1/3}, \qquad E^* = \frac{1-\gamma_1^2}{E_1} + \frac{1-\gamma_2^2}{E_2}, \qquad and \quad R = \frac{1}{R_1} + \frac{1}{R_2}$$

where F is the applied load, a is the contact radius, R is the reduced radius of curvature, γ is the poisson's ratio of the material, E is the elastic modulus, and $E^*$ is the contact modulus. The initial theoretical contact stress is expected to decrease rapidly at the start of the test as the run-in wear occurs and the material pairs experience wear which increases the contact area thus reducing the contact stress. Therefore the actual contact stress that is based on the measured values of the contact area is expected to give a true representation of the stress at the material contact.

### 7.3.12 Microscopy

Surface analysis was performed at different intervals of the wear test after the specimens had been cleaned and weighed to obtain wear results. Microscopy of the specimens was performed using an Olympus BHM optical microscope with a MTV-3 photometrics cool snap CCD image capture device using image pro plus image processing software by Media Cybernetics.

Scanning electron microscopy was also performed using a JSM-6460 (JEOL, Peabody, MA) scanning electron microscope to allow for some quantification of surface damage. A conductive coating of gold was required for the OPT specimens to prevent charge build-up. The CFR specimens were not coated because the carbon in the specimens limits the electron build-up, however some small bright areas were noted on the surface during imaging where the surface was charged with electrons.

## 7.4 Results

### 7.4.1 PEEK Fluid Absorption

The fluid absorption characteristics of PEEK were investigated for both unfilled and carbon fiber reinforced versions in a pre-soak study. In addition to being a necessary wear test procedure, the fluid absorption observed in the pre-soak operation could be studied and used to provide an estimate for some of the random error in the later evaluation of wear in the present testing. Both undamaged (new) and damaged (worn) specimens were investigated to determine if surface damage affected the rate and amount of fluid uptake observed and to estimate the error associated with the load soak compensation procedure due to specimen variation.

5 sets (pins and plates) of unfilled PEEK Optima specimens and 4 sets of filled PAN carbon fiber reinforced PEEK were soaked in phosphate buffer solution (PBS) at room temperature and pressure for long enough to establish a low and relatively linear rate of fluid uptake (Figure 7-9). All of these specimens were later used in wear test 1 as discussed in later sections.

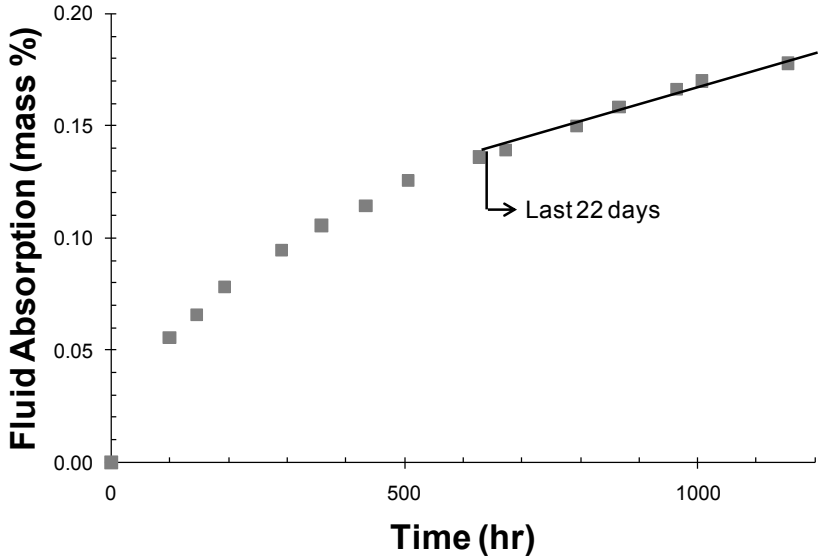


**Figure 7-9: Fluid uptake for a typical OPT plate specimen (Plate 7) during the pre-soak testing.**

This low linear rate of fluid uptake was important because the true mass loss of a specimen was determined by subtracting the fluid uptake during the test interval as estimated from the load-soak control specimens. The conditions imposed on the specimens in the load-soak apparatus were somewhat different than those imposed in the wear test apparatus. For example, the load-soak apparatus did not impose relative motion on the specimens and did not have frictional heating of the specimen surfaces. Thus, there was a bias error introduced by the assumption that fluid uptake could be estimated from the load-soak control specimens. There was also a random error associated with the scatter in the measurements caused by the accuracy limitations of the gravimetric assessment procedures such as fluctuations in the calibration precision of the balance, incomplete removal of fluid from the specimen surfaces and fluid loss from the specimens during the mass measurement. If the fluid uptake

were increasing in an exponential manner (as it did when a specimen was first immersed in fluid) the above errors would be likely to increase.

In the wear testing protocols, the average fluid absorption since the start of the test was evaluated after each wear test interval for each of the four types of specimen (OPT pins, OPT plates, CFR pin and CRF plates) in the load-soak apparatus. The corresponding average values were then added to the apparent mass loss of each of the wear specimens since the start of the wear test to get the true mass loss related to wear. Following Scholes and Unsworth (2007, 2010), specimens were not subjected to vacuum drying for a period of time before measuring their mass as was done by Austin (2008) and as advocated for polyethylene wear testing. This change in protocol was adopted to prevent any *potential* damage to the specimens from the vacuum drying as suggested by Scholes and Unsworth (2007) and did not seem to introduce any decrease in the consistency of the present results compared with those of Austin. Although it was recognized that the mass of the specimen might change during its measurement due to fluid desorption, this did not occur to any detectable extent. There remained the distinct possibility that the fluid absorption of the load-soak controls might differ somewhat from that occurring in the specimens being subjected to the wear testing. This possibility did suggest a potential source of error in the wear testing of the present study. However, as previously mentioned Scholes and Unsworth (2007) performed an elaborate vacuum oven drying procedure on half of their specimens in a fairly large scale wear test program in addition to performing a protocol similar to that of the present study that completely avoided vacuum drying. The differences in wear factors that were determined using the vacuum oven drying procedure versus those using the procedure that avoided vacuum drying were very small in comparison with the scatter in the wear factors of their nominally similar specimen pairs. Thus, the errors in the present study arising from the procedures for treating fluid absorption were deemed to be small.

However, there was scatter and physical inconsistency in the wear data. For example, our CFR specimen pairs appeared to have unrealistic negative wear during some test intervals. Therefore, it was considered important to estimate the scatter in the evaluation of fluid absorption from the load-soak control specimens in order to determine its contribution to the overall scatter and inconsistency. One approach to this estimate was to consider the pre-soak experiments described in Section 4.6. The scatter in the fluid absorption of the load-soak controls could have been considered directly but there seemed to be some merit in examining the long term behavior of the specimens as they hydrated over time in the pre-soak experiments. This allowed some expectations regarding the subsequent fluid absorbing characteristics of the load-soak control and wear specimens. It was noted that the specimens had been soaking in PBS for 48 days(1152 hours) and showed a small essentially constant rate of fluid adsorption (rather than the expected asymptotic approach to a constant level of fluid absorption) over about the last 22 days (528 hours) as shown for a typical specimen in Figure 7-9. Since the specimens were not subjected to wear debris or potential protein adhesion from the use alpha calf based lubricant, the cleaning procedure was modified to remove the steps involving submerging the specimens in cleaning solution in the ultrasonicator, while all other steps were followed. All the specimens had fairly similar rates of fluid absorption in the last 22 days but differed most in their magnitudes, presumably due to different initial levels of hydration. Thus, to obtain some measure of the random scatter that would be likely to occur in the measurement of fluid absorption that was

needed for the gravimetric evaluation of wear, all of the pre-soak specimens had their *change* in fluid absorption in mass % from their values at 26 days plotted against time (from 26 to 48 days). A least squares fit of a straight line, forced through zero, was applied to each of the four types of specimens and a corresponding standard error of estimate was calculated.

The standard error of estimate ($SE_E$) is a type of standard deviation and can be calculated using a formula of the following general form:

$$SE_E = \sqrt{\frac{\sum (y_i - bx_i)^2}{n - 1}}$$

where the data points are ($x_i$, $y_i$), $b$ is the slope and $n$ is the number of data points. If the fluid absorption in mass percentage has a precise linearly proportional relationship with time, the $SE_E$ is very small and the fluid absorption correction to the mass loss used to assess wear is considered to be applied with precision.

Finally, the $SE_E$ in mass percentage was converted to an equivalent wear volume in $mm^3$ ($S_{EQ}$) that would have been mistakenly considered as wear in the gravimetric assessment if the measured fluid absorption was one $SE_E$ higher than the true average value in the following manner:

$$S_{EQ} = \frac{SE_E \, m_{AVG}}{100 \, \rho}$$

where $m_{AVG}$ was the average mass of the specimen after soaking for 26 days (mg) and ρ was the specimen material density (mg $mm^{-1}$).

The $S_{EQ}$ values were fairly small (Table 7-5) but large enough to contribution to the interval-to-interval fluctuations in the measured wear. It was recognized that the protein components of the lubricant used in the wear experiments and in the load-soak apparatus might have influenced the behavior and scatter of the fluid absorption. This issue remains to be investigated and perhaps could be done using the record of the fluid absorption of the load-soak controls in the load-soak apparatus.

**Table 7-5: Standard error of estimate ($SE_E$) and its equivalent wear volume ($S_{EQ}$)**

| Specimen Group | $m_{AVG}$ (g) | $\rho$ (mg $mm^{-3}$) | $SE_E$ ($10^{-3}$ mass%) | $S_{EQ}$ ($mm^3$) |
|---|---|---|---|---|
| OPT pins | 1.774 | 1.265 | 4.87 | 0.0683 |
| OPT plates | 6.343 | 1.265 | 2.81 | 0.1409 |
| CFR pins | 1.934 | 1.400 | 5.00 | 0.0691 |
| CFR plates | 7.072 | 1.400 | 3.28 | 0.1657 |

The "standard error of estimate" associated with the measured fluid absorption was about 0.07 $mm^3$ for pins and about 0.15 $mm^3$ for plates. These values were quite small but did seem likely to have contributed to the

fluctuations of wear from interval to interval, particularly for the CFR specimen pairs, as revealed in the wear test results section.

### 7.4.2 Wear Test Plan

The present study investigates the wear of self-mating PEEK material pairs in several individual tests including up to 6 wear pairs and up to 5 load soak pairs (Table 7-6).

**Table 7-6: Test plan**

| Test # - material | Number of wear test pairs | Number of load soak pairs | Load F (N) | Lubricant Protein ($gL^{-1}$) | Duration (Mc) | Sph. Contact Radius (mm) | Fibre orient. to contact surface | |
|---|---|---|---|---|---|---|---|---|
| | | | | | | | Pin | Plate |
| **1a** – OPT | 3 | 2 | 120 – 400* | 12 | 1.05 | 100 | - | - |
| **1a** – CFR | 2 | 2 | 120 – 400* | 12 | 1.05 | 100 | perp. | parallel |
| **1b** – OPT | 2** | 2 | 80 | 12 | 2.00 | 100 | - | - |
| **1b** – CFR | 2 | 2 | 80 | 12 | 2.00 | 100 | perp. | parallel |
| **2a** – OPT | 3 | 2 | 80 | 12 | 1.00 | conical | - | - |
| **2a** – CFR | 3 | 3 | 80 | 12 | 1.00 | 60 | parallel | parallel |
| **2b** – OPT | 3 | 2 | 80 | 6 | 1.00 | conical | - | - |
| **2b** – CFR | 3 | 3 | 80 | 6 | 1.00 | 60 | parallel | parallel |
| **3a** – OPT | 6 | 4 | 80 | 12 | 1.00 | 60 | - | - |
| **3b** – OPT | 6 | 4 | 80 | 6 | 1.00 | 60 | - | - |
| **4a** – CFR | 6 | 4 | 80 | 12 | 1.00 | 60 | parallel | parallel |
| **4b** – CFR | 6 | 4 | 80 | 6 | 2.00 | 60 | parallel | parallel |

### 7.4.3 Wear Test 1

In the first test, pin-on-plate wear testing was performed using 3 OPT and 2 CFR (30 wt% PAN fibres) PEEK specimen pairs that were originally provided by Invibio Ltd. (Thornton-Cleveleys, Lancashire, UK). These specimens had been used as load-soak controls in a previous study performed by Austin (2008). The actual wear test specimens that had been worn (2 OPT and 2 CFR) from the previous study of Austin were used in the present study for the load-soak controls. The contact geometry consisted of pins having a spherical radius of 100 mm articulating on a flat plate. For the CFR specimens, the fibers were perpendicular to the contact surface in the pins and parallel to the contact surface in the plates. These are the same parameters as used by Austin (2008).

The five specimen pairs used in the wear testing were first subjected to "adverse" load conditions (test 1a), starting at 120 N increasing every 0.15 *Mc* to a maximum load of 400 N for a total of 1.05 *Mc*. An error in the wear test controller caused the 180 N trial to extend to a length of 0.24 *Mc*, as a result the 210 N trial was shortened to 0.06 *Mc* in order to re-establish the original interval plan. Following this, a load of 80 N (test 1b) was applied for an additional 2.00 *Mc*. Friction forces were measured throughout the wear testing.

The adverse load conditions (ranging from 120 – 400 N) were chosen to investigate the extreme limits of contact tribology in a "test to failure scenario" originally investigated by Austin (2008). Also, testing was performed under a load of 80 N that had been selected to approximate the *in vivo* contact stress of an implant subject to the weight of the head and loading of the neck musculature. The present study applied the adverse load conditions first, whereas Austin performed the testing under a load of 80 N first. Thus, the protocols and test intervals of test 1 were essentially the same as those of Austin except for having a different overall order. This was done to investigate whether the damage sustained in the adverse load testing would damage the specimen surfaces enough to cause accelerated wear during the 2.00 *Mc* of testing under the load of 80 N. One of the OPT specimen pairs did sustain extensive damage during the initial adverse load testing and was removed from the study as an outlier and thus only 2 OPT specimen pairs were tested under the load of 80 N (test 1b).

## Results

The wear amounts were plotted as a function of the number of cycles (Figure 7-10) and it was clear that the wear of CFR was much lower than that of the OPT specimen pairs under virtually all loading conditions. Although the loads were increased dramatically during the first 1.05 *Mc*, the wear rates were not much different than during the subsequent testing under the mild 80 N load. However, it was important to note that one specimen pair (OPT3) did exhibit high wear with extensive surface damage in the last interval of the adverse conditions testing (0.9 – 1.05 *Mc*) and was so different from the other two OPT specimen pairs that it was classified as an outlier and withdrawn from the remainder of its scheduled wear testing (2.0 *Mc* under a load of 80 N).

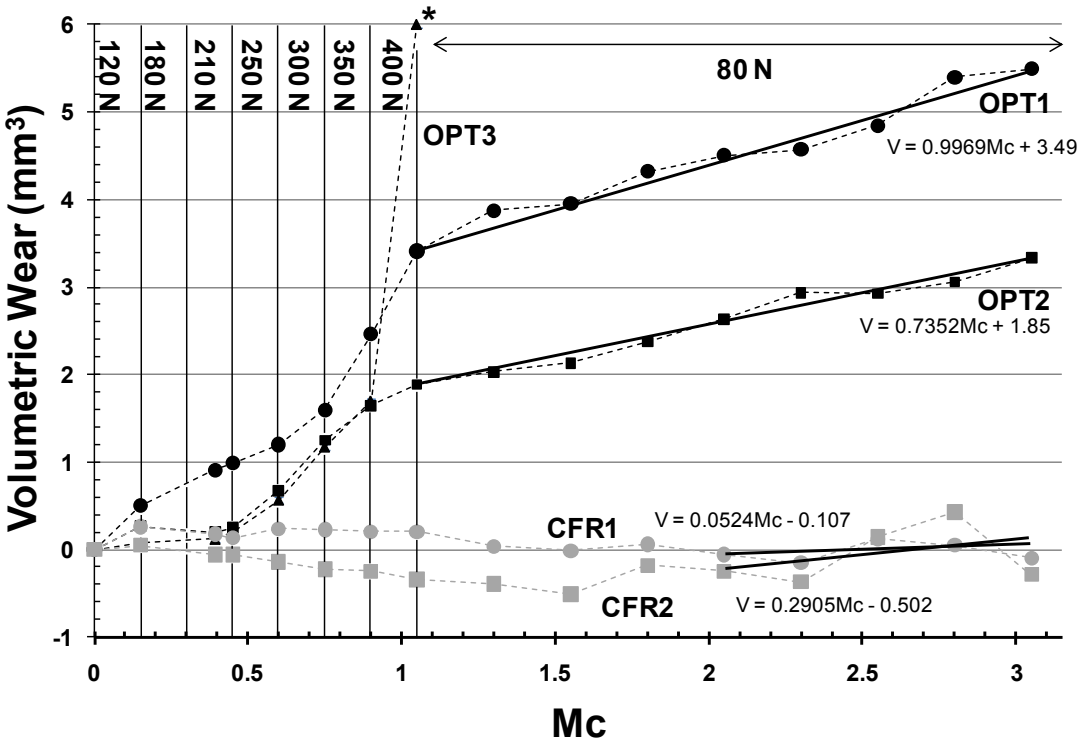


(* one OPT specimen pair exhibited severe cascading wear under 400 N load and was removed from the study)

**Figure 7-10: Wear of the OPT and CFR specimen pairs under various loads during wear test 1**

In the 1.05 *Mc* of testing under the adverse loading conditions, both OPT and CFR specimen pairs were likely to have exhibited some run-in wear at the beginning of the test and at the beginning of each interval when the load was increased. Despite the increasing loads both OPT and CFR specimen pairs seemed to experience an early drop in wear rate. The measured wear rate of the CFR specimens remained low (or negative) for the rest of the adverse load test period while the OPT specimens had their wear rate increase in the middle of the adverse load test period, presumably in response to the increasing loads. As previously mentioned, the adverse load conditions did not cause drastic increases in wear rate.

After the adverse load condition testing, the OPT specimen pairs had a drop in wear rate during the 2.0 *Mc* of testing under a load of 80 N to apparently constant values (Figure 7-10). The CFR specimen pairs essentially had such low wear rates that various random and bias errors made an accurate determination impossible. To estimate wear rates, the last few data points of the two CFR specimen pairs were fitted to straight lines that had positive slopes but the accuracies of these representations were considered low.

The wear amounts of the individual pins and plates were compared throughout the wear testing (Figure 7-11). The wear amounts of the pins and plates after they had been subjected to the adverse load conditions and the additional wear amounts observed after they had been subjected to the 80 N load conditions were also compared (Figure 7-12).

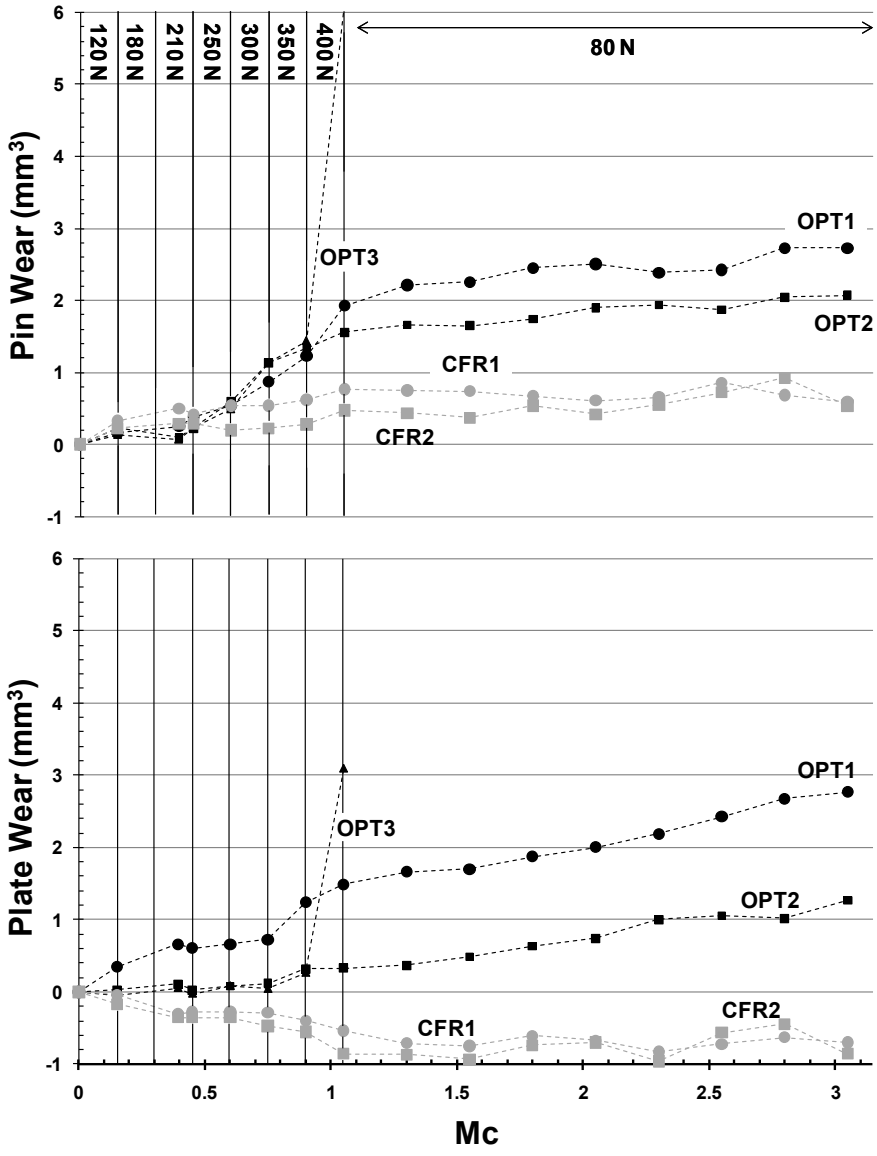


**Figure 7-11: Wear of the pins and plates during wear test 1**

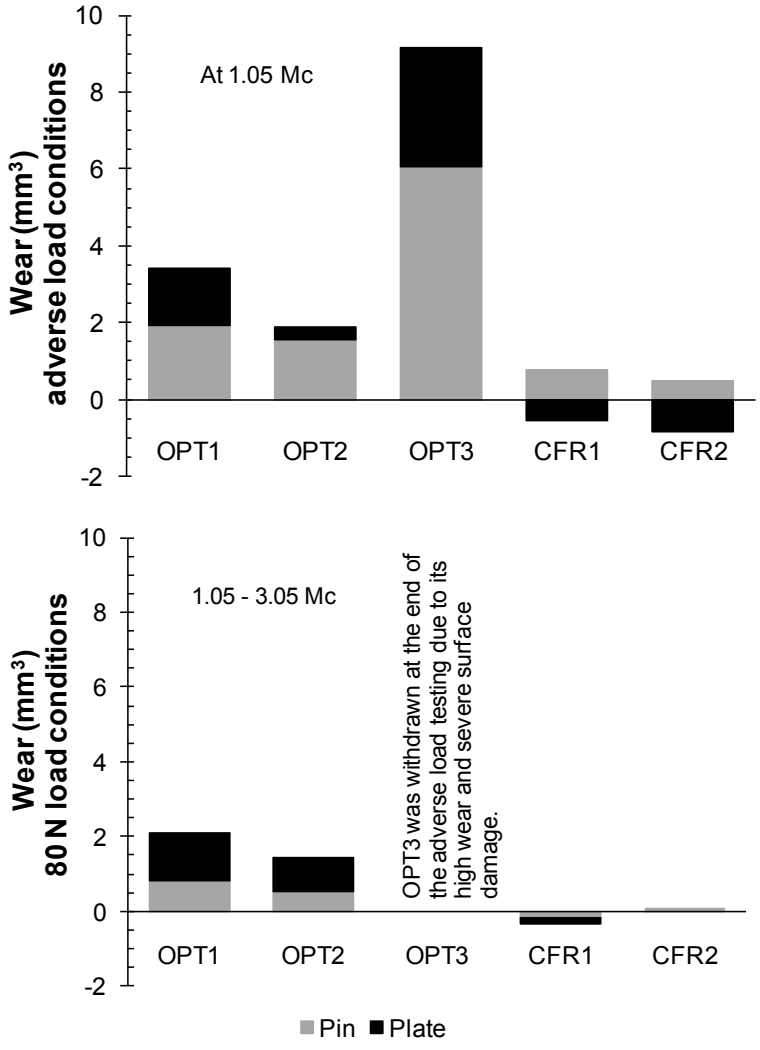


(1.05 Mc under adverse load conditions and the additional wear after they had been subjected to the 2.00 Mc at 80 N)

**Figure 7-12: Cumulative wear of individual pins and plates during wear test 1**

Both OPT pins and plates followed similar wear trends with the OPT pins showing more wear than the plates under the adverse loading conditions followed by a more even split in the wear under the 80 N loading conditions. However, throughout the wear testing under the adverse loading conditions, the CFR pins exhibited a fairly consistent reduction in mass while the CFR plates exhibited a similarly consistent increase in mass. Furthermore, the magnitude of the mass loss of the pins approximately corresponded to the mass losses of the plates. This clearly suggested a net mass transfer from the pins to the plates during wear of the specimen pairs. It was observed that the contact surfaces of the CFR pins did exhibit some obvious damage but the CFR plates did not show much visual evidence of wear with only a shiny track resulting from the testing.

Throughout the testing, it was apparent that the OPT specimens pairs seemed to sustain mild adhesive and abrasive wear (Figure 7-13). The cause of the abrasive wear was somewhat of a mystery. It was considered

possible that PEEK OPT wear particles might be harder than some regions of the surface and thus produce third body abrasion.

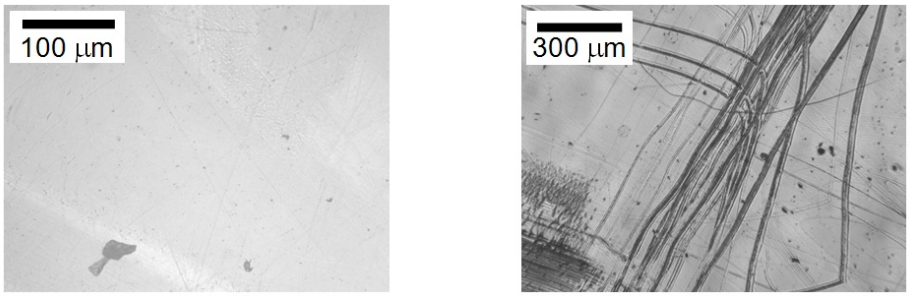


**Figure 7-13: Typical optical microscopy images of the OPT1 pin and OPT1 plate**

One specimen pair (OPT3) did exhibit high wear with severe surface damage (Figure 7-14) evident after the last interval of the adverse load testing (0.9 – 1.05 *Mc*). As explained earlier, this specimen pair was withdrawn from the remainder of its scheduled wear testing (2.0 *Mc* under a load of 80 N).

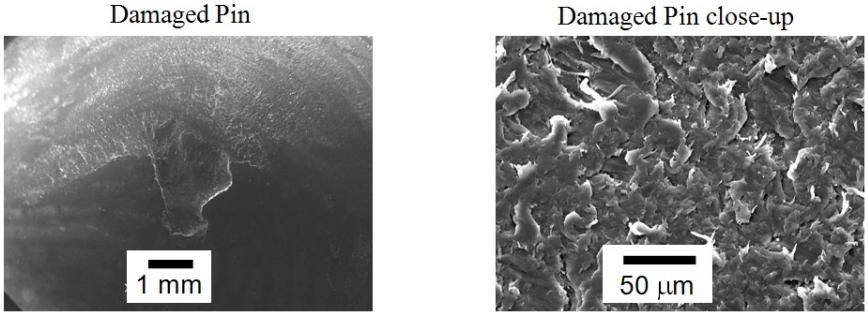


**Figure 7-14: OPT3 pin that sustained damage in the first 1.05 Mc at adverse load conditions**

The CFR specimens showed only mild surface damage but the carbon fibres were clearly visible and quite close to the surface (Figure 7-15). Furthermore, all of the CFR pins showed some delamination at their centres, thus suggesting a surface fatigue wear mechanism that could lead to abrasive action from the exposed fibres.

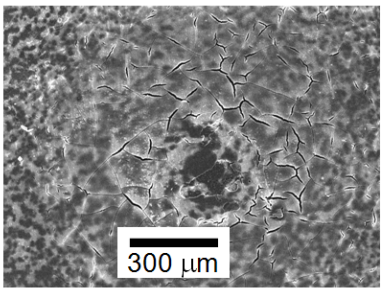


Pin delamination at centre

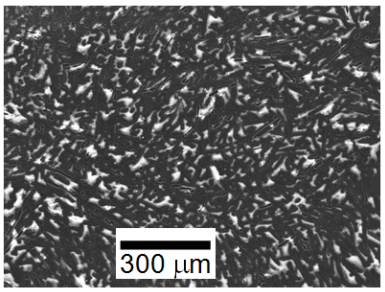


Plate showing parallel fibres near the surface

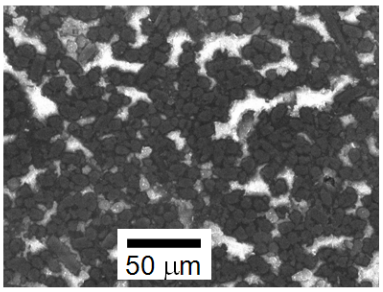


Pin showing fibre ends near the surface

**Figure 7-15: CFR1 pin and plate after the first 1.05 Mc under adverse load conditions**

## Comparison with Austin et al

The wear amounts of the present study were compared with those obtained by Austin et al (2010) and they showed quite good agreement (Figure 7-16). In particular, the wear of the OPT specimen pairs during the 80 N load conditions for the present study was about the same as that of Austin et al despite the specimens being first subjected to testing under adverse load conditions. This suggested that, in the present study, testing under the adverse load conditions *had not* seriously damaged the specimen pairs.

However, there were some differences that seemed rather inconsistent. When the wear of the present study was compared with that of Austin et al (2010) after the first 0.75 *Mc* of testing under the adverse load conditions (Austin et al had stopped wear testing here due to excessive surface damage), it was found to be statistically significantly higher ($p = 0.044$). This result suggested that the specimen pairs of Austin et al *had* sustained some damage during their prior testing for 2.0 *Mc* under the 80 N load conditions. This suggests that not only must high loads be applied but also some number of cycles at lower loads might be part of a "threshold condition" for severe surface damage and the subsequent high wear.

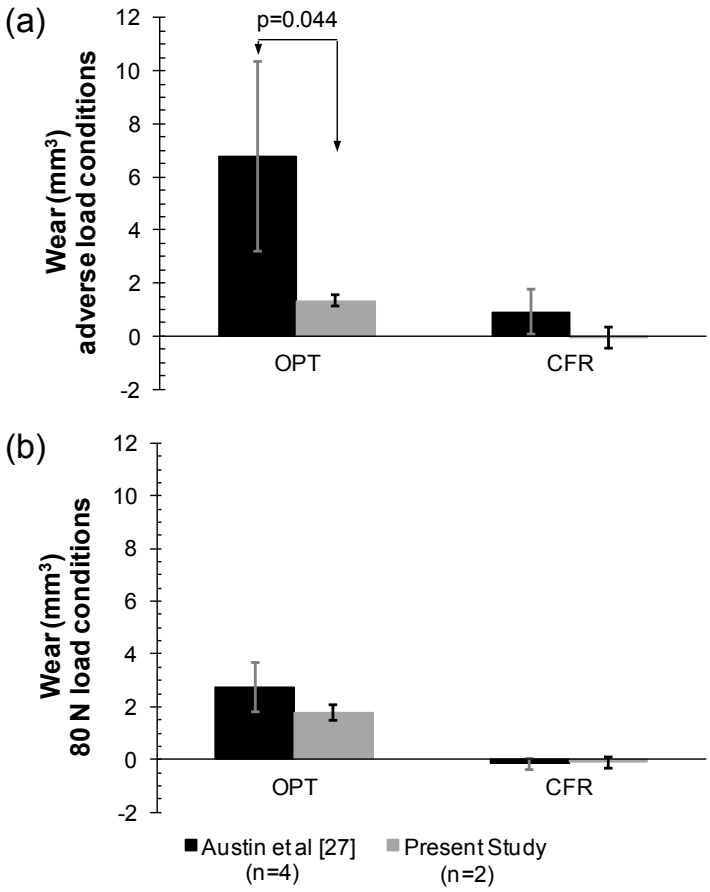


(Austin et al (2010) had sample sizes of 4 compared to 2 for the present study and stopped testing at 0.75 Mc)

**Figure 7-16: Wear during (a) the first 0.75 Mc of adverse loads and (b) 2.00 Mc at 80 N**

However, in the present study, the sample size was only 2 and the standard deviation was relatively high. Thus, it could only be considered pilot study from a statistical perspective. Also, the 'OPT3' specimen pair in the present study was withdrawn as an outlier at the end of the adverse load conditions when it exhibited high wear and severe surface damage. While it was included in the above statistical comparison (since the severe damage occurred after 0.9 *Mc* under the 400 N load condition), it was also noted that perhaps if more specimen pairs had been tested, this high wear and damage might have occurred more often and sooner, thus precluding any outlier classification. If so, both the average wear and standard deviation would have increased for the testing under the adverse load conditions of the present study and the apparent difference with Austin et al might not be prominent.

For the CFR specimen pairs, both studies showed much lower wear than for the OPT specimen pairs and recorded small amounts of physically unrealistic negative wear, thus indicating bias errors in the accuracy of the wear measurements. Both studies also showed a tendency towards higher wear amounts occurring during the adverse loading conditions but this effect was apparently reduced in the present study where adverse load conditions were applied first compared with Austin et al (2010) where the adverse loading followed testing under 80 N load conditions. For the CFR specimen pairs in both studies, these tendencies were obscured by the bias errors and essentially a high "noise-to-signal ratio" at low wear levels. The previously mentioned discussion of

the precision of the fluid absorption predictions from the load-soak controls suggested that this was a source of some of this random error.

## Contact Stress

Wear mechanisms, particularly those related to fatigue, were considered likely to be related to the average contact stress. Thus, the contact stress was determined by dividing load by the contact area as measured on the pin surfaces using a ruler (Table 7-7). It was recognized that at the beginning of wear testing, the average contact stress could be estimated using Hertzian theory. However, almost immediately, wear removed the pin tip and contact area increased rapidly, with a subsequent drop in the average contact stress. However, the contact area soon stabilized and then only gradually increased in size during wear testing. These data values were not deemed interesting enough to be included in the results of the present study.

**Table 7-7: Average contact stress during wear test 1**

| Test | F (N) | Number of specimen pairs measured | Average contact stress (MPa) | |
|---|---|---|---|---|
| | | | avg | std dev |
| 1a – OPT | 120 | 3 | 2.21 | 0.16 |
| | 400 | 3 | 5.96 | 0.32 |
| 1a – CFR | 120 | 2 | 4.62 | 0.015 |
| | 400 | 2 | 13.59 | 0.117 |
| 1b – OPT | 80 | 2 | 1.167 | 0.015 |
| 1b – CFR | 80 | 2 | 2.485 | 0.117 |

*To the precision of the measuring scale the two CFR pins exhibited the same sized contact areas after 0.15 Mc under loads of 120 N and thus the same contact stress

It was more interesting to note that the contact stress on the CFR specimen pairs was about twice that of the contact stress acting on the OPT specimen pairs. According to Kurtz and Devine (2007), the elastic modulus was about 20 GPa for CFR and 4 GPa for OPT, Thus, it was likely that the higher elastic modulus CFR had a small initial contact area that did not become enlarged quickly because wear was so low and thus remained much smaller than that of OPT during the various phases of the wear testing. It was also interesting to note that the wear of CFR remained low compared with the OPT despite being subjected to higher contact stress. However, high contact stress over longer wear test periods might promote sub-surface fatigue wear processes and thus implant designers for disc arthroplasty devices should probably consider highly conforming surfaces if they were to be made from CFR.

## Coefficients of Friction

Friction forces were measured at the end of each test interval and used to calculate the average coefficient of friction for the two material pairs during the testing under the 80 N load conditions (Table 7-8).

**Table 7-8: Coefficient of friction evaluated at the end of each interval (test 1) when F=80 N**

| Material | Number of evaluations | Coefficient of friction | |
|---|---|---|---|
| | | avg | std dev |
| OPT | 16 | 0.54 | 0.09 |
| CFR | 16 | 0.47 | 0.07 |

Although friction forces did fluctuate somewhat, they were fairly constant over this test period. Interestingly, the average coefficient of friction was 0.54 for the OPT and 0.47 for the CFR, a difference that was statistically significant ($p = 0.016$). The average coefficients of friction were also measured at the end of the test interval when the load was 400 N load. Once again, the OPT had a higher average value than the CFR, but they were both about half the values obtained for the 80 N load (Table 7-9). Thus, the coefficient of friction decreased with increasing load. The implications of the friction force behavior on long term wear and implant design remained uncertain.

**Table 7-9: Load dependence of the coefficient of friction during wear test 1**

| Material | Average coefficient of friction | |
|---|---|---|
| | F = 400 N | F = 80 N |
| OPT | 0.36 | 0.54 |
| CFR | 0.25 | 0.47 |

## Wear factors

As previously mentioned, wear factors were only determined for the wear results obtained when the 80 N load conditions were applied. The wear factors were calculated based on the slope of a least squares best fit line in the "steady-state" region of the wear versus *Mc* plots and recorded in Table 7-10.

**Table 7-10: Wear factor (k) at steady state when F=80 N during wear test 1**

| Material | k ($10^{-6}$ $mm^3$ $N^{-1}$ $m^{-1}$) | | |
|---|---|---|---|
| | Wear Test 1 avg ± std dev | Austin *et al* (2010) avg (range) | Scholes & Unsworth (2010) avg (range) |
| OPT | 0.64 ± 0.13 | 0.41 (0.31 – 0.47) | 4.5 (1.32 – 8.20) |
| CFR | 0.13 ± 0.12 | 0.21 (0.03 – 0.27) | 0.30 (0.25 – 0.51) |

The OPT seemed to exhibit steady state wear during the entire 2.0 *Mc* while steady state wear was observed in the second *Mc* for the CFR. The OPT wear factors from the present study were quite similar to those obtained by Austin et al (2010) but were substantially lower than those obtained by Scholes and Unsworth (2008).

The reasons for the much higher wear factors of Scholes and Unsworth (2008) were not clear. They performed crossing-path pin-on-plate testing with fairly similar test protocols. While it was noted that their sliding distances were about three times larger than those of the present study for the same number of cycles, this difference should have been accounted for to some extent by the wear factor calculation. It could be speculated that their use of flat-ended pins might have caused a gouging action by the pin edges and the continual rotation of the pins ensured that the edges would not be rounded very quickly by wear processes. Unlike the present study, the plates in the wear testing of Scholes and Unsworth always had higher wear than the pins. However, there could be many other more subtle reasons for the differences between the wear found in the present study and that of Scholes and Unsworth. In terms of wear amounts, Scholes and Unsworth had substantially higher levels than the present study, Austin et al (2010) and all of the previously discussed simulator studies (Schwenke *et al*, 2007; Wimmer *et al*, 2008; Brown *et al*, 2010; Grupp *et al*, 2010).

### 7.4.4 Wear Test 2

In the second wear test, a new set of specimens was used to investigate the effects of changing the spherical radius of the pins and the fiber orientation in the CFR PEEK specimens. Testing was performed with 3 OPT and 3 MOTIS-G (Pitch-based) CFR specimen pairs provided by Invibio Ltd. (Thornton-Cleveleys, Lancashire, UK). In wear test 2, the OPT pins were manufactured with a ‘cone like’ contact geometry (Figure 7-17), and the CFR pins were given a spherical contact radius of 60 mm. As before, both the OPT and CFR pins articulated with a flat plate. These modifications were performed to investigate the wear effects of the contact geometry. During wear test 1 it was also observed that the wear scar on the OPT pins approached, but did not reach, the full diameter of the pin near the end of the adverse wear conditions testing. If the wear is allowed to reach the edge of the pin, the contact geometry essentially becomes a flat pin on a flat plate. This may allow for the edge of the pin to dig into the surface of the plate thus generating some ‘edge effects’ that would not be apparent in a properly designed implant. Therefore this was also a deciding factor in modifying the geometry of the pin because a smaller radius or conical shape results in a higher dome on the end of the pin and thus more wear must occur to flatten the pin.

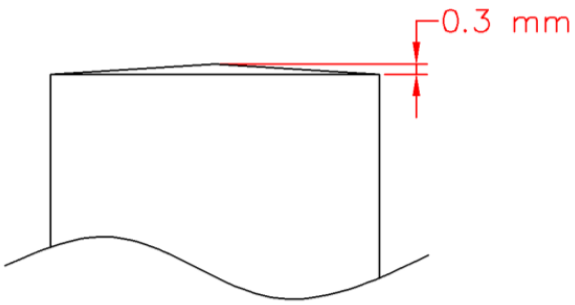


**Figure 7-17: Wear test 2 OPT pin conical contact geometry**

The fiber orientation in the CFR pins was also modified to be parallel to the contact surface rather than perpendicular as was investigated wear test 1. The fiber orientation of the plates was maintained as parallel to the contact surface. During wear test 1, concern was raised over whether the perpendicular fiber reinforcements in the pin were 'digging' into the surface of the plate resulting in increased wear. Therefore in order to investigate if this had any affect on wear; the fiber orientation was modified to be parallel to the contact in both the pin and plate.

The six specimen pairs were subjected to a loading of 80 N for a total of 2 Mc. This load was selected to provide a contact stress similar to what a spinal implant *in vivo* would be subjected to *in vivo*. Alpha calf fraction serum (with an antibiotics package) that was diluted with phosphate buffer solution to a specified protein concentration was used as the test lubricant. The protein concentration was 12 g/L from 0-1 Mc (test 2a), and 6 g/L from 1-2 Mc (test 2b). This was done to investigate the effects of this parameter, if any, on the wear performance of the material pairs. The temperature of the lubricant was maintained at 37° C. Friction forces were measured at the start and end of each wear test interval, with the start friction obtained after the specimens were cycled for a count of 100, and the final count immediately after the interval count was reached. As before, the actual contact area was obtained by measuring the pin wear scar.

## Results

Volumetric wear amounts of both the OPT and CFR specimen pairs were plotted as a function of number of cycles (Figure 7-18). The wear of both OPT and CFR was very similar for the first 1.0 Mc, with both materials exhibiting run-in wear during the first 0.25 Mc. Surprisingly, from 0.25–1.0 Mc OPT exhibited a steady state wear rate of 0.094 $mm^3Mc^{-1}$ which was lower than the CFR which exhibited a rate of 0.170 $mm^3Mc^{-1}$. The average contact areas of the OPT and CFR pairs during this period were 6.4 and 22.4 $mm^3$ respectively, resulting in average contact stresses of 15.5 and 3.6 MPa. Thus the OPT exhibited a higher contact stress than the CFR, but exhibited lower wear.

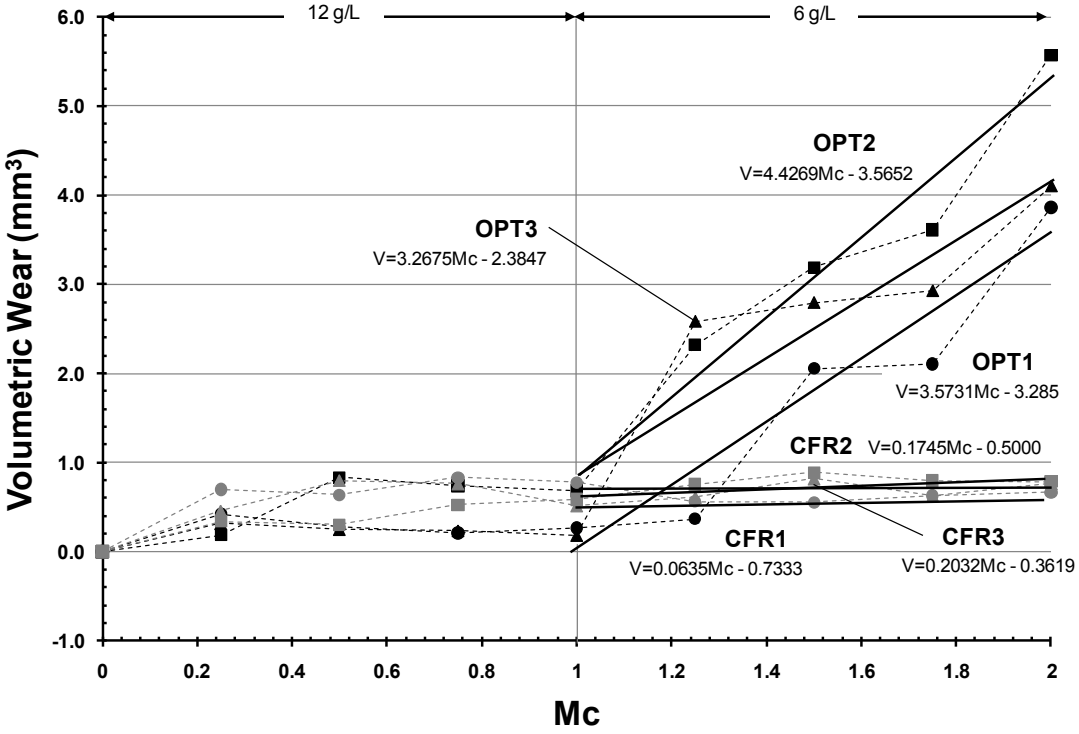


**Figure 7-18: Wear of the OPT and CFR specimen pairs during wear test 2**

When the protein concentration of the lubricant was reduced from 12 to 6 $gL^{-1}$, a statistically significant increase in wear rate was observed for OPT ($p=0.001$) while no significant difference in wear was detected for CFR (Table 7-11). Between 1.0-1.50 Mc all OPT pairs exhibited significant wear, resulting in increased contact area (33.6 $mm^3$) and reduced contact stress (3.6 MPa). It is not immediately apparent whether the decrease in protein concentration was the cause of the significant increase in OPT wear rate, or whether the increased wear was due to the surface reaching some 'threshold' level due to the high levels of contact stress observed for the first Mc and observing consequent high wear.

**Table 7-11: Average volumetric wear rates during wear test 2**

| Specimen Type | Average Volumetric Wear Rate ($mm^3Mc^{-1}$) | |
|---|---|---|
| | 12 $gL^{-1}$ (0.25-1 Mc) | 6 $gL^{-1}$ (1-2 Mc) |
| OPT PEEK | 0.062 ± 0.436 | 3.756 ± 0.601 |
| CFR PEEK | 0.203 ± 0.169 | 0.147 ± 0.074 |

The contact surfaces of both OPT and CFR specimens exhibited highly polished areas, with some signs of light surface scratches appearing on the OPT specimens after 0.5 Mc (Figure 7-19). Surprisingly the central pitting of the CFR pin that was seen in wear test 1 was not observed in the current test.

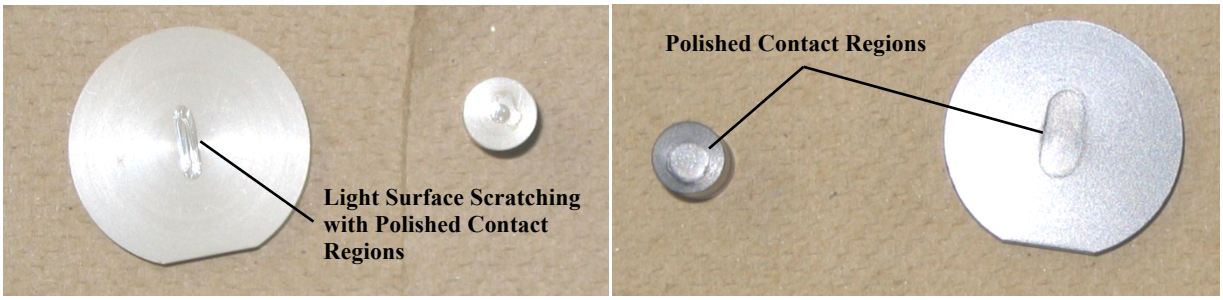


**Figure 7-19: OPT (left) and CFR (right) specimens after 0.5 Mc (test 2)**

It is immediately apparent that the conical pin contact geometry of the OPT specimens resulted in a smaller contact area which resulted in subsequent wear after 1 Mc at 80 N. It is also interesting to note that this reduced contact area, with associated significantly higher contact stresses, resulted in the OPT exhibiting similar wear rates to CFR for the initial Mc. However, during the second Mc significant wear was exhibited by the OPT specimens suggesting either a sensitivity to lubricant protein concentration (since this is where the protein concentration was reduced from 6 to 12 $gL^{-1}$), or that the surface succumbed to the high contact stresses after 1 Mc resulting in increased wear.

The average wear of the pins and plates was plotted individually for both the OPT and CFR specimens after 1 and 2 Mc of testing (Figure 7-20). For the OPT specimens it appears that the pins experienced the majority of wear during the first Mc, whereas after 2 Mc the wear appears to be shared more equally between the pins and plates, with the latter observing more wear on average. This suggests that while the wear during the initial 1 Mc was low, the pins experienced most of this wear and the plates didn't wear much. During the second Mc, when wear was observed to increase, the plates observed more wear than the pins which brought the cumulative wear amounts to similar levels.

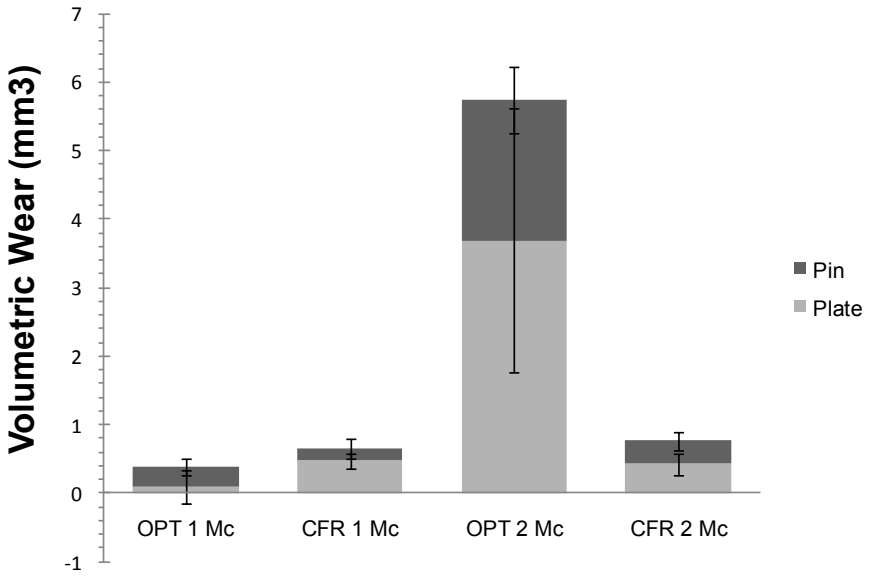


**Figure 7-20: Average pin and plate wear during wear test 2 after 1 and 2 Mc**

In this case, net material transfer from the pin to the plate was not observed for the CFR specimens, with both the pins and plates wearing evenly through 2 Mc. This is different from wear test 1 during which material transfer from the CFR pins to the plates was observed. This may be due to the parallel fiber orientation used in wear test 2 compared to the perpendicular fibers used in wear test 1.

## Contact Stress

As before, the contact stress was determined by dividing load by the contact area as measured on the pin surfaces using a ruler (Table 7-12). All specimens in the present test exhibited growth of the contact area as wear progressed. The OPT specimens in the present test exhibited much higher contact stress than the CFR specimens for the first 1 Mc, after which significant wear grew the contact area and reduced the contact stress to levels less than the CFR specimens.

**Table 7-12: Average contact stress during wear test 2**

| Test | F (N) | Protein Concentration ($gL^{-1}$) | Number of specimen pairs measured | Average contact stress (MPa) | |
|---|---|---|---|---|---|
| | | | | avg | std dev |
| 2a – OPT | 80 | 12 | 3 | 15.47 | 9.89 |
| 2a – CFR | 80 | 12 | 3 | 3.60 | 0.36 |
| 2b – OPT | 80 | 6 | 3 | 2.57 | 0.82 |
| 2b – CFR | 80 | 6 | 3 | 2.83 | 0.14 |

In this case the contact stress of the OPT specimens was larger (for the first Mc) or comparable (second Mc) to the contact stress of the CFR specimen pairs. This was a result of the different OPT contact geometry used in the present wear test which was conical and caused a smaller overall contact area. It is interesting to note that the wear of the OPT remained low despite the high contact stresses for the first Mc, however significant wear during the second Mc reduced contact stresses.

The contact stresses exhibited by the CFR specimens remained relatively stable over the entire test, decreasing slightly as wear increased the size of the contact area.

## Wear Factors

Wear factors were determined for regions of steady state wear observed during the different test parameters; 0.25-1.0 and 1.0-2.0 Mc for both the OPT and CFR specimens. This removed the initial run-in wear and included the two distinct regions of wear that the OPT specimens exhibited. The wear factors were calculated based on the slope of a least squares best fit line in the “steady-state” region of the wear versus *Mc* plots and recorded in Table 7-13.

**Table 7-13: Steady state wear factors during wear test 2**

| Material | k (10-6 $mm^3$ $N^{-1}$ $m^{-1}$) avg ± std dev | |
|---|---|---|
| | 0.25-1.0 Mc | 1.0-2.0 Mc |
| OPT | 0.13 ± 0.29 | 2.76 ± 0.44 |
| CFR | 0.15 ± 0.12 | 0.11 ± 0.05 |

The OPT specimen pairs exhibited a significant increase in wear during the second Mc of the test whereas the CFR wear remained relatively constant. When the wear factors are compared to wear test 1, the CFR wear rates are similar, but the OPT wear rates for wear test 2 are lower for the first Mc, and then significantly higher for the second Mc than previous work. Surprisingly the OPT wear rates during the second Mc are similar (about one half) to those reported by Scholes & Unsworth (2010).

## Coefficients of Friction

Friction forces were measured at the end of each test interval and used to calculate the average coefficient of friction for both material pairs during the testing under both the 12 and 6 g/L protein concentration under 80 N of loading (Table 7-14).

**Table 7-14: Coefficient of friction for each different protein concentration (test 2)**

| Material | Protein Concentration (g/L) | Number of evaluations | Coefficient of friction | |
|---|---|---|---|---|
| | | | avg | std dev |
| OPT | 12 | 12 | 0.12 | 0.03 |
| CFR | 12 | 12 | 0.18 | 0.02 |
| OPT | 6 | 12 | 0.28 | 0.10 |
| CFR | 6 | 12 | 0.18 | 0.01 |

The measured friction forces were relatively consistent over the test period, with the majority of variation occurring early in the test (0-0.25 Mc) for both specimens. Surprisingly the most variation was observed in the OPT specimens during the second Mc of testing when the lubricant had a protein concentration of 6 g/L. The friction of the OPT specimens was actually lower than the CFR specimens during the initial 1 Mc having values of 0.12 and 0.18 respectively. This result was statistically significant (p=0.0001) and was probably due to the

small contact area exhibited by the conical OPT specimens during this period compared to the larger contact provided by the spherical CFR specimens. During the second Mc with a protein concentration of 6 g/L and during which time the OPT specimens exhibited a high rate of wear, the friction of the OPT specimens increased significantly to 0.28 while the CFR remained relatively constant throughout the entire wear test at an average value of 0.18, with no significant difference detected between the two protein concentrations that were tested. Again this difference in friction as statistically significant ($p=0.0049$), although reversed from the first Mc during which OPT exhibited lower friction. It is interesting to note that the friction values observed during wear test 2 were lower than wear test 1, this may be a result of the reduced contact radius and/or conical contact used (in the case of OPT specimens).

## Discussion

Surprisingly, the present study shows similar OPT and CFR wear for the first 1.0 Mc where previous studies show much lower wear for CFR. This may be due to the reduced OPT contact area due to the conical pin contact geometry. After 1.0 Mc the OPT contact area increases similar to CFR values. Coincidentally this corresponds to the occurrence of significant OPT wear. It is currently not clear if the reduction in protein concentration is the cause of this increased wear. The wear rate of the CFR remains relatively unchanged after the reduction in protein concentration.

The low OPT wear observed from 0-1 Mc may be due to improved heat removal from the relatively small contact area through the surrounding lubricant. An increased contact area may retain more thermal energy that may negatively affect the material strength. The increased and significantly higher OPT wear observed in the second Mc of testing is either a result of the reduced lubricant protein concentration, or the surface succumbing to the 1 Mc of testing at large contact stresses. Since the start of the increased wear coincided with the modification of the lubricant protein concentration, another test is warranted to investigate if OPT is sensitive to lubricant changes.

While the net CFR wear in the present study was slightly larger than observed in previous studies, which is thought to be due to increased run-in wear, the steady state wear rates and wear factors are similarly low. The increase run-in wear may have been a result of the reduced pin radius or the different fiber orientation tested in the present study. Austin (2009) postulated that the axial orientation of carbon fibers in the pin might have resulted in increased abrasive wear of the plate. It is possible that the parallel orientation of the carbon fibers allowed more PEEK matrix to be worn away during run-in to expose the underlying, wear resistant carbon fibers whereas with perpendicular reinforcing fibers less matrix material is needed to be removed since the ends of the fibers were already exposed by the machining process.

The present study seems to show a weak correlation between protein concentration and wear for the CFR specimens, while a strong link between contact area and wear was observed for the OPT material pairs. Parallel fiber orientation at the contact area and/or reduced contact radius appeared to increase to run-in wear in CFR. The effects of protein concentration is important as different implant applications will be subjected to varying lubrication properties with a lower protein concentration expected in the spinal disc space compared to a

synovial joint. Contact area in many articulations is maximized to reduce contact stress. While the present study suggests that for OPT smaller contact areas, and thus higher contact stresses results in lower wear, there is the risk of large amounts of wear that occur rapidly in this configuration.

### 7.4.5 Wear Test 3

The third wear test focused on the investigation of unfilled PEEK OPTIMA specimen pairs. Testing was performed with 6 OPT specimen pairs provided by Invibio Ltd. (Thornton-Cleveleys, Lancashire, UK), including 4 load soak specimens that were used for fluid absorption compensation. In wear test 3, the OPT pins were manufactured with a 60 mm spherical radius on the contact end identical to the CFR pins used in wear test and as before, articulated with a flat plate. With a 60 mm spherical contact radius is was unlikely that enough wear would occur for the wear scar to reach the edge of the pin, thus any potential 'edge effects' were avoided. Also, an identical radius to the CFR pins used in wear test 2 would allow direct comparison of wear results between OPT and CFR PEEK specimens.

The six specimen pairs were again subjected to a loading of 80 N for a total of 2 Mc, selected to provide a contact stress similar to what a spinal implant *in vivo* would be subjected to. Alpha calf fraction serum (with an antibiotics package) that was diluted with phosphate buffer solution to a specified protein concentration was used as the test lubricant. The protein concentration was 12 g/L from 0-1 Mc (test 3a), and 6 g/L from 1-2 Mc (test 3b). This was done to investigate the effects of this parameter, if any, on the wear performance of the PEEK OPTIMA having a contact radius of 60 mm. The temperature of the lubricant was maintained at 37° C. Friction forces were measured at the start and end of each wear test interval, with the start friction obtained after the specimens were cycled for a count of 100, and the final count immediately after the interval count was reached. As before, the actual contact area was obtained by measuring the pin wear scar.

#### Results

The volumetric wear of the six OPT specimens used in wear test 3 were plotted against number of cycles (Figure 7-21), and the volumetric wear functions for each specimen were also calculated for each lubricant protein concentration (Table 7-15).

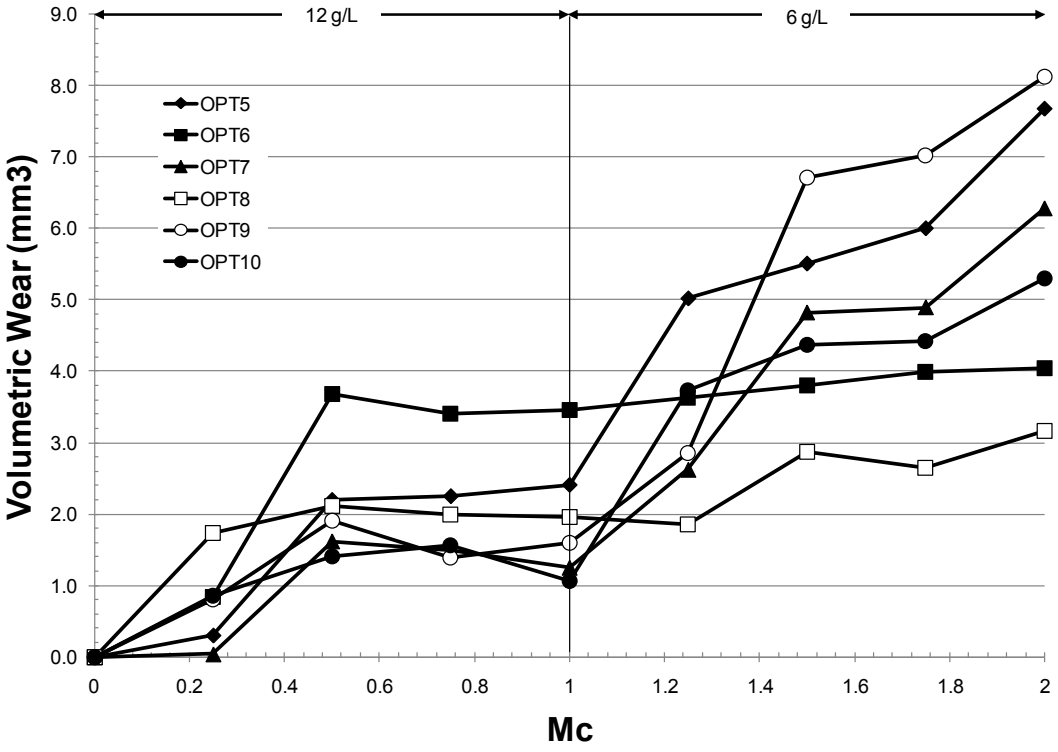


**Figure 7-21: Volumetric wear vs. number of cycles for OPT specimen pairs in wear test 3**

**Table 7-15: OPT specimen pair wear rates during wear test 3**

| Specimen Pair | Volumetric Wear Function ($mm^3$) | |
|---|---|---|
| | 0.25-1.00 Mc (12 g/L) | 1.00-2.00 Mc (6 g/L) |
| OPT5 | 2.551Mc + 0.1976 | 4.603Mc – 1.582 |
| OPT6 | 3.057Mc + 0.935 | 0.609Mc + 2.871 |
| OPT7 | 1.402Mc + 0.224 | 4.930Mc – 3.422 |
| OPT8 | 0.232Mc + 1.805 | 1.283Mc + 0.578 |
| OPT9 | 0.738Mc + 0.962 | 6.891Mc + 5.071 |
| OPT10 | 0.316Mc + 1.013 | 3.66Mc - 1.719 |

During the first million cycles a relatively steady rate of wear was observed for 5 of the six specimens, with one specimen pair exhibiting slightly higher wear than the others. A relatively small amount of run in wear was observed during the first 0.25 Mc. During the second million cycles a marked change in wear rate was observed (Table 7-16), this change coincides with the point at which the protein concentration in the lubricant is reduced from 12 to 6 g/L. This change in wear rate is clearly visible when the average volumetric wear is plotted against Mc (Figure 7-22).

**Table 7-16: Average wear rates at different protein concentrations during wear test 3**

| Wear Test Period | Average Wear Rate ($mm^3$/Mc) |
|---|---|
| 0.25-1.00 Mc (12 g/L) | 1.3825 +/- 1.1867 |
| 1.00-2.00 Mc (6 g/L) | 3.6717 +/- 2.0737 |

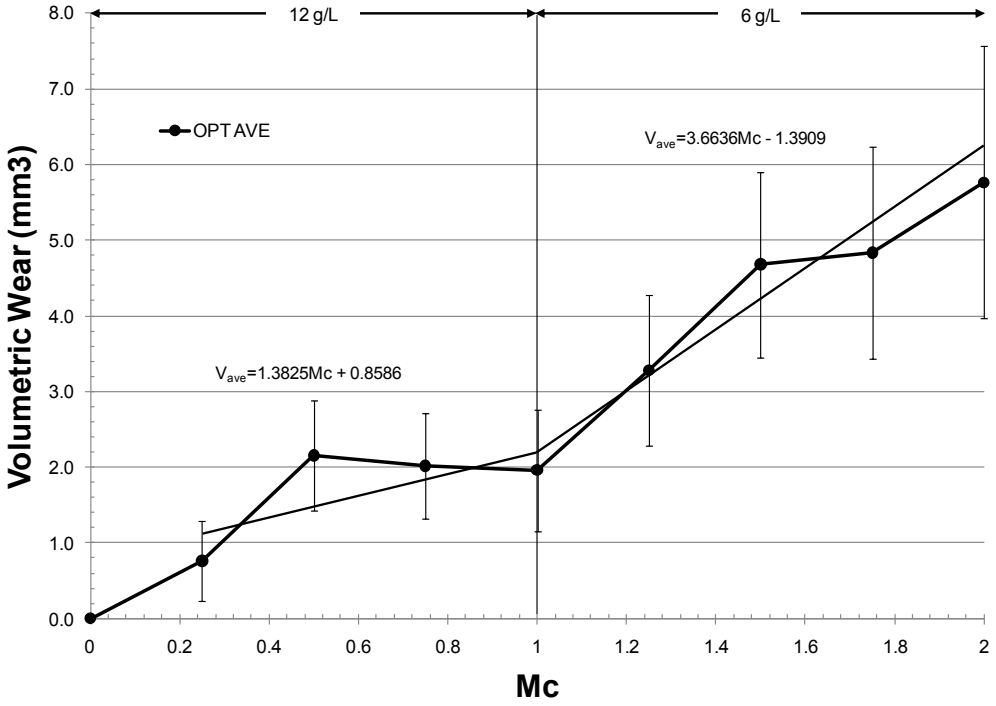


**Figure 7-22: Average OPT wear during wear test 3**

As previously described, the specimens exhibited a polished contact region that exhibited some signs of surface scratching upon initial inspection after 0.25 Mc (Figure 7-23). The surface characteristics did not appear to vary significantly for the duration of the test, other than small increases in contact area as wear progressed.

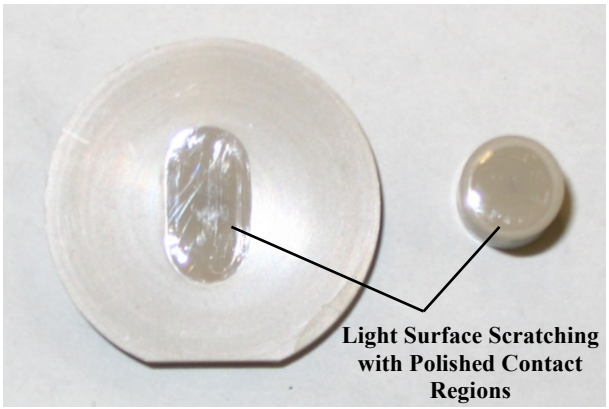


**Figure 7-23: OPT specimens after 2 Mc of testing at 80 N (test 3)**

The wear of the pins and plates can be individually compared (Figure 7-24) to investigate if one or the other was experiencing higher wear or if some material transfer was occurring during testing.

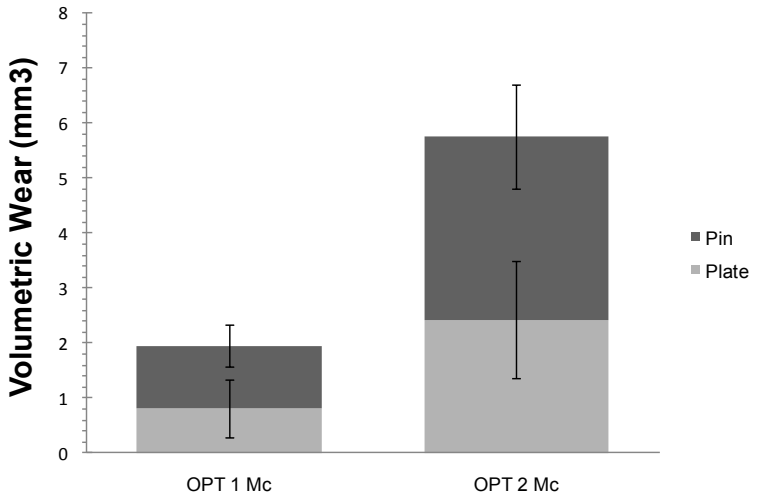


**Figure 7-24: Individual pin and plate wear during wear test 3**

It can be seen that, on average, both the pins and plates exhibit the same amount of wear and thus the wear appears to be shared equally between both contact surfaces. Also, unlike what was exhibited by some of the CFR specimens, no material transfer as indicated by a negative wear rate was observed in during wear test 3.

## Contact Stress

The contact stress during the first Mc was larger than the second Mc as wear increased the contact area (Table 7-17).

**Table 7-17: Contact stress during wear test 3**

| Test Period | Average Contact Stress (MPa) |
|---|---|
| 0-1 Mc | 4.58 +/- 3.21 |
| 1-2 Mc | 2.30 +/- 0.45 |

The contact stress exhibited greater variation during the first Mc and then stabilized during the final Mc as shown by the standard deviations of both intervals. The contact stress of the OPT specimens during the first Mc in wear test 3 (4.58 MPa) was significantly lower than what was observed with the conical OPT specimens in wear test 2 (22.36 MPa). This is due to the much smaller contact area observed by the conical specimens, compared to the larger contact provided by the 60 mm radius spherical tip used in wear test 3. Not surprisingly the contact stress of wear test 3 was larger than the stress observed during wear test 1 where the pins had a spherical contact radius of 100 mm. A larger radius results in a higher contact area and thus a lower contact stress.

## Wear Factors

Wear factors were determined for regions of steady state wear observed during the different test parameters; 0.25-1.0 at 12 g/L protein concentration and 1.0-2.0 Mc at 6 g/L protein concentration for the OPT specimens. This removed the initial run-in wear and included the two distinct regions of wear that was observed for the OPT specimens. The wear factors were calculated based on the slope of a least squares best-fit line in the "steady-state" region of the wear versus *Mc* plots and recorded in Table 7-18.

**Table 7-18: Steady state wear factors during wear test 3**

| Material | k (10-6 $mm^3 N^{-1} m^{-1}$) avg ± std dev | |
|---|---|---|
| | 0.25-1.0 Mc (12 g/L) | 1.0-2.0 Mc (6 g/L) |
| OPT | 1.02 ± 0.87 | 2.70 ± 1.53 |

The OPT specimen pairs exhibited a significant increase in wear during the second Mc of the test when the protein concentration of the lubricant was reduced from 12 to 6 g/L. This difference is statistically significant ($p=0.041$) and thus there are two individual wear regimes occurring in both the first and second Mc. Again, it in unclear whether the increased wear rate was due to the breakdown of the OPT after 1 Mc, or whether the reduction in lubricant protein concentration from 12 to 6 g/L was the cause. This is similar to the results of wear test 2 where the OPT specimens exhibited a significant increase in wear rate for similar test conditions.

When the wear factors are compared to wear test 1 (0.63 for the duration of testing at 80 N in 12 g/L lubricant), the OPT wear rates for wear test 3 are higher for both the first and second Mc. When compared to the OPT wear factors obtained during wear test 2 (0.125 for the first Mc and 2.76 for the second Mc), the wear factor for the first Mc was significantly lower for the conical pins in wear test 2 compared to the spherical radius pins in wear test 3. This is surprising because the reduced contact area exhibited by the conical pins resulted in a much higher contact stress than what was exhibited by the spherical pins. During the second Mc, the OPT wear factors are almost identical, these values were obtained at similar contact areas and stresses. This similarity may be a result of the effect of the reduced lubricant protein concentration or the breakdown of the OPT surfaces after 1 Mc of wear testing.

## Coefficients of Friction

Friction forces were measured at the end of each test interval and used to calculate the average coefficient of friction for both material pairs during the testing under both the 12 and 6 g/L protein concentration under 80 N of loading (Table 7-19).

**Table 7-19: Coefficient of friction during each different protein concentration for wear test 3**

| Material | Protein Concentration (g/L) | Number of evaluations | Coefficient of friction | |
|---|---|---|---|---|
| | | | avg | std dev |
| OPT | 12 | 24 | 0.24 | 0.09 |
| OPT | 6 | 24 | 0.39 | 0.11 |

Again, the measured friction forces were relatively consistent over the test period, with the majority of variation occurring early in the test (0-0.25 Mc) for both specimens, with very little variation occurring during the subsequent 1.75 Mc of testing during both the 12 and 6 g/L lubricant protein concentrations. The coefficient of friction was measured to be lower during the first Mc than during the second Mc, when increased wear rates were observed to be significantly higher. This difference was statistically significant ($p<0.0001$). This increase in friction was observed to occur at the point where the lubricant protein concentration was reduced from 12 to 6 g/L, this is similar to the transition that was observed during wear test 2. In both cases increased wear was accompanied by increased coefficients of friction.

When the friction during wear test 3 is compared to the values obtained for OPT during wear test 1 it can be seen that lower friction was obtained for both lubricant protein concentrations with specimens having a spherical contact radius of 60 mm compared to those having a radius of 100 mm. When compared to the conical OPT specimens tested during wear test 2, the friction during wear test 3 was higher for both protein concentrations. These differences were statistically significantly different with p values of $p<0.0001$ for 0.25-1 Mc and 12 g/L and $p=0.0022$ for 1-2 Mc and 6 g/L. Clearly the conical contact produced lower friction in all cases, but much lower wear during the first Mc and similar wear rates during the second Mc of testing.

### 7.4.6 Wear Test 4

The fourth wear test focused on the investigation of CFR PEEK specimen pairs. Testing was performed with 6 MOTIS-G (Pitch-based) CFR specimen pairs provided by Invibio Ltd. (Thornton-Cleveleys, Lancashire, UK). The pins were manufactured with a spherical contact radius of 60 mm and articulated on a flat plate. The fiber orientation in the CFR pins was parallel to the contact surface. The fiber orientation of the plates was maintained as parallel to the surface. Test parameters were identical to those used in wear test 2 for CFR pairs.

The six specimen pairs were subjected to a loading of 80 N for a total of 3 Mc. This load was selected to provide a contact stress similar to what a spinal implant would be subjected to *in vivo*. Alpha calf fraction serum (with an antibiotics package) that was diluted with phosphate buffer solution to a specified protein concentration was used as the test lubricant. The protein concentration was 12 g/L from 0-1 Mc (test 2a), and 6 g/L from 1-3 Mc (test 2b). This was done to investigate the effects of this parameter, if any, on the wear performance of the material pairs. The temperature of the lubricant was maintained at 37° C. Friction forces were measured at the start and end of each wear test interval, with the start friction obtained after the specimens were cycled for a count of 100, and the final count immediately after the interval count was reached. As before, the actual contact area was obtained by measuring the pin wear scar.

#### Results

As observed in wear test 2 the CFR pins and plates exhibited polished contact regions after the first test interval, with the only notable change being a small amount of contact area growth as the test progressed (Figure 7-25). No central pitting was observed on the CFR pins; again this is similar to wear test 2 and different from wear test 1. The main differences between these tests were the contact radius and fiber orientation.

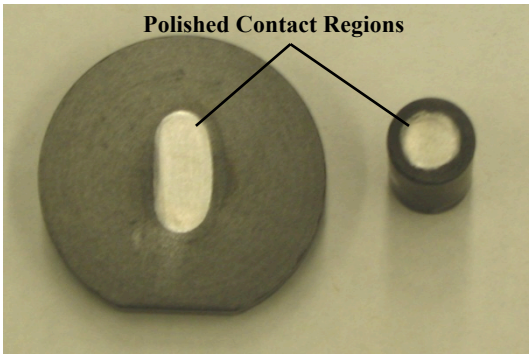


**Figure 7-25: CFR Specimens after 3 Mc of testing at 80N (test 4)**

The volumetric wear of the 6 CFR specimen pairs can be plotted against the number of cycles (Figure 7-26). It is immediately apparent that there are two distinct groups of specimens; two of the six specimens exhibited steady positive wear rates, while the remaining 4 specimen pairs showed a steady negative rate of wear over the entire 3 Mc of testing. When all six specimens are considered, the average rate of wear over the entire 3 Mc is -0.254 $mm^3Mc^{-1}$; an impossible value since material was not added to the specimen pairs. When only the

specimen pairs with a positive wear rate are considered, the average wear rate becomes 0.278 $mm^3Mc^{-1}$, a value that is much more physically realistic.

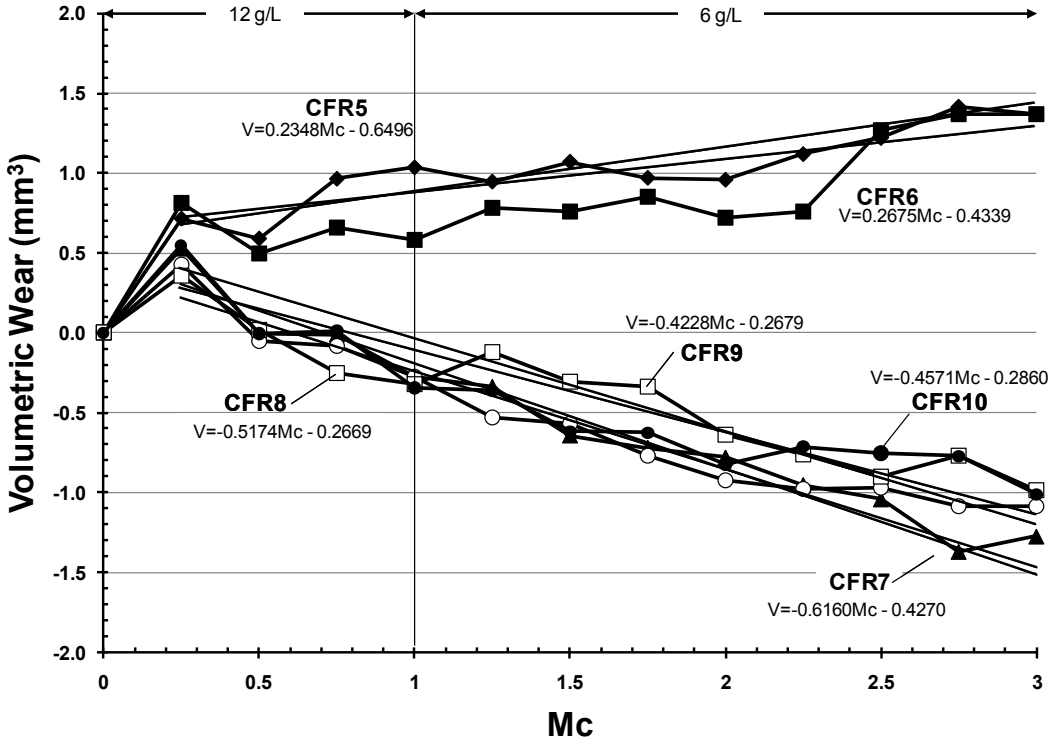


**Figure 7-26: Volumetric wear of CFR specimens vs. number of cycles during wear test 4**

There is an error associated with the specimen pairs that exhibited negative wear rates, probably involving fluid absorption that was not accommodated with the load soak compensation process. However, since realistic wear values were observed with two material pairs, the entire fluid absorption process was not entirely biased, but the problem seems to be confined to 4 of the 6 specimen pairs. While the wear rates of these 4 material pairs may not provide valid insight into CFR wear rates, they will allow for investigation into the possibility of catastrophic failure at high cycling; a failure which would present as high wear. This was not observed in the present testing.

When the protein concentration of the lubricant was reduced from 12 to 6 $gL^{-1}$, the wear rate of the high wearing specimen pairs decreased slightly while the negative wear group showed a small change to a less negative rate (Table 7-20). During the first 0.25 Mc all of the specimen pairs experienced some run-in wear at a higher rate of wear than observed during the subsequent testing.

**Table 7-20: Average volumetric wear rates during wear test 4**

| Specimen Type | Average Volumetric Wear Rate ($mm^3Mc^{-1}$) | |
|---|---|---|
| | 12 $gL^{-1}$ (0.25-1 Mc) | 6 $gL^{-1}$ (1-2 Mc) |
| CFR – Positive wear group | 0.593 ± 0.559 | 0.371 ± 0.106 |
| CFR – Negative wear group | -0.598 ± 0.112 | -0.421 ± 0.148 |

All of the contact surfaces appeared polished as observed after the initial 0.25 Mc through to the end of testing, as previously seen in wear test 2. The average wear of the pins and plates was plotted individually for all the CFR specimens after 1, 2 and 3 Mc of testing (Figure 7-27).

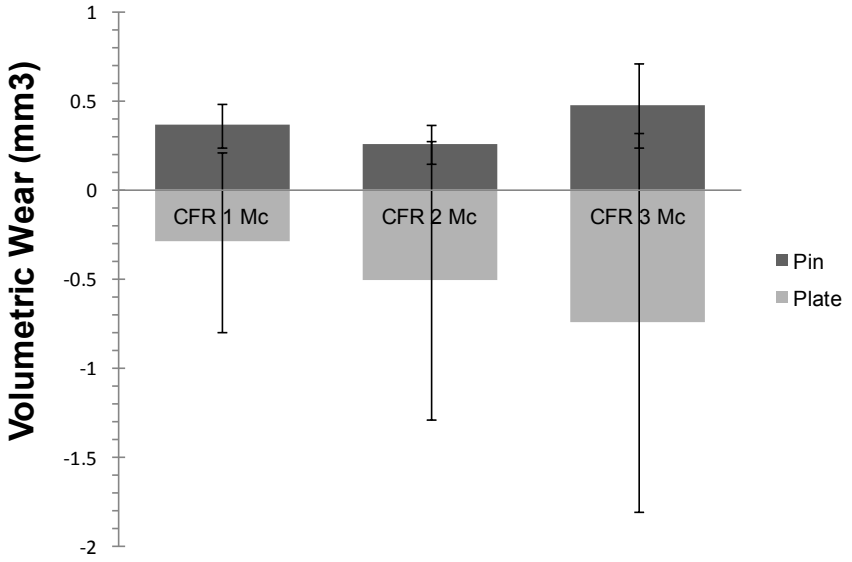


**Figure 7-27: Average pin and plate wear at 1, 2 and 3 Mc during wear test 4**

Examination of this data could lead to the conclusion that net material transfer occurred from the pin to the plate, with the pins experiencing a positive wear and the plates exhibiting negative wear (or a net increase in mass). While this was observed during wear test 1 with the CFR specimens, this was not generally found for the CFR specimens tested in wear test 2 (which are identical to the specimens tested in the current test. Further examination of the data was performed for the two subsets of specimen pairs; the 2 positive wear rate, and 4 negative wear rate material pairs (Figure 7-28). It is clearly visible that in this wear test the hi wear material couples observed wear on both the pins and plates whereas the negative wear couples exhibited some positive wear of the pins with significant negative wear (or mass increase) on the plates. On average for all three intervals investigated, the increase in mass of the plates exceeded the mass loss of the pins due to wear and therefore it is expected that this error is due to fluid uptake. Some material transfer may have occurred from the pins to plates, however the pin wear was not large enough to account for all the mass increase of the pins.

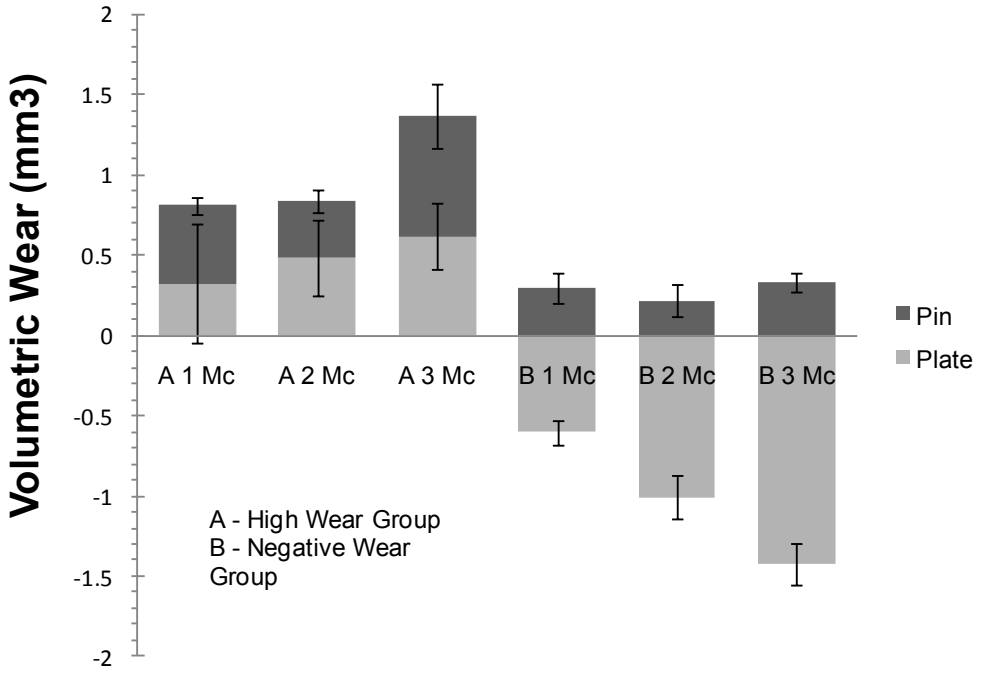


**Figure 7-28: Individual pin and plate wear for high wear and negative wear groups (test 4)**

In order to further investigate this anomaly, the volumetric wear of just the pins was plotted against the number of cycles (Figure 7-29) since the fluid uptake error only seemed to afflict the plates and not the pins.

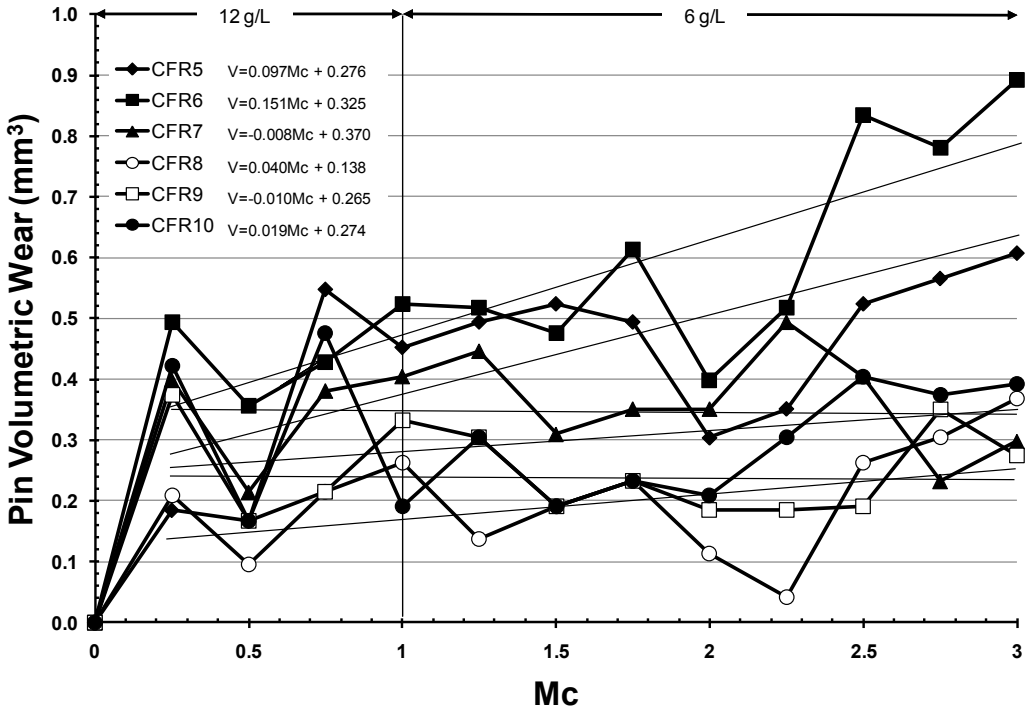


**Figure 7-29: CFR pin volumetric wear vs. number of cycles during wear test 4**

The wear rates of all the pins are similarly positive with a relatively consistent slope. Surprisingly the wear pin wear trends seem to be noisier than the wear trends of the specimen pairs. The reason for this is unknown but may be due in part to the reduced mass and volume of the pins making them more sensitive to fluid absorption and the accompanying compensation procedure. The volumetric wear rates of the pins were calculated and compared to the pin wear rates observed in wear test 2 (Table 7-21).

**Table 7-21: Comparison of pin volumetric wear rates from wear test 2 and 4**

| Pin Group | Average Volumetric Wear Rate ($mm^3Mc^{-1}$) |
|---|---|
| Wear Test 2 | 0.0502 ± 0.1030 |
| Wear Test 4 | 0.0482 ± 0.0638 |

No significant difference between the wear of the pins in wear test 2 and wear test 4 was detected; this supports the hypothesis that excess fluid absorption of CFR plates 7-10 caused the negative wear rates, and that the tribology at the contact of the negative wear group was not significantly different than the positive wear group or those observed in wear test 2.

## Contact Stress

As before, the contact stress was determined by dividing load by the contact area as measured on the pin surfaces using a ruler (Table 7-22). All specimens in the present test exhibited small amounts of growth of the contact area as wear progressed. There was no significant difference between the contact areas of the positive and negative wear groups; again supporting that the tribology of the contact was similar for both groups and that excess plate fluid absorption contributed to the observed error.

**Table 7-22: Contact stresses of CFR specimen pairs during wear test 4**

| Material | k (10-6 $mm^3 N^{-1} m^{-1}$) avg ± std dev | |
|---|---|---|
| | 0.25-1.0 Mc (12 g/L) | 1.0-3.0 Mc (6 g/L) |
| CFR | 3.65 ± 0.45 | 2.77 ± 0.17 |

When the contact stresses exhibited during wear test 4 are compared to the CFR specimens tested during wear test 2 under identical testing conditions it can be seen that the values are very similar for both the testing in protein concentrations of 12 and 6 g/L. This is to be expected as the specimens and test parameters are identical. It is important to note that the contact stress did not change much during testing from 2-3 Mc, this means that once the contact area has been created mainly by run in wear it does not change much during subsequent testing.

## Wear Factors

Wear factors were determined for regions of steady state wear observed during the different test parameters; 0.25-1.0 and 1.0-3.0 Mc for the CFR specimens. This removed the initial run-in wear and included the two regions during which test parameters were modified to determine if they had an affect on overall wear rates. The wear factors were calculated based on the slope of a least squares best-fit line in the "steady-state" region of the wear versus *Mc* plots and recorded in Table 7-23.

**Table 7-23: Steady state wear factors during wear test 4**

| Material | k (10-6 $mm^3$ $N^{-1}$ $m^{-1}$) avg ± std dev | |
|---|---|---|
| | 0.25-1.0 Mc (12 g/L) | 1.0-2.0 Mc (6 g/L) |
| CFR – all material pairs | -0.186 ± 0.310 | |
| CFR – positive wear group | 0.436 ± 0.411 | 0.204 ± 0.019 |
| CFR – negative wear group | -0.439 ± 0.082 | -0.382 ± 0.084 |

In this case the CFR specimens exhibited a change in wear factor when the protein lubricant was reduced, the difference was more marked with the positive wear group compared to the negative wear group. What is interesting is that the wear rate actually decreased with the reduction in lubricant protein concentration. This is opposite to what was seen with OPT specimens where the wear rate increased for the same conditions. Since the positive wear group consists only on two specimens it is expected that this difference is just due to scatter. When the wear rates of all six pins are compared to remove the fluid absorption error associated with the plates, no significant difference in wear rate was detected (p=0.73) for the two different protein concentrations investigated.

### 7.4.7 Coefficients of Friction

Friction forces were measured at the end of each test interval and used to calculate the average coefficient of friction for both material pairs during the testing under both the 12 and 6 g/L protein concentration under 80 N of loading (Table 7-24).

**Table 7-24: Coefficient of friction during each different protein concentration (test 4)**

| **Material** | **Protein Concentration (g/L)** | **Number of evaluations** | **Coefficient of friction** | |
|---|---|---|---|---|
| | | | **avg** | **std dev** |
| CFR | 12 | 24 | 0.17 | 0.01 |
| CFR | 6 | 48 | 0.18 | 0.03 |

The friction forces as measured were relatively consistent over the test period, with the majority of variation occurring early in the test (0-0.25 Mc). The friction measured in both lubricant protein concentrations were almost identical, and were almost indifferent from the friction obtained during the same testing conditions for the CFR specimens in wear test 2. Again, no significant difference in friction was detected between the positive and negative wear groups, further supporting the hypothesis that the error was attributed to the increased fluid absorption of the plates. It is plausible to expect that any difference at the point of contact that would result in increased (or decreased) wear would produce discernable coefficients of friction. Overall the friction of the CFR specimens was consistent and low as expected from the results of wear test 2.

### 7.4.8 Discussion and Concluding Remarks

The volumetric wear vs. number of cycles was plotted for OPT (Figure 7-30) material pairs subjected to 80 N loading conditions. For the OPT specimen pairs, the conical contact pins exhibit markedly less wear for the first Mc, but during the second Mc the specimen wear increased to levels near the 60 mm spherical radius pins.

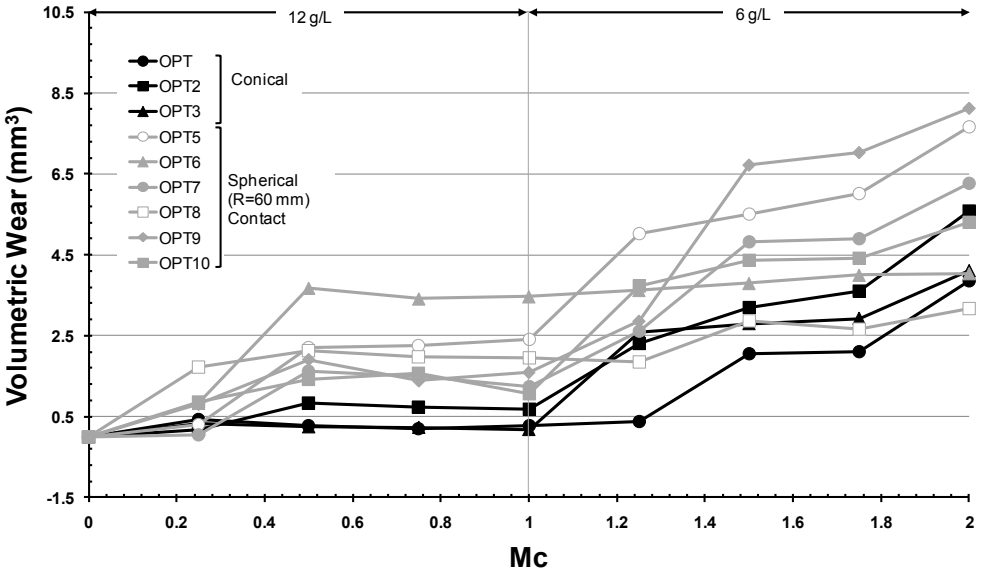


**Figure 7-30: Volumetric wear of all OPT pairs at 80 N vs. number of cycles**

The results of wear tests 1 and 2 were also plotted against data obtained by Austin (2008) who used the same test parameters as wear test 1 (Figure 7-31) with a constant lubricant protein concentration of 12 $gL^{-1}$. The wear observed in the present study is similar to the range of values obtained by Austin for both OPT and CFR material pairs. The conical OPT specimens exhibited much lower wear for the first Mc, but during the second Mc reached wear levels equal to or higher than Austin. The wear of the CFR specimens in the present study is slightly, but not significantly higher than the wear reported by Austin (2008).

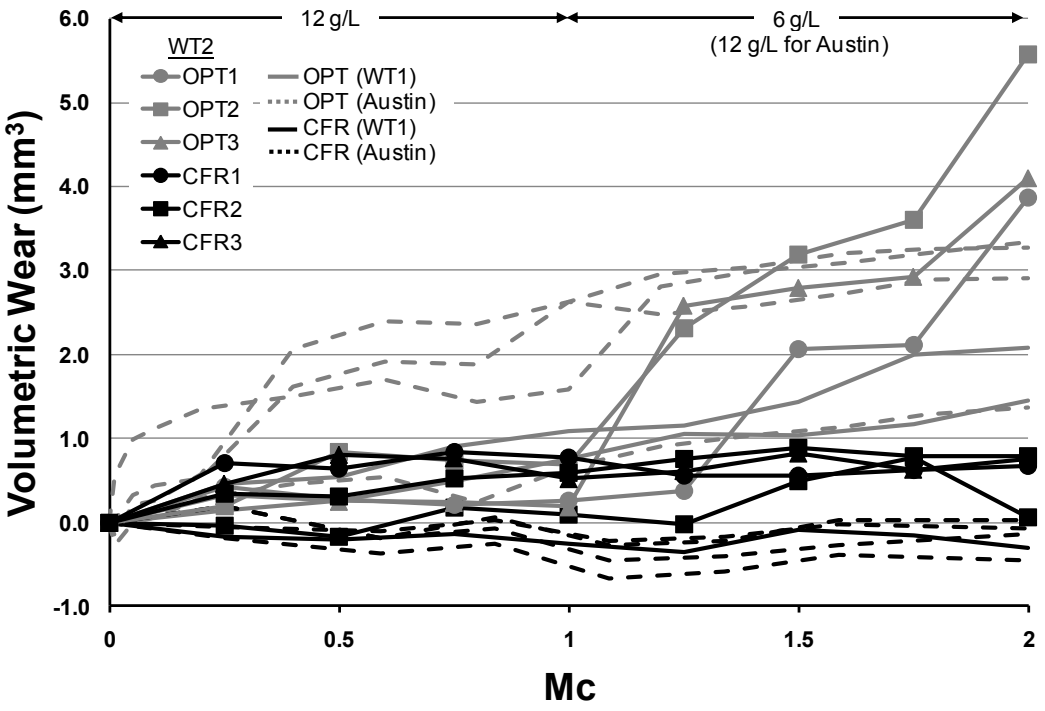


**Figure 7-31: WT1 and WT2 volumetric wear plotted with data from Austin (2008)**

The volumetric wear of all the 60 mm spherical radius CFR specimens in the present study was also plotted as a function of the number of cycles (Figure 7-32). With the exception of the negative wear group, all the CFR specimens exhibited a steady rate of positive wear under both lubricant protein concentrations.

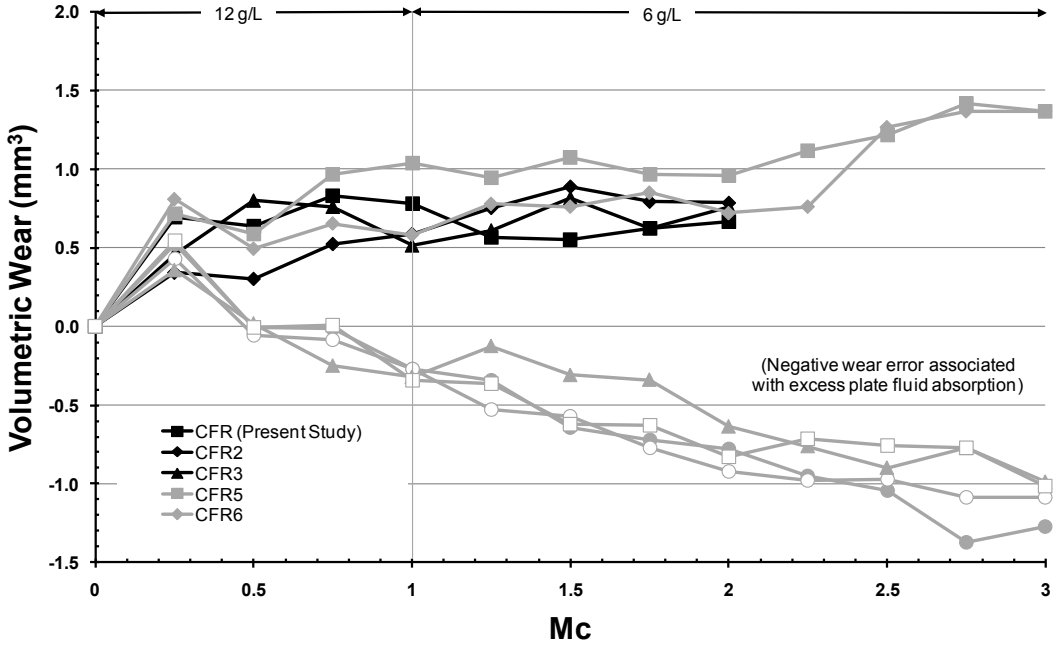


**Figure 7-32: Volumetric wear of all CFR pairs at 80 N vs. number of cycles**

In order to facilitate easy comparison of wear rates, the results of the present study can be plotted against Austin (2008), Scholes & Unsworth (2009), Grupp et al (2010) and Schwenke et al (2007) for all OPT material pairs (Figure 7-33) and CFR material pairs (Figure 7-35).

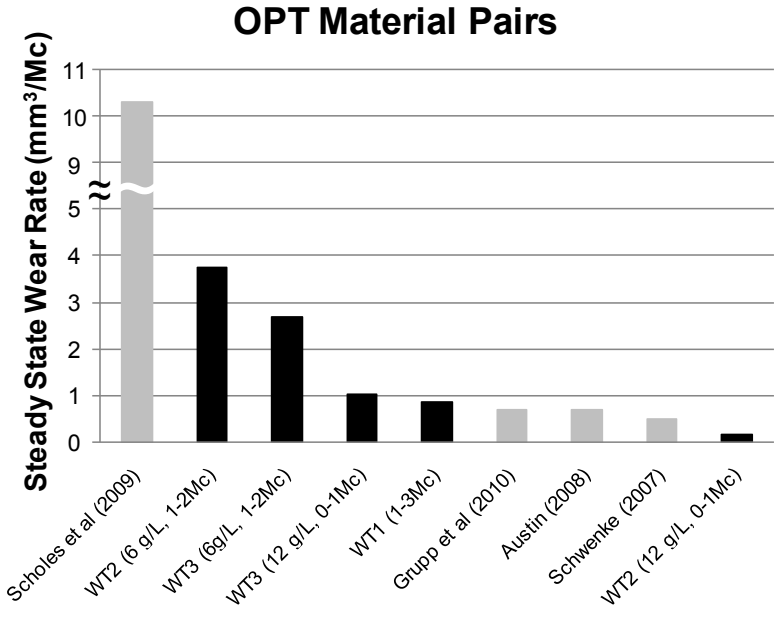


**Figure 7-33: OPT material pair overall wear rate comparison**

For the OPT specimen pairs, the highest wear rate is reported by Scholes & Unsworth (2009) who tested all-OPT articulations consisting of flat ended pins on flat plates in continuous rotation. The next highest wear rates were reported by the present study in the second half of wear tests 2 and 3 when the protein concentration was reduced to 6 $gL^{-1}$. During this time both sets of samples exhibited a large increase in wear rate; the cause of which is expected to be due to either a sensitivity to protein concentration or the breakdown of the surfaces after exposure to 1 Mc of testing at 80 N. An increase in wear rate in the second Mc of testing was not reported by Austin (2008) in a constant lubricant protein concentration but the test parameters in that study included OPT pins with a larger spherical contact radius, and thus a larger contact area. This resulted in a lower contact stress, a value which may have been low enough not to produce the breakdown of the surface after the 1 Mc of testing at 80 N. The difference in contact stress is more marked in wear test 2 where conical OPT pins were used to produce stress levels greater than what was experienced by the CFR specimens. Since a larger wear rate was observed during the second half of wear test 2 under the same conditions of wear test 3 it is expected that the OPT is sensitive to the contact stress and thus OPT wear can be described using some function of applied load (and thus contact stress) and number of cycles. There may also be some sensitivity to lubricant protein concentration as the change in wear rate occurred in both cases at the point of reduction of this test parameter.

Low overall wear rates were observed during the first Mc of wear test 3 in lubricant having a protein concentration of 12 $gL^{-1}$. Even lower rates of wear were observed during the 2 Mc of testing in wear test 1 even after 1 Mc of loading under adverse conditions with applied loads of up to 400 N. This result seems to show that an all-OPT articulation is resistant to wear even after significant loading and exposure to high contact stresses. This is interesting to compare to the results of wear tests 2 and 3 where OPT experienced a large increase in wear after subjected to a relatively low load of 80 N for only 1 Mc. This seems to point to a sensitivity of OPT wear to lubricant protein concentration, but it is important to note that the contact stresses observed in wear tests 2 and 3 were still, on average, larger than the contact stresses observed by the OPT specimens during the adverse conditions. This is because the larger 100 mm contact radius provided a larger contact area during testing.

Therefore based on the current study, the wear of OPT is expected to be more strongly linked to applied contact stress and less on the lubricant protein concentration. The fact that the material pairs exhibited more wear immediately after reducing the protein concentration may have just coincided with the point of material breakdown. While this is not conclusive, further testing employing the same test parameters without the lubricant change at 1 Mc will provide insight into this question.

Testing of OPT specimens with a 100 mm spherical contact radius yielded the lowest wear rates of all compared studies. Again, this leads to the conclusion that lower contact stresses result in lower wear for self-mating OPT articulations. When the run in wear observed from 0-0.25 Mc is compared (Figure 7-34) no significant difference can be detected between pins having either a 60 or 100 mm spherical radius, however the conical OPT pins did exhibit much less run-in wear during wear test 2.

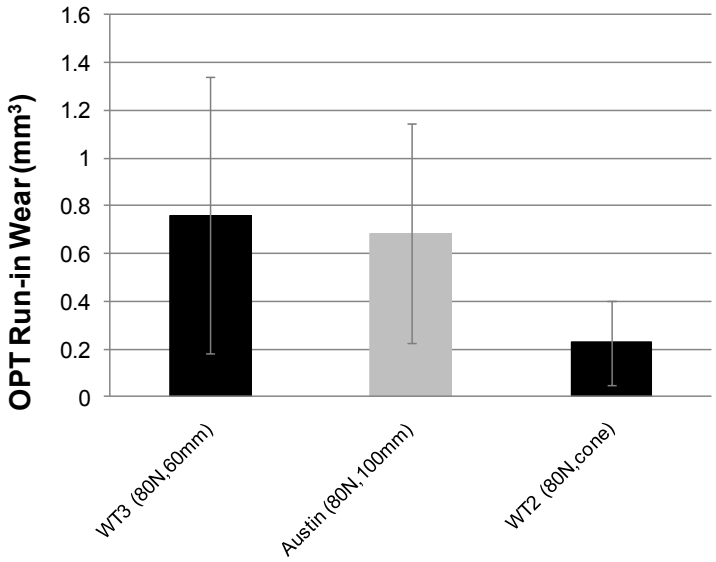


**Figure 7-34: OPT run in wear comparison under 80 N loading**

This result shows that for short periods of time, all-OPT articulations can exhibit low wear even at high contact stresses, however over longer periods of time wear may increase as the surfaces break down due to some surface damage mechanism.

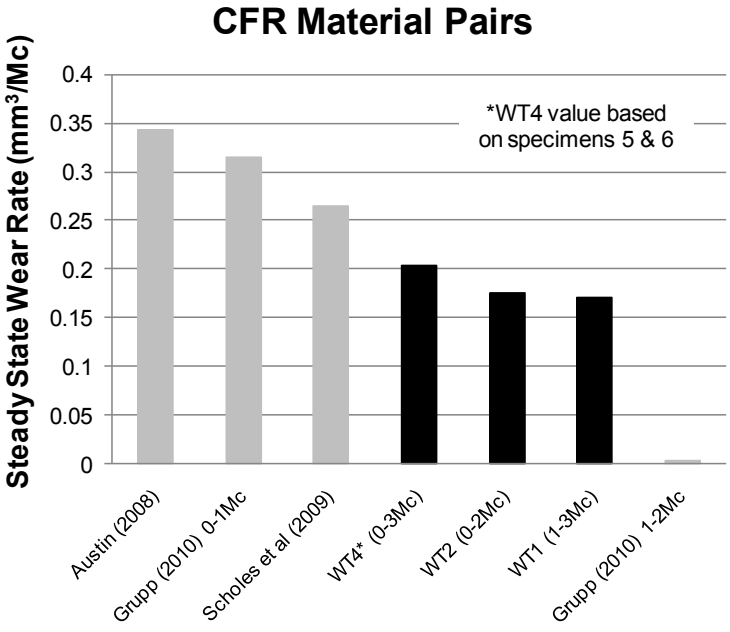


**Figure 7-35: CFR material pair overall wear rate comparison**

The wear of the CFR material pairs in the present study were lower than all other studies except for Grupp et al (2010) who reported almost no wear. When the wear rates of wear test 1 are compared to Austin (2008) who

tested using the exact same parameters, it is interesting to find that the present study observed almost a 50% reduction in wear rate. The only difference in this case is the specimens in the present study were subjected to adverse loading prior to the 2 Mc of testing at 80 N when the steady state wear rate was assessed. This difference may have been a result of the wearing away of the PEEK matrix to expose the underlying, more wear resistant reinforcing carbon fibers during the initial 1 Mc of adverse loading. Austin (2008) measured the wear rate during the initial 2 Mc at 80 N during which time the PEEK matrix would have observed wear to expose the underlying carbon fibers.

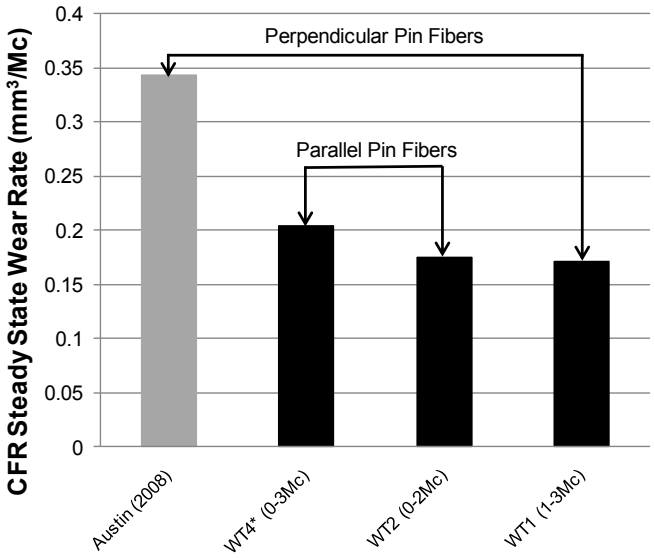


**Figure 7-36: Wear rate effects of CFR pin fiber orientation**

The wear of the 60 mm spherical radius CFR pins with reinforcing fibers that are parallel to the contact was similar to the 100 mm CFR pins after being subjected to adverse loading (Figure 7-36), and lower than results reported by Austin (2008). In this case, it was postulated that having two surfaces that had parallel meshes of carbon fibers would produce lower wear since the reinforcing fibers would articulate with one another along their longitudinal axes as opposed to the ends of fibers articulating on the sides of fibers. However when the run-in wear of both types of fiber orientations are compared (Figure 7-37) a significant difference can be seen.

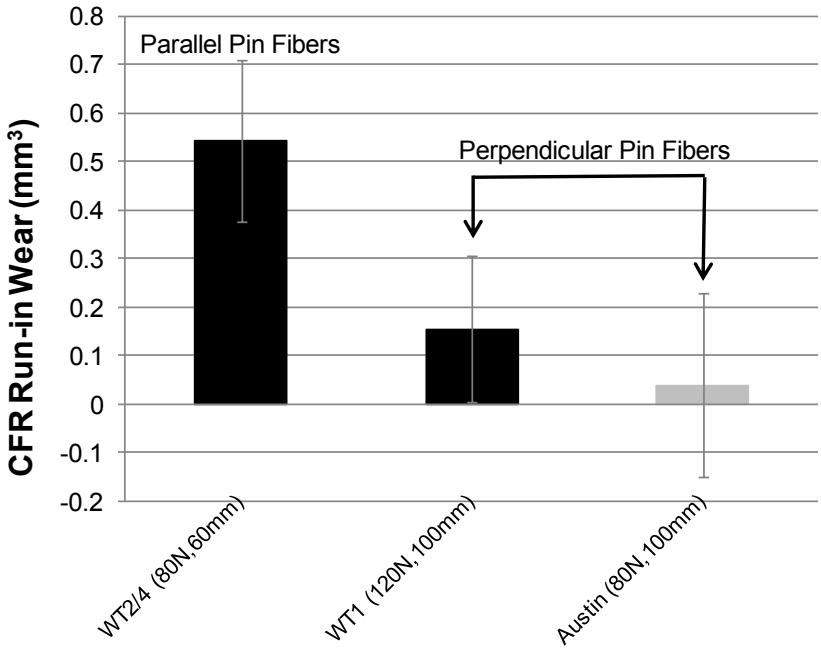


**Figure 7-37: Run-in wear effects of CFR pin fiber orientation**

The CFR pins having a parallel fiber orientation exhibited much higher run-in wear than those having a perpendicular fiber orientation. This may be a result of the need for PEEK matrix to be removed from both the pin and plate to expose the underlying, wear resistant carbon fibers for the parallel on parallel configuration. For parallel on perpendicular fiber orientation, only the PEEK matrix on the plate needs to be removed since the perpendicular fibers in the pin are already at the surface providing resistance to wear. Thus it was seen that the parallel on parallel fiber orientation produced a lower steady state wear rate, but exhibited more run in wear.

The average steady state wear factors of all wear tests were also compared (Table 7-25). It can be seen that while the wear factors obtained in wear test 3 are high, they are still not at the same levels reported by Scholes and Unsworth (2010); this may be to the continuous rotation employed in their wear test. A marked difference in OPT wear rates between lubricant protein concentrations and first and second Mc is also observed; the reason again is either due to a sensitivity to lubricant protein concentration or surface breakdown due to elevated surface contact stresses. The CFR specimen pairs consistently exhibit lower wear factors than the OPT specimens except for the first Mc of wear test 2 where the conical OPT specimen pins exhibited high contact stresses with little or no wear. The wear factor during the second Mc for the OPT specimens was however significantly higher than the CFR as the OPT surfaces exhibited high wear.

**Table 7-25: Steady state wear factors from all wear tests**

| Material | k (10-6 $mm^3$ $N^{-1}$ $m^{-1}$) avg ± std dev or [range] | | | | | | | | |
|---|---|---|---|---|---|---|---|---|---|
| | Austin (2008) | Scholes & Unsworth (2010) | WT1 | WT2 (12 g/L) | WT2 (6 g/L) | WT3 (12 g/L) | WT3 (6 g/L) | WT4 (high wear couples) | WT4 (all wear couples) |
| **OPT** | 0.412 [0.40-0.45] | 4.5 [.312-.471] | 0.637 ± 0.136 | 0.061 ± 0.435 | 3.76 ± 0.601 | 1.017 ± 0.873 | 2.700 ± 1.525 | - | - |
| **CFR** | 0.213 [.002-0.26] | 0.3 [.132-.267] | 0.126 ± 0.124 | 0.203 ± 0.168 | 0.147 ± 0.074 | - | - | 0.204 ± 0.019 | -0.187 ± .310 |

The average coefficient of friction was also plotted for each wear test (Figure 7-38). Like in the wear factor comparison, the CFR specimen pairs consistently exhibit lower friction than the OPT specimen pairs except for the first Mc of wear test 2, again when the conical OPT pins exhibited very little wear. During this period the CFR friction was higher than the OPT friction, but this was reversed during the second Mc when the OPT exhibited high wear.

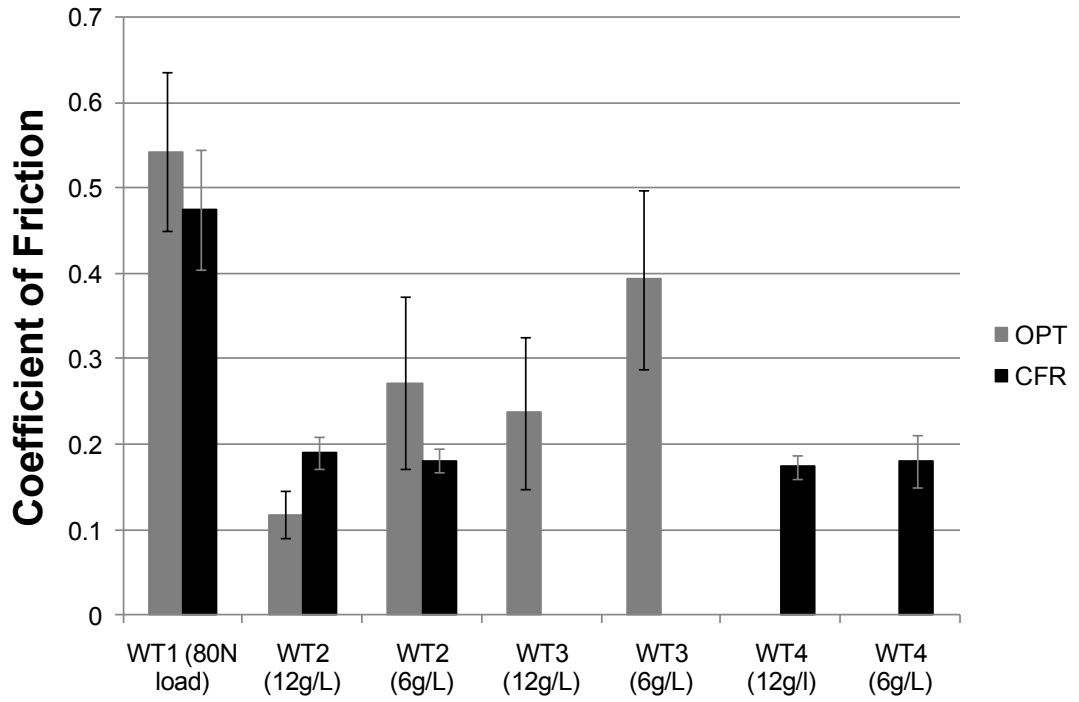


**Figure 7-38: Average coefficients of friction from all wear tests**

While a lower wear factor and friction was achieved with the conical OPT specimens for the first Mc of testing during wear test 2, during the second Mc these advantages were lost and subsequent high wear increased the wear factor and friction to levels above the CFR specimen pairs under the same conditions. Thus the strategy of reducing the contact area to improve wear resistance and friction is not viewed as a suitable long term solution for OPT specimens. Overall the CFR material pairs exhibited lower and more stable wear and friction than the OPT specimens under all conditions.

## 7.5 Limitations of the Current Study

The present study investigated the wear of all-polymer PEEK articulations in a pin-on-plate configuration for both unfilled and carbon fiber reinforced variants. While the results of the present study seem to show that CFR PEEK is significantly more wear resistant than unfilled PEEK, there are some limitations in the results.

Central pitting was observed during the testing of the 100 mm CFR pins; the cause of this is currently unknown although other studies have also observed this. Surprisingly this was not recorded for the 60 mm CFR pins, or any of the unfilled OPT pins. It is important to note that the overall wear of the CFR material pairs was still quite low, but the cause of this central pitting and any resulting clinical implications is currently unknown and needs to be the focus of future investigation.

Also, four of the nine 60 mm CFR specimen pairs exhibited a negative wear rate that was attributed to excessive fluid absorption of the plates. Because the wear of the CFR was so low, the fluid absorption was large enough to mask the actual wear resulting in a physically impossible negative wear rate. While it is clear that the CFR wear rate was very low over the 3 Mc of testing, the negative wear rate observed presents the concept that PEEK may absorb fluids at different rates. While this may not have a clinical implication since it is not expected that the amount of wear will be affected by fluid absorption, future wear testing of PEEK may also be affected by this phenomenon and therefore should be considered for future studies.

In order to strengthen the conclusions of the current study, further testing should be performed to increase the number of specimen pairs tested for each set of test parameters. This will increase the confidence in the results. Also, the present study is strictly a pin-on-plate study that subjected the specimens to a representative contact stress with crossing path motion. In order to gain an understanding of the actual performance of the all-polymer PEEK articulation, full-scale spine simulator wear testing using actual implant geometry and spinal kinematics and loading should be performed. This will provide a more accurate prediction of the expected *in vivo* performance of the device.

The results of the current study do show that CFR PEEK articulations are better than unfilled OPT versions in terms of wear, friction and sensitivity to test parameters. Also, the threshold for increased wear was not reached for CFR PEEK even under adverse loading and up to 3 Mc of testing. Therefore the present study shows that CFR seems to be a more resilient material than OPT for use in joint replacement in the cervical spine. This knowledge should be used to direct future wear studies and investigations.

# Chapter 8
# Conclusions and Recommendations

## 8.1 Conclusions

A cervical total level arthroplasty system (CTLAS) was developed and introduced in Chapter 6 to illustrate the potential of PEEK-on-PEEK articulations for spinal disc and facet implants. Although firm conclusions regarding this design could not be made, detailed "concluding remarks" were presented in section 6.11.

The selected 'best design' includes both disc and facet replacement implant; the disc replacement promotes motion about the natural helical axis of the cervical spine and the facet replacement mimics the anatomy of the natural facet. There is still significant work required before this concept could be brought to clinical use. Fixation, surgical procedure, and instrumentation all need to be addressed. Device implementation includes three distinct treatment paths depending on the type of deterioration presented initially by the patient; disc and facet pain warrants the combined disc and facet replacement system, disc or facet pain individually warrants replacement of only the damaged component. In the case of future deterioration of the other spinal structure(s), replacement can be accommodated with the present design. This allows the system to be tailored to the individual patient's needs to be as minimally invasive as possible. The proposed CTLAS design represents a significant advancement in spinal disc arthroplasty that includes a cervical disc replacement that better replicates the kinematics of the cervical spine and a facet replacement that allows for the removal of damaged facets while preserving segmental motion (where fusion was required in the past).

In Chapter 7, the tribology of PEEK-on-PEEK articulations was examined in some detail using a pin-on-disc apparatus. In agreement with other studies (Grupp *et al*, 2010; Scholes and Unsworth, 2008; Austin *et al*, 2010; Scholes and Unsworth, 2010), CFR was found to have much lower wear than OPT.

Under all testing conditions, except when the contact area was reduced with the conical OPT pins which resisted wear for the first Mc and then exhibited significant wear during the subsequent Mc, the CFR material pairs exhibited significantly lower wear than the OPT specimens. These observations are the result of the reinforcing carbon fibers providing a stronger composite with a higher modulus (resulting in a smaller contact area), and possibly some resistance to wear via fiber interaction. CFR was found to perform well, exhibiting low wear up to 3 Mc at 80 N loading for a moderate contact stress of about 3 MPa.

In all cases, the CFR exhibited a much more consistent, predictable wear trend under varying contact geometries, loading and lubricant protein content. Once a linear wear trend was identifiable, the wear followed this trend with very little deviation. This consistency in wear is desirable because in the case of orthopedic implants different patients demand varying levels of performance and subject the implant to a wide range of applied motions and loadings. The present study suggests that CFR PEEK exhibits a weak sensitivity to these parameters and thus there is a high probability that it will provide low wear in a wide variety of articulating conditions.

On the other hand, the OPT specimens seemed to show some sensitivity to the test parameters, in particular the lubricant protein concentration. In two separate instances at the point where the protein concentration was reduced from 12 to 6 $gL^{-1}$, the wear of the OPT significantly increased. This suggests that OPT material pairs are sensitive to lubricant protein concentration. However, as previously mentioned, it is unclear whether this was due to the changes in lubricant or the result of the breakdown of the surface after 1 Mc of testing since in both cases the OPT material pairs were subjected to higher contact stresses than previously tested via adjustment of the contact geometry.

Similar to the wear comparison, the coefficient of friction of the CFR specimen pairs was consistently lower than the OPT specimen pairs except for the conical OPT pins during the first Mc. This difference was statistically significant and suggests that, much like in the case of wear, the reinforcing carbon fibers reduce the coefficient of friction. This is probably due to some combination of the higher elastic modulus and/or interaction of the reinforcing fibers of the articulating surfaces. It is interesting that the wear seems to correlate with the coefficient of friction and is probably a result of surface damage creating both higher sliding resistance and increased wear through abrasion.

The 60 mm radius CFR specimen pairs also exhibited less surface damage than the OPT specimen pairs, with the latter observing light surface scratching during the first Mc of wear testing. Surprisingly the CFR pins with a 100 mm spherical radius and perpendicular reinforcing fibers developed a central pit at the centre of the pin. This is postulated to be due to the high contact stresses near the beginning of the test causing subsurface damage and subsequent material removal. This was not seen in the 60 mm pins with reinforcing fibers parallel to the contact surface, which is surprising because the contact stresses of the smaller diameter pins are expected to be higher due to the reduced contact area. It is important to note that the reinforcing fiber orientation was difference for these two groups and therefore this parameter may have been a contributing factor to the development of the central pits.

The wear factors for the present study and that of Austin et al (2010) were lower than those found by Scholes and Unsworth (2010) for the OPT material pairs. Furthermore, the absolute wear amounts in Scholes and Unsworth were much higher than the present study, the study of Austin et al and the simulator studies of OPT articulations. All these suggested that the laboratory "wear model" of Scholes and Unsworth might be overly severe. The same difference was not as apparent for the wear factors of the CFR material pairs.

During wear test 1, the testing under the adverse loading conditions preceded testing under the milder 80 N load conditions. When compared with the results of Austin et al (2010) who tested in the opposite order, it seemed that the wear under adverse loading conditions was lower but the wear under the 80 N load conditions was about the same. However, one implant in the present study did sustain severe surface damage under the adverse load conditions and was judged to be an outlier. It was considered possible that if the testing had been a little longer in duration, such severe damage might have been triggered in all the specimens. However, since the two OPT specimens that performed well during the adverse conditions did not exhibit significant wear in the subsequent 2 *Mc* at 80N, high loads might be more damaging than the number of cycles. It is also important to note that the wear of both OPT and CFR specimen pairs under a load of 80 N remained low and thus exhibited a remarkable

lack of sensitivity to previous wear during the adverse load testing regime. Overall, the PEEK was quite resistant to damage accumulation, in that it could survive the adverse load testing and still have a similar wear rate to that of the as-received specimens tested by Austin (2008). This bodes well for PEEK as a cervical spinal arthroplasty material. For the pins with a spherical contact radius of 100 mm and reinforcing fibers perpendicular to the contact, there appeared to be some material transfer from pin to plate during testing of CFR under the adverse loading regime. The same was not seen for the CFR pins that had a 60 mm spherical contact radius and reinforcing fibers that were oriented parallel to the contact surface. Also, none of the OPT material pairs exhibited this material transfer behavior.

During wear test 2, the conical OPT pins surprisingly exhibited lower wear and friction than the CFR material pairs during the first Mc despite being subjected to significantly higher contact stresses due to the point-like contact. However, during the second Mc the OPT specimen pairs exhibited high wear and friction as a result of either the reduced lubricant protein concentration or breakdown of the surface after 1 Mc at elevated contact stresses. The CFR specimen pairs exhibited a steady positive wear rate for the duration of the test showing no detectable sensitivity to the changes in lubricant protein concentration. Also, despite being subjected to higher contact stresses, due to the reduced 60 mm spherical contact radius, the CFR specimen pairs showed similarly low wear as the pins with a 100 mm radius tested in wear test 1. This again suggests that CFR PEEK is a more robust material pairing with low sensitivity for contact stress and lubricant protein content.

The results of wear test 3 again suggested that OPT material pairs are sensitive to lubricant protein concentration as significantly higher wear was observed during the second Mc when the protein was reduced from 12 to 6 $gL^{-1}$. In this case OPT pins having a spherical contact geometry of 60 mm were tested, which again provided larger contact stresses than the 100 mm geometry tested in wear test 1. As in wear test 2, it is unclear whether the increase in wear is due to the reduced lubricant protein content or a breakdown of the OPT articulating surfaces due to 1 Mc at elevated contact stresses. It is important to note that the contact stresses in wear test 3 were larger than wear test, but lower than those of wear test 2. Therefore if the increase in wear rate was solely due to contact stress, it is interesting that the increase occurred after the same cycling as in wear test 1 (1 Mc) because the contact stress was significantly lower. While these results seem to point to a sensitivity of OPT material pairs to lubricant protein content, it is still unclear if this is entirely the case.

Wear test 4 employed the same test parameters as wear test 2 and allowed for testing of a set of 6 more CFR material pairs having a spherical contact radius of 60 mm for a total of 3 Mc at 80 N. Results similar to wear test 2 were observed, with all six CFR specimen pairs showing no sensitivity to lubricant protein concentration. There was some error detected with 4 of the 6 specimen pairs exhibiting negative (but linear) wear with the remaining 2 showing a normal, positive wear trend. Further examination of this outcome showed that for the 4 negative wear couples, the pins showed normal amounts of wear with decreasing masses, but the plates showed a net mass increase that was significantly larger than the mass reduction in the pins. While net material transfer from the pins to plates was observed with the 100 mm radius pins, this was not observed under identical conditions during wear test 2. Also, since the mass increase of the plates was larger than the mass loss of the pins, the cause of the negative wear was attributed to an increased amount of fluid absorption by the plates of the four

negative wear couples was significantly different from the load soak pairs and thus was not accommodated by the fluid absorption compensation procedure. Furthermore, the friction from all 6 specimen pairs was similar and therefore if there was a difference in surface tribology for the 4 negative wear specimen pairs, it would be expected that the friction would also be different. Therefore it was concluded that the negative wear was a result of an increased fluid uptake of the four corresponding plates. The reason for the erroneous fluid uptake is not known, although it has been postulated that material variation may be at fault. Even with the aforementioned error, it is clear that over the 3 Mc of testing no material pair exhibited significant surface damage, central pitting, or wear, independent of the applied number of cycles and lubricant protein concentration. This adds to the conclusion that CFR exhibits low wear under a variety of testing conditions, providing a predictable, linear wear rate.

The picture that emerged from the present study and the quite similar study of Austin et al (2010) was the likelihood that PEEK-on-PEEK articulations could carry loads for a certain number of cycles up to some threshold condition after which the surfaces could no longer resist the accumulated damage or energy input, perhaps associated elevated surface temperatures and other wear mechanisms without sustaining a severe and cascading damage. It is important to note that this 'threshold' was not reached for the CFR PEEK in the present study during testing of up to 3 Mc under both normal and adverse loading conditions of up to 400 N. A more fundamental and specific identification of this threshold condition and whether it could, under any circumstances, arise in a clinical scenario was considered an important issue in the future development of PEEK-on-PEEK implant systems.

Under moderate loads OPT and CFR for durations of 2 and 3 Mc respectively, the all-polymer articulations in the present pin-on-plate study exhibited relatively low wear and surface damage. Under higher, adverse loading conditions the wear of CFR remained relatively low exhibiting almost not sensitivity to applied load. OPT on the other hand, showed increased wear under increased loads, with some signs of increased surface damage. Both material pairs surprisingly exhibited low wear rates under normal loading conditions after a period of adverse loading of up to 400N. Under all wear criteria however, the CFR material pairs performed more favorably than the OPT pairs exhibiting less overall wear, lower wear rate, less run-in wear and lower friction, surprisingly even at higher contact stresses compared to the OPT specimens.

The CFR had a higher elastic modulus, smaller contact areas, higher contact stresses and lower wear than the OPT. While this clearly made CFR look better than OPT, the possibility of subsurface fatigue exposing carbon fibers to direct contact and wear remains a concern. If this concern is adequately addressed with further wear test data including simulator studies of the proposed design, then CFR PEEK is clearly better than PEEK OPTIMA for use in a spinal disc and facet arthroplasty device for its lower wear, almost non-existent sensitivity to applied loading, lubricant protein concentration and contact geometry.

## 8.2 Recommendations

Based on the results of the present study as previously described, the following recommendations are proposed.

### *The proposed CTLAS requires more design work.*

The present study outlines the development of a cervical total level arthroplasty system for use in the replacement of both the disc and facet joints of the cervical spine in a modular fashion. The proposed design represents a significant advancement in the field of spinal arthroplasty since at the present time facet joint damage typically limits patients to spinal fusion which arrests spinal motion and can result in adjacent level degeneration. Further design work is required to develop the design including simulator testing to validate the wear properties of the proposed material pairing and cadaver testing to evaluate the range of motion and kinematics provided by the device to assess the accuracy of the restore motion.

### *CFR is the most suitable formulation of PEEK for use in spinal arthroplasty devices.*

When OPT and CFR versions of PEEK are compared, it is clear that the CFR PEEK provides lower wear, friction and surface damage and is, at the present time, viewed as the most favorable material for use in an all-polymer spinal arthroplasty device. Concerns of sub-surface fatigue at high cycling still remain and need to be addressed in future wear studies.

### *Determine the cause of the central pit developed in the 100 mm radius CFR PEEK pins.*

The only significant surface damage observed for the CFR PEEK in the present study was the development of a central pit in the 100 mm radius CFR pins during wear test 1. This result was also reported by Austin (2008) for identical test parameters. The root cause for this damage needs to be determined as this could have serious implications for future articulations that employ CFR PEEK material. Central pitting was not observed when the spherical radius was reduced to 60 mm and when the reinforcing fiber orientation was parallel to the contact surface. The effects of both these parameters need to be investigated to assess their effects on surface damage and wear as both the fiber orientation and contact geometry of any implant will need to be specified as to minimize wear and surface damage. This will maximize the longevity and *in vivo* performance of the implant.

### *Determine whether high cycle sub-surface fatigue is a concern for CFR PEEK.*

Failure of the articulating surfaces is a concern for any orthopedic implant material, especially a two-phase material such as CFR PEEK. In order to determine the sensitivity of CFR PEEK to sub-surface fatigue, long-term wear testing should be performed in both pin-on-plate and wear simulator configurations to quantify this possible effect, if any, on the long term performance of this articulation.

*Perform spinal simulator wear testing of the proposed CTLAS.*

While pin-on-plate wear testing allows for screening of orthopedic material pairings, more accurate wear testing using a full scale simulator that recreates the actual kinematics of the natural joint is required to fully evaluate the device under the actual *in vivo* conditions. Therefore spine simulator testing of the proposed CTLAS device is recommended to aid in the evaluation of the actual *in vivo* performance of the device. It is expected that this will accommodate further design improvements that are not possible with pin-on-plate wear testing. Testing parameters should allow for the investigation of fiber orientation and contact geometry including the reduced radii of conforming contacts.

*Quantify the lubricant protein sensitivity of PEEK OPTIMA articulations.*

While the wear performance of OPT PEEK is not as favorable as CFR PEEK, it still may have application in other joint replacement applications, possible those which observe reduced loading and motion. Therefore in order to further understand this material pairing and assess the potential sensitivity of this material pairing to the lubricant protein concentration that was suggested by the results of the present study, further wear testing should investigate the wear performance of 60 mm OPT pins without reducing the lubricant protein concentration from 12 to 6 $gL^{-1}$ after 1 Mc. Removing the reduction in protein concentration from the test plan it will be determine cause of the increased wear observed in the present study. If increased wear is observed during the second Mc, then increased contact stresses were a factor in the increased wear. If wear does not increase, then it is clear that the OPT material pairing is indeed sensitive to lubricant protein content. There may also be some combination of effect.

# References


Acosta, F.L., Lotz, J., Ames, C.P. (2005) The potential role of mesenchymal stem cell therapy for intervertebral disc degeneration: a critical overview. *Neurosurg Focus* 19(3), E4.

Adams, M.A., Hutton, W.C. (1982) Prolapsed intervertebral disc. A hyperflexion injury. *Spine* 7, 184–191.

Adams, M.A., Hutton, W.C. (1985) Gradual disc prolapse. *Spine* 10, 524–531.

Advanced Mechanical Technology Inc. (AMTI) (2004) *AMTI's OrthoPOD™ Friction and Wear Testing Machine Manual.* AMTI Technical Manual, Watertown, MA, USA.

Agency for Healthcare Research and Quality (AHRQ) (2007) *Healthcare Cost and Utilization Project, HCUPnet* [Online] Available at: http://www.hcup-us.ahrq.gov/ [Accessed 10 July 2009].

American Society for Testing and Materials (ASTM) (2006) *Standard guide for functional, kinematic, and wear assessment of total disc prosthesis.* ASTM F 2423-05, PA, United States.

Amevo, B., Worth, D., Bogduk, N. (1991) Instantaneous axes of rotation of the typical cervical motion segments: a study in normal volunteers. *Clin. Biomech.* 6(2), 111-117.

Amevo, B., Macintosh, J.E., Worth, D., Bogduk, N. (1991) Instantaneous axes of rotation of the typical cervical motion segments. *Clinical Biomechanics* 6, 31-37.

Amstutz, H. C., Campbell, P., Kossovsky, N. (1992) Mechanism and clinical significance of wear debris-induced osteolysis. *Clinical Orthopaedics and Related Research*, 276, 7-18.

Andersson, E.A., Oddsson, L.I., Grundstrom, H., Nilsson, J., Thorstensson, A. (1996) EMG activities of the quadratus lumborum and erector spinae muscles during flexion-relaxation and other motor tasks. *Clin Biomech* 11, 392–400.

Andersson, G.B.J., Lavender, S.A. (1997) *Evaluation of muscle function*. In: Frymoyer JW, The Adult Spine: Principles and Practice. Lippincott-Raven.

Austin, H. A. (2008) Wear of PEEK All-Polymer Articulations for Cervical Spinal Disc Arthroplasty. *MASc Thesis*, University of Waterloo, Waterloo, Ontario.

Austin, H.A., Langohr, G.D.G., Harper, M.L. and Medley, J.B. (2010) Performance of PEEK all-polymer articulations for spinal applications. *56th Annual Meeting of the Orthopaedic Research Society*, New Orleans, LA, Paper 275 (poster and short talk presentation). 6-9 March, New Orleans, LA.

Austin, H.A., Harper, M.L. and Medley, J.B. (2008) PEEK-on-PEEK for application in cervical disc arthroplasty? *8th World Biomaterials Congress*, Amsterdam, The Netherlands, 28 May – 1 June, Poster P-Sat-A-182.

Bagnall, K.M., Ford, D.M., McFadden, K.D., Greenhill, B.J., Raso, V.J. (1984) The histochemical composition of human vertebral muscle. *Spine* 9, 470–473.

Bao, Q.B., Songer, M., Pimenta, L., Werner, D., Reyes-Snachez, A., Balsano, M. Agrillo, U., Coric, D., Davenport, K. and Yuen, H. (2007) Nubac disc arthroplasty: preclinical studies and preliminary safety and efficacy evaluations. *SAS Journal*, 1 (1), 36-45. (online at doi: SASJ-2006-0007-RR)

Baptiste, D.C., Fehlings, M.G. (2006) Pathophysiology of cervical myelopathy. *Spine* 6, 190S–197S.

Bergmark, A. (1989) Stability of the lumbar spine. A study in mechanical engineering. *Acta Orthop Scand Suppl* 230, 1–54.

Berkson, M.H., Nachemson, A.L., Schultz, A.B. (1979) Mechanical properties of human lumbar spine motion segments – Part 2: responses in compression and shear; influence of gross morphology. *J Biomech Eng* 101, 52–57.

Bertagnoli, R., Yue, J.J., Pfeiffer, F., Fenk-Mayer, A., Lawrence, J.P., Kershaw, T., Nanieva, R. (2005) Early results after ProDisc-C cervical disc replacement. *J Neurosurg Spine* 2, 403–10.

Best, B.A., Guilak, F., Setton, L.A., Zhu, W., Saed-Nejad, F., Ratcliffe, A.,Weidenbaum, M.,Mow, V.C. (1994) Compressive mechanical properties of the human anulus fibrosus and their relationship to biochemical composition. *Spine* 19, 212–221.

el Bohy, A.A., Yang, K.H., King, A.I. (1989) Experimental verification of facet load transmission by direct measurement of facet lamina contact pressure. *J Biomech* 22, 931–941.

Bohlman, H.H., Emery, S.E., Goodfellow, D.B., Jones, P.K. (1993) Robinson anterior cervical discectomy and arthrodesis for cervical radiculopathy. Long-term follow-up of one hundred and twenty-two patients. *J Bone Joint Surg (Am)* 75-A, 1298–1307.

Boos, N., Aebi, M. (2008) *Spinal Disorders: Fundamentals of Diagnosis and Treatment*., Springer Publishing.

Bragdon, C.R., O'Connor, D.O., Lowenstein, J.D., Jasty, M. and Syniuta, W.D. (1996) The importance of multidirectional motion on the wear of polyethylene. *Proc. IMechE, Part H, Journal of Engineering in Medicine*, 210, 157-65.

Brinckmann, P., Frobin, W., Hierholzer, E., Horst, M. (1983) Deformation of the vertebral endplate under axial loading of the spine. *Spine* 8, 851–856.

Brown, T., Bao, Q-B, Kilpela, T., Schwenke, T. and Wimmer, M.A. (2008) A comprehensive wear assessment of self mating PEEK-OPTIMA for disc arthroplasty applications. 8th World Biomaterials Congress, Amsterdam, The Netherlands, 28 May – 1 June, Poster P-Sat-K-661.

Brown, T., Bao, Q.B. and Hallab, N. (2009) Biotribological assessment of NuBac, a PEEK on PEEK cervical disc replacement according to ISO and ASTM recommendations. *9th Meeting of the Spine Arthroplasty Society*, London, England, 28 April – 1 May, SAS9 abstract no. 94, 110.

Brown, T., Bao, Q.B., Kilpela, T. and Songer, M. (2010) An in vitro biotribological assessment of NUBAC, a polyetheretherketone-on-polyetheretherketone articulating nucleus replacement device. Spine, 35 (16), E774-E781.

Bryan, V.E. Jr. (2002) Cervical motion segment replacement. *Eur Spine* J 11 (Suppl 2), S92–S97.

Burklein, D., Lochmuller, E., Kuhn, V., Grimm, J., Barkmann, R.,Muller, R., Eckstein, F. (2001) Correlation of thoracic and lumbar vertebral failure loads with in situ vs. ex situ dual energy Xray absorptiometry. *J Biomech* 34, 579–587.

Burrows, E.H. (1963) The sagittal diameter of the spinal canal in cervical spondylosis. *Clin Radiol* 14, 77–86.

Butler, D., Trafimow, J.H., Andersson, G.B.H., McNeil, T.W., Huckman, M.S. (1990) Discs degenerate before facets. *Spine* 15, 111-113.

Cappozzo, A. (1984) Compressive loads in the lumbar vertebral column during normal level walking. *J Orthop Res* 1, 292–301.

Chang, U., Kim, D.H., Lee, M.C., Willenberg, R., Kim, S., Lim, J. (2007a) Changes in adjacent-level disc pressure and facet joint force after cervical arthroplasty compared with cervical discectomy and fusion. *J Neurosurg Spine* 7, 33-39.

Chang, U.K., Kim, D.H., Lee, M.C.,Willenberg, R., Kim, S.H., Lim, J. (2007b) Range of motion change after cervical arthroplasty with ProDisc-C and prestige artificial discs compared with anterior cervical discectomy and fusion. *J Neurosurg Spine* 7, 40–46. [Otherwise you cannot reference them uniquely!]

Chazal, J., Tanguy, A., Bourges, M., Gaurel, G., Escande, G., Guillot, M., Vanneuville, G. (1985) Biomechanical properties of spinal ligaments and a histological study of the supraspinal ligament in traction. *J Biomech* 18, 167–176.

Chen, C., Lu, Y., Kallakuri, S., Patwardhan, A., Cavanaugh, J.M. (2006) Distribution of A-delta and C-fiber receptors in the cervical facet joint capsule and their response to stretch. *J Bone Joint Surg Am* 88, 1807–1816.

Chen, S.H., Zhong, Z.C., Chen, C.S., Chen, W.J., Hung, C. (2009) Biomechanical comparison between lumbar disc arthroplasty and fusion. *Medical Engineering & Physics* 31, 244-253.

Cherubino, P., Benazzo, F., Borromeo, U., Perle, S. (1990) Degenerative arthritis of the adjacent spinal joints following anterior cervical spinal fusion: clinicoradiologic and statistical correlations. *Ital J Orthop Traumatol* 16, 533–543.

Clark, Charles R. (2005) *The Cervical Spine*. Lippincott Williams & Wilkins.

Clausen, J.D., Goel, V.K., Traynelis, V.C., Scifert, J. (1993) Unicate process and Lushka joints influence the biomechanics of the cervical spine: quantification using a finite element model of the C5-C6 segment. *Journal of Orthopaedic Research* 15, 342-347.

Cleland, J.A., Fritz, J.M.,Whitman, J.M., Heath, R. (2007) Predictors of short-termoutcome in people with a clinical diagnosis of cervical radiculopathy. *Phys Ther* 87, 1619–1632.

Cohen, S.P. (2007) Pathogenesis, Diagnosis, and Treatment of Lumbar Zygapophysial (Facet) Joint Pain. *Anesthesiology* 106, 591-614.

Coric, D., Regan, J. and Songer, M.N. (2010) Two year follow-up results from the US IDE feasibility of NUBAC, an articulating PEEK on PEEK nucleus replacement device. *SAS10 Annual Conference*, New Orleans, U.S.A. 27-30 April, Poster 458.

Cote, P., Cassidy, J.D., Carroll, L.J., Kristman, V. (2004) The annual incidence and course of neck pain in the general population: a population-based cohort study. *Pain* 112, 267–73.

Crawford, R.P., Cann, C.E., Keaveny, T.M. (2003) Finite element models predict in vitro vertebral body compressive strength better than quantitative computed tomography. *Bone* 33, 744–750.

Cusick, J.F., Yoganandan, N., Pintar, F., Myklebust, J., Hussain, H. (1988) Biomechanics of cervical spine facetectomy and fixation techniques. *Spine* 13, 808-812.

Cyron, B.M., Hutton, W.C., Troup, J.D. (1976) Spondylolytic fractures. *J Bone Joint Surg Br* 58-B, 462–466.

Delamarter, R.B, D.M. Fribourg, L.E. Kanim, Bae, H. (1976) Prodisc Artificial Total Lumbar Disc Replacement: Introduction and Early Results from the United States Clinical Trial. *Spine* 28, S167-S175.

Deyo, R.A., Nachemson, A., Mirza, S.K. (2004) Spinal-Fusion Surgery – The Case for Restraint. *The New England Journal of Medicine* 350(7), 722-726

Dillon, W., Booth, R., Cuckler, J., Balderson, R., Simeone, F., Rothman, R. (1986) Cervical Radiculopathy. A review. *Spine* 11, 998-991.

Dunlop, R.B., Adams, M.A., Hutton, W.C. (1984) Disc space narrowing and the lumbar facet joints. *J Bone Joint Surg* Br 66, 706–710.

Dvorak, J., Frohlich, D., Penning, L. (1988a) Functional radiographic diagnosis of the cervical spine: flexion/extension. *Spine* 13, 748-755.

Dvorak, J., Penning, L., Hayek, J. (1988b) Functional diagnostics of the cervical spine using computer tomography. *Neuroradiology* 30, 132-137.

Edwards, W.C., LaRocca, H. (1983) The developmental segmental sagittal diameter of the cervical spinal canal in patients with cervical spondylosis. *Spine* 8, 20–27

Emery, S.E., Fisher, J.R.S., Bohlman, H.H. (1997) Three-level anterior cervical discectomy and fusion. Radiographic and clinical results. *Spine* 22, 2622–2625.

EOrthopod (Medical MultiMEDIA Group LLC.). (2009) *Surgical Content Images* [Online] Available at: http://www.eorthopod.com [Accessed 9 March 2009].

eSpine. (2009) *Artificial Disc Prosthesis Devices* [Online] Available at: http://www.espine.com/ [Accessed 9 June 2009].

Evans, J.H., Nachemson, A.L. (1969) Biomechanical study of human lumbar ligamentum flavum. *J Anat* 105, 188–189.

Facet Solutions. (2009) *ACADIA™ Facet Replacement System* [Online] Available at: http://www.facetsolutions.com/Device.html [Accessed 14 July 2009].

Farfan, H.F. (1975) Muscular mechanism of the lumbar spine and the position of power and efficiency. *Orthop Clin North Am* 6, 135–144.

Ferlic, D.C. (1963) The nerve supply of the cervical intervertebral disc in man. *Bull Johns Hopkins Hosp* 113, 347–351.

Fernstrom, U. (1966) Arthroplasty with intercorporal endoprothesis in herniated disc and in painful disc. *Acta Chir Scand* S357, 154–159.

Fitz, W.R. (2000) *Artificial facet joint*, US Patent RE36758.

Fouyas, I.P., Statham, P.F., Sandercock, P.A. (2002) Cochrane review on the role of surgery in cervical spondylotic radiculomyelopathy. *Spine* 27, 736–747

Fujiwara, A., Tamai, K., Yamato, M., An, H.S., Yoshida, H., Saotome, K., Kurihasi, A. (1999) The relationship between facet joint osteoarthritis and disc degeneration of the lumbar spine: an MRI study. *Eur Spine J* 8, 396-401.

Galante, J.O. (1967) Tensile properties of the human lumbar anulus fibrosus. *Acta Orthop Scand* 100(Suppl), 1–91.

Galbusera, F., Fantigrossi, A., Raimondi, M.T., Sassi, M., Fornari, M., Assietti, R. (2006) Biomechanics of the C5-C6 spinal unit before and after placement of a disc prosthesis. *Biomechan Model Mechanobiol* 5, 253-261.

Galbusera, F., Bellini, C.M., Brayda-Bruno, M., Fornari, M. (2008) Biomechanical studies on cervical total disc arthroplasty: A literature review. *Clinical Biomechanics* 23, 1095-1104.

Galbusera, F., Bellini, C.M., Raimondi, M.T., Fornari, M., Assietti, R. (2008b) Cervical spine biomechanics following implantation of a disc prosthesis. *Medical Engineering & Physics* 30, 1127-1133.

Goel, V.K., Clark, C.R., Harris, K.G., Schulte, K.R. (1988) Kinematics of the cervical spine: effects of multiple total laminectomy and facet wiring. *J Orthop Res* 6, 611-619.

Goel, V.K., and Clausen, J.D. (1998) Prediction of Load Sharing Among Spinal Components of a C5-C6 Motion Segment Using the Finite Element Approach. *Spine* 23(6), 684 – 691.

Goffin, J., Casey, A., Kehr, P. (2002) Preliminary clinical experience with the Bryan Cervical Disc Prosthesis. *Neurosurgery* 51, 840–847.

Grant, J.P., Oxland, T.R., Dvorak, M.F. (2001) Mapping the structural properties of the lumbosacral vertebral endplates. *Spine* 26, 889–896.

Grant, J.P., Oxland, T.R., Dvorak, M.F., Fisher, C.G. (2002) The effects of bone density and disc degeneration on the structural property distributions in the lower lumbar vertebral endplates. *J Orthop Res* 20, 1115–1120.

Gray, H. (1918) Anatomy of the Human Body. Lea & Febiger, Philadelphia, Bartleby.com, 2010.

Green, S. (2005) Using Implantable-Grade PEEK for *in vivo* devices. *Medical Device & Diagnostic Industy* (May), 104.

Grupp, T.M., Meisel, H.J., Cotton, J.A., Schwiesau, J., Fritz, B., Blomer, W. and Jansson, V. (2010) Alternative bearing materials for intervertebral disc arthroplasty. *Biomaterials*, 31, 523-531.

Guez, M., Hildingsson, C., Nasic, S., Toolanen, G. (2006) Chronic low back pain in individuals with chronic neck pain of traumatic and non-traumatic origin: a population-based study. *Acta Orth,* 77, 132–137.

Harris, W. H. (1995) The problem is osteolysis. *Clinical Orthopaedics and Related Research,* 311, 46-53.

Hasegawa, K., Takahashi, H.E., Koga, Y., Kawashima, T., Hara, T., Tanabe, Y., Tanaka, S. (1993) Mechanical properties of osteopenic vertebral bodiesmonitored by acoustic emission. *Bone,* 14, 737–743.

Hattori, S., Oda, H., Kawai, S. (1981) Cervical Intradiscal Pressure in Movements and Traction of the Cervical Spine. *Zeitschrift Fur Orthopadie* 119, 568-569.

Hayashi, H., Okada, K., Hamada, M., Tada, K., Ueno, R. (1987) Etiologic factors of myelopathy. A radiographic evaluation of the aging changes in the cervical spine. *Clin Orthop Relat Res,* 214, 200–209.

Hilibrand, A.S., Carlson, G.D., Palumbo, M.A., Jones, P.K., Bohlman, H.H. (1999) Radiculopathy andmyelopathy at segments adjacent to the site of a previous anterior cervical arthrodesis. *J Bone Joint Surg Am,* 81, 519–528.

Hunter, C.J., Matyas, J.R., Duncan, N.A. (2003) The Notochordal Cell in the Nucleus Pulposus: A Review in the Context of Tissue Engineering. *Tissue Engineering,* 9(4), 667-677.

Hutton, W.C., Cyron, B.M., Stott, J.R. (1979) The compressive strength of lumbar vertebrae. *J Anat* 129, 753–758.

Impliant Inc. (2009) TOPS System [Online] Available at: http://www.impliant.com/ [Accessed 14 July 2009].

International Organization for Standardization (ISO) (2005) *Implants for surgery – wear of total intervertebral spinal disc prosthesis – Part 1: Loading and displacement parameters for wear testing and corresponding environmental conditions for test*. ISO 18192-1, United States.

Invibio Biomaterial Solutions (2009) *MOTIS™ Polymer Typical Material Properties [Online]*. Available at: http://www.invibio.com/ [Accessed 8 July 2010].

Jones, D.P., Leach, D.C., Moore, D.R. (1985) Mechanical Properties of Poly-Ether-Ether-Ketone for Engineering Applications. *Polymer* 26(9), 1385-1393.

Kalichman, L., Hunter, D.J. (2007) Lumbar Facet Joint Osteoarthritis: A Review. *Semin Arthritis Rheum*. 2, 69-80.

Kasimatis, G.B., Michopoulou, S., Boniatis, I., Dimopoulos, P., Panayiotakis, G., Panagiotopoulos, E. (2009) The impact of fusion on adjacent levels in cervical spine injuries: It is really important? *Clinical Neurology and Neurosurgery* 111, 816-824.

Kim, D.H., Cammisa, F.P., Fessler, R.G. (2006) *Dynamic Reconstruction of the Spine*. Thieme Medical Publishers Inc.

Kirkady-Willis, W.H., Wedge, J.H., Yong-Hing, K., Reilly, J. (1978) Pathology and pathogenesis of lumbar spondylosis and stenosis. *Spine* 3, 319-328.

Kumaresan, S., Yoganandan, N., Pintar, F.A., Mainman, D.J. (1999) Finite element modeling of the cervical spine: role of intervertebral disc under axial and eccentric loads. *Medical Engineering and Physics* 21, 689-700.

Kurtz, S.M. & Edidin, A.A. (2006) *Spine Technology Handbook*., New York: Elsevier.

Kurtz, S.M., Devine, J.N. (2007) PEEK Biomaterials in Trauma, Orthopedic, and Spinal Implants. *Biomaterials* 28 (32), 4845-4869.

LaRocca, H. (1988) Cervical spondylotic myelopathy: natural history. *Spine* 13, 854–855.

Lavender, S.A., Tsuang, Y.H., Andersson, .G.B.J. (1992) Trunk muscle cocontraction: the effects of moment direction and moment magnitude. *J Orthop Res* 10, 691–670.

Le, H., Thongtrangan, I., Kim, D.H. (2004) Historical review of cervical arthroplasty. *Neurosurg Focus* 17(3), E1.

Link, H.D. (2002) History, design and biomechanics of the LINK SB Charite artificial disc. *Eur Spine J* 11 S2, S98–S105.

Lipson, J.L., Muir, H. (1981) Proteoglycans in experimental intervertebral disc degeneration. *Spine* 6, 194-210.

Long, R., Sairyo, K., Goel, V., Phares, T., Biyani, A., McGowan, D. (2005) Biological Evaluation of Gelfoam as a Bioabsorbable Scaffold for Nucleus Pulposus Cells. *In: 32nd Annual Meeting of International Society of Study for the Lumbar Spine.* New York, NY.

Lorenz, M., Patwardhan, A., Vanderby, R., Jr. (1983) Load-bearing characteristics of lumbar facets in normal and surgically altered spinal segments. *Spine* 8, 122–130.

Marawar, S., Girardi, F.P., Sama, A.A., Ma, Y., Gaber-Baylis, L.K., Besculides, M.C., Memtsoudis, S.G. (2010) National Trends in Anterior Cervical Fusion Procedures. *Spine*, doi: 10.1097/BRS.0b013e3181bef3cb (Published Ahead of Print)

Marchand, F., Ahmed, A.M. (1990) Investigation of the laminate structure of lumbar disc annulus fibrosus. *Spine* 15, 402–410.

Marieb, E. (2000) *Human Anatomy & Physiology 5th Edition*., Benjamin-Cummings Publishing Company.

Martins, A. (1976) Anterior cervical discectomy with and without interbody bone graft. *J Neurosurg* 44, 290-295.

Matsumoto, M., Okada, E., Ichihara, D., Watanabe, K., Chiba, K., Toyama, Y., Fujiwara, H., Momoshima, S., Nishiwaki, Y., Iwanami, A., Ikegami, T., Takahata, T., Hashimoto, T. (2009) Anterior Cervical Decompression and Fusion Accelerates Adjacent Segment Degeneration. *Spine* 35(1), 36-43.

McBroom, R.J., Hayes, W.C., Edwards, W.T., Goldberg, R.P.,White, A.A.III (1985) Prediction of vertebral body compressive fracture using quantitative computed tomography. *J Bone Joint Surg Am* 67, 1206–1214.

McGlashen, K.M., Miller, J.A., Schultz, A.B., Andersson, G.B. (1987) Load displacement behavior of the human lumbo-sacral joint. *J Orthop Res* 5, 488–496.

McKellop, H.A. and Clarke, I.C. (1984) Evolution and evaluation of materials-screening machines and joint simulators in predicting *in vivo* wear phenomena. *Functional Behaviour of Orthopedic Biomaterials, Vol. II: Applications* (Edited by P. Ducheyne and G.W. Hastings), CRC Press, Boca Raton, FL, 51-85.

McGill, S.M., Santaguida, L., Stevens, J. (1993) Measurement of the trunk musculature from T5 to L5 using MRI scans of 15 young males corrected for muscle fiber orientation. *Clin Biomech* 8, 171–178.

McLain, R.F. (1994) Mechanoreceptor endings in human cervical facet joints. *Spine* 19, 495–501.

Medtronic Inc. (2009) The Prestige® Cervical Disc [Online] Available at: http://www.prestigedisc.com/ [Accessed 11 July 2009].

Miller, J.A.,Haderspeck, K.A., Schultz, A.B. (1983) Posterior element loads in lumbar motion segments. *Spine* 8, 331–337.

Mochida, K., Komori, H., Okawa, A.,Muneta, T.,Haro, H., Shinomiya, K. (1998) Regression of cervical disc herniation observed on magnetic resonance images. *Spine* 23, 990–995.

Mochida, J. (2005) New Strategies for Disc Repair: Novel Preclinical Trials. *J. Orthop. Sci* 10, 112-118.

Moroney, S.P., Schultz, A.B., Miller, J.A., Andersson, G.B. (1988) Load-displacement properties of lower cervical spine motion segments. *J Biomech* 21, 769–779.

Moroney, S.P., Schultz, A.B., Miller, J.A.A. (1998) Analysis and Measurement of Neck Loads. *Journal of Orthopaedic Research* 6, 713-720.

Myers, B.S., McElhaney, J.H., Doherty, B.J., Paver, J.G., Nightingale, R.W., Ladd, T.P., Gray, L. (1989) Responses of the Human Cervical Spine to Torsion. In: *Applied Biomechanics Paper Abstracts,* Ref. #892437, 215-222.

Nabhan, A., Ahlhelm, F., Shariat, K., Pitzen, T., Steimer, O., Steudel, W.I., Pape, D. (2007) The ProDisc-C prosthesis: clinical and radiological experience 1 year after surgery. *Spine* 32, 1935–41.

Nachemson, A.L. (1960) Lumbar intradiscal pressure. Experimental studies on post-mortem material. *Acta Orthop Scand* 43(Suppl), 1–104.

Nachemson, A.L. (1960b) Lumbar intradiscal pressure. Experimental studies on post-mortem material. *Acta Orthop Scand* 43(Suppl), 1–104.

Nachemson, A.L. (1963) The influence of spinal movements on the lumbar intradiscal pressure and on the tensile stresses in the anulus fibrosus. *Acta Orthop Scand* 33, 183–207.

Natarajan, R.N., Chen, B.H., An, H.S., Andersson, G.B.J. (2000) Anterior cervical fusion: a finite element model study on motion segment stability including the effect of osteoporosis. *Spine* 25(8), 955-961.

Nemeth, G., Ohlsen, H. (1986) Moment armlengths of trunkmuscles to the lumbosacral joint obtained *in vivo* with computed tomography. *Spine* 11, 158–160.

Ng, H.W., Teo, E.C. (2001) Nonlinear finite element analysis of the lower cervical spine (C4-C6) under axial loading. *Journal of Spinal Disorders* 16(1), 201-210.

Orr, R.D., Postak, P.D., Rosca, M., Greenwald, A.S. (2007) The Current State of Cervical and Lumbar Spinal Disc Arthroplasty. *J Bone Joint Surg Am* 89, 70-75.

Orthopedic Institute. (2009) *Patient Education - Neck* [Online] Available at: http://www.ortho-i.com [Accessed 2 August 2009].

Orthopedics International. (2009) *Lumbar Degenerative Disc Disease* [Online] Available at: http://www.oispine.com/photos/spine_path [Accessed 10 March 2009].

Oxland, T.R., Panjabi, M.M. (1992) The onset and progression of spinal injury: a demonstration of neutral zone sensitivity. *J Biomech* 25, 1165–1172.

Ozgur, B.M. (2009) *Minimally Invasive Spine Surgery*., Springer Science & Business Media, LLC.

Panjabi, M.M., White, A.A., III, Johnson, R.M. (1975) Cervical spine mechanics as a function of transection of components. *J Biomech* 8, 327–336.

Panjabi, M.M., Brand, R.A., Jr., White, A.A.III (1976) Mechanical properties of the human thoracic spine as shown by three-dimensional load-displacement curves. *J Bone Joint Surg Am* 58, 642–652.

Panjabi, M.M., White, A.A., Keller, D., Southwick, W.O., Friedlaender, G. (1978) Stability of the Cervical Spine Under Tension. *J. Biomechanics* 11, 189-197.

Panjabi, M.M., Goel, V.K., Takata, K. (1982) Physiologic strains in the lumbar spinal ligaments. An in vitro biomechanical study. 1981 Volvo Award in Biomechanics. *Spine* 7, 192–203.

Panjabi, M. M., Summers, D. J., Pelker, R. R. (1986) Three-Dimensional Load-Displacement Curves due to Forces on the Cervical Spine. *Journal of Orthopedic Research*, **4**(2), 152-161.

Panjabi, M.M. (1992) The Stabilizing System of the Spine. Part I. Function, Dysfunction, Adaptation, and Enhancement. *Journal of Spinal Disorders* 5(4), 383-389.

Panjabi, M.M. (1992b) The Stabilizing System of the Spine. Part II. Neutral Zone and Instability Hypothesis. *Journal of Spinal Disorders* 5(4), 390-397.

Panjabi, M.M., Oxland, T., Takata, K., Goel, V., Duranceau, J., Krag, M. (1993) Articular facets of the human spine. Quantitative three-dimensional anatomy. *Spine* 18, 1298–1310.

Panzer, M.B. (2006) 'Numerical Modeling of the Human Cervical Spine in Frontal Impact.' *MASc Thesis*, University of Waterloo, Ontario, Canada.

Panzer, M.B., Cronin, D.S. (2009) C4-C5 segment finite element model development, validation, and load-sharing investigation. *Journal of Biomechanics* 42, 480-490.

Pathria, M., Sartoris, D.J., Resnick, D. (1987) Osteoarthritis of the lumbar facet joints: accuracy of oblique radiographic assessment. *Radiology* 164, 227-230.

Penning, L. (1978) Normal Movement of the cervical spine. *AJR Am J Roentgenol* 130, 317-326.

Penning, L., Wilmink, J.T., Van Woerden, H.H., Knol, E. (1986) CT myelographic findings in degenerative disorders of the cervical spine: clinical significance. *AJR Am J Roentgenol* 146, 793–801.

Penning, L., Wilmink, J.T. (1987) Rotation in the cervical spine; a CT study in normal subjects. *Spine* 14, 1135-1139.

Phillips, F.M., Reuben, J., Wetzel, F.T. (2002) Intervertebral disc degeneration adjacent to a lumbar fusion. *The Journal of Bone and Joint Surgery* 84-B, 289-294.

Phillips, F., Tzermiadianos, M., Voronov, L., Havey, R., Carandang, G., Renner, S., Rosler, D., Ochoa, J., Patwardhan, A. (2009) Effect of the Total Facet Arthroplasty System after complete laminectomy-facetectomy on the biomechanics of implanted and adjacent segments. *The Spine Journal* 9, 96-102.

Pointillart ,V. (2001) Cervical disc prosthesis in humans: first failure. *Spine* 26, E90–E92.

Powell, M.L., Medley, J.B. and Varano, R. (2005) Metal-metal cervical disc implants: material investigation using pin-on-plate tests. *Trib and Interface Eng Series* 48, 845-852.

Punt, I.M., Visser, V.M., van Rhijn, L.W., Kurtz, S.M., Antonis, J., Schurink, G.W.H., van Ooij, A. (2008) Complications and reoperations of the SB Charite lumbar disc prosthesis: experience in 75 patients. *Eur Spine J* 17, 36-43.

Radhakrishnan, K., Litchy, W.J., O'Fallon, W.M., Kurland, L.T. (1998) Epidemiology of cervical radiculopathy. *Brain* 117(2), 325–35.

Rao, R.D., Currier, B.L., Albert, T.J., Bono, C.M.,Marawar, S.V., Poelstra, K.A., Eck, J.C. (2007) Degenerative cervical spondylosis: clinical syndromes, pathogenesis, and management. *J Bone Joint Surg Am* 89, 1360–78.

Raynor, R.B., Pugh, J., Shapiro, I. (1985) Cervical facetectomy and its effect on spine strength. *J Neurosurg* 64, 278-282.

Raynor, R.B., Moskovich, R., Zidel, P., Pugh, J. (1987) Alterations in primary and coupled neck motions after facetectomy. *J Neurosurg* 12, 681-687.

Rohlmann, A., Graichen, F., Weber, U., Bergmann, G. (2000) Volvo Award winner in biomechanical studies: Monitoring *in vivo* implant loads with a telemeterized internal spinal fixation device. *Spine* 25, 2981–2986.

Rohlmann, A., Zander, T., Schmidt, H., Wilke, H.J., Bergmann, G. (2006) Analysis of the influence of disc degeneration on the mechanical behavior of a lumbar motion segment using the finite element method. *Journal of Biomechanics* 39, 2484-2490.

Rydevik, B., Garfin, S. (1989) Spinal nerve root compression. In: Szabo RM (ed) Nerve root compression syndromes: diagnosis and treatment. Slack Medical, New York, pp 247–261.

Sasso, R.C., Smucker, J.D., Hacker, R.J., Heller, J.G. (2007) Clinical outcomes of BRYAN cervical disc arthroplasty: a prospective, randomized, controlled, multicenter trial with 24-month follow-up. *J Spinal Disord* Tech 20, 481–491.

Schulte, K.R., Clark, C.R., Goel, V.K. (1989) Kinematics of the cervical spine following discectomy and stabilization. *Spine* 14, 1116-1121.

Schultz, A.B., Warwick, D.N., Berkson, M.H., Nachemson, A.L. (1979) Mechanical properties of human lumbar spine motion segments. Part 1: Responses in flexion, extension, lateral bending and torsion. *J Biomech Eng* 101, 46–52.

Scholes, S., Unsworth, A. (2001) Pin-on-Plate studies on the effects of rotation on the wear of metal on-metal samples. *J Materials Science: Materials in Medicine* 12, 299-303.

Scholes, S.C. and Unsworth, A. (2007) The wear properties of CFR-PEEK-OPTIMA acticulating against ceramic assessed on a multidirectional pin-on-plate machine. *Proc IMechE, Part H, Engng in Med,* **221***,* 281-89.

Scholes S and Unsworth A. (2008) Comparison of PEEK/PEEK, CFR-PEEK/CFR-PEEK and alternative PAEK couplings for use in orthopaedic applications. *8th World Biomaterials Congress*, Amsterdam, The Netherlands, 28 May – 1 June, Poster P-Sat-I-598.

Scholes, S.C., Unsworth, A. (2009) Wear studies on the likely performance of CFR-PEEK/CoCrMo for use as artificial joint bearing materials. J Mater SciL Mater Med, 20, 167-170.

Scholes, S.C., Unsworth, A. (2010) The wear performance of PEEK-OPTIMA based self-mating couples. Wear, 268, 380-387.

Schultz, A., Andersson, G., Ortengren, R., Haderspeck, K., Nachemson, A. (1982) Loads on the lumbar spine: Validation of a biomechanical analysis by measurements of intradiscal pressures and myoelectric signals. *J Bone Joint Surg Am* 64, 713-720.

Schwenke, T., Brown, T., Bao, Q., Kilpela, T. and Wimmer, M. (2007) Wear assessment of a self mating polymer for nucleus replacement devices. *53rd Annual Meeting of the Orthopaedic Research Society*, San Diego, CA, 11-14 February, Poster 1125.

Scoville, W.B. (1961) Cervical spondylosis treated by bilateral facetectomy and laminectomy. *J Neurosurg* 18, 423-428.

Shin, W.R., Kim, H.I., Shin, D.G., Shin, D.A. (2006) Radiofrequency neurotomy of cervical medial branches for chronic cervicobrachialgia. *J Korean Med Sci* 21, 119–25.

Shirazi-Adl, A., Ahmed, A.M., Shrivastava, S.C. (1986) Mechanical response of a lumbar motion segment in axial torque alone and combined with compression. *Spine* 11, 914–927.

Shirazi-Adl, A., Drouin, G. (1987) Load Bearing Role of Facets in a Lumbar Segment under Sagittal Plane Loadings. *J. Biomechanics* 20(6), pp 601-613.

Silva, M.J.,Wang, C., Keaveny, T.M., Hayes, W.C. (1994) Direct and computed tomography thicknessmeasurements of the human, lumbar vertebral shell and endplate. *Bone* 15, 409–414.

Skaggs, D.L., Weidenbaum, M., Iatridis, J.C., Ratcliffe, A., Mow, V.C. (1994) Regional variation in tensile properties and biochemical composition of the human lumbar anulus fibrosus. *Spine* 19, 1310–1319.

Spine-Health. (2009) *Treatment: Artificial Disc Replacement – Facet Technologies* [Online] Available at: http://www.spine-health.com/treatment/artificial-disc-replacement/facet-technologies [Accessed 11 July 2009].

Spivak, J. & Bendo, J. (2002) Lumbar Degenerative Disorders. In: *Koval K, ed. Orthopaedic knowledge update. American Academy of Orthpaedic Surgeons*, pp 627-44, Rosemont, IL, USA.

Stokes, I.A. (1987) Surface strain on human intervertebral discs. *J Orthop Res* 5, 348–355.

Stokes, I.A. (1988) Bulging of lumbar intervertebral discs: non-contacting measurements of anatomical specimens. *J Spinal Disord* 1, 189–193.

Synthes International. (2009) *PDF Files - Surgical Technique ProDisc®-C* [Online] Available at: http://www.synthesprodisc.com/html/Surgical-Technique.105.0.html [Accessed 23 Oct. 2009].

Szpalski, M., Gunzburg, R., Mayer, M. (2002) Spine arthroplasty: a historical review. *Eur Spine J* 11(S2), S65–S84.

Tan, L.C. (1999) Medial cervical facetectomy for radiculopathy due to foraminal stenosis: 71 personal consecutive cases, *Journal of Clinial Neuroscience* 5(3), 207-211.

Tencer, A.F., Ahmed, A.M. (1981) The role of secondary variables in the measurement of the mechanical properties of the lumbar intervertebral joint. *J Biomech Eng* 103, 129–137.

Tencer, A.F., Ahmed, A.M., Burke, D.L. (1982) Some static mechanical properties of the lumbar intervertebral joint, intact and injured. *J Biomech Eng* 104, 193–201.

Terayama, K., Ohtsuka, K.,Merlini, L., Albisinni, U., Gui, L. (1987) Ossification of the spinal ligament. A radiographic reevaluation in Bologna, Italy. *Nippon Seikeigeka Gakkai Zasshi* 61, 1373–8.

Tjandra, J.J. (2006) *Textbook of Surgery (3rd Ed.),* Blackwell Publishing Inc.

Tkaczuk, H. (1968) Tensile properties of human lumbar longitudinal ligaments. *Acta Orthop Scand* 115(Suppl):1

Tracy, M.F., Gibson, M.J., Szypryt, E.P., Rutherford, A., Corlett, E.N. (1989) The geometry of the muscles of the lumbar spine determined by magnetic resonance imaging. *Spine* 14, 186–193.

Traynelis, V.C. (2006) Cervical Arthroplasty. *Clinical Neurosurgery* 53, 203-207.

Tsuang, Y.H., Novak, G.J., Schipplein, O.D., Hafezi, A., Trafimow, J.H., Andersson, G.B. (1993) Trunk muscle geometry and centroid location when twisting. *J Biomech* 26, 537–546.

United States Department of Health & Human Services, Food and Drug Administration. (2009) *Medical Device Approvals* [Online] Available at: http://www.fda.gov/MedicalDevices/ProductsandMedicalProcedures/ [Accessed 3 August 2009].

Vaccaro, A., Smith, H.E., Wimberley, D.W. (2004) Cervical Arthroplasty: Material Properties. *Neurosurg Focus* 17(3).

Van Ooij, A., Oner, F.C., Verbout, A.J. (2003) Complications of artificial disc replacement: a report of 27 patients with the SB Charite disc. *J Spinal Disord Tech* 16, 369–383.

Van Zundert, J., Harney, D., Joosten, E.A., Durieux, M.E., Patijn, J., Prins, M.H., Van Kleef, M. (2006) The role of the dorsal root ganglion in cervical radicular pain: diagnosis, pathophysiology, and rationale for treatment. *Reg Anesth Pain Med* 3, 152–67.

Vital, J.M., O. Gille, P.G., Pointillart, V., Obeid, A.I. (2008) The Mobi-C® cervical disc prosthesis: indications, techniques and results. *Interact Surg* 3, 181-186.

Voronov, L.I., Havey, R.M., Sjovold, S.G., Funk, M. Carandang, G. Zindrick, D. Rosler, D.M. and Patwardhan, A.G. (2009) Kinematics of total facet replacement (TFAS-TL) with total disc replacement. *SAS Journal*, 3, 85-90.

Wainner, R.S., Gill, H. (2000) Diagnosis and nonoperative management of cervical radiculopathy. *J Orthop Sports Phys Ther* 30, 728–44.

Waters, R.L., Morris, J.M. (1973) An in vitro study of normal and scoliotic interspinous ligaments. *J Biomech* 6, 343–348.

Whang, P.G., Simpson, A.K., Rechtine, G., Grauer, J.N. (2009) Current trends in spinal arthroplasty: an assessment of surgeon practices and attitudes regarding cervical and lumbar disk replacement. *J Spinal Disord Tech* 22(1), 26-33.

White A.A., Johnsson R.M., Panjabi M.M., Southwick W.O. (1975) Biomechanical analysis of the clinical stability in the cervical spine. *Clin Orthop* 109, 85-95

White A.A., Southwick W.O., Panjabi M.M. (1976) Clinical instability in the lower spine. A review of past and current concepts. *Spine* 1, 15-27.

White, A.A, Panjabi, M.M. (1990) *Clinical Biomechanics of the Spine 2nd Edition*. J.B. Lippincott Company.

Wigfield, C., Gill, S., Nelson, R. (2002) The new Frenchay artificial cervical joint: results from a two-year pilot study. *Spine* 27, 2446–2452.

Wigfield, C., Gill, S., Nelson, R. (2002) Influence of an artificial cervical joint compared with fusion on adjacent-level motion in the treatment of degenerative cervical disc disease. *J Neurosurg* 96, 17–21.

Williams, J.A. (1994) *Engineering Tribology*., New York: Oxford University Press.

Wilson, D., Campbell, D. (1977) Anterior cervical discectomy without bone graft. *Neurosurgery* 47, 551-555.

Wimmer, M.A., Schwenke, T., Brown, T., Kilpela, T. and Bao, Q.B. (2008) The effect of accelerated aging on the wear of PEEK for use in disc arthroplasty. 54th Annual Meeting of the Orthopaedic Research Society, San Francisco, CA, 2 -5 March, Poster 1922.

Womack, W., Woldtvedt, D., Puttlitz, C.M. (2008) Lower cervical spine facet cartilage thickness mapping. *Osteoarthritis and Cartilage* 16, 1018-1023.

Wong, D.A., Annesser, B., Birney, T., Lamond, R., Kumar, A., Johnson, S., Jatana, S., Ghiselli, G. (2007) Incidence of contraindications to total disc arthroplasty: a retrospective review of 100 consecutive fusion patients with a specific analysis of facet arthrosis. *The Spine Journal* 7, 5-11.

Yang, K.H., King, A.I. (1984) Mechanism of facet load transmission as a hypothesis for lowback pain. *Spine* 9, 557–565.

Yoganandan, N., Larson, S.J., Pintar, F.A., Gallagher, M., Reinartz, J., Droese, K. (1994) Intravertebral pressure changes caused by spinal microtrauma. *Neurosurgery* 3, 415–421.

Yoganandan, N., Kumaresan, S., Pintar, F.A. (2000) Geometric and mechanical properties of human cervical spine modeling. *Spine* 21(15), 1824-1834.

Yonenobu, K. (2000) Cervical radiculopathy and myelopathy: when and what can surgery contribute to treatment? *Eur Spine J* 9, 1–7.

Yuan, H., Coric, D., Songer, M. Pimenta, L. Reyes-Sanchez, A., Werner, D., Balsano, M., Argrillo, U. and Bucciero, A. (2010) Two year follow-up results of NUBAC, a peek on peek nucleus replacement device: a prospective worldwide multi-center clinical study. *SAS10 Annual Conference*, New Orleans, U.S.A., 27-30 April, Poster 483.

Zdeblick, T.A., Abitbol, J.J., Kunz, D.N., McCabe, R.P., Garfin, S. (1993) Cervical stability of the cervical spine sequential capsule resection. *Spine* 18, 2005-2008

Zigler, J. (2005) Lumbar *Artificial Disc Surgery for Chronic Back Pain: Spine Health* [Online] Available at: http://www.spine-health.com/treatment/artificial-disc-replacement/ [Accessed 21 April 2010].